Proceedings of the 15th Meeting

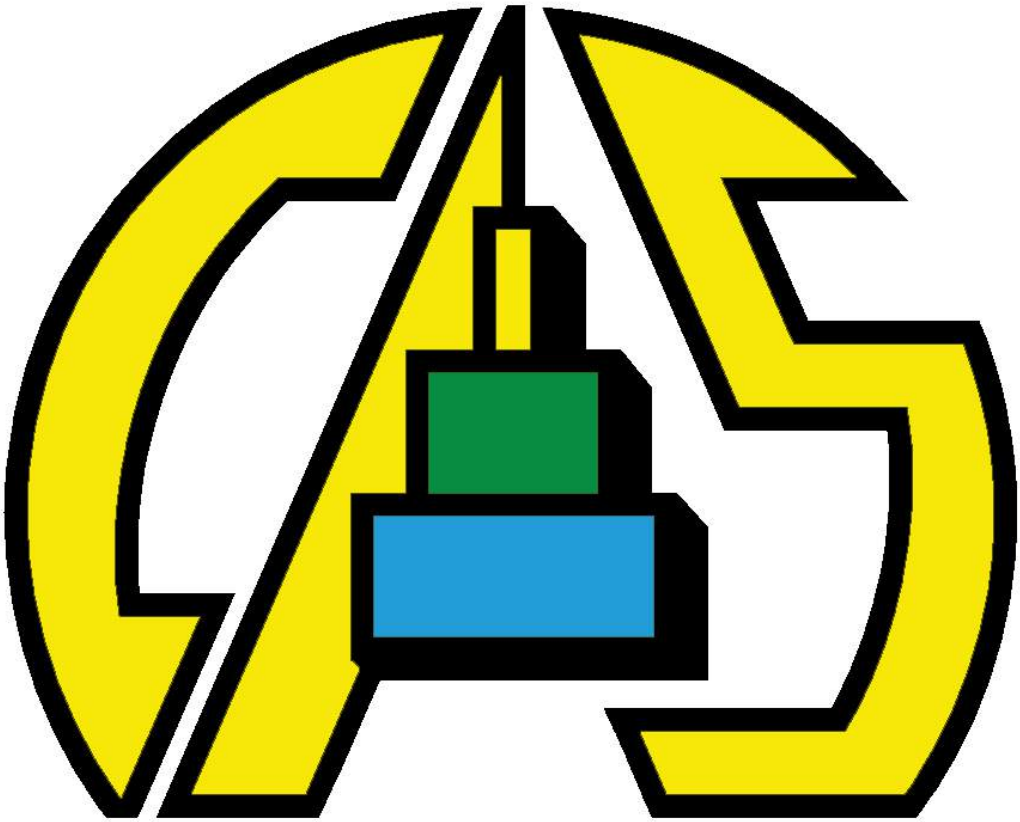

Caribbean Academy of Sciences

Science and Technology in a Caribbean Environment

Creole Beach Hotel - Guadeloupe

May 21 - 23 , 2006

The Caribbean Academy of Sciences

Science and Technology in a Caribbean Environment

Proceedings
of the
15th Meeting & Conference

hosted by
The DFA Chapter of the Caribbean Academy of Sciences

Venue
Creole Beach Hotel - Gosier, Guadeloupe
May 21 – 23, 2006

Edited by
D. Himmel, GTSI,
Université des Antilles et de la Guyane, Guadeloupe, France

Invited speakers :

Prof. Claude COHEN-TANNOUDJI
Laureate of Physics Nobel Prize 1997
"Manipulating atoms with light"

Dr. Edouard FABRE Emeritus CNRS Director
"World Energy Survey"

Presentations on USB-Stick

CAS Executives

President :	Pr. W. MELLOWES
Foreign Secretary :	Pr. G.N. MELVILLE
Secretary :	Mr. J. CAESAR
Treasurer :	Dr. T. ALLEYNE
Public Relations Officer :	Dr. C. STARR

Scientific Committee

Pr. B. DESHAIES
Dr. J. DUMONT
Pr. E. HICKS
Pr. O. HUE
Pr. M. LOUIS
Pr. J.L. MANSOT
Pr. W. MELLOWES
Pr. R.H. PETIT
Pr. A. PIETRUS
Pr. R. SAUNDERS

Organisation

Dr. N. BADRIE
Dr. P. BILAS
Dr. S. BLONC
Dr. T. CÉSAIRE
Dr. J. DUMONT
M. K. DELBÉ
Dr. V. GOLABKAN
Dr. D. HIMMEL
Pr. J.L. MANSOT
Mrs. N. NOMEDE MARTYR
Pr. L. ROMANA
Dr. Ph. THOMAS

Participants

Mohamed ABADI	mabadi@univ-ag.fr
Gisèle ALEXANDRE	Gisele.Alexandre@antilles.inra.fr
Shazaad ALI SHAH	sali-shah@fsa.uwi.tt
Clara ALLAYOUS	Clara.Allayous@univ-ag.fr
Trevor ALLEYNE	trevnmar@tstt.net.tt
S. ALTENOR	sgaspard@univ-ag.fr
F. ALVAREZ	falvarez@univ-ag.fr
Lilliam ALVAREZ-DIAZ	lilliam@citma.cu
Abdullah Adil ANSARI	ansari_adil@hotmail.com
Sophie ANTOINE-JONVILLE	sophie.jonville@wanadoo.fr
Hilary G. ARSCOTT	ianmar5757@yahoo.com
C. ASSELIN de BEAUVILLE	christian.asselin@univ-ag.fr
Marlene ATTZS	mattzs@fss.uwi.tt
Hervé AZALOUX	azaloux@wanadoo.fr
Neela BADRIE	nbadrie@fans.uwi.tt
Veena BADRIE-MAHARAJ	Trinidad and Tobago
Eric BANDOU	ebandou@univ-ag.fr
Céline BASSETTE	Celine.Bassette@univ-ag.fr
M. BENGOUBOU-VALERIUS	mendy@ipgp.jussieu.fr
Philippe BILAS	pbilas@univ-ag.fr
Fabian BLANCHARD	Fabian.Blanchard@Ifremer.fr
Rudy BLONBOU	rblonbou@univ-ag.fr
Stephen BLONC	stephen.blonc@univ-ag.fr
Noël M.BROWN	nbrown@utech.edu.jm
John Cartey CAESAR	jccaesar@yahoo.com
Marlena CASTELLANOS	marlena@citma.cu
Thierry CESAIRE	Thierry.cesaire@univ-ag.fr
Sophie COAT	sophiecoat@yahoo.fr
Claude COHEN-TANNOUDJI	France
Philippe CONNES	pconnes@yahoo.fr
Simeon CORNWALL	cornwall@myway.com
B.COULANGES	France
John CRAIN	John.crain@icann.org
Emanuel CUMMINGS	roweper1@yahoo.co.uk
Karl DELBE	kdelbe@univ-ag.fr
Antoine DELCROIX	Antoine.Delcroix@univ-ag.fr
Deryk CHEN	uwideryk@yahoo.com
Samuel DUFOUR-KOWALSKI	samuel.dufour-kowalski@antilles.inra.fr
Jacques DUMONT	jacques.dumont@univ-ag.fr
Kimathy ELISE	kelise@univ-ag.fr
Gaius D.EUXODIE	geudoxie@fsa.uwi.tt
Edouard FABRE	France
Audrey FANCHONE	Audrey.Fanchone@antilles.inra.fr
Tony FEUILLARD	tony.feuillard@univ-ag.fr
Carine FEVRIERE	†
Sandie FIGARO	sfigaro@univ-ag.fr
Jean Marie FLOWER	jean-marie.flower@wanadoo.fr
Alain FOUERE	Alain.Fouere@antilles.inra.fr
Dawn Iona FOX	dawniking@yahoo.com
Yann FREJAVILLE	Yann.Frejaville@univ-ag.fr
Sara GASPARD	sgaspard@univ-ag.fr
Vanyna GOLABKAN	Vanyna.golabkan@univ-ag.fr
Alexander Oliver GOSSETT	goliver@utech.edu.jm
Jean-Philippe GOURDINE	jpgourdine@univ-ag.fr
E. GRANDCHAMP	egrandch@univ-ag.fr
Jean Sebastien GUIBERT	jsebguibert@hotmail.com
Seetharaman HARIHARAN	uwi.hariharan@gmail.com
Maximilian F. HASLER	mhasler@martinique.univ-ag.fr
Michel Le HER	michel.le-her@univ-ag.fr
Elizabeth HICKS	Elizabeth.Hicks@univ-ag.fr
David HIMMEL	dhimmel@univ-ag.fr
David HINDS	dhinds@fsa.uwi.tt
Lionel HIRSCH	hirsch@ixl.fr
Olivier HUE	HueO@wanadoo.fr
E. INGADASSAMY	alain.rousteau@univ-ag.fr
Gillian B. ISABELLE	gisabelle@edenscapes.com
Sandra JACOBY-KOALY	Sandra.jacoby-koaly@univ-ag.fr
Olivier JACQUET	Olivier.jacquet@univ-ag.fr
Raymond C. JAGESSAR	raymondjagessar@yahoo.com
Célia JEAN-ALEXIS	cjeanale@univ-ag.fr
Cédric JEAN-CHARLES	cedric.jean-charles@univ-ag.fr
Marie-Odile JOANNES	mo_joannes@yahoo.fr
Ian C. JOSEPH	iancallistus@yahoo.com
Dorothée KOPP	dorothee.kopp@univ-ag.fr
Abilio LAGUNA GRANJA	cebimar@infomed.sld.cu
Mélina C.Z. LAURENT	memelili@hotmail.com
Marc LAVOIE	mlavoie@uwichill.edu.bb
Jean F. LEBRUN	jflebrun@univ-ag.fr
G. LEQUELLEC	christian.asselin@univ-ag.fr
Leticia LIMEA	limea@antilles.inra.fr

Max LOUIS	max.louis@univ-ag.fr
Jean-Louis MANSOT	Jean-louis.mansot@univ-ag.fr
Carine MARIE-MAGDELEINE	marie@antilles.inra.fr
Jean-André MARTI	jean-andre.marti@univ-ag.fr
Gisèle MASSENGO	gmophou@univ-ag.fr
Sebastien MATHOURAPARSAD	smathour@univ-ag.fr
Leslie C. MAURIN	lmaurin@univ-ag.fr
Winton A. MELLOWES	wmellowe@eng.uwi.tt
Nathalie MICHALON	nathalie_michalon@yahoo.fr
Shareeda MOHAMMED	shareeda.mohammed@gmail.com
F. MOLIA	France
Jacques MOLINIE	jmolinie@univ-ag.fr
Dominique MONTI	dominique.monti@univ-ag.fr
Charmagne E. MORTLEY.	nbrown@utech.edu.jm
Marilaine MOTA - MEIRA	motameira@yahoo.com
Jimmy NAGAU	jnagau@univ-ag.fr
Nathalie NATHOU	nnathou@univ-ag.fr
Nadiege NOMEDE MARTYR	nadiege.nomede-martyr@univ-ag.fr
Abdennebi OMRANE	aomrane@univ-ag.fr
Nady PASSE-COUTRIN	Nady.Passe-Coutrin@univ-ag.fr
Rosehelen PETIT	rhpetit@univ-ag.fr
Jacques PIGERRE	jacques.pigerre@guyane.univ-ag.fr
Pedro PORTILLO	pedroportillo2@yahoo.com
Christan POSTHOFF	cposthoff@fans.uwi.tt
Jérôme PRUNEAU	Pruneau.j@wanadoo.fr
Gaelle RAMDINE	slemoine@univ-ag.fr
H. RAMPADARATH	rsaunders@fsa.uwi.tt
Auran RANDRIANASOLO	Auran.randrianasolo@univ-ag.fr
Christelle ROBIN	Krisrob1@hotmail.com
Laurence ROMANA	lromana@univ-ag.fr
Alain ROUSTEAU	alain.rousteau@univ-ag.fr
Sebastien RUFFIE	jacques.dumont@univ-ag.fr
Mohammad SAQUIB	mohammadaqib@hotmail.com
Fagnété SARA	fagnetesara@yahoo.fr
Ramsey SAUNDERS	rsaunders@fsa.uwi.tt
E. SENATUS	stephen.blonc@univ-ag.fr
Willy SICOT	wsicot@univ-ag.fr
Stéphane SINNAPAH	stephane.sinnapah.toulouse@caramail.fr
Ted SOUBDHAN	ted.soubdhan@univ-ag.fr
Ollivier TAMARIN	ollivier.tamarin@guyane.univ-ag.fr
Vanessa TARER	v.tarer@voila.fr
K.D. THOMAS	Trinidad & Tobago
Philippe THOMAS	pthomas@univ-ag.fr
Alain TORRENS	torrab@yahoo.com
Julien TRIPETTE	juliustrip@hotmail.com
Jean VAILLANT	jean.vaillant@univ-ag.fr
Olga VALDES IGLESIAS	cebimar@ama.cu
Amandine VASLET	amandine.vaslet@univ-ag.fr
V.N. VERMA	Chemistry88@lycos.com
Bernard VICENS	prepasub.971@orange.fr
Carl WALTERS	cwalters582@yahoo.com
Thomas WESSEL	wthomas@utech.edu.jm
Thierry WOIGNIER	woignier@crit.univ-montp2.fr
Mark N. WUDDIVIRA	wuravnakka@yahoo.com
Xavier XANDE	Xavier.xande@antilles.inra.fr
Gail YOUNG	gyoung@fsa.uwi.tt
Farid F. YOUSSEF	fmyoussef@ tstt.net.tt
Narcisse ZAHIBO	nzahibo@univ-ag.fr

Table of contents

Computer Science & Maths

The Interdisciplinary Importance of Computer Science 11
C. Posthoff

Parallel Mining of Association Rules 13
W. Thomas

Boundary controllability with constraints on the state 15
G. Massengo and O. Nakoulima

Characteristic Cauchy Problem for Nonlinear Unidirectional Wave Equation 18
J.A. Marti

The sentinel method for mixed boundary condition dissipative problem with incomplete data 20
A. Omrane

Angles & Logarithms 23
A. Torrens

Estimation of the Large Multifractal Deviation Spectrum 28
M. Abadi, E. Grandchamp

A Variant of Newton's Method for Generalized Equations 29
C. Jean Alexis and A. Pietrus

An Accurate Projection Method for Incompressible Flows 30
C. Février, P. Angot, J. Laminie and P. Poullet

Introduction to and Implication of Emergent Global Internet Protocols and Policies for the Caribbean Region 30
J. Crain

Kernel Theorems in Spaces of Colombeau Generalized Functions 31
A. Delcroix

Chemistry / Physics of Materials

The Diels Alder Reaction, a Useful Synthetic Methodology 35
R.C. Jagessar and J.J. Hingree.

The Sol-Gel Process: a Method to Prepare Synthetic Materials and to Understand Natural Materials 38
T. Woignier, P. Dieudonné, J. Primera and A. Charlier de Chilly

Extraction and Isolation of Natural Products From *Momordica Charantia* 40
R.C. Jagessar and A. Mohamed

Ground and Excited States Vibrational Frequencies of 3-Amino-2-Chloropyridine 41
V.N. Verma

Effect of Processing Method on Shelf Stability of Coconut Water 43
H. G. Arscott and I. A. Lambert

Introduction of Electron Microscopy to The University of the West Indies, St. Augustine, Trinidad and Tobago 45
D. Hinds and R. Saunders

Analytical Scanning Electron Microscopy approach for Caribbean Ceramics Identification 47
B. Vicens, J.S. Guibert, D. Himmel and J.L. Mansot

High Spatial Resolution Raman Spectroscopic Mappings in Dynamic Lubricated Sphere - Plane Contacts: Application to Pressure and Thickness Profile Measurements 49
D. Himmel, Y. Bercion and J.L. Mansot

Band Structure Calculations Applied to Structural Determination of Graphite Intercalation Compounds: the Case Of CaC_6 51
K. Delbé, Ph. Thomas, N. Emery, C. Hérold, F. Boucher, J.-P. Buisson, P. Lagrange and J.L. Mansot

Development and Applications of a Flash Test Using High Powered Ultrasounds for the Fast Evaluation of the Durability of Painted Galvanized 52
J. Pigerre, P. Rodriguez , Y. Bercion and J.L. Mansot
Nano Friction of Low Dimensional Compounds Using Atomic and Lateral Force Microscopy: Toward An Atomic Interpretation 57
P. Bilas, L. Romana, F. Bade, K. Delbe, P. Thomas and J.L. Mansot
Nanomechanical Characterizations of Submicrometer Thick-Tribologic Films 59
L. Romana, P. Bilas, V. Golabkan and J.L. Mansot
Theoretical Approach of Nanocristallized Graphite Phases: Influence of Cluster Size Electronic Band Structure–Correlation to EELS Near Edges Structures 62
T. Césaire, V. Jeanne-Rose, N. Nomède Martyr, L.Largitte and J.L. Mansot
Antiwear and Antifriction Action Mechanisms of Colloidal Lubricant Additives 63
V. Golabkan, P. Bilas, L. Romana, J. Pigerre and J.L. Mansot
Tribological Properties of Room Temperature Graphite Fluorides Heat-Treated Under Fluorine Atmosphere 64
P. Thomas, K. Delbé, D. Himmel, J.L. Mansot, C. Delabarre, M. Dubois, K. Guérin and A. Hamwi
Kinetic Study of Sulfation of Natural Limestones from Guadeloupe 66
N. Passé-Coutrin and A. Ouensanga
Experimental Aqueous Phase Adsorbents Made From Purple heart *(Peltogyne venosa)* Sawdust And Rice Husk 68
D. I. Fox and R. Singh
Organic Electronics: From Molecules to Devices 70
L. Hirsch, G. Wantz, N. Huby, M. Urien, L. Vignau and J.P. Parneix
Characterization of Vetiver Roots Activated Carbon and Absorption Of Phenolic Compounds 70
S. Altenor, B. Carene, J. Lambert, J.J Ehrhardt, A. Ouensanga and S. Gaspard
A Comparative Study of Biological Indigenous Products Used to Increase Surface Hardness of Low Plain Carbon Steel 71
D. Gossett and A. Oliver
Industrial Production of Value-Added Chemicals From Sugarcane Bagasse 71
G.B. Isabelle
Multi technique approach of chemical and mechanical properties of hotmelts 72
N. Nomede Martyr, A. Gruda,S. Radegonde , T. Cesaire, D. Himmel and J.L. Mansot

Energy / Environment / Pollution

A Day – Night Solar Air Dryer with the Temperature and Flow Rate Controls: Numérical Simulation and Experimental Results 75
O. Tamarin, J.L. Bernard, F. Dupont, H. Clergeot and M. Dupont
Lack of Significance of Usual Ecological Indicators in Predicting Pesticides Contamination: Specificities of Tropical Islands Freshwaters 79
S. Coat and D. Monti
A Reactor for the Decontamination of Water Using Titanium Dioxide Nanoparticles and Solar Energy 81
S. Ali Shah, R. Saunders and R. Clarke.
Metallic Contaminations in Two Bays of Guadeloupe - Set Up of a Biomonitoring Survey by Using a Biomarker of Genotoxicity on the Mangrove Oyster (*Crassostrea rhizophorae*) 85
G. Ramdine, D. Fichet and S. Lemoine
Short-Time Scales Variability of the Global Solar Radiation in Guadeloupe 87
T. Soubdhan, F. Dupont, R. Calif and B. Deshaies
Acceptance, Applicability and Efficiency of Batch Disinfection of Rainwater for Human Consumption in Rural Communities of Trinidad Using Solar Radiation 87
W.A. Mellowes and K.D. Thomas
Retrieval of Aerosol Optical Thickness from Solar Radiation Data: Study of a Saharan Dust Event In Guadeloupe 88
T. Feuillard, R. Bonhomme, J. Molinié, S. Jacoby-Koaly, R.H. Petit and F. Brute

High Particles Concentration Levels and Relationship with Air Conditioning: Study of Three Cases of Intoxication in Public Offices 89
J. Molinié, R.H. Petit, S. Jacoby-Koaly and A. Roussas

Measurement and Analysis of Wind Velocity and short Time Scale Wind Speed Forecast 89
R. Blonbou, R. Calif, F. Dupont, T. Soubdhan and B. Deshaies

Simulation of Rainfall Interception Processes for Pollution Hazards Estimation Under Banana Plants 90
C. Bassette and F. Bussière

Molasse Spentwash Treatment by Two Processes: Adsorption on AC and Biodegradation 90
S. Figaro, C. Jean-Marius, O. Gros, L. Farhasmane, B. Ganou, F. Bazile, W. Achouack, M.A. Roncato, A. Ouensanga and S. Gaspard

Measurement and Computer Representation of Banana Plants for Environmental Studies 91
S. Dufour-Kowalski, and F. Bussière

Energy Production and Pollutant Mitigation from Broiler Houses on Poultry Farms in Pennsylvania and Jamaica 92
N. M. Brown and C.E. Mortley

Root Growth Responses of a wheat Cropland Weed, *Melilotus indicus(L.) All.,* Papilionaceae to Air Pollution 93
Mohammad Saquib

Environment / Climate / Naural Hazards / Simulation

Mathematical Tools for Modeling Natural Risks 97
M.F. Hasler

Climatological Analysis of Deep Convective Days in Guadeloupe 100
N. Nathou and E. Hicks

Modelling of The Wind Field Produced During a Hurricane Passage in the Vicinity of an Island. A Case Study: The Island of Guadeloupe (FWI) 104
K. Elise. and C. Asselin de Beauville

Behavioral Change: an Original Application of Health Belief Models for the Prevention of Natural Hazards 108
N. Michalon

Two Numerical Experiments for the Investigation of Possible Influences of a Climate Change on the Global Atmospheric Electrical Circuit 111
N. Michalon

Facing Natural Hazards: Policies, Strategies, role of Basic Sciences 114
L. Alvarez-Diaz

CDSA: A New Seismological Data Center for French West Indies 114
M. Bengoubou-Valérius, D. Bertil, S. Bazin, A. Bosson, F. Beauducel and A. Randrianasolo

Seismogenic Potential of Fore-Arc Tectonic Structures: Onshore - Offshore Geology Helps to Understand the Tectonic Activity at the Marie-Galante Basin - Lesser Antilles 115
J.F. Lebrun, J.L. Léticée, S. Bes de Berc, J.J. Cornée, P. Munch, A. Randrianasolo, I. Thinon and M. Villeneuve

Evaluation of the Tsunami Risk for Guadeloupe (Lesser Antilles) 116
N. Zahibo, E. Pelinovsky and I. Nikolkina

North Atlantic Hurricanes Trajectories; Important Forecast Parameters: a Case Study, 2006 Hurricane Season 116
G. Lequellec and C. Asselin de Beauville

A Method of Analysis and Identification of Clouds of Satellite Images Coming from GOES Satellite 117
J. Nagau and J-L Henry

Initialization of an Atmospheric Mesoscale Model for the Prediction of the Track and Intensity of Hurricanes 118
W. Sicot

Climatology of African Dust using Meteosat IR throughout the Period 1984-1998 118
M. Legrand, O. Pancrati, N. J. Brooks and L. J. Shipman

Table of contents

Evaluation of Rainfall Over Guadeloupe by Four Cumulus Parameterization Schemes: Case of the Tropical Depression Jeanne 119
C. Jean-Charles and C. Asselin De Beauville
Estimation of Downward Longwave Radiation in Guadeloupe 119
A. Fouéré, R. Bonhomme, F. Busière and S. Dufour-Kowalski
Early Observations of the Blazar OJ 287: Further Evidence for the Binary Black Hole Model 120
H. Rampadarath, M.J. Valtonen, R. Saunders and H.J. Lehto

Agriculture / Plant Biology

Statistical Study of Spatio-Temporal Evolution of Plant Infection by SCYLV in a Disease Free Plot 123
O. Jacquet, C. Edon, J. Vaillant and J.H. Daugrois
Tentative Estimates of Carbon Storage Ability Within Coastal Forested Wetlands in The Caribbean 125
J.M. Flower
Evaluation of a Direct Field Method of Soil Salinity Appraisal 127
G. Eudoxie
Paddy Cultivation in Sodic Soil through Vermitech 131
A. A. Ansari
Soil Texture and Organic Matter Effects on Structural Stability, Infiltration, Runoff and Seal Formation 134
M.N. Wuddivira, R.J. Stone and E.I. Ekwue
Effects Of *Musa x paradisiaca* Plant Extracts on the Digestive Parasitic Nematode *Haemonchus contortus* in the French West Indies 136
C. Marie-Magdeleine, M. Mahieu, H. Hoste and H. Archimède
The Ectomycorrhizal Fungus *Scleroderma bermudense* Improves Water Status and Limits Sodium and Chloride in Seagrape (*Coccoloba uvifera* L.) Seedlings 138
E. Bandou, F. Lebailly, F. Muller, M. Dulormne, A. Toribio, J. Chabrol, R. Courtecuisse, Y. Prin, B. Dreyfus and A. Bâ
Leaf Allometry in Long and Short Shoots of *Betula papyrifera* 138
J. C. Caesar
Biodiversity in Rain Forests of the Lesser Antilles 139
E. Ingadassamy and A. Rousteau

Agriculture / Animal Biology

A Low Cost Mechanism for Restraint and Handling of the Collared Peccary 143
(*Tayassu tajacu; Pecari tajacu*), **applied in Kourou, French Guiana**
G. Young, A. Steil and G. Garcia
The Ability of Near Infrared Reflectance Spectroscopy (NIRS) to Assess Quality and Level of Tropical Grass Intake by Creole Sheep 145
A. Fanchone, M. Boval, P. Lecomte and H. Archimede
Influence of a Sugar Cane Diet on Growth Performance, Carcass Traits and Meat Quality in Creole Growing Pigs 148
X. Xandé, D. Renaudeau, E. Despois, M. Giorgi and B. Bocage
How to Produce Heavy Goat Carcass With Lean Meat? 150
L. Limea, G. Alexandre, R. Arquet, G. Gravillon, B. Bocage

Marine Biology / Bacteriology

Marine Biotechnology in the Caribbean: Study of *Codakia orbicularis* Gill Proteins 155
J.P.F. Gourdine and E.J. Smith-Ravin

The Post Larval Settlement of Fishes on a Coral Reef of Guadeloupe (FWI) 157
Y. Frejaville, Y. Bouchon-Navaro, M. Louis and C. Bouchon

Antimicrobial Substances from Marine Bacteria 159
C. Walters

The CHALOUPE Project: Global Change, Dynamics of Exploited Marine Diversity, and Viability of Fisheries 161
F. Blanchard and O. Thèbaud

A Spatial and Temporal Study of the Benthic Communities in the Coral Reefs of the Bay Islands, Honduras 163
P. Portillo, Y. Bouchon-Navaro, M. Louis and C. Bouchon

Significance of Environmental Variables for the Structure of Fish Assemblages in the Lagoon of the Grand Cul-De-Sac Marin (Guadeloupe – FWI) 165
A. Vaslet, C. Bouchon, Y. Bouchon-Navarro and M. Louis

Seagrass Beds as Important Habitats for Juvenile Fishes in the Bay of the Grand Cul-De-Sac Marin (Guadeloupe, F.W.I.) 167
D. Kopp, Y. Bouchon-Navarro, C. Bouchon and M. Louis

Colonization of Sunken Wood in the Caribbean Area: Influence of the Environment 169
M.C.Z. Laurent and O. Gros

Bacterial Symbiosis in Wood Fall Bivalves 169
M.C.Z. Laurent and O. Gros

Description of the Extracellular Bacterial Interactions in Marine Nematodes From t*halassia testudinum* Environment 170
L.C. Maurin and O. Gros

Observation of Marine Nematodes Along a Transect Beach-Seagrass Beds of t*halassia testudinum*: a SEM Analysis 170
L.C. Maurin, C. Grateloup, M. Delannay and O. Gros

Health / Social Sciences

The Design and Application of a Biomedical Sensor for Blood Volume Pulsations 173
S. Cornwall, K. De Souza and R. Saunders

Modeling Economic Impact of Changes in Tourism for the French Overseas Region: the Guadeloupean Case 175
S. Mathouraparsad, A. Maurin and J.G. Montauban

Evaluation of Intensive Care in Trinidad – a Comparison with the Developed World 181
S. Hariharan, D. Chen

Fighting Against Sedentarity in the Caribbean Area: on the Interest of a Pluridisciplinar Approach 183
S. Antoine-Jonville, S. Sinnapah, S. Ruffié, S. Jacquelin, J.P. Donnet and O. Hue

Impact of Science on Gender Ideology in Society 184
K. Philip, N. Badrie and G. Sirju-Charran

Sickle Cell Trait Carriers: are they Comparable to Subjects with Normal Haemoglobin? From Cellular Biology to the Cardiovascular Approach 186
F. Sara, P. Connes, M.D. Hardy-Dessources, L. Marlin, M. Montout-Hedreville, J. Tripette, M. Etienne-Julan, C. Saint-Martin, J.C. Barthélémy and O. Hue

Comparing Physical Behaviors and Dietary Habits of Guadeloupeans Originating and Not Originating From India: Need for a Multidimensional Approach 188
S. Sinnapah, S. Antoine-Jonville, J.P. Donnet, S. Ruffié, and O. Hue

Factors influencing food choices by secondary school children with specific reference to health and nutrition in Trinidad, West Indies 190
N. Badrie, V. Leith, C. Serrette and T. Marie Rousseau

An Example of Applied Underwater Archaeological Studies in the West Indies 193
B. Vicens and J.S. Guibert

Table of contents

HLA Alleles Distribution Among a French Caribbean Population 195
M.O. Joannes, F. Agis and R. Chout
Neuroprotection: Activation of Novel Endogenous Pathways? 197
F.F. Youssef
Women in Sciences in the Caribbean: Some Data and Reflections 197
L. Alvarez-Diaz
Social Sciences, an Indispensable View on West Indian Health 198
J. Dumont, J. Pruneau, S. Ruffié, S. Laupa and G. Villoing
Social Dialogue in Conflictual Settings : The Case of Guadeloupe 198
F. Alvarez and H. Ernatus
Risk Factors of Acute Chest Syndrome in Guadeloupean Sickle Cell Anemia Children 199
V. Tarer, V. Chaar, M. Etienne-Julan, J.P. Diara, L. Doumdo, J. Elion and M. Romana
Sickle Red Cells Dynamic Behavior Under Venular Blood Flow 200
C. Allayous, A. Bruel, D. Schoëvaërt, R. Emilion and T. Marianne-Pepin
Sport and Sickle Cell Disease in 12-19 Years Old Adolescents in Guadeloupe: Best Enemies 200
J. Pruneau, F. Maillard and B. Philippon
The Effect of Tropical Environment on Sports Performances 201
S. Blonc, E. Senatus, C. Robin, M. Le Her and O. Hue
Modern Biotechnology and Biosafety Policy Issues for Guyana 201
J. C. Caesar
Eléments de Prospective et l'Environnement 202
M. Castellanos, J.G. Montauban, A. Rodrigue and L. Alvarez
Climate Change and Caribbean Economic Development: an Opportunity for Convergence of the Sciences 203
M. Attzs
A New Recombinant Geminivirus Infecting *Sida* in Jamaica 203
C.S. Stewart and M.E. Roye
Setting up of a Pet - Ct Center in Martinique: Interest and Feasibility 204
H. Azaloux, J. Baudin-Veronique, J.M. Caignon, C. Draganescu, M. Dieye and J. Smith-Ravin
Revitalizing Science and Technology Policy for Sustainable Development in Guyana: Leveraging Lessons from the Developing World 205
J. C. Caesar
Low brain cytochrome c oxydase activityIn two rabbit models of Alzheimer's Disease 205
T. Alleyne, J. Joseph, N. Mohan and A. Adogwa
The effect of *Apium graveolens* and *Momordica charantia* on plasma lipids and blood pressure in laboratory rats 206
E. Cummings and M. Varswyk
The Effects of *Apium graveolens* and *Trigonella foenumgraecum* on Plasmolipids in Laboratory Rats 206
E. Cummings and G. Coopsammy

Computer Science & Maths

The Interdisciplinary Importance of Computer Science 11
C. Posthoff

Parallel Mining of Association Rules 13
W. Thomas

Boundary controllability with constraints on the state 15
G. Massengo and O. Nakoulima

Characteristic Cauchy Problem for Nonlinear Unidirectional Wave Equation 18
J.A. Marti

The sentinel method for mixed boundary condition dissipative problem with incomplete data 20
A. Omrane

Angles & Logarithms 23
A. Torrens

Estimation of the Large Multifractal Deviation Spectrum 28
M. Abadi, E. Grandchamp

A Variant of Newton's Method for Generalized Equations 29
C. Jean Alexis and A. Pietrus

An Accurate Projection Method for Incompressible Flows 30
C. Février, P. Angot, J. Laminie and P. Poullet

Introduction to and Implication of Emergent Global Internet Protocols and Policies for the Caribbean Region 30
J. Crain

Kernel Theorems in Spaces of Colombeau Generalized Functions 31
A. Delcroix

Computer Science & Maths

The Interdisciplinary Importance of Computer Science

PROF. CH. POSTHOFF

Department of Mathematics & Computer Science, UWI, Trinidad & Tobago, cposthoff@fans.uwi.tt

Introduction

Historically, Computer Science has been strongly associated with Mathematics. During the 60's and 70's of the last century, Computer Science was nurtured at Universities in Departments of Mathematics. By the late 70's and early 80's, however, Computer Science had matured sufficiently and many universities spun out Computer Science as a discipline distinct from Mathematics. Its position in the organization structure was not uniform and several models emerged: a Department of Computer Science within the Science Faculty or within the Faculty of Engineering or even within Social Sciences (Dept. of Information Systems). By the 90's, the model that emerged as the preferred placement was a School of Computer Sciences (names vary) with links to Science, Engineering, Social Studies, and even Medical Sciences (Bioinformatics and Medical Computing).

These developments are especially crucial because the level of one discipline is strongly dependent on another discipline, and only the efficient cooperation and combination of Computer Science and other disciplines results in a modern education and application of this knowledge.

The Interdisciplinary Importance

The guiding principle will be that ***the level of university education is only as good as the level of Computer Science application and knowledge***. The paper will give some examples to underline this principle and show the responsibility of academic staff to cope with this responsibility. It can be seen very clearly that the production of transparencies, course material etc. is only a first and tiny step. And it must also be understood that this is only a small set of examples, an exhaustive survey would require much more time and space.

1- Mathematics

At present very powerful systems for Mathematics are available, such as MAPLE, MATHEMATICA, MATLAB, MATHCAD, among others. It still can be discussed what really has to be done with these systems in teaching Mathematics, however, there is no doubt at all that courses must be available for other Science disciplines (such as Physics, Biology, Chemistry, …) that present and use these systems. Based on these systems, **Mathematics is more applicable than ever before**. However, no longer the computational part is the core of applications, it is most important to express a problem in Physics, … in a mathematical format - hence, ***mathematical modeling*** is crucial, and thereafter, it is very necessary to understand the solutions and to use them properly. Thus a Science Faculty has an urgent need of courses in **Modeling and Simulation** or **Scientific Computing**, compulsory for all science students. This approach can immediately be extended to all the Engineering disciplines that are also very related to Mathematics. Special systems are dealing with **Statistics** and **Financial Mathematics**, they must also be used, however, in a narrower environment.

2- Other Science Disciplines

In addition to the influence of Mathematics to the respective Science disciplines or by using Mathematics as a bridge, we see the development of special disciplines that represent exactly the combination of the Science discipline and/or Mathematics with Computer Science. The development of areas such as *Computational Physics, Computational Chemistry, Bioinformatics, DNA-Computing, Quantum Computing* can be seen, at present the teaching of these sub-disciplines or even an introduction do not exist.

3- Medicine

The role of Computer Science in *Medicine* is rapidly growing, many areas of *Medicine* get more and more computerized. Very often these developments are based on the union of Medicine, different developments in Electronics and computer-based methods. Internationally developments such as ***Telemedicine*** or ***Medical Informatics*** can be found. Very interesting and useful in the very near future is, for instance, the cooperation between ***Artificial Intelligence*** or ***Soft Computing*** methods and Medicine. Learning from examples (that exist in Medicine in large numbers) and the creation of very powerful ***Diagnostic Systems*** are only one example. All kinds of methods for ***image processing*** are another rapidly growing field. The arrival and use of digital cameras plays an important role even in the daily life. There is no doubt that students of Medicine must be educated in these areas.

4- Education

An urgent need to educate Computer Science teachers as well as to train all teachers in the use of computers for educational purposes. The development of Computer Science Didactics and the ***Didactics of computer-based instruction and teaching*** need much more attention. These areas are mainly not existing or restricted to the use of some commercial systems. ***Distance Education*** is another important factor that can considerably extend University education to distant places and islands and improve considerably the quality of education and of life in distant areas.

5- Social Sciences

The required overlap with Computer Science (*Information systems, E-Commerce, Database Systems Applications, Internet Technologies, Financial Systems, Security Issues)* is only rudimentarily discussed and defined. Internationally, however, we can see enormous developments in many of these areas. ***E-Government*** is another "hot topic" that requires efforts to be implemented and that can considerably improve the quality of the Public Service and many branches of the business life. The use of Computer Science in the legal system is a very broad part of these issues and can considerably improve the efficiency of this system.

6- Scientific Writing

This is another very typical situation in this changing world of education based on computerization. Any publisher requires nowadays manuscripts that are more or less ready for publication. Science-related publications rely heavily on Mathematics, however, typing of Mathematics requires special knowledge and understanding. All our graduate students should acquire this knowledge compulsorily, based on advanced type-setting systems to make them competitive in this area.

7- Conclusions

These are only some examples that show the enormous responsibility of each staff member to acquire the necessary knowledge and to work, more than ever before, in an interdisciplinary way for the improvement of the quality of the level of our university education.

Computer Science & Maths

Parallel Mining Of Association Rules

THOMAS WESSEL

University of Technology, 237 Old Hope Road, Kingston 6, Jamaica - thomaswe@scis.nova.edu

Abstract

In this paper we present a parallel algorithm for the mining of association rules. We implemented a parallel algorithm that used a lattice approach for mining association rules. The Dynamic Distributed Rule Mining (DDRM) is a lattice-based algorithm that partitions the lattice into sub-lattices to be assigned to processors for processing and identification of frequent item sets. We implemented the DDRM using a dynamic load balancing approach to assign classes to processors for analysis of these classes in order to determine if there are any rules present in them. Experimental results show that DDRM utilizes the processors efficiently and performed better than the prefix-based algorithm that uses a static approach to assign classes to the processors. The DDRM algorithm scales well and shows good speedup.

Introduction

Many organizations are now finding it feasible economically to create ultra large databases of business and scientific data. This is made possible by the availability of inexpensive storage devices and developments in data capture technology (Agrawal & Shafer, 1996). Bar-code technology has made it possible to collect and store large amounts of sales data in retail organizations. The records associated with retail data are typically made up of transaction data and items bought in the transaction. These databases are viewed by organizations as important pieces of marketing infrastructure. Organizations are now using this data for the mining of association rules.

Problem Statement

The goal of data mining is the discovery of unknown patterns in large databases using efficient techniques to find these rules.

An association rule is of the form, "87% of customers that purchase a computer also purchase a printer." Agrawal, Imielinski and Swami (1993) first introduced the problem of mining association rules. According to Zaki (2000) the search space for the discovery of all frequent associations in very large databases is exponential in the number of database attributes. In addition this is further complicated by I/O requirements for the millions of database objects.

In this paper we present the Dynamic Distributed Rule Mining (DDRM) algorithm that uses a lattice to represent the search space for the generation of the frequent item sets. DDRM partitions the search space and assigns each partition dynamically to the next available processor. An evaluation of the algorithm was carried out and its performance relative to the prefix-based with bottom-up search, which is a parallel algorithm for mining of association rules, was also determined (Zaki, 2000).

The DDRM algorithm does not require any special architecture for its implementation. It is designed to operate on an existing LAN where the PCs can be added to the cluster and used to participate in the computations of the classes. The database of transactions can also be distributed over the network. This flexibility of the algorithm will result in significant savings to the organization as it uses the resources that are already available within the organization. This reduction in cost is due to the fact that there is no need for specialized architecture and makes the algorithm attractive to an organization that currently operates a network with databases distributed over it.

The Message Passing Interface (MPI) model consists of P processors each with local memory, connected over a communication network. MPI facilitates communications among a set of processors that have only local memory through the mode of sending and receiving of messages.

Experimental Results

The DDRM algorithm was developed and implemented using C/C++ as the programming language on an Ethernet LAN consisting of 7 workstations and one server. Each workstation on the network is an AMD Athlon XP 2800+ with 512 Mbytes of memory. The processors are interconnected via a 10/100 Mbps switch. The switch used 100BASE-T (Fast Ethernet) technology, which provided greater bandwidth and improved the client/server response time. For communications we used the message passing interface (MPI). We used the windows message passing interface (WMPI) for 8 workstations from Critical Software Ltd to implement our algorithm

We used the 1987 census data from the Statistical Institute of Jamaica to generate the data used in this experiment. The size of the database was 25 Mbytes with 1.1 million records. The support count used was 8% with a confidence of 50%. The experiment was conducted by partitioning the database among the processors.

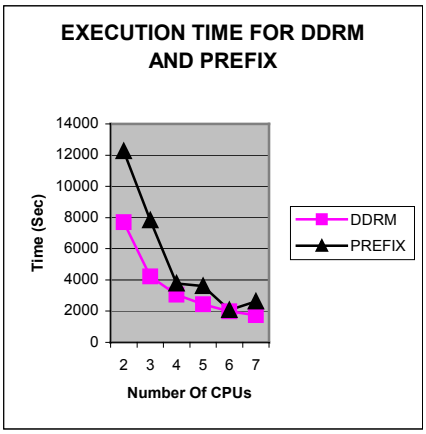

Figure 1 Execution Time for DDRM and Prefix

In Figure 1 we show a plot of the response time on the vertical axis and the number of processors on the horizontal axis. The database was partitioned based on the number of processors. The search space was partitioned into 32 classes, which were assigned dynamically to the processors participating in the cluster. It can be seen that as we increase the number of processors the response time decreases as well. We compare the response time for DDRM with that of the Prefix-based algorithm. The response time for DDRM is better than that for the Prefix-based.

We also obtained a maximum speedup of approximately 4.5. The DDRM algorithm also scales well.

Conclusion

This paper has presented the Dynamic Distributed Rule Mining (DDRM), which is a lattice-based algorithm that partitions the lattice into sublattices to be assigned to processors for processing and identification of frequent itemsets. We implemented the DDRM using a dynamic load balancing approach to assign classes to processors for analysis of these classes in order to determine if there are any rules present in them. Experimental results show that DDRM utilizes the processors efficiently and performed better than the prefix-based algorithm that uses a static approach to assign classes to the processors. The DDRM algorithm scales well and shows good speedup.

References

Agrawal, R., Imielinski, T., & Swami, A. (1993). Mining association rules between sets of items in large databases. *Proceedings of ACM SIGMOD International Conference on Management of Data*, 207-216.

Agrawal, R., & Shafer, J. C. (1996). Parallel mining of association rules. *IEEE Transaction on Knowledge and Data Engineering,* 8 (6), 962-969.

Zaki, M. J. (2000). Scalable algorithms for association mining. *IEEE Transactions on Knowledge and Data Engineering*, 12(3), 372-390.

Computer Science & Maths

Boundary controllability with constraints on the state

GISÈLE MASSENGO MOPHOU AND OUSSEYNOU NAKOULIMA
Laboratoire de Mathématiques et Informatique
Université des Antilles et de La Guyane, Campus Fouillole
97159 Pointe-à-Pitre GUADELOUPE *(FWI)*
Gisele.Mophou@univ-ag.fr, Ousseynou.Nakoulima@univ-ag.fr

Abstract

We consider a boundary controllability problem with a finite number of constraints on the state. Interpreting each constraint, we transform the problem into an equivalent controllability problem with constraint on the control. Then using an inequality of observability which derives from the boundary inequality of Carleman, we prove that the equivalent controllability problem has a solution.

Key-words : Heat equation, controllability, inequality of Carleman.

1 Introduction

Let N, $M \in \mathbf{N}^*$ and Ω be a bounded open subset of $\mathbb{R}^N$ with boundary Γ of class $\mathcal{C}^2$. Let $\omega \subset \Gamma$ be an open non empty subset. For a time $T > 0$, we set $Q = \Omega \times (0,T)$ and $\Sigma = \Gamma \times (0,T)$ and we consider the semilinear heat equation:

$$\left\{ \begin{array}{rcll} \dfrac{\partial y}{\partial t} - \Delta y + a_0 y & = & 0 & \text{in } Q, \\ y & = & v\chi_\omega & \text{on } \Sigma, \\ y(0) & = & y^0 & \text{in } \Omega \end{array} \right. \tag{1}$$

where $a_0 \in L^\infty(Q)$, $y^0 \in L^2(\Omega)$, the control v belongs to $L^2(\Gamma \times (0,T))$ and χ_ω represents the characteristic function of the control set ω.
Since $v\chi_\omega \in L^2(\Gamma \times (0,T))$, $a_0 \in L^\infty(Q)$ and $y^0 \in L^2(\Omega)$, one can prove using transposition method (see [5]) that the problem (1) has a unique solution $y \in L^2(Q)$.
In this paper, we are interested in the following boundary controllability problem with a finite number of constraints: *Given* $e_i \in L^2(Q)$, $1 \leq i \leq M$ *and* $y^0 \in L^2(\Omega)$, *find a control* $v \in L^2(\Gamma \times (0,T))$ *such that the solution of (1) satisfies*

$$\int_0^T \int_\Omega e_i \, dx \, dt = 0, \quad 1 \leq i \leq M. \tag{2}$$

There is a large literature on controllability of the heat equations. Let us mention briefly some of the existing works.
In the context of linear heat equation, G. Lebeau and L. Robbiano in [4], solved the null controllability using Fourier series and sharp estimates on the eigenfunctions of the Laplacian obtained by means of Carleman inequalities. In the nonlinear case, A. Fursikov A. and O. Yu. Imanuvilov in [2], showed using a Carleman's estimate that, when the control acts on the boundary, null controllability holds for bounded continuous and sufficiently small initial data.
There is a large literature on approximate controllability problem as well. For instance in [1], C. Fabre, J.-P. Puel and E. Zuazua proved, using the minimization of a particular functional, that the following approximate controllability holds: *Given* y^0, $y^1 \in L^2(\Omega)$ *and* $\alpha > 0$, *find a control* $v \in L^2(Q)$ *such that the solution of (1) satisfies* $\|y(T) - y^1\|_{L^2(\Omega)} \leq \alpha$. The method is supported by a unique continuation theorem.
Recently, O. Nakoulima proved [6], using an adapted Carleman inequality, that the following null controllability with constraint on the control holds: *Given an open non empty subset* γ *of* Ω, *a finite dimensional subspace* Y *of* $L^2(\gamma \times (0,T))$ *and* $y^0 \in L^2(\Omega)$, *find a control* $v \in Y^\perp$, *the orthogonal of* Y *in* $L^2(\gamma \times (0,T))$, *such that the solution of (1) satisfies* $y(T) = 0$ *in* Ω.

In this paper, we prove by means of Carleman inequality that the controllability problem with constraints on the state (1) and (2) holds.
Without loss of generality, we can assume that

$$\left\{ \begin{array}{l} \{e_1\chi_\omega, \cdots, e_M\chi_\omega\} \text{ is a family of} \\ \quad M \text{ independent functions.} \end{array} \right. \tag{3}$$

The main result of the paper is the following theorem.

Theorem 1.1 *Assume that the hypotheses above on* Ω *and* ω *are satisfied. Then for every* $e_i \in L^2(Q)$, $1 \leq i \leq M$, *every* $T > 0$, *there exists* $v \in L^2(\Gamma \times (0,T))$ *such that the solution of (1) sastifies (2). Moreover, there exists*

$C = C(\Omega, \omega, \|a_0\|_{L^\infty(Q)}, \sqrt{M}) > 0$ *such that*

$$\|v\|_{L^2(\Sigma)} \leq C\|y^0\|_{L^2(\Omega)}. \tag{4}$$

The rest of the paper is devoted to the proof of Theorem 1.1.

2 Proof of Theorem 1.1

To prove Theorem 1.1, we proceed in three steps.
Step 1. We prove that controllability with constraints on the state (1) and (2) is equivalent to controllability with constraint on the control.
To this end, we interpret the relations (2), using the notion of adjoint. More precisely, for each e_i, $1 \leq i \leq M$, we consider the ajoint system:

$$\left\{ \begin{array}{rcll} -\dfrac{\partial p_i}{\partial t} - \Delta p_i + a_0 p_i &=& e_i \quad \text{in} \quad Q, \\ p_i &=& 0 \quad \text{on} \quad \Sigma, \\ p_i(T) &=& 0 \quad \text{in} \quad \Omega. \end{array} \right. \tag{5}$$

Since $a_0 \in L^\infty(Q)$ and $e_i \in L^2(Q)$, the problem (5) admits a unique solution p_i in
$H^{2,1}(Q) = L^2(0,T; H^2(\Omega)) \cap H^1(0,T; L^2(\Omega))$.

Lemma 2.1 *Assume (3). Then the functions* $\dfrac{\partial p_i}{\partial \nu}\chi_\omega$, $1 \leq i \leq M$ *are linearly independent.*

Proof. We use the unique continuation theorem due to Mizohata [7] and the fact that the functions $e_i\chi_\omega$, $1 \leq i \leq M$ are linearly independent. ■

From now on, we assume that the functions

$$\{\frac{\partial p_i}{\partial \nu}\chi_\omega,\ 1 \leq i \leq M\} \text{ are orthonormal.} \tag{6}$$

Remark 1 *If the functions* $\dfrac{\partial p_i}{\partial \nu}\chi_\omega$, $1 \leq i \leq M$ *are not orthonormal, it suffices to apply the algorithm of Gram-Schmidt on the* $\dfrac{\partial p_i}{\partial \nu}\chi_\omega$ *to obtain a family of orthonormal functions since the functions* $\dfrac{\partial p_i}{\partial \nu}\chi_\omega$, $1 \leq i \leq M$ *are linearly independent.*

Thus, multiplying both sides of the differential equation in (1) by p_i and integrating by parts in Q, we have using (5),

$$\int_0^T \int_\omega v \frac{\partial p_i}{\partial \nu} d\Gamma\, dt = -\int_0^T \int_\Omega y e_i\, dx\, dt + \int_\Omega y^0 p_i(0)\, dx, \quad 1 \leq i \leq M.$$

Therefore, taking into account the conditions (2), we obtain

$$\int_0^T \int_\omega v \frac{\partial p_i}{\partial \nu} d\Gamma\, dt = \int_\Omega y^0\, p_i(0)\, dx,\ 1 \leq i \leq M. \tag{7}$$

Let

$$\mathcal{U} = \text{Span}\left(\frac{\partial p_1}{\partial \nu}\chi_\omega, \cdots, \frac{\partial p_M}{\partial \nu}\chi_\omega\right), \tag{8}$$

be the real vector subspace of $L^2(\Gamma \times (0,T))$ generated by the M independent functions $\dfrac{\partial p_i}{\partial \nu}\chi_\omega$. Then, there exists a unique $u_0 \in \mathcal{U}$ such that

$$\int_\Omega y^0 p_i(0) dx = \int_0^T \int_\omega u_0 \frac{\partial p_i}{\partial \nu}\, dx dt,\ 1 \leq i \leq M. \tag{9}$$

Consequently, (7) holds if and only if:

$$v - u_0\chi_\omega = u\chi_\omega \in \mathcal{U}^\perp \tag{10}$$

where $\mathcal{U}^\perp$ is the orthogonal of $\mathcal{U}$ in $L^2(\omega \times (0,T))$. Thus,

$$v = (u_0 + u)\chi_\omega \tag{11}$$

and (1) becomes

$$\left\{ \begin{array}{rcll} \dfrac{\partial y}{\partial t} - \Delta y + a(z)y &=& 0 \quad & \text{in} \quad Q, \\ y &=& (u_0 + u)\chi_\omega \quad & \text{on} \quad \Sigma, \\ y(0) &=& y^0 \quad & \text{in} \quad \Omega. \end{array} \right. \tag{12}$$

Conversely, assume that $a_0 \in L^\infty(Q)$, $y^0 \in L^2(\Omega)$ and $e_i \in L^2(Q)$, $1 \leq i \leq M$ are given. Then solving (5), we get the functions p_i, $1 \leq i \leq M$. Next, we define $\mathcal{U}$ as in (8) and we denote by $\mathcal{U}^\perp$ its orthogonal in $L^2(\omega \times (0,T))$. Multiplying both sides of the differential equation in (12) by p_i and integrating by parts in Q, we have

$$\int_0^T \int_\omega (u_0 + u) \frac{\partial p_i}{\partial \nu}\, d\Gamma\, dt = -\int_0^T \int_\Omega y\, e_i\, dx\, dt + \int_\Omega y^0\, p_i(0)\, dx, \quad 1 \leq i \leq M.$$

Then, since $(u_0(z), u(z)) \in \mathcal{U} \times \mathcal{U}^\perp$ is such that (9) and (10) hold, this latter identity is reduced to (2). In short, we have proved in the first step that the controllability problem with constraints on the state: *Given* $a_0 \in L^\infty(Q)$, $y^0 \in L^2(\Omega)$ *and* $e_i \in L^2(Q)$, $1 \leq i \leq M$, *find* v *in* $L^2(\Gamma \times (0,T))$ *such that the solution* y *of (1) sastifies (2)* is equivalent to the controllability problem with constraint on the control: *Given* $a_0 \in L^\infty(Q)$, $u_0 \in \mathcal{U} \subset L^2(\omega \times (0,T))$ *and* $y^0 \in L^2(\Omega)$, *find* $u \in L^2(\omega \times (0,T))$ *so that*

$$u \in \mathcal{U}^\perp \tag{13}$$

and such that $y = y(u)$ *is solution of (12).*

Step 2. According to (10), the controllability problem with constraint on the control (13) and (12) has an infinitely many solutions. Since among the controls $u \in \mathcal{U}^{\perp}$ such that $y = y(u)$ is solution of (12), $u = 0$ is the control which has the minimal norm in $L^2(\omega \times (0,T))$, we choose

$$u = 0. \tag{14}$$

Therefore from (11), we have

$$v = u_0 \chi_\omega. \tag{15}$$

Thus, we can find $v \in L^2(\Gamma \times (0,T))$ verifying (15) such that $y = y(v)$ which is solution of (1) satisfies (2).

Step 3. We show that the control v given by (15) verifies (4).

First of all, let us recall the following inequality of observability which derives from the boundary Carleman inequality (see [3]):

Proposition 2.1 *There exists* $C = C(\Omega, \gamma, \|a_0\|_{L^\infty(Q)}) > 0$ *such that, for any* ρ *verifying* $\rho \in L^2(Q)$, $-\dfrac{\partial \rho}{\partial t} - \Delta \rho + a_0 \rho \in L^2(Q)$ *and* $\rho = 0$ *on* Σ,

$$\int_\Omega |\rho(0)|^2 \, dx \leq C \left[\int_0^T \int_\gamma \left| \frac{\partial \rho}{\partial \nu} \right|^2 d\Gamma \, dt + \int_0^T \int_\Omega \left| -\frac{\partial \rho}{\partial t} - \Delta \rho + a_0 \rho \right|^2 dx \, dt \right]. \tag{16}$$

Now, since u_0 verifies (9), applying the inequality of Cauchy-Schwartz to right hand side of this identity, we obtain

$$\left| \int_0^T \int_\omega u_0 \frac{\partial p_i}{\partial \nu} d\Gamma \, dt \right| \leq \|y^0\|_{L^2(\Omega)} \|p_i(0)\|_{L^2(\Omega)}.$$

Therefore, a_0 being in $L^\infty(Q)$ and $p_i = 0$ on Σ, using (5) and the inequality of observability (16), we have

$$\left| \int_0^T \int_\omega u_0 \frac{\partial p_i}{\partial \nu} d\Gamma \, dt \right| \leq C \|y^0\|_{L^2(\Omega)} \left(\left\| \frac{\partial p_i}{\partial \nu} \right\|^2_{L^2(\omega \times (0,T))} + \|e_i\|^2_{L^2(Q)} \right)^{1/2}$$

where $C = C(\Omega, \omega, \|a_0\|_{L^\infty(Q)})$. Hence, we deduce, since $\left\| \dfrac{\partial p_i}{\partial \nu} \right\|_{L^2(\Sigma)} = 1$,

$$\left| \int_0^T \int_\omega u_0 \frac{\partial p_i}{\partial \nu} d\Gamma \, dt \right| \leq C \sqrt{1 + \|e_i\|^2_{L^2(Q)}} \|y^0\|_{L^2(\Omega)}.$$

Consequently,

$$\begin{aligned} \|u_0\|^2_{L^2(\omega \times (0,T))} &= \sum_{i=1}^M \left| \int_0^T \int_\omega u_0 \frac{\partial p_i}{\partial \nu} d\Gamma \, dt \right|^2 \\ &\leq C^2 \left(M + \sum_{i=1}^M \|e_i\|^2_{L^2(Q)} \right) \|y^0\|^2_{L^2(\Omega)}. \end{aligned}$$

Therefore, v verifying (15), we deduce from this latter inequality the estimate (4). ■

References

[1] Fabre C., Puel J.-P., Zuazua E., Approximate controllability of the semilinear heat equation, Proc. Royal Soc. Edinburgh, 125A, (1995); pp. 31-61.

[2] Fursikov A. and Imanuvilov O. Yu., Controllability of evolution equations. Lecture Notes, Research Institute of Mathematics, Seoul National University, Korea, (1996).

[3] Imanuvilov O. Yu., Controllability of parabolic equations. Sbornik Mathematics 186 : 6 (1995); pp. 879-900.

[4] Lebeau G. and Robbiano L., Contrôle exacte de l'équation de la chaleur, Comm. P.D.E., 20, (1995); pp. 335-356.

[5] Lions J.-L. Optimal control of systems governed by partial differential equations. Springer, NY, (1971).

[6] Nakoulima O., Optimal control for distributed systems subject to null-controllability. Application to discriminating sentinels. ESAIM: Control, Optimisation and Calculus of Variations, Vol.13, 4(2007); pp. 623-638.

[7] Mizohata S., Unicité du prolongement des solutions pour quelques équations différentielles paraboliques, Memoirs of sciences University of Kyoto, 31(1958); pp. 219-239.

Computer Science & Maths

Characteristic Cauchy problem for nonlinear unidirectional wave equation

J.-A. MARTI

Laboratoire GTSI – Université des Antilles et de la Guyane, Guadeloupe - jamarti@univ-ag.fr

During the last three decades, theories of nonlinear generalized functions have been developed by many authors. These theories have proved their efficiency to pose and solve differential problems with irregular data and operators or characteristic problems.

In this paper we consider this last question, not from a general point of view, but with a thorough study of some typical example which has no solution in the classical theory.

The non linear characteristic initial value (or Cauchy) problem we choose to study can be written

$$\left\{ \begin{array}{c} \dfrac{\partial u}{\partial t} + (\varphi' \otimes 1_x) \dfrac{\partial u}{\partial x} = F(.,.u) \\ u\,|_S = f \end{array} \right. \qquad \text{(CIVP)}$$

where $S = \Gamma_\varphi$ is the characteristic curve given by $x = \varphi(t)$, φ a smooth function, with $\varphi(0) = 0$ and $\varphi' > 0$ on $\mathbb{R}$ and f a function in $\mathrm{C}^\infty(\mathbb{R})$. We suppose, in addition, that F is a continuous function of all its arguments verifying a Lipschitz condition given by the following hypothesis

$$\forall K \Subset \mathbb{R}^2, \ \sup_{(t,x)\in K} |\partial_z F(t,x,z)| = m_K < +\infty$$

where the symbol $K \Subset \mathbb{R}^2$ means that K is a compact subset of $\mathbb{R}^2$. We know that the problem is ill posed, and cannot be solved by any classical procedure.

We approach (CIVP) by the one parameter family

$$\left\{ \begin{array}{c} \dfrac{\partial u_\varepsilon}{\partial t} + (\varphi' \otimes 1_x) \dfrac{\partial u_\varepsilon}{\partial x} = F(.,.u_\varepsilon) \\ u_\varepsilon(t, \varphi(t) + \varepsilon t) = f(t) \end{array} \right. \qquad (\mathrm{CIVP}_\varepsilon)$$

and we consider the family $(u_\varepsilon)_\varepsilon$ of the solutions to $(\mathrm{CIVP}_\varepsilon)$. They have to verify the integral

$$u_\varepsilon(t,x) = f[x - \varphi(t)] + \int_0^t F\left[\tau, x, u_\varepsilon(\tau, x)\right] d\tau. \qquad (1)$$

Picard's procedure to solve (1) is to set up a sequence of successive approximation $u_{\varepsilon,n}$ defined by the formula

$$u_{\varepsilon,n+1}(t,x) = f[x - \varphi(t)] + \int_0^t F\left[\tau, x, u_{\varepsilon,n}(\tau, x)\right] d\tau.$$

We prove the uniform convergence on any compact set of the sequence $u_{\varepsilon,n}$ to the solution u_ε of $(\mathrm{CIVP}_\varepsilon)$. Then, we can construct the generalized function belonging to the Colombeau algebra $\mathcal{G}\left(\mathbb{R}^2\right)$ (see the Appendix)

$$\mathbf{u} = (u_\varepsilon)_\varepsilon + \mathcal{N}\left(\mathbb{R}^2\right) \qquad (2)$$

and consider it as the generalized solution of (CIVP).

Some association processes of generalized functions with distributions are defined in $\mathcal{G}\left(\mathbb{R}^2\right)$. For example, for $u = [u_\varepsilon] \in \mathcal{G}\left(\mathbb{R}^2\right)$ (class of $(u_\varepsilon)_\varepsilon$), $T \in \mathcal{D}'\left(\mathbb{R}^2\right)$, Φ a mapping from $\mathbb{R}_+$ to $\mathbb{R}_+$ such that the class of $(\Phi_\varepsilon)_\varepsilon$ is a generalized number we define

$$u \sim T \Leftrightarrow \lim_{\substack{\varepsilon \to 0 \\ \mathcal{D}'(\mathbb{R}^2)}} u_\varepsilon = T$$

$$u \underset{\Phi}{\sim} T \Leftrightarrow \lim_{\substack{\varepsilon \to 0 \\ \mathcal{D}'(\mathbb{R}^2)}} \Phi(\varepsilon) u_\varepsilon = T.$$

Let us suppose $F = 0$ and $f \in \mathrm{C}^\infty(\mathbb{R}) \cap \mathrm{L}^1(\mathbb{R})$ with $\int f(x)dx = 1$. We know that if $f_\varepsilon(x) = \frac{1}{\varepsilon} f(\frac{x}{\varepsilon})$, then $\lim\limits_{\substack{\varepsilon \to 0 \\ \mathcal{D}'(\mathbb{R})}} f_\varepsilon = \delta$. Putting

$$\frac{1}{\varepsilon} u_\varepsilon(t,x) = \frac{1}{\varepsilon} f(\frac{x - \varphi(t)}{\varepsilon})$$

one can show that

$$u \underset{\varepsilon}{\sim} \delta_{\Gamma_\varphi}.$$

In other words, u have a bidimensional soliton structure, and $\operatorname{supp} u = \operatorname{supp} \delta_{\Gamma_\varphi} = \Gamma_\varphi$: the solution of the characteristic Cauchy problem for the unidirectional wave equation is associated to a bidimensional soliton whose support is the characteristic curve. In the general case ($F \neq 0$) the solution is associated to the sum of such a soliton and another generalized function corresponding to the nonlinearity.

Appendix : the sheaf of Colombeau simplified algebras

Let C^∞ be the sheaf of complex valued smooth functions on $\mathbb{R}^d$ ($d \in \mathbb{N}$), with the usual topology of uniform convergence. For every open set Ω of $\mathbb{R}^d$, this topology can be described by the family of semi norms

$$p_{K,l}(f) = \sup_{|\alpha| \leq l, K \Subset \Omega} \left| \partial^\alpha f(x) \right|,$$

where the notation $K \Subset \Omega$ means that the set K is a compact set included in Ω.

Let us set

$$\mathcal{E}_M(\Omega) = \left\{ (f_\varepsilon)_\varepsilon \in \mathrm{C}^\infty(\Omega)^{(0,1]} \,\middle|\, \forall l \in \mathbb{N},\ \forall K \Subset \Omega,\ \exists q \in \mathbb{N},\ p_{K,l}(f_\varepsilon) = \mathrm{o}\left(\varepsilon^{-q}\right) \text{ for } \varepsilon \to 0 \right\},$$

$$\mathcal{N}(\Omega) = \left\{ (f_\varepsilon)_\varepsilon \in \mathrm{C}^\infty(\Omega)^{(0,1]} \,\middle|\, \forall l \in \mathbb{N},\ \forall K \Subset \Omega,\ \forall p \in \mathbb{N},\ p_{K,l}(f_\varepsilon) = \mathrm{o}\left(\varepsilon^{p}\right) \text{ for } \varepsilon \to 0 \right\}.$$

We have the following

Lemma

i. The functor $\mathcal{F} : \Omega \to \mathcal{E}_M(\Omega)$ defines a sheaf of subalgebras of the sheaf $(\mathrm{C}^\infty)^{(0,1]}$.

ii. The functor $\mathcal{N} : \Omega \to \mathcal{N}(\Omega)$ defines a sheaf of ideals of the sheaf $\mathcal{F}$.

We shall not prove in detail this lemma but quote the two mains arguments:

(a) For each open subset Ω of X, the family of seminorms $(p_{K,l})$ related to Ω is compatible with the algebraic structure of $\mathrm{C}^\infty(\Omega)$; In particular:

$$\forall l \in \mathbb{N},\ \forall K \Subset \Omega,\ \ \exists C \in \mathbb{R}_+^*,\ \ \forall (f,g) \in \left(\mathrm{C}^\infty(\Omega)\right)^2 \ \ p_{K,l}(fg) \leq C p_{K,l}(f)\, p_{K,l}(g),$$

(b) For two open subsets $\Omega_1 \subset \Omega_2$ of $\mathbb{R}^d$, the family of seminorms $(p_{K,l})$ related to Ω_1 is included in the family of seminorms related to Ω_2 and

$$\forall l \in \mathbb{N},\ \forall K \Subset \Omega_1,\ \ \forall f \in \mathrm{C}^\infty(\Omega_2),\ \ p_{K,l}\left(f_{|\Omega_1}\right) = p_{K,l}(f).$$

This leads to the following

Definition

The sheaf of factor algebras

$$\mathcal{G}(\cdot) = \mathcal{E}_M(\cdot) / \mathcal{N}(\cdot)$$

is called the sheaf of *Colombeau simplified algebras.*

The sheaf $\mathcal{G}$ turns to be a sheaf of differential algebras and a sheaf of modules on the factor ring $\overline{\mathbb{C}} = \mathcal{F}(\mathbb{K}) / \mathcal{N}(\mathbb{K})$ with

$$\mathcal{F}(\mathbb{K}) = \left\{ (r_\varepsilon)_\varepsilon \in \mathbb{K}^{(0,1]} \,\middle|\, \exists q \in \mathbb{N},\ |r_\varepsilon| = \mathrm{o}\left(\varepsilon^{-q}\right) \text{ for } \varepsilon \to 0 \right\},$$

$$\mathcal{N}(\mathbb{K}) = \left\{ (r_\varepsilon)_\varepsilon \in \mathbb{K}^{(0,1]} \,\middle|\, \forall p \in \mathbb{N},\ |r_\varepsilon| = \mathrm{o}\left(\varepsilon^{p}\right) \text{ for } \varepsilon \to 0 \right\},$$

with $\mathbb{K} = \mathbb{C}$ or $\mathbb{R}$.

Computer Science & Maths

The sentinel method for mixed boundary condition dissipative problem with incomplete data

A. OMRANE

Laboratoire d'Analyse, Optimisation et Contrôle, AOC, Université des Antilles et de la Guyane, Campus Fouillole, 97159 Pointe-à-Pitre, Guadeloupe, France – aomrane@univ-ag.fr

(A part of this work can be found in [4])

***Abstract*— Many environmental problems contain incomplete data. We propose a sentinel method for the detection of pollution present in the state equation of a dissipative system of incomplete initial condition. In the present case, the control and the observation have their supports in different open sets.**
The problem of determining a sentinel is equivalent to a controllability problem, for which we use Carleman inequalities. We then prove the existence of a non nul sentinel.

Key words. Dissipative systems, sentinels, incomplete data, mixed boundary conditions.

I. INTRODUCTION

Let be $T > 0$, and Ω an open subset of $\mathbf{R^d}$ of regular boundary $\partial\Omega$, and denote by $Q = \Omega\times]0,T[$ the space-time cylinder. We are intersted in systems not completely known, where some of the conditions are not entirely available; we consider here the parabolic equation :

$$\left\{\begin{array}{rcll} y' - \Delta y + f(y) &=& \xi + \lambda\hat{\xi} & \text{in } Q, \\ y(0) &=& y^0 + \tau\hat{y}^0 & \text{in } \Omega, \\ y &=& 0 & \text{on } \Sigma_1, \\ \dfrac{\partial y}{\partial \nu} &=& 0 & \text{on } \Sigma_2, \end{array}\right. \tag{1}$$

where $y = y(x,t;\lambda,\tau)$, and where Σ_1 is a part of the boundary $\Sigma = \partial\Omega\times]0,T[$ and $\Sigma_2 = \Sigma\backslash\Sigma_1$. In the present situation we assume that $f : \mathbf{R} \to \mathbf{R}$ is a given application of class C^1, the functions ξ and y^0 are known with $\xi \in L^2(Q)$ and $y^0 \in L^2(\Omega)$. However, the terms : $\lambda\hat{\xi}$ (called pollution term) and $\tau\hat{y}^0$ (called perturbation term) are unknown. We only assume that

$$\|\hat{\xi}\|_{L^2(Q)} \leq 1, \quad \|\hat{y}^0\|_{L^2(\Omega)} \leq 1$$

where the reals λ, τ are small inough.

Let be now a non empty open subset $O \subset \Omega$, called observatory, and an observation of y on O, during the time T. We denote by y_{obs} this observation

$$y_{obs} = m_o \in L^2(O\times(0,T)). \tag{2}$$

We suppose that (1) admits a unique solution denoted

$$y(\lambda,\tau) := y(x,t;\lambda,\tau)$$

in a suitable space. The question is

> how to calculate the pollution $\lambda\hat{\xi}$ present in the state equation, independent of the variation $\tau\hat{y}^0$ around the initial data ? (3)

a) Least squares: Question (3) is natural since the main interest is the detection of the pollution term. One can use the least squares method. Here, we consider the unknowns $\{\lambda\hat{\xi},\tau\hat{y}^0\} = \{v,w\}$ as control variables, then the state $y(x,t;v,w)$ has to be as close as possible to m_o.
Technically, this is an optimal control problem. With this method we search for v and w together, so there is no real possibility to separate the two variables.

b) Sentinels: The sentinels method of Lions [3] is a least squares method particularly adapted to the detection of pollution in ecosystems of incomplete data; many models can be found in litterature. It relies on the following three considerations : a state equation (for instance (1)), an observation function (2), and a control function w to determine.
This method is not the only one; we can distinguish the data assimilation method (a least squares method using inertial manifolds) and some other more or

less known methods.

Below, we consider the sentinel method of Lions which is an other attempt and brings better answer to question (3), as we will explain now :
Let h_0 be a given function in $L^2(O \times (0,T))$. Let besides ω be an open and non empty subset of Ω. For a control function $\mathsf{w} \in L^2(\omega \times (0,T))$, we introduce the functional

$$S(\lambda,\tau) = \int_0^T \int_O h_0\, y(\lambda,\tau)\, dxdt + \int_0^T \int_\omega \mathsf{w}\, y(\lambda,\tau)\, dxdt. \quad (4)$$

We shall say that S defines a sentinel for the problem (1) if there exists w such that S is insensitive (at first order) with respect the to missing terms $\tau\hat{y}^0$ which means

$$\frac{\partial S}{\partial \tau}(0,0) = 0 \quad (5)$$

for any $\hat{y}^0$ where here $(0,0)$ corresponds to $\lambda = \tau = 0$, and if w has the property of minimal norm in the sense

$$\|\mathsf{w}\|_{L^2(\omega\times(0,T))} = \text{minimum}. \quad (6)$$

Remark *1:* The Lions sentinels S correspond to the case where $\omega = O$. In this case, the observation and the control have the same support, and so $\mathsf{w} = -h_0$ is an evident solution of (5), and we only have to solve (6). We then have to be sure that the minimal solution of (6) is different from $-h_0$.
Many papers use the definition of Lions in the theoretical aspect as well as in the numerical one (see Kernevez [2]). Here we consider the case $\omega \neq O$. We then avoid the case $\mathsf{w} = -h_0$.

c) Informations given by the sentinel: Because of (5) we can write

$$S(\lambda,\tau) \simeq S(0,0) + \lambda \frac{\partial S}{\partial \tau}(0,0), \quad \text{for} \quad \lambda, \tau \quad \text{small}.$$

In (4), $S(\lambda,\tau)$ is observed and using (2), it equals

$$\int_Q (h_0\chi_O + \mathsf{w}\chi_\omega) m_o\, dxdt$$

so that (5) becomes

$$\lambda \frac{\partial S}{\partial \lambda}(0,0) \simeq \int_Q (h_0\chi_O + \mathsf{w}\chi_\omega)(m_o - y_0)\, dxdt, \quad (7)$$

with

$$\frac{\partial S}{\partial \lambda}(0,0) = \int_Q (h_0\chi_O + \mathsf{w}\chi_\omega) y_\lambda\, dxdt = 0.$$

The derivative y_λ only depends on $\hat{\xi}$ and other known data. Consequently, the estimates (7) contains the informations on $\lambda\hat{\xi}$.

II. Equivalence to a controllability problem

We shall show in this section that the existence of a sentinel is equivalent to a null controllability problem. We begin by transforming the insensibility condition (5).
Let us introduce

$$y_\tau = \frac{d}{d\tau} y(\lambda,\tau)\Big|_{\lambda=\tau=0}.$$

Then the function y_τ is given by

$$\begin{cases} y'_\tau - \Delta y_\tau + f'(y_0) y_\tau = 0 & \text{in } Q, \\ y_\tau(0) = \hat{y}^0 & \text{in } \Omega, \\ y_\tau = 0 & \text{on } \Sigma_1, \\ \dfrac{\partial y_\tau}{\partial \nu} = 0 & \text{on } \Sigma_2, \end{cases} \quad (8)$$

where $y_0 = y(0,0)$. Problem (8) admits a unique solution y_τ under general assumptions on f; for example $f(y) = y^3$.

The insensibility condition (5) is equivalent to

$$\int_Q \left(h_0\chi_O + \mathsf{w}\chi_\omega\right) y_\tau\, dxdt = 0 \quad (9)$$

where χ_O and χ_ω denote the characteristic functions of O and ω respectively.
Denote by

$$L = \frac{\partial}{\partial t} - \Delta + f'(y_0)\, I_d \quad (10)$$

and by

$$L^* = -\frac{\partial}{\partial t} - \Delta + f'(y_0)\, I_d \quad (11)$$

its adjoint. We can transform (9) by introducing the classical adjoint state. More precisely, we define the function $q = q(x,t)$ as the solution of the backward problem :

$$\begin{cases} L^* q = h_0\chi_O + \mathsf{w}\chi_\omega & \text{in } Q, \\ q(T) = 0 & \text{in } \Omega, \\ q = 0 & \text{on } \Sigma_1, \\ \dfrac{\partial q}{\partial \nu} = 0 & \text{on } \Sigma_2. \end{cases} \quad (12)$$

As for the problem (8), the problem (12) also admits a unique solution q (under very general assumptions on $f'(y_0)$). The function q depends on w that we shall determine :

If we multiply the first equation in (12) by y_τ, and we integrate by parts over Q, we obtain

$$\int_Q \Big(h_0\chi_O + \mathsf{w}\chi_\omega\Big)\, y_\tau\, dxdt \;=\; \int_\Omega q(0)\hat{y}^0 dx$$

for every $\hat{y}^0$ such that $\|\hat{y}^0\|_{L^2(\Omega)} \leq 1$. Hence, condition (5) (or (9)) is equivalent to

$$q(0) \quad = \quad 0. \tag{13}$$

Finally, (12) with (13) is a null-controllability problem.

III. Existence of a sentinel

We begin by giving an observability inequality. Consider

$$\mathcal{V} = \Big\{ v \in \mathcal{C}^\infty(\overline{Q}) \text{ such that } v_{|\Sigma_1} = \frac{\partial v}{\partial t}\Big|_{\Sigma_1} = \frac{\partial v}{\partial \nu}\Big|_{\Sigma_2} = 0 \Big\}. \tag{14}$$

Then we have :

Corollary *1:* Let be $u \in \mathcal{V}$ defined by (14), then there exists a positive constant $C = C(\Omega, \omega, O, T, f'(y_o))$ such that

$$\int_Q \frac{1}{\theta^2}\,|u|^2\, dxdt \leq C\Big(\int_Q |L\,u|^2\, dxdt + \int_0^T\int_\omega |u|^2\, dxdt\Big) \tag{15}$$

where $\theta \in \mathcal{C}^2(Q)$ positive with $\dfrac{1}{\theta}$ a bounded weight function.

Proof - For the proof of this result which is based on the classical Carleman estimates for the heat equation, we refer to Imanuvilov [1] for the case $\Sigma_2 = \emptyset$ and $\Sigma_1 = \Sigma$, and to Miloudi *et* al. [4] in the more general case (14). ■

According to the RHS of (15), we consider the space $\mathcal{V}$ endowed with the bilinear form $a(.,.)$ defined by :

$$a(u,v) = \int_Q Lu\, Lv\, dxdt + \int_0^T\int_\omega u\, v\; dxdt. \tag{16}$$

Let V be the completion of $\mathcal{V}$ with respect to the norm

$$v \mapsto \|v\|_V = \sqrt{a(v,v)}, \tag{17}$$

then, V is a Hilbert space for the scalar product $a(v,\hat{v})$ and the associated norm. Moreover, $\mathcal{V}$ is dense in V.

Remark *2:* We can precise the structure of the elements of V. Indeed, let $H_\theta(Q)$ be the weigthed Hilbert space defined by

$$H_\theta(Q) = \Big\{ v \in \mathcal{V} \text{ such that } \int_Q \frac{1}{\theta^2}\,|v|^2\, dxdt < \infty \Big\}$$

endowed with the natural norm $\|v\|_\theta = (\int_Q \frac{1}{\theta^2}\,|v|^2\, dxdt)^{\frac{1}{2}}$. Then the left hand side in (15) shows that V is imbedded continuously in $H_\theta(Q)$. In the same way, we have

$$\|v\|_\theta \leq C\,\|v\|_V\,. \tag{18}$$

Now if $h_0 \in L^2(Q)$ and $\theta h_0 \in L^2(Q)$ (i.e : $h_0 \in L^2_\theta(Q)$), then thanks to (15) and the Cauchy-Schwartz inequality, we deduce that the linear form defined on V by

$$v \mapsto \int_Q h_0\chi_O\, v\, dxdt$$

is continuous.

Therefore, from the Lax-Milgram theorem there exits a unique u in V solution of the variational equation :

$$a(u,v) = \int_Q h_0\chi_O\, v\, dxdt \qquad \forall v \in V. \tag{19}$$

Theorem *1:* Let be $h_0 \in L^2_\theta(Q)$, and let u be the unique solution of (19). We set

$$\mathsf{w} = -u\chi_\omega \qquad \text{and} \quad q = Lu.$$

Then, the pair (w, q) is such that (12)-(13) hold (i.e. then there exists an insensitive sentinel defined by (4)-(5)).

■

References

[1] O. Yu. Imanuvilov Controllability of parabolic equations. Sbornik Mathematics 186 : 6, 1995, pp 879 – 900.

[2] Kernevez J.-P., The Sentinel Method and its Application to Environmental Pollution Problems, CRC. Press, Boca Raton, FL, 1997.

[3] Lions J.-L. Sentinelles pour les systèmes distribués à données incomplètes. Masson, Paris, 1992.

[4] Miloudi Y., Nakoulima O., Omrane A., A method of detecting pollution in dissipative systems of incomplete data, ESAIM:Proceeding, Vol 17, 2007, pp 67 – 79.

[5] Nakoulima O., Contrôlabilité à zéro avec contraintes sur le contrôle. C. R. Acad. Sci. Paris, Ser. I 339, 2004, pp 405 – 410.

Angles & Logarithms

ALAIN B. TORRENS

Université Quisqueya, BP 796, Port-au-Prince, Haïti - torrab@yahoo.com

Introduction

Angles are physical quantities endowed with a dimension [0], as indicated by the fact that they are expressed in some unit - typically, the degree (°), radian (rad), or revolution (r). For example, one will quote an angle of '36°', or '0.628 rad', but not '0.628'.

On the other hand, a truly dimensionless quantity is expressed as a simple number: an efficiency could be written as '0.62', or '62 %'; a gain (ratio of two voltages) could be equal to 15.8, and an index of refraction, 1.42.

Fig·0

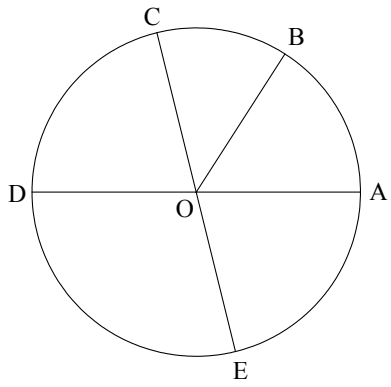

Two angles can be compared, added or subtracted; e.g. , in Fig·0:

B**O**C<C**O**D = A**O**E; A**O**C = A**O**B + B**O**C;

A**O**E = B**O**E − B**O**A;

But one cannot compare an angle with a number, which should be possible if, as some assert [1, Table 3, Note b; sec.2.2.3], angles have no dimension. Furthermore, if angles were dimensionless, their unit would be the unit number 1 (one).

The angle as a fundamental quantity

Not only can angles not be compared with numbers; they cannot be compared with, or added to, any other physical quantity, such as force, time, volume, etc… This implies that they are a **fundamental quantity**, on a par with mass, length, time,…

Particular angles

The **radian** is defined as the angle subtended at the center of a circle by an arc of circumference equal in length to the radius of the circle. (Notice that the radian is defined as an *angle*, not as the ratio of two lengths.)

The natural unit of angle is the **revolution** r. It is the minimum, non-zero, angle of rotation about O that transforms a point M into itself.

The **straight angle** is equal to the half a revolution: $\Pi = ½\ \mathrm{r} = 180° = \pi\cdot\mathrm{rad}$ **:1**.

Notice the distinction between the *angle* Π and the *number* π. With this notation, the revolution may be noted '2Π' (not 2π), the right angle 'Π/2', etc.

The angular constant

Let us consider the angle $\theta = \mathrm{A}\mathbf{O}\mathrm{B}$ in Fig·0; the length s of the arc AB subtended by the angle θ is, traditionally, written as

$$s = R\theta \qquad \textbf{:2}.$$

Since the angle θ has a dimension A (just as the radius R has the dimension L of a length), this equation is dimensionally incorrect, since it implies that the dimension of s is $[s] = \mathsf{LA}$ instead of L.

In fact, s is not *equal* to $R\theta$, but only *proportional* to it, through a factor η called **angular constant** [0]:

$$s = \eta R\theta \qquad \textbf{:3}.$$

The value of η is determined by the lengths of particular arcs:

- If θ = r, the arc is a complete circle: $2\pi\mathrm{R} = \eta R\cdot\mathrm{r} \Rightarrow \eta = 2\pi/\mathrm{r}$;
- If θ = rad, by definition of the radian, $s = R = \eta R\cdot\mathrm{rad} \Rightarrow \eta = \mathrm{rad}^{-1}$.

With Rel·1, we summarize:

$$\eta = \frac{2\pi}{r} = \frac{\pi}{\Pi} = \frac{1}{rad} \approx 0.01745\ (°)^{-1} \qquad \textbf{:4}.$$

The question arises: If Rel·2 is incorrect, how has it been used so often, and for so long? The answer: with many cautions and arbitrary rules, the basic one being: *all angles must be in radians*. Why this rule? Because Rel·2 should be written

$$s = Ru \qquad \textbf{:5},$$

where u is not the *angle* θ but its *measure in radian*. Indeed, in Rel·3, one can replace η by its expression with respect to the radian:

$$\eta\theta = \theta/\text{rad}.$$

Unlike Rel·2, Rel·5 is correct (since the measure u of θ in radian is, like all measures, dimensionless), but it has the drawback of being a *mixed equation*: both a *quantity equation* (independent of any unit that may eventually be used to express s and R) and a *measure equation*, since it is valid only with the radian as unit of angle. On the other hand, Rel·3 is a true quantity equation, independent of *any* unit.

One can also define the **analytical angle** [0] u not as an the measure of θ in radian, but as the product $\eta\theta$:

$$u == \eta\theta \qquad \textbf{:6}.$$

Rel·3&6 ⇒ Rel·5. In this perspective, u is a new variable which *happens* to be equal to the measure of θ in radian but is really independent from it, since η is (like Planck's constant or the celerity of light in vacuum) a *physical constant* which preexists any unit, and which can be expressed in units other than the radian - Rel·4.

If u is defined by Rel·6, then Rel·3 et Rel·5 are equivalent. However, it must be emphasized that u is *not* an angle (in the usual sense of the word, adopted in this paper) but a pure number, and should be expressed as such, without any unit (other than the number 1 [1, Sec.2.2.3]) ─not even the radian, which is unit of *angle*, not of number.

Confusing the geometrical angle θ and the analytical angle u leads to confusion of their respective units and bizarre conclusions. For example, according to the BIPM, the radian, classed as a 'supplementary unit' from 1960 to 1995, is now a derived unit equal to m/m (m = mètre). Since m/m = 1, then rad = 1, and 'radian' is 'special name for the number one' [1, Sec.2.2.2; Table 3, note b]. It this is true, then one can write a length of two metres as

$$a = 2\ \text{m} = 2\ \text{m}\cdot\text{rad} = 2\ \text{m/rad}^2 = \ldots!.$$

In fact, the radian is a *fundamental* (not derived) unit of *angle*, distinct from the *number* 1, which is a most fundamental unit, not a 'dimensionless derived unit' [1, Sec.2.2.3; Table 3, note b], since numbers exist independently of any physical quantity. (Is the number 1 'derived' from the meter, by m/m = 1, from the second, by s/s = 1, or from the coulomb, by C/C = 1?)

Trigonometric functions

To define the cosine and sine of an angle $\theta = (\mathbf{Ox},\mathbf{Or})$, one considers the intersection M of Or with the trigonometric circle, and the coordinates of M (Fig·1):

$$\text{Cos}\theta = x = \underline{\text{OJ}} \qquad \textbf{:7},$$

$$\text{Sin}\theta = y = \underline{\text{OK}} \qquad \textbf{:8}.$$

Fig·1

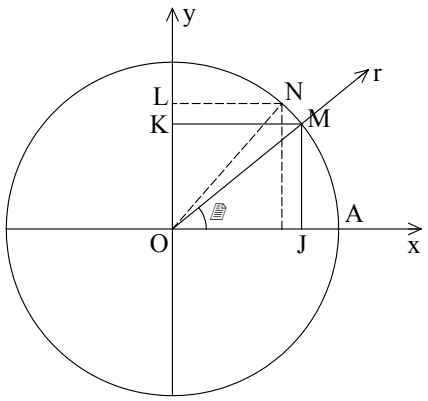

To evaluate the derivative of Sinθ, let us consider a variation $\Delta\theta$ of θ. Point M moves to N, and its projection K moves to L. Since the radius of the trigonometric circle is 1, Rel·3 ⇒

$$s = \text{AM} =^{3} \eta\theta, \quad \text{and} \quad \text{MN} = \Delta s = \eta\Delta\theta,$$

so that $\Delta y = \underline{\text{KL}} = \text{MN}\cdot\text{Cos}\ (\mathbf{Oy},\mathbf{MN})$ **:9**,

where

$(\mathbf{Oy},\mathbf{MN}) = (\mathbf{Oy},\mathbf{Ox}) + (\mathbf{Ox},\mathbf{OM}) + (\mathbf{OM},\mathbf{MN})$

$= -\Pi/2 + \theta + \Pi/2 = \theta$

Rel·9&10 ⇒ $\Delta y/\Delta\theta = \eta\cdot\text{Cos}\theta$ **:11**.

The limit value of this ratio when $\Delta\theta \to 0$ is the **derivative** of Sinθ: $\frac{d\,Sin\theta}{d\theta} = \eta\cdot Cos\theta$ **:12.**

The above proof was developed in detail to show how the angular constant η appears in Rel·12. According to this relation, the dimension of d(Sinθ)/dθ is that of η, namely A^{-1}. This is consistent with the definition, since the ratio $\Delta y/\Delta\theta$ (Rel·11) is a number divided by an angle.

To reconcile Rel·12 with the well-known formula $\frac{d\,Sin\,u}{du} = \cos u$ **:13**,

one must realize that the mathematical functions sin (u), cos (u), tan (u) require a (dimensionless) *analytical angle* as argument, while the angular functions Sinθ, Cosθ, Tanθ require an *angle* as argument. In other words, their respective **domains** [2] are the set of **reals** (**R**) and the set of **angles**; they share the same **codomain**, since their values are reals. They satisfy the identities

Sin (θ) ≡ sin (ηθ);
Cos (θ) ≡ cos (ηθ);
Tan (θ) ≡ tan (ηθ) **:14**.

Common practice is to confuse these functions and write, for example, sin (30°) = ½, which is incorrect since the angle 30° is not an acceptable argument for the function sin; instead, one could write:
sin (π/6) = Sin (π/6 rad) = Sin (30°) = ½.

With Rel·6, Rel·13 & 14a

$$\Rightarrow \frac{d\,Sin\theta}{d\theta} = \frac{d\,Sin\,u}{du}\times\frac{d\,u}{d\theta}$$

$=^{6}$ η·cos (u) = η·Cos (θ),

which confirms Rel·12. Similarly,

$$\frac{d\,Cos\theta}{d\theta} = \eta\cdot\frac{d\,Cos\,u}{du} = -\eta\cdot Sin\theta \quad \textbf{:15},$$

and $\frac{d\,Tan\,\theta}{d\theta} = \eta\cdot\frac{d\,Tan\,u}{du} = \eta/Cos^2\theta.$

Conversely, the **primitive** of Cosθ is

$\int Cos\theta\cdot d\theta = \eta^{-1}\cdot Sin\theta$ **:16**;

its dimension is that of dθ (left-hand side of Rel·16) and η^{-1} (right-hand side), namely **A**.

Frequency; angular frequency

Let us consider a point M in uniform motion on a circle of radius R (Fig·1): $\theta = \Omega t$ **:17**.

The **period** is the duration of one revolution:

$T = r/\Omega$ **:18**,

the **frequency** of the movement is

$f = T^{-1} = \Omega/r$ **:19**.

and the **angular velocity** is

$d\theta/dt = \Omega = r\cdot f = 2\Pi\cdot f$ **:20**.

The projection J of M on the x-axis is at

$x = R\cdot Cos\theta = R\cdot Cos\Omega t$ **:21**,

and its velocity is, with Rel·15,

$v_x = dx/dt = -R\cdot\eta\Omega\cdot Sin\Omega t = -v_{max}\cdot Sin\Omega t$ **:22**,

where, with Rel·4b & 19,

$v_{max} == RW$ **:23**,

where $W == \eta\Omega = 2\pi f$ **:24**.

Example: If f = 30 Hz; Rel·19

$\Rightarrow \Omega = 30\cdot rHz = 30\cdot r/s = 1800$ r/min **:25**.

If R = 40 cm, Rel·23,24,25

$\Rightarrow v_{max} = 40\text{ cm}\times 2\pi\times 30\text{ Hz} = 75.4$ m/s

Traditionally, one would set the factor η to unity (as in Rel·2), confuse W with Ω (Rel·24), write $\Omega = 2\pi\cdot f \approx 188.5\text{ Hz} = 188.5\text{ s}-1$,

add 'we know that an angular velocity must be in rad/s', then conclude: Ω = 188.5 rad/s.

Then, one would calculate

$v_{max} = R\cdot\Omega = 40\text{ cm}\times 188.5\text{ rad/s} = 75.4\text{ m}\cdot\text{rad/s}$,

add 'we know that a velocity must be in m/s' and 'drop' (arbitrarily) 'rad' from the result.

Not only are such questionable acrobatics (introducing or removing the radian where that seems appropriate) not required to apply Rel·19 & 23, but such a result as Rel·25 involves *practical* units ─ r/s, r/min. (Even to the mathematically-inclined, a speed of 188.5 rad/s is difficult to grasp.)

Circlance

The voltage $V = V_{max}\cdot\mathrm{Sin}\,\omega t$ **:26**

varies with time t with a frequency f and an **angular frequency** $\omega = 2\Pi f = \mathrm{r}\,f$ **:27**.

This voltage, applied to a capacitor of capacitance C, produces an electric current of intensity

$$i = C\cdot \mathrm{d}V/\mathrm{d}t;$$

with Rel·12,

$i = C\cdot V_{max}\cdot\eta\omega\cdot\mathrm{Cos}\,\omega t = Y\cdot V_{max}\cdot\mathrm{Cos}\,\omega t$,

where Y is the admittance: $Y == wC$ **:28**,

Where $w == \eta\omega = 2\pi f$ **:29**.

Example: If $f = 10$ kHz and $C = 47$ nF, Rel·29

$\Rightarrow w = 62.8$ kHz, and Rel·28$\Rightarrow Y = 2.95$ mS.

Traditionally, one would write:

$\omega = 2\pi f = 62.8\times10^3\ \mathrm{s}^{-1}$,

and express the result as 62.8×10^3 rad/s (because 'ω must be in rad/s'),

then calculate $Y == \omega C$

$= (62.8\times10^3\ \mathrm{rad/s})\times(47\times10^{-9}\mathrm{F}) = 2.95$ rad·mS,

then drop 'rad' from the result because it obviously does not belong there…

W (Rel·24) or w (Rel·29) are similar quantities that have the dimension T^{-1} of a frequency, but are not *the* frequency f; they are usually called 'angular velocity' or 'angular frequency', but these terms apply to Ω and ω (Rel·20,27), which have the angular dimension AT^{-1}. The quantity $2\pi f$ associated with a sinusoidal oscillation of frequency f could be called **circlance** (from the verb 'to circle'), by analogy with the circumference of a circle of radius R: $\mathrm{c} = 2\pi\mathrm{R}$.

Remark

Different quantities have different names and symbols, yet may have the same dimension and, *consequently*, the same unit. For example, Rel·29 implies that the frequency f and the circlance w have the same dimension T^{-1}, and therefore the same unit Hz. One should *not* use a special unit for w just to show that it is different from f, as suggested by some, including the BIPM [1, Sec.2.2.2]. (In particular, the unit rad/s is applicable to ω, but not to w.) Similarly, the radius R, diameter D, and circumference c of a circle all have the same dimension (L) and unit (m, cm, ft,…).

Angular exponential

Consider an angle θ and another real quantity ξ of the same dimension A. The complex quantity

$$\zeta == \xi + \mathrm{i}\cdot\theta \qquad \textbf{:30}$$

also has the dimension A, because the imaginary unit i is a pure number. (The quantities ζ, ξ and θ must, by homogeneity, have the same dimension for the expression $|\zeta|^2 = \xi^2 + \theta^2$ to be meaningful.)

On ther other hand, $x == \eta\xi$ **:31,**

$$u == \eta\theta \qquad \textbf{:32}$$

and $g == \eta\zeta = x + \mathrm{i}\cdot u$ **:33**,

are dimensionless numbers; as such, they are acceptable as arguments of the exponential function. Consistently with Rel·14, the **angular exponential** function Exp (capitalized, to distinguish it from the numeric function exp) is defined over the angle domain by

$\mathrm{Exp}\,(\zeta) == \exp(g) = \exp(x + \mathrm{i}u)$

$= \exp(x)\cdot\exp(\mathrm{i}u) = \exp(x)\cdot(\cos u + \mathrm{i}\cdot\sin u)$

In particular, for $\zeta = \xi$, $\mathrm{Exp}\,(\xi) = \exp(x)$ **:36**

and, for $\zeta = \mathrm{i}\cdot\theta$,

$\mathrm{Exp}\,(\mathrm{i}\cdot\theta) == \exp(\mathrm{i}\cdot u)$

$= \cos u + \mathrm{i}\cdot\sin u = \mathrm{Cos}\,\theta + \mathrm{i}\cdot\mathrm{Sin}\,\theta$ **:37**.

Rel·35 may therefore be written

$\mathrm{Exp}\,(\xi + \mathrm{i}\cdot\theta) \equiv \mathrm{Exp}\,(\xi)\cdot\mathrm{Exp}\,(\mathrm{i}\cdot\theta)$

$\equiv \mathrm{Exp}\,(\xi)\cdot(\mathrm{Cos}\,\theta + \mathrm{i}\cdot\mathrm{Sin}\,\theta)$ **:38**.

Note: in Rel·35, $\exp(g)$ may be calculated as e^g (where the pure number g is an acceptable power), but e^ζ (where ζ has a dimension) is not defined, and may not be used as a substitute for Exp (ζ).

Angular logarithm

The complex natural logarithm is defined as the inverse function of the complex *numeric* exponential:

$$z = \exp(g) = \exp(x + iu)$$

$$\Leftrightarrow g = \ln z = x + i\cdot(u + n\cdot 2\pi) \qquad \textbf{:39},$$

where n is any integer.

The inverse function, noted Log, of the angular exponential is similarly defined: if $z == \mathrm{Exp}(\zeta)$, Rel·33 $\Rightarrow$ $\mathrm{Log}\, z = \zeta = 33\ \eta{-}1\cdot g = 39\ \eta{-}1\cdot \ln z$

$$= \eta{-}1\cdot[x + i\cdot(u + n\cdot 2\pi)]$$

$$= 31{,}32\ \xi + i\cdot(\theta + n\cdot r) \qquad \textbf{:40}.$$

Just as $\ln z$ is defined modulo $i\cdot 2\pi$ (where π is a *number*) (Rel·39), $\mathrm{Log}\, z$ is defined modulo $i\cdot r$, where the revolution r is an *angle*:

Rel·1 $\Rightarrow r = 2\Pi = 360°$. From here on, we will consider the principal value of $\mathrm{Log}\, z$, defined by $-\Pi < \theta \leq \Pi$ and $n = 0$ (Rel·40).

The **angular logarithm** Log is therefore a *quantity*, defined intrinsically, having the dimension A of η^{-1}, ζ, ξ and θ (Rel·40); it is also called 'indefinite logarithm' by Frank_MP, who stresses that 'no specific base is implied at all' in its definition [3]. It is 'angular' only in a broad sense: while the imaginary part (θ) of ζ is an angle; the real part ξ is of a different nature - see below -, even though it has the same dimension.

Since $\eta^{-1} = \mathrm{rad}$ (Rel·4), Rel·40b

$$\Rightarrow \mathrm{Log}\, z = \ln z\ \mathrm{rad} \qquad \textbf{:41}.$$

Therefore, the measure of $\mathrm{Log}\, z$ in radian is $\ln z$. However, Rel·41 should be regarded as an *interpretation* (in terms of a particular unit, the radian) of Log z; the definition (Rel·40) is intrinsic, independent of any unit.

Conclusion

►Using the angular constant (Rel·4) instead of the number 1, and the angle Π (Rel·1) instead of the number π, where required (Rel·3, 12, 15, 16, 20, 27) removes all inconsistencies in relations between rotational and translational quantities, and obviates the need to introduce or delete the radian (or neper, decibel, etc.) 'where appropriate' [1, Sec.2.2.2, Table 3, Note b]. It also removes the requirement that angles be expressed in radians in some equations and permits, instead, the use of practical angle units such as the revolution or the degree, without the need for an explicit conversion into radians. In fact, it lets one write any relation intrinsically, in dependently of any unit.

►As an unit of angle, the **radian** is impractical. In real-life calculations, η is always expressed as $2\pi/r$ or $\pi/180°$ (Rel·4); of course, expressing it as rad^{-1} simplifies the calculation (since the measure of η is, then, 1), but only temporarily, since a result such as 377 rad/s is so obscure that it must be converted (via another calculation) to a more comprehensible form, such as 60 r/s, or 3600 r/min.

In the end, the radian becomes useless because, as geometrical angles and the anguler constant are used systematically, there is no more need to convert angles into radians. In hindsight, we can see that the radian was invented just to avoid the use of the angular constant.

►The definitions of angular trigonometric and exponential functions lead to the conclusion that neper and radian are actually equal (Rel·45), with the consequence that one should be abandoned in favour of the other. I suggest keeping the neper, because:

- Naming units after scientists has been the recent trend;
- The name must be 'neutral' to apply to quantities as diverse as angles, logarithmic gains, entropy; 'radian' is perceived strictly as an angle unit, as suggested by its etymology [8].
- The neper will be used mostly for the real part of logarithm (as it currently is), seldom to express angles −see above.

►Since angles and logarithms constitute a fundamental quantity, of dimension A, the **neper** (so far, not even recognized as an SI unit [1, Sec.4.1, Table 8]) should become a **base unit** of the SI [1, Sec.2.1].

►While the angular frequency (Rel·27) has dimension AT−1 and is expressed in r/s (or r·Hz, or °/s, etc.), the circlance w (Rel·29) has dimension T−1 of a frequency and is expressed in Hz, not in rad/s. It is used (instead of ω) to express the susceptance of a capacitor or the reactance of a coil: $B = wC$, $X = wL$.

►The angular functions have the general properties of the traditional mathematical functions, so that one need not 're-learn' mathematics; for example:

$\mathrm{Cos}(\alpha+\beta) \equiv \mathrm{Cos}\alpha\cdot\mathrm{Cos}\beta - \mathrm{Sin}\alpha\cdot\mathrm{Sin}\beta$;
$\mathrm{Exp}(\alpha+\beta) \equiv \mathrm{Exp}\alpha\cdot\mathrm{Exp}\beta$;
$\mathrm{Log}(ab) \equiv \mathrm{Log}\,a + \mathrm{Log}\,b$.

$\mathrm{Sin}\,\theta \equiv \sin u = u - u^3/3! + u^5/5! - u^7/7! + \ldots$,

Where $u == \eta\theta$.

►It is possible (and permitted!) to prefer analytical (numerical) angles to geometrical ones. This simplifies the language (all 'angles' are, by convention, numerical) and mathematical formulas (by replacing Rel·3 with Rel·5, Rel·12 with Rel·13, etc.), and eliminates the need for such angular functions as Cos, Exp and Log.
By denying the existence of geometrical angles, this viewpoint even eliminates the need for, and use of, angular units - *even the radian*. It, therefore, forces one to quote an angle as a number (which it *is*), as '$\pi/3$' or '1.2' ─at the expense of clarity, because most people understand angles as geometrical entities. To make the expression clearer, one would therefore express the angle of '1.2' as '1.2 rad', thereby switching (implicitly) to the concept of geometrical angles.

References

0: Torrens A B: 'On angles and angular quantities', Metrologia 22, 1-7; 1986 Jan. See also Metrologia 23, 155; Metrologia 23, 57; Metrologia 24, 155.

1: BIPM (Bureau international des Poids et Mesures): 'The International System of Units (SI)', 8th edition (1998): www1.bipm.org/en/si/si_brochure/

2: http://en.wikipedia.org/wiki/Domain_%28mathematics%29.

3: Frank_Michael_P., The Indefinite Logarithm, Logarithmic Units, and the Nature of Entropy, http://www.eng.fsu.edu/~mpf/IndefLog_paper/indef-log.pdf#search='logarithm%20units'

4: http://en.wikipedia.org/wiki/Neper

5: http://en.wikipedia.org/wiki/Ban_%28information%29

6: http://PlanetMath.org/encyclopedia/ShannonsTheoremEntropy.html

7: http://en.wikipedia.org/wiki/Entropy_%28statistical_views%29.

8: http://members.aol.com/jeff570/r.html

Estimation of the Large Deviation Multifractal Spectrum

M. ABADI AND E. GRANDCHAMP

GRIMAAG UAG, Campus de Fouillole, BP 250, 97157 Pointe-à-Pitre Cedex,
Université Antilles Guyane, Guadeloupe, France - mabadi@univ-ag.fr - egrandch@univ-ag.fr

Keywords. multifractal theory, multifractal spectrum, quasi-continuous histogram, kernel, methods.

Abstract

Within the framework of the multifractal analysis, we propose to use the quasi-continuous histogram (QCH) method for the estimation the probability density in order to be able to compute the large deviation spectrum (LDS). The QCH is a statistical tool related to the kernel for density estimation. The application of this tool and the comparison with kernel methods on binomial measures is a new point in this field.

Computer Science & Maths

A Variant of Newton's Method for Generalized Equations

C. JEAN ALEXIS AND A. PIETRUS

Laboratoire AOC, Université des Antilles et de la Guyane, Département de Mathématiques et Informatique, Campus de Fouillole, F–97159 Pointe à Pitre, France
celia.jean-alexis@univ-ag.fr, apietrus@univ-ag.fr

Keywords: Set–valued mapping, generalized equation, linear convergence, Aubin continuity.

Abstract

Throughout this statement X and Y are two Banach spaces. We consider a generalized equation of the form

$$0 \in f(x) + F(x) \tag{1}$$

where $f : X \to Y$ is Frechet-differentiable and $f : X \to 2^Y$ is a set-valued map with closed graph. Let us note that the equation (1) is an abstract model for various problems.

- When $F = 0$, (1) is an equation,
- when F is the positive orthant in R^m, (1) is a system of inequalities,
- when F is the normal cone to a convex and closed set in X; (1) may represent variational inequalities.

Let us remark that when $F = \{0\}$ and x^* is a solution of (1) of order $h > 1$; the Newton method of the form

$$0 \in f(x_k) + \nabla f(x_k)(x_{k+1} - x_k) + F(x_{k+1}), \quad k = 0,1... \tag{2}$$

is no longer valid. To avoid this drawback, in [1, 2] the authors proposed a variant of the Newton method of the form

$$x_{k+1} = x_k - h \nabla f(x_k)^{-1} f(x_k) \tag{3}$$

Following this work, we introduce to solve (2), the following sequence of the form

$$0 \in f(x_k) + h\nabla f(x_k)(x_{k+1} - x_k) + F(x_{k+1}), \quad k = 0,1... \tag{4}$$

Let us remark that when $h = 1$, the method (4) is exactly the Newton type method (2). This statement is organized as follows : at first time, we recall a few preliminary results then in the second time, we show that the method (4) is locally convergent and to finish, we prove the stability of this method.

References:

[1] J.M. Ortega and W.C Rheinboldt, Iterative solution of nonlinear equations in several variables, Academic Press, New-York and London, 1970.

[2] A.M Ostrowski, Solution of equations in Euclidean and Banach spaces, Academic Press, New-York and London, 1970.

Computer Science & Maths

An Accurate Projection Method for Incompressible Flows

C. FEVRIERE† (1), P. ANGOT (2), J. LAMINIE (1), P. POULLET (1)

(1) *GRIMAAG, Groupe de Recherche en Informatique et en Mathématiques Appliquées des Antilles et de la Guyane, Université des Antilles et de la Guyane, Campus de Fouillole, 97159 Pointe-à-Pitre Cedex, Jacques.Laminie@univ-ag.fr , Pascal.Poullet@univ-ag.fr*
(2) *LATP, Laboratoire d'Analyse, Topologie et Probabilités, Université de Provence, 39 rue Joliot-Curie, 13453 Marseille Cedex 13, angot@cmi.univ-mrs.fr*

Abstract

The most important dif_culty for the numerical simulation of imcompressible _ows is that the velocity and the pressure are coupled by the imcompressibility constraint. Since the precursory works of Chorin and Temam [1, 8], several papers have treated about this subject [7, 6, 3], (and [2] for an overview), but research on this topic remains still active [4]. Our study is concerned with the implementation and study of projection methods, known to offer
a methodology to solve such a problem. The most attractive feature of projection methods is that, at each time step one only needs to solve a sequence of decoupled elliptic equations for the velocity and the pressure, making it very ef_cient for large scale numerical simulations. We focus our attention on the pressure correction schemes and particularly, the capabilities of the implementation with staggered mesh, to compute accurate solutions of problems with realistic boundary conditions. We study the incremental and penality projection methods in theirs standard and rotational forms. A comparative study of the four schemes for the time-dependent Stokes problem will help users to select the projection methods using MAC mesh which is more accurate.

Références

[1] A.J. Chorin, Numerical solution of the Navier-Stokes equations, *Math. Comput.* 22, pp. 745-762, (1968).
[2] J.L. Guermond, P. Minev and J. Shen, An overview of projection methods for incompressible flows *Comput. Methods Appl. Mech. Engrg.* (to appear).
[3] J.L. Guermond, L. Quartapelle, An the approximation of the unsteady Navier-Stokes equations by finite element projection methods *Numer. Math.* 80, pp. 207-238, (1998).
[4] M. Jobelin, C. Lapuerta, J.-C. LatchÈ, Ph. Angot and B. Piar A Finite Element penalty-projection method for incompressible flows, *J. Comput. Phys.* (to appear).
[5] P. Poullet, Staggered Incremental Unknowns for solving Stokes and generalized Stokes problems, *Applied Num. Math.* 35(1), pp. 23-41, (2000).
[6] J. Shen, On error estimates of projection methods for Navier-Stokes equations : Second-order schemes, *Math. Comput.* 65(215), pp. 1039-1065, (1996).
[7] J. Van Kan, A second-order accurate pressure-correction scheme for viscous incompressible flow, *SIAM J. on Scient. Stat. Comput.* 7(3), pp. 870-891, (1986).
[8] R. Temam, Sur l'approximation de la solution des équations de Navier-Stokes par la méthode à pas fractionnaires (II), *Archive for Rat. Mech. and Anal.* 33, pp. 377-385, (1969).

Introduction to and Implications of Emergent Global Internet Protocols and Policies for the Caribbean Region

J. Crain

Crain, John – Chief Technical Officer ICANN - Internet Corporation for Assigned Names and Numbers, Marina Del Rey, USA - john.crain@icann.org

The global internet continues to expand around the world. More than one billion people now have access to this network of networks. In addition to adding users, increasing demand for mobile internet access and convergence between Internet protocols, supply chain and other resource management systems is creating the potential for an internet of things.

This rapidly evolving landscape presents both opportunities and challenges for the science and technology sector. How are the systems that keep the Internet functioning responding to these changes? How are these systems governed? What are the potential implications for small island states and the scientific community?

This presentation will provide a user-friendly overview of basic Internet functions. It will also introduce some of the key systems and policies under discussion at a global level and outline how they are agreed on. Topics will include:

IPv6 and the extension of Internet addresses into physical space.
Internationalised domain names at the top level: developing a multi-lingual Internet infrastructure
Top level domain name current policy issues.
Bottom up policy making: who runs the Internet? You do.

Kernel Theorems in Spaces of Caribbean Generalized Functions

A. DELCROIX

Equipe AANL - Laboratoire AOC - Faculté des sciences exactes et naturelles
Université des Antilles et de la Guyane - 97110 Pointe-à-Pitre – GUADELOUPE & IUFM de Guadeloupe - Morne Ferret - BP 517 - 97178 Abymes Cedex – GUADELOUPE
Antoine.Delcroix@univ-ag.fr

Abstract

During the three last decades, theories of non-linear generalized functions have been developed by many authors, mainly based on the ideas of J.-F. Colombeau, which we are going to follow in the sequel. Those theories appear to be a natural continuation of the distributions' one, specially efficient to pose and solve differential or integral problems with irregular data. We continue here the investigations in the field of generalized integral operators initiated by D. Scarpalézos and carried out by various authors (S. Bernard, J.-F. Colombeau, A. Delcroix, C. Garetto, V. Valmorin). The importance of these operators is that they exactly generalize, in the Colombeau framework, the operators with distributional kernels in spaces of distributions.

More specifically, we show that any moderate net of linear maps - that is satisfying some growth properties with respect to a small parameter - gives rise to a linear map $L : G_C(\mathrm{R}^n) \to G(\mathrm{R}^m)$ ($G_C(\mathrm{R}^d)$ and $G(\mathrm{R}^d)$ denote respectively the space of generalized functions and the space of compactly supported ones.) The main result is that L can be represented as a generalized integral operator in the spirit of Schwartz Kernel Theorem. Moreover, through now classical results of embeddings of $D(\mathrm{R}^n)$ (*resp.* $D'(\mathrm{R}^m)$) into $G_C(\mathrm{R}^n)$ (*resp.* $G(\mathrm{R}^m)$), we show that the classical kernel theorem is contained in our result.

Going further in this direction, we show that the generalization of the classical isomorphism theorem between $S'(\mathrm{R}^{n+m})$ and the space of continuous linear mappings acting between $S(\mathrm{R}^n)$ and $S'(\mathrm{R}^m)$ is possible. In this case, the spaces of generalized functions considered are the space $G_S(\mathrm{R}^n)$ of rapidly decreasing generalized functions (in which $S(\mathrm{R}^n)$ is embedded) and the space $G_\tau(\mathrm{R}^m)$ of tempered generalized functions (in which $S'(\mathrm{R}^m)$ is embedded). In this case, we also obtain a kernel result for moderate nets. Once more, the generalized kernel theorem contains the classical one.

Chemistry / Physics of Materials

The Diels Alder Reaction, a Useful Synthetic Methodology 35
R.C. Jagessar and J.J. Hingree.

The Sol-Gel Process: a Method to Prepare Synthetic Materials and to Understand Natural Materials 38
T. Woignier, P. Dieudonné, J. Primera and A. Charlier de Chilly

Extraction and Isolation of Natural Products From *Momordica Charantia* 40
R.C. Jagessar and A. Mohamed

Ground and Excited States Vibrational Frequencies of 3-Amino-2-Chloropyridine 41
V.N. Verma

Effect of Processing Method on Shelf Stability of Coconut Water 43
H. G. Arscott and I. A. Lambert

Introduction of Electron Microscopy to The University of the West Indies, St. Augustine, Trinidad and Tobago 45
D. Hinds and R. Saunders

Analytical Scanning Electron Microscopy approach for Caribbean Ceramics Identification 47
B. Vicens, J.S. Guibert, D. Himmel and J.L. Mansot

High Spatial Resolution Raman Spectroscopic Mappings in Dynamic Lubricated Sphere - Plane Contacts: Application to Pressure and Thickness Profile Measurements 49
D. Himmel, Y. Bercion and J.L. Mansot

Band Structure Calculations Applied to Structural Determination of Graphite Intercalation Compounds: the Case Of CaC_6 51
K. Delbé, Ph. Thomas, N. Emery, C. Hérold, F. Boucher, J.-P. Buisson, P. Lagrange and J.L. Mansot

Development and Applications of a Flash Test Using High Powered Ultrasounds for the Fast Evaluation of the Durability of Painted Galvanized 52
J. Pigerre, P. Rodriguez , Y. Bercion and J.L. Mansot

Nano Friction of Low Dimensional Compounds Using Atomic and Lateral Force Microscopy: Toward An Atomic Interpretation 57
P. Bilas, L. Romana, F. Bade, K. Delbe, P. Thomas and J.L. Mansot

Nanomechanical Characterizations of Submicrometer Thick-Tribologic Films 59
L. Romana, P. Bilas, V. Golabkan and J.L. Mansot

Theoretical Approach of Nanocristallized Graphite Phases: Influence of Cluster Size Electronic Band Structure–Correlation to EELS Near Edges Structures 62
T. Césaire, V. Jeanne-Rose, N. Nomède Martyr, L.Largitte and J.L. Mansot

Antiwear and Antifriction Action Mechanisms of Colloidal Lubricant Additives 63
V. Golabkan, P. Bilas, L. Romana, J. Pigerre and J.L. Mansot

Tribological Properties of Room Temperature Graphite Fluorides Heat-Treated Under Fluorine Atmosphere 64
P. Thomas, K. Delbé, D. Himmel, J.L. Mansot, C. Delabarre, M. Dubois, K. Guérin and A. Hamwi

Kinetic Study of Sulfation of Natural Limestones from Guadeloupe 66
N. Passé-Coutrin and A. Ouensanga

Experimental Aqueous Phase Adsorbents Made From Purple heart *(Peltogyne venosa)* Sawdust And Rice Husk 68
D. I. Fox and R. Singh

Organic Electronics: From Molecules to Devices 70
L. Hirsch, G. Wantz, N. Huby, M. Urien, L. Vignau and J.P. Parneix

Characterization of Vetiver Roots Activated Carbon and Absorption Of Phenolic Compounds 70
S. Altenor, B. Carene, J. Lambert, J.J Ehrhardt, A. Ouensanga and S. Gaspard

A Comparative Study of Biological Indigenous Products Used to Increase Surface Hardness of Low Plain Carbon Steel 71
D. Gossett and A. Oliver

Industrial Production of Value-Added Chemicals From Sugarcane Bagasse 71
G.B. Isabelle

Multi technique approach of chemical and mechanical properties of hotmelts 72
N. Nomede Martyr, A. Gruda,S. Radegonde , T. Cesaire, D. Himmel and J.L. Mansot

Chemistry / Physics of Materials

The Diels Alder reaction, a useful synthetic methodology,

R.C.JAGESSAR, J.JHINGREE

Department of Chemistry, University of Guyana, Guyana - raymondjagessar@yahoo.com

The Diels-Alder reaction is a useful synthetic tool, providing one of the best ways to make six membered rings with diverse functions. It involves the reaction of a diene with a dienophiles, scheme 1.0. The diene is the electron rich nucleophile and the dienophile is electron poor electrophile. It is also a (4 + 2) cycloaddition, because a ring is formed by the interaction of four pi electrons in the diene with two pi-electrons of the alkene or alkyne. It converts two pi bonds into two sigma bonds.

The Diels-Alder reaction is like a nucleophilic-electrophilic reaction.

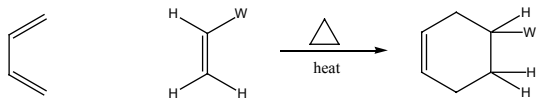

Scheme 1.0

The presence of electron releasing groups such as alkyl groups or alkoxy (-OR) groups will further enchance the reactivity of the diene.A good dienophile has one or more electron withdrawing groups (-W) such as carbonyl (C=O) or cyano ((-CN) pulling electron density away from the pi bond. A variety of different dienes and dienophiles can be used. An example is shown in Fig 1.0.

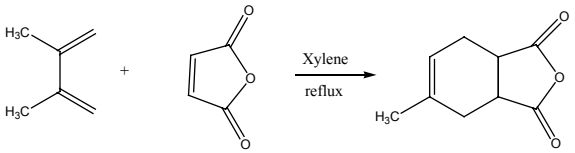

Fig.1.0 An examples of a Diels Alder Reactions.

The Diels Alder reaction follow a concerted mechanism which involves the simultaneous cyclic movement of six electrons: four in the diene and two in the dienophile, Scheme 2.0.

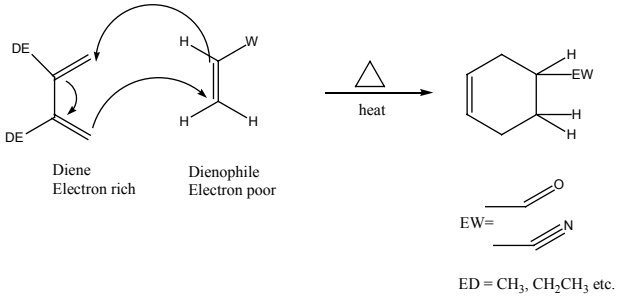

Scheme 2.0: Diels Alder Mechanism

The stereochemical features of the Diels-Alder reaction are controlled by the requirements of the transition state. The diene must be in the s-cis conformation to react. When the diene is in the s-trans conformation, the end p-orbitals are too far apart to overlap with the p orbitals of the dienophile.The s- trans conformation has a lower energy than the s-cis, but this energy difference is not enough to prevent most dienes from undergoing Diels-Alder reactions. For example, The s-trans conformation of butadiene is 2.3 kcal/mol lower in energy than the s-cis conformation.

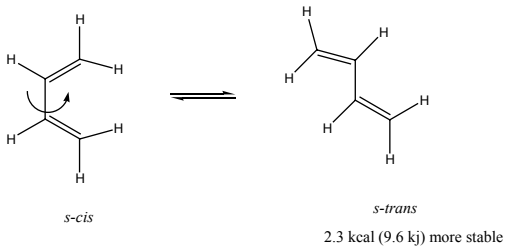

Fig. 2.0

Thus, structural features that aid or hinder the diene in achieving the s-cis conformation affect its ability to participate in Diels-Alder reactions.Dienes with functional groups that hinder the s-cis conformation react slower than butadiene and vice versa. Dienes with functional groups that hinder the s-trans conformation react faster than butadiene and vice versa. The Diels Alder reaction also proceed via a syn addition with respect to both the diene and the dienophile.

Secondary overlap is another important feature of the Diels-Alder reaction. This occurs when the dienophile has a pi bond in its electron withdrawing group (as in a carbonyl group or a cyano group), the p-orbitals in that electron withdrawing approach the central carbon atoms (C2 and C3) of the diene. This stabilizes the transition state and foster the Diels Alder reaction.

Hence, there is a preference for the electron withdrawing substituent to occupy a position closest to the central atoms of the diene, the endo position and thus observing the endo rule.The endo rule is useful for predicting the products of many types of Diels Alder reactions in which the dienophile bears electron withdrawing groups, Fig 3.0.

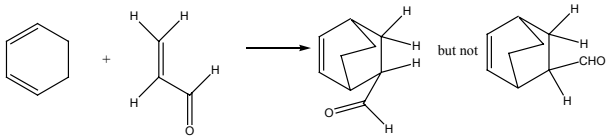

Fig: 3.0 Endo rule

Reagent (Dienophile)	Limiting reagent (Diene)	Product	Yield (%)
Maleic anhydride	Anthracene (Diene)	9,10-dihyrdro-anthracene-9,10-endo α,β-succinic anhydride (1)	10.47
Cyclohexene	Anthracene (Diene)	9,10-dihydro-anthracene-9,10-endo-α,β-cyclohexane (2)	78
Succinic anhydride (Not a Dienophile)	Anthracene (Diene)	No product as anticipated	-----
Cinnamaldehyde	Anthracene	9,10-dihydro-anthracene-9,10-endo phenyl propanal-dehyde (3)	65
Crotonaldehyde	Anthracene	9,10-dihydro-anthracene-9,10-endo butanal-dehyde (4)	55

Scheme 3.0

In our experiment, anthracene the planar fused aromatic compound was used as the diene and reacted individually with several dienophiles such as maleic anhydride, cyclohexene, cinnamaldehyde, crotonaldehyde in the presence of xylene to yield compounds of white flaky crystalline nature to white solids in yields of 10% to 65% after purification via crystallization. These results are summarized in Scheme 3.0.

Synthetically, reaction of anthracene with succinic anhydride in xylene yielded compound (1), 9,10 dihydroanthracene-9,10-endo-α,β-succinic anhydride as a white solid in yield of 10.5% , whereas reaction of anthracene with cyclohexene yielded compound (2), 9,10-endo-α,β-cyclohexane as a white gray solid in yield of 28%. Also, reaction of anthracene with other dienophiles such as phenyl propenaldehyde and but-2-ene aldehyde yielded compounds (3), 9,10-dihydroanthracene-9,10-endo butanaldehyde and 9,10-dihydroanthracene-9,10-endo phenyl propanaldehyde (4) as white solids in yields of 55 and 65% respectively. Under standard conditions as expected, the reaction of anthracene with a non dienophile maleic anhydride was negative. A representative example of these reactions is shown in *Scheme. 4.0*.

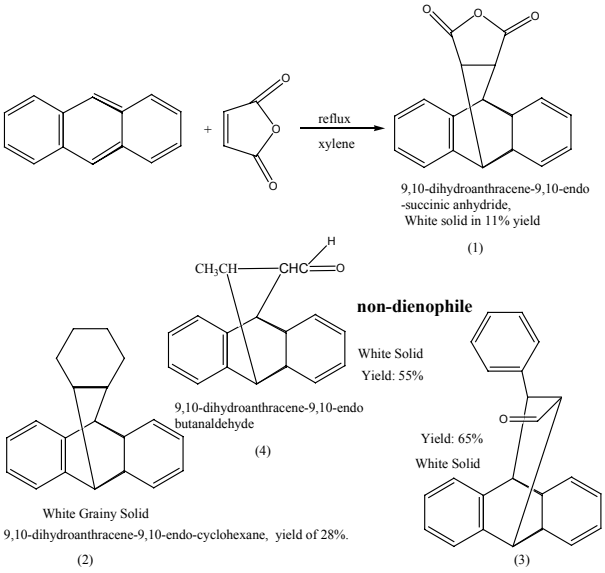

Scheme. 4.0

UV/Vis spectroscopy as the only means of characterization available here indicates that for compound (1), 9,10-dihydroanthracene-9,10-*endo*-α,β-succinic anhydride λ_{max} occurs at 330 nm with an absorbance of 0.16 and a shoulder at 370 nm as shown on the poster. There is also an intense band in the region 310nm-350 nm. This intense band is due to the

conjugated nature of the system. The UV/Vis spectrum for compound (2) indicates the presence of two peaks. One peak could result from the anhydride product and the other from the diacid product. Conformational rotation in solution can also contribute to the two different peaks.

The feasibility of a Diels Alder reaction is predicted using Molecular Orbital Theory which takes into account the symmetry of the molecular orbitals of the reactants and product. The theory of conservation of orbital symmetry indicates that the MOs of the diene must flow smoothly into the MOs of the dienophile without any drastic changes in symmetry. As an example, consider the Diels-Alder reaction of butadiene with ethylene. Molecular orbitals of butadiene and ethylene are shown in Fig. 4.0.

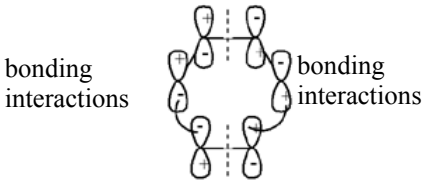

Fig. 4.0 Ethylene LUMO

The HOMO of butadiene forms a constructive bonding overlap with the LUMO of ethylene because the orbitals have similar symmetry. Symmetry allowed.

Butadiene with four atomic p-orbitals, has four molecular orbitals: two bonding.

MOs (filled) and two antibonding Mos (vacant). Ethylene, with two atomic p orbitals, has two MOs: a bonding MO(filled) and an antibonding MO (vacant). For a thermally induced reaction, the electrons move from the HOMO into the LUMO. As shown, the HOMO of butadiene has the correct symmetry to overlap in phase or constructively with the LUMO of ethylene. Hence, bonding occurs.

The Diels Alder reaction has several applications. These include the synthesis of pesticides such as Dieldrin and Aldrin. Also, the syntheses of flame retardants and the agricultural fungicide, Captan.

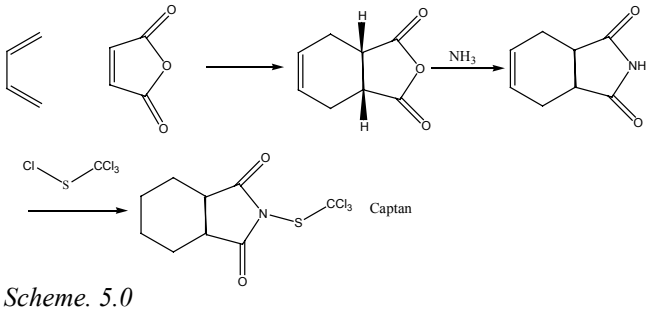

Scheme. 5.0

Compounds (1)–(4) will be fully characterized via 13CNMR, DEPT, COSY, HMBC, HMQC etc. Also, the medicinal activities of these synthesized compounds will be investigated.

Chemistry / Physics of Materials

The sol-gel Process: a method to prepare synthetic materials and to understand natural materials.

THIERRY WOIGNIER (1,2), J. PRIMERA (3), L. ANES (3)

(1) UR Seqbio IRD-PRAM, Le Lamentin, Martinique, France, woignier@univ-montp2.fr
(2) CNRS, Université de Montpellier 2, France
(3) Departamento de fisica, FEC, LUZ, Maracaibo, Venezuela

Introduction

Since the "First International Conference on Glasses from gels", in Padova (1981) it has been shown that the sol - gel process could be a new way to synthesise materials as different as ceramics, glasses or composites, in the form of bulk products, films or fibres.
The main advantages of the sol - gel route are :

- the high purity of the starting compounds which can be preserved during the process,
- for multicomponent systems, a good homogeneity of the different chemical species can be achieved by chemical reactions in the starting solution,
- the control of the morphology of the product, film, fibre, bulk materials, by the adjustment of the viscosity at room temperature,
- in the case of glass composition the gel is amorphous and can be transformed into a glass in a low temperature range, without melting or refining .

However , the gel science techniques and concepts could be extrapolated for natural materials like allophanic soils. Allophanic soils are interesting in terms of environmental properties especially because of their potentialities as sinks for "greenhouse gases": Allophanic soils exhibit higher organic carbon content (usually by a factor 4) than the one measured in other clay soils. So, there is a need to establish correlation between the sequestration mechanism of carbon in allophanic soils and other soils physical parameters.
These volcanic soils comprise weathering products such as allophanes originating from the sedimented volcanic ash and volcanic and allophanes aggregates have physical features very close to that of synthetic gels. Like synthetic gels, allophane are amorphous minerals, very porous, a density close to 0.5 g/cm^3 and a high specific surface area (700-1100 m^2/g). Like gels allophanes aggregates have fractal geometry. We use this analogy between allophanes aggregates and synthetic gels and we present results on the physical properties of allophanic soils preserved by supercritical drying technique (largely used in the gel science). The objective is to characterize the true structural properties of these soils, at the microscopic scale.We will also discuss the C content of these soils and possible correlation with the pore volume features.

Results

The figure1 shows the evolution of the C percent versus allophane percent in different volcanic soils in the Caribbean French island "Martinique" and confirm the influence of the allophanic structure on the C (or N) content.

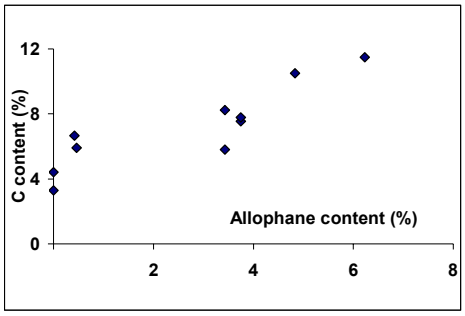

Figure 1: evolution of the C content versus the soil allophane content

Allophanic soils behave as gels during a classical drying with an important irreversible shrinkage which can modify the soil physical properties. The supercritical drying is a technique successfully used to carefully dry synthetic gels like silica gels and we have applied the supercritical drying procedure to control the drying step for allophanic soils. The objective is to preserve the structure and physical properties of the soils, which is affected by the classical drying .
We show that the textural properties such as specific surface area or mean pore size are higher for the supercritical dried samples compared to the classical dried samples, indicating the preserving effect of the SCD.

So, the allophanic features are preserved showing the interest of this drying method to have a correct description of the porous soils features. Thanks to this approach we show correlation between the true specific surface area (preserved by the supercritical drying) and the C content in the allophanic soil.

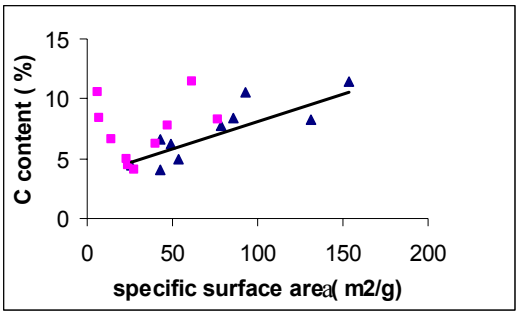

Figure 2: evolution of the C content versus the specific surface area (the blue triangles corresponds to the supercritically dried samples and the pink squares to the classical drying.

This study has clearly evidenced that the supercritical drying could be useful to preserve the organization of the solid phase of allophanic soils. This new way to dry the soil before analysis would allow getting a more precise and truer description of the soil organization.

Figure 3 :TEM micrograph of an allophanic soil (the micrograph width is 600nm).

To confirm our analogy where allophane aggregate could be considered as natural gels the figure 3 shows the TEM micrograph of allophanic soils. The allophane structure is a very open structure made of aggregated small particles (≤ 5 nm) building clusters with size close to 30-50 nm. This clusters can stick and form larger aggregates. This description is in agreement with a qualitative fractal description and SAXS experiments have estimated the fractal dimension Df close to 2.5 (similar to the fractal dimension of gels aggregates).

All of these results allow proposing of an explanation for the mechanism of the C sequestration in allophanic soils. The large specific surface area is the signature of small pore size. Associated to the fractal (and consequently tortuous) structure, the permeability at the scale of the allophane aggregates would be very low. For C species located in or near the allophane aggregates, possible exchange or chemical reactions with others chemical species will be difficult because of this low permeability. So, C should be preserved and trapped in the fractal aggregates. It is not possible to measure the permeability at the scale of the allophane aggregates but fractal geometry allows deriving the permeability at the aggregates scale.

What is the permeability of a fractal aggregate? A simple approach of this question could be resumed as follows. It exists in the literature a relationship which relates the permeability K with the relative density ρ_r and the mean pore size d of a porous object. This relation is called Carman- Kozeni equation. $K \propto (1- \rho_r)\, d^2$.

This equation express that the K value increases with porosity and with the size of the pores, allowing the fluid flow. This equation has been successfully applied to many type of granular material. In the case of a fractal aggregate we know that the evolution of the local bulk density is $\rho\,(l) \propto l^{Df-3}$. If we apply the scaling relation between ξ and a, the limits of the fractal aggregates we get:

$$\rho\,(l) \propto \rho\,(a)\,[l/a]^{Df-3}.$$

The mean pore size decreases when the length scale decrease and we find that the local permeability (inside the fractal aggregate) varies as: $K\,(l) \propto (1-(l/a)^{Df-3})\, l^2$, showing that the permeability strongly decreases when the length scale decreases.

Conclusions

These results mean that the fluids will have more difficulty to migrate inside the porous and tortuous porosity of the fractal aggregates. The fluid will be confined and trapped in the porosity and the chemical exchanges inside the fractal aggregates will be poor. This lower and lower permeability can be a part of the explanation concerning the high carbon content sequestrated in allophanic soils.

Chemistry / Physics of Materials

Extraction and Isolation of Natural Products from Momordica *Charantia*,

R.C.JAGESSAR*, A. MOHAMED.

Department of Chemistry, University of Guyana, Guyana - raymondjagessar@yahoo.com

Abstract

Natural products are the secondary constituents of plants, organisms and microorganisms that are of restricted occurrence to the plant or organism. There is an urgent need at the moment to screen plants for natural products, both from a chemical and economic point of view. These include their use in the field of medicine as drugs, components of drugs and as herbal medicines. Also, their use as poisons, stimulants, perfumes, spices, narcotics, hallucinogens and their application in industrial processes.

We are particularly interested in the medicinal aspect of natural products as drugs derived from natural products can result in the influx of huge financial investment. Also, research in natural products can lead to the discovery of drugs that have anticancer, antiaids, antiSARS activities and even useful against the fight of the recent H5N1 bird flu virus. Over sixty percent of the pharmaceutical drugs currently in use have their origins in natural products. Examples, include morphine for pain relief, quinine for malaria and digitoxin for cardiac disorders.Taxol, the diterpenoid anti cancer drug was first isolated from *Taxus brevifolia* in 1962.Since then two drugs were approved, one for breast and the other for ovarian cancer.

Band carylla, *Mormordica Charantia* is a slender climbing vine with long stalked leaves and yellow solitary male and female flowers borne in the leaf axils. The fruit is oblong, resembling a cucumber. The dried leaves of *Mormordica Charantia* were solvent extracted repeatedly thrice with distilled hexane, dichloromethane and methanol over a period of several days. Solvents were removed in *vacuo* to yield viscous oils of varying colour. The viscous oils of the hexane, dichlormethane and methanol extracts were separated via silica gel column chromatography to yield white solids, yellow solids, yellow viscous liquid, green solid of varying R_f values. For example, the dichloromethane extract was separated and yielded three useful fractions of R_f values 0.27, 0.48 and 0.53. The hexane extract yielded fractions of R_f values 0.34, 0.53. The methanol extract yielded five fractions of R_f values: 0.65, 0.88, 0.97, 0.98, and 0.92. Their spectroscopic nature is currently been investigated to establish purity and structural assignments. For example, the hexane fraction yielded a component that is mainly lipophilic in structure as suggested by ^{1}HNMR and ^{13}CNMR spectrum shown on the poster presented. The medicinal activity of these compounds is currently been investigated.

Chemistry / Physics of Materials

Ground and excited states vibrational frequencies of 3-amino-2-chloropyridine

V. N VERMA

Department of Chemistry, Faculty of Natural Sciences, University of Guyana, Turkeyen Campus
GUYANA (SOUTH AMERICA) - chemistry88@lycos.com

Abstract

The electronic transitions in pyridine are n-II* and II – II* transitions in which the n-II* transition corresponds to the longer side of the wavelength and the II-II* to the shorter wavelength side (Sponer and Stucken, 1946). Further it is now established that the most probable transition in substituted pyridines is due to the n-II* transition.

The present study of the ultraviolet absorption spectrum of 3-Amino- 2-Chloropyridine reports the changes occurring due to the substituted amino- and chloro- groups simultaneously in the pyridine molecule.

Manson has discussed the effect of the substitution and has shown that for each specific type of transition, substitution effect depends upon the nature of the substituents and the position of substitution with respect to the ring nitrogen which has occurred in the analysis of the spectrum.

Experimental details

3-Amino-2-Chloropyrine is a solid molecule having its mp around 80°C. A special design of the experimental set up is therefore required. The spectra were photographed on a Q-24 Zeiss Medium Quartz Spectrograph. The hydrogen lamp of 150W was used as a source of Continuum. To get the optimum condition to develop the bands, the lengths of the absorption tubes of a diameter 2.5 cm were chosen as 30, 40 and 50 cm. The quartz windows were fixed on either side with the help of sealing wax. The sample of an amount 0.5 g was placed inside the absorption tube though an other narrow tube connected in the middle of this absorption tube. A vacuum rotary pump was connected then with this narrow tube to evacuate the air from the absorption tube. Thus the pressure inside the absorption tube was approximately below the normal pressure. The narrow tube was then sealed using the gas burner. The above process was repeated for each absorption tube. The absorption tube is then placed inside a suitable length of the heating furnace. The absorption spectra were then photographed at different temperatures of 25, 30, 35, 40°C on the proper photographic plates. The exposures were given for 15- 30 minutes. A copper arc was also photographed as a standard source for the purpose of measurement. The bands were found developed at the length of 50cm at a temperature of 30°C.

Measurement of the plates

After washing and getting dried, the plates were measured to locate the positions of the absorption bands using the comparator and standard chart. The wavelengths of the absorbed bands are given in Table 1.

Analysis of the spectrum

The molecule ($C_5H_5N_2Cl$) belongs to C_{2v} point group for the mass point consideration of the amino and chlorine groups. The molecule is a non-linear molecule. There are 39 bands observed in the present investigation. The most strong band observed at 32982 cm^{-1}(3031.95A^0) is assigned as the (0,0) band. Thus a red shift of 5368 cm^{-1} has been observed with respect to pyridine. The shift in the position of the (0,0) band in comparison to the other similar molecules is shown in Table 2. The table 2 shows that the position of the (0,0) band in 3-Amino-2-Chloropyridine is near to the (0,0) band of the 3-Aminopyridine than the 2-Chloropyridine and thus a dominating effect of the amino group is observed.

Table 1: Vibrational Assignments for 3-Amino-2-Chloropyridine Vapour

Wave-number (cm^{-1})	Intensity from (relative)	Separation (0,0) band (cm^{-1})	Assignments
32410	w	-572	C-C-C in- plane bending
32459	w	-523	0+650-572-2x286
32584	m	-398	0+153-572
32609	w	-373	0+650-572-2x151
32698	m	-284	C-Cl in- plane bending
32761	m	-221	0+650-572-2x151
32796	s	-186	0+538-151-572
32831	ms	-151	C-Cl out of plane bending
32855	m	-127	0+153-284
32876	m	-106	0+650-284-3x151
32961	m	-21	0+538-2x284
32982	vs	0	(0,0) band
33013	w	31	0+2x284-538
33044	w	62	0+650-286-2x153
33071	w	89	0+650-572
33097	w	115	0+650-538
33135	m	153	C-Cl out of plane bending
33170	m	188	0+727-538
33197	w	215	0+650-286-153
33239	w	257	0+538-284
33268	m	286	C-Cl in plane bending
33291	m	309	0+2x153
33314	mw	332	0+2x727-2x572
33333	w	351	0+650-284
33411	m	429	0+153+286
33442	w	460	0+3x153
33481	w	499	0+650-151
33520	s	538	C-C-C in-plane bending
33542	ms	565	0+2x286
33595	ms	613	0+2x153+286
33632	m	650	C-Cl stretching
33679	m	697	0+153+538
33709	m	727	C-C ring breathing
33813	w	831	NH_2 wagging
33964	w	982	0+153+831
34002	m	1020	C-C-C trigonal bending
34038	m	1056	0+2x538
34245	w	1263	0+538+727
34305	w	1323	0+286+1020

s=strong intensity, ms= medium strong, m= medium, w=weak

Table 2: Position of the (0,0) Band in some Substituted Pyridines

Molecules	Position (in cm-1)	(in A0)
3-Amino-2-Chloropyridine	32982	3031.95
Pyridine	38350	2607.56
2-Aminopyridine	33465	2988.19
3-Aminopyridine	33049	3025.81
3-Chloropyridine(II-II*)	35795	2793.68
(n-II*)	34900	2865.32
4-Chloropyridine	36455	2743.10
2,6-Dichloropyridine	36083	2771.39
3,5-Dichloropyridine	35498	2817.06

Acknowledgement

The author is grateful to the Laser and Spectroscopy Laboratory, Department of Physics, Banaras Hindu University to provide the experimental facilities to perform this experiment

References

Sponer ,H & Stucken, H. (1946) J.Chem.Phys. 14, 101

Mason, S.F. (1960) J.Chem.Soc. 219 & (1962), 493.

Pandey, B.R. (1967) Ind.J.Pure Appl. Phys. 5,288.

Pandey, B.R. (1968) Ind.J..Phys. 42, 269.

Bhujle , V.V. & Pandey, M.R., (1970) Ind.J.Pure Appl.Phys. 8,820

Tripathi,R.S. & Pandey, B.R. (1974) Ind.J.Pure Appl. Phys. 12, 64.

Chemistry / Physics of Materials

Effect of Processing Method on Shelf Stability of Coconut Water

HILARY G. ARSCOTT AND IAN A. LAMBERT

Department of Chemical Engineering, University of The West Indies, St. Augustine Campus
Trinidad and Tobago - ianmar5757@yahoo.com

Abstract

The effect of different processing methods on the shelf life of refrigerated coconut water at 2ºC was investigated. Processing methods included pasteurization, microfiltration and/or UV sterilization. The primary objective was to extend the refrigerated life of the bottled product to a minimum of one month.

Water from green coconut, harvested at the age of approximately seven months (with no or very little jelly), was extracted, quickly chilled and coarse filtered through muslin cloth to remove solids and particulate material. The water was then clarified with polyvinylpyrrolidone (PVPP), with and without added ascorbic acid and then further processed using the above methods. The bottled product was stored under refrigeration (2ºC) for shelf life studies. Analyses included changes in pH, turbidity, total soluble solids, total plate counts, yeasts and moulds and coliforms for microbial load and organoleptic testing.

Results showed that the shelf life of the refrigerated bottled product was extended to a month after pasteurization and the natural flavour and colour of coconut water were retained. Sensory evaluation showed that the taste and odour of coconut water prepared by pasteurization without the addition of ascorbic acid and PVPP were consumer acceptable after one month on storage at 2ºC ($P \leq 0.05$). The use of microfiltration and/or UV sterilization was not successful in achieving a product lasting more than seven days.

Introduction

The production of shelf stable coconut water has long interested food processors, and within the last few years the regional and international markets for fresh coconut water have grown tremendously. Most commercial production of coconut water is currently carried out in Indonesia, the Phillipines and Thailand using high temperature/short time (HTST) pasteurization, but this method of thermal processing has a major drawback - it eliminates not only the risk of bacteria, but some of the coconut's water nutrients and almost all of its delicate flavour. As a result this severely limits the product's marketability. In an attempt to address this problem, the FAO (2001) developed a cold sterilization process that retained its flavour and all its nutritional characteristics. The major drawback for small scale processors in the Caribbean is that the coconut water produced by the FAO process was packaged using an aseptic filling operation with standard Tetra-Pak like packaging. This aseptic filling operation requires a major investment which cannot be met by small scale processors. It is therefore still necessary to develop appropriate process conditions and packaging forms to extend the shelf life of coconut water to beyond the ten days currently obtained. The process however should be as simple and inexpensive as possible so that the technology could easily be transferred to, and adopted by the small scale farmer while at the same time providing a shelf life so that the more lucrative export markets can be easily accessed. The basic objective of this research project was to determine the effect of several processing methods on the preservation and shelf life of coconut water under refrigerated conditions. Processing methods include pasteurization, filtration, micro-filtration and ultraviolet radiation. The effect of processing on taste and microbial load of the product were also investigated.

Materials and Methods

Water from green coconut, harvested at the age of approximately seven months (with no or very little jelly), was extracted, quickly chilled and coarse filtered through muslin cloth to remove solids and particulate material. The water was then clarified with polyvinyl-pyrrolidone (PVPP), with and without added

ascorbic acid and then further processed using pasteurization, microfiltration and/or UV sterilization. The bottled product was stored under refrigeration (2ºC) for shelf life studies. Analyses included changes in pH, turbidity, total soluble solids, total plate counts, yeasts and moulds and coliforms for microbial load and organoleptic testing.

Results and Discussion

The treatment of fresh coconut water with coarse filtration, with or without ascorbic acid (150 mg/L), packaged, nitrogen flushed, pasteurized and subsequently stored at 2ºC was found to produce a good quality drink up to four weeks. Minimal changes in pH and ºBrix were observed and the microbial load after processing was within the standards specified.

In the case where the fresh coconut water was additionally treated with PVPP and pasteurized results show that the product was microbiologically safe. Also, in terms of taste and colour, there was no significant change in the product.

However in the experiments where UV sterilization was used the coconut water was not acceptable as it had a burnt/scorched and bland flavour. This may have resulted from too high a temperature or too long a residence time in the UV chamber. In addition the microbial load of the coconut water exiting the lamp was high.

Sensory evaluation of bottled coconut water samples which lasted for at least one month were statistically analyzed using the Analysis of Variance (ANOVA). The pasteurized coconut water containing no ascorbic acid and PVPP after four weeks of storage was the most preferred of the three samples tested by the panelists. The smell of the fresh coconut water was preferred over the one month old coconut water samples. However there was no significant difference detected in the smell of the fresh versus the stored product at the 5% level.

Chemistry / Physics of Materials

Introduction of Electron Microscopy to The University of the West Indies, St. Augustine, Trinidad and Tobago

DAVID HINDS AND R. SAUNDERS

Electron Microscope Facility, Physics Department, The University of the West Indies, St Augustine, Trinidad and Tobago - dhinds@fsa.uwi.tt

Abstract

Two Electron Microscopes, one Scanning Electron Microscope (SEM- Phillips 515) and one Transmission Electron Microscope (TEM- Phillips 420) were installed, in 1987, at the Eric William's Medical Sciences Complex in Trinidad. These microscopes were expected to be used for tissue and bone microanalysis in the Pathology and Microbiology Department. However, up to when these microscopes were transferred to the University of the West Indies in 2001 they were never used on account of the lack of important ancillary equipment and a management and technical infrastructure for the microscopes. In 2002 the Microscopes were made operational by a small UWI team under the guidance of Prof R. Saunders of the Physics Department. They were subsequently optimised and certified by an engineer from Philips Holland, the manufacturer. Since then the University of the West Indies, has digitised the SEM and purchased some key equipment to enhance the operation of the Electron Microscope facility.

Introduction

The two Electron Microscopes were handed over by the Eric Williams Medical Science Complex to the University of the West Indies in 2001 and were made operational by the University of the West Indies Physics Department. The Department has these two microscopes operational and available for use inside and outside of the University.

Scanning Electron Microscope

Transmission Electron Microscope

To date the University has had three workshops at the Electron Microscope Suite to assist in training and sensitising academic and technical staff to the contribution that electron microscopy can make to teaching and research.

One workshop was on TEM sample preparation and operation of the TEM, another was on the SEM operation and sample preparation. Finally there was a Nephrology Workshop, which focused on Electron Microscope techniques for renal biopsies. The workshop presenters were all well respected regional and international electron micro-scopists from Jamaica, Guadeloupe and Canada.

Materials and Methods

As mentioned the university has purchased some key equipment to enhance the Em facility they include a Critical point dryer for freeze drying tissues and other soft biological material for the SEM. A sputter coater for coating samples for the SEM. A vacuum oven for the drying of resin in the Tem sample preparation process. Other Tem sample preparation material to include chemicals,

stirrers, resin, grids and all that is needed for Tem sample preparation.

Critical point dryer

Sputter coater

Results and Discussion

The analyses done by these microscopes to date are from various disciplines. The Physics Department has been analysing clays, ceramics and other materials. The Life Sciences have been addressing the micro-analysis of plants and insects. The work of the Engineering Faculty has been on fossils related to oil drilling. Finally the Medical Faculty has been doing work on the microanalysis of tissue, viruses and bones.

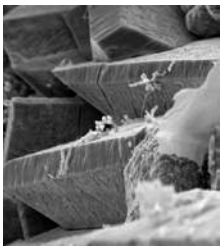

Kidney Stones

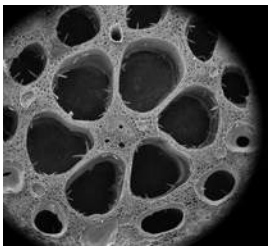

Stem cross-section

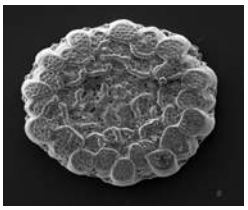

Fossils

Insect

Conclusion

These microscopes are expected to make a significant contribution to the work of students, staff and private organizations in the future. Our hope is to work with many of our Caribbean neighbours as possible to enhance our research capabilities in this region.

Acknowledgements

MR. Shazaad Ali Shah (UWI, Trinidad)

Department of physics (UWI, Trinidad)

Chemistry / Physics of Materials

Analytical Scanning Electron Microscopy approach for Caribbean ceramic identification

B.VICENS*, J.S. GUIBERT*, J.L. MANSOT, D. HIMMEL

** Protection Recherche et Etude du Patrimoine Subaquatique (PREPASUB), 2729 Chemin de Tabanon, 97170 Petit-Bourg , Guadeloupe – prepasub.971@orange.fr*
Groupe de Technologie des Surfaces et Interfaces (GTSI EA 2423), Université des Antilles et de la Guyane, Faculté des Sciences Exactes et Naturelles, Campus Fouillole, 97159 Pointe à Pitre cedex Guadeloupe (France)

Abstract

One of the problems encountered with pottery in archaeological studies is the identification of the place of manufacture. To achieve this purpose, chemical and physical analyses can be envisaged, as far as they are non-destructive or require extremely small samples to avoid visible damages of the pieces. In this work Analytical Scanning Electron Microscopy (ASEM) is advantageously used in order to identify the chemical composition of micro samples (10^{-3} mm^3) from original pieces in order to establish the material of production.

Experimental background

At the end of 18th century, it is admitted that potter's workshops from south of France as Vallauris are supplying Guadeloupe with cooking utensils. Old pottery pieces found in the bay of Le Moule (North East of Guadeloupe) during sub aquatic surveys present characteristic shapes of Vallauris manufacture. During that period Fidelin's potter's workshop mainly produced sugar moulds and started to product cooking utensils. Analytical Scanning Electron Microscopy is used to try to identify the origin of the potteries found in the bay of Le Moule. For that purpose, pieces collected at the Fidelin's workshop archaeological site, considered as standards, were chemically analysed by ASEM. The ASEM analyses of the pieces discovered in the bay of Le Moule are compared to Fidelin's standard ones.

Experimental conditions

The experiments were carried out on an Analytical Scanning Electron Microscope Hitachi associated with a Link Energy Dispersive X rays Spectrometer (EDXS).
The electron microscope was running at an acceleration voltage of 20 kV using a LaB_6 filament as electron source.

Samples preparation

Micro samples of ceramics and superficial varnish of archaeological pieces are extracted by slight scratching of the surfaces (the sampling is not visible after extraction). The fine particles are deposited onto an aluminium support and coated under vacuum with a thin carbon film by evaporation.

Materials

The samples studied are potteries.
Those used as standards were collected on the archaeological site of the Fidelin's workshop. This one, located in the Sainte Island "Terre de Bas", was operating at the end of 18th century. At that period its main production was concerned with sugar moulds [1].
The other unidentified pieces were collected during sub aquatic surveys in the bay of Le Moule well known as the main port destinated to sugar exportation [2].
Some cooking utensils were discovered and initially identified as a Vallauris production (south of France) due to their shape and internal varnish [3].

Cooking utensils, 19th century, from 'Le Moule'

Conclusion

X rays analyses pointed out that the chemical compositions of the clay an internal varnish of the two types of samples are similar. This seems to support the hypothesis that, during this period, Fidelin's utensils started to supersede French production in the supplying of Guadeloupe. Other analyses are in progress to confirm these first results. Sub aquatic surveys on various sites of Guadeloupe coast aim to establish the commercial routes used by Fidelin's workshop to share out its production.

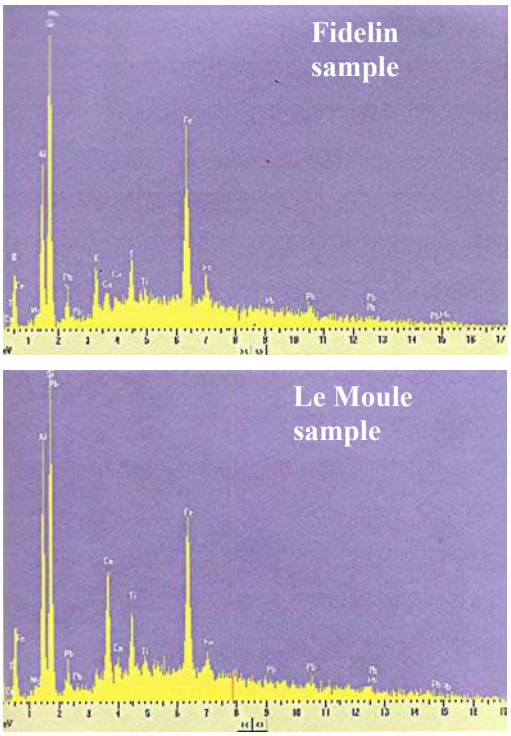

Clay X Ray analysis showing similar compositions

Bibliography

[1] GABRIEL Isabelle, Rapport de la seconde campagne de fouilles programmées de l'habitation-poterie Fidelin à Terre de Bas, DRAC Guadeloupe Basse-Terre, 2005

[2] VICENS Bernard, Prospection sondage dans le port du Moule, Rapport, Petit-Bourg, 2002- 2003.

[3] Pignates et poêlons poterie culinaire de Vallauris, Catalogue d'exposition, Réunion des musées nationaux, Paris, 1996.

High Spatial Resolution Raman Spectroscopic Mappings in Dynamic Lubricated Sphere - Plane Contacts: Application to Pressure and Thickness Profile Measurements

D. HIMMEL, Y. BERCION, J.L. MANSOT

Groupe de Technologie des Surfaces et Interfaces (GTSI EA 2432)
Université des Antilles et de la Guyane, Faculté des Sciences Exactes et Naturelles, Campus Fouillole, 97159 Pointe à Pitre cédex Guadeloupe (France) - dhimmel@univ-ag.fr

Keywords: Raman microspectroscopy, Tribology, Pressure

Abstract

Photonic microscopes are extensively used for morphologic studies in various fields of material science. The coupling of a photonic microscope with a visible spectrometer in the early eighties led to the development of Raman microprobes [1] which capabilities today allow us to acquire high energy (0.5 cm^{-1} resolution) and high spatial resolution (probe diameter less than 10 µm) spectroscopic images.

In this work, quantitative Raman microscopy is applied to acquire spectroscopic images in elastohydrodynamic lubricated (EHL) sphere / plane contacts. For this purpose, an experimental set-up coupling a Raman microprobe to an elasto-hydrodynamic ball on disc tribometer is developed (Fig. 1). It allows us to acquire Raman spectra in the dynamic lubricated contact on areas of 10 µm diameter and film thicknesses down to 0.1 µm.
The model lubricant used is 5P4E presenting a strong Raman band near 1000 cm^{-1} corresponding to the trigonal breathing vibration mode of the aromatic rings.

Spectroscopic images composed of 15x15 spixels (spectroscopic pixel corresponding to the spectrum of one point in the contact) are obtained (Fig. 1 b,c).
The frequency shift of the 1000 cm^{-1} Raman band is classically interpreted in terms of pressure changes [2]. Due to the cylindrical shape of the Raman probe, the intensity of the 1000 cm^{-1} Raman band is linearly related to the thickness of the lubricant film in the contact.

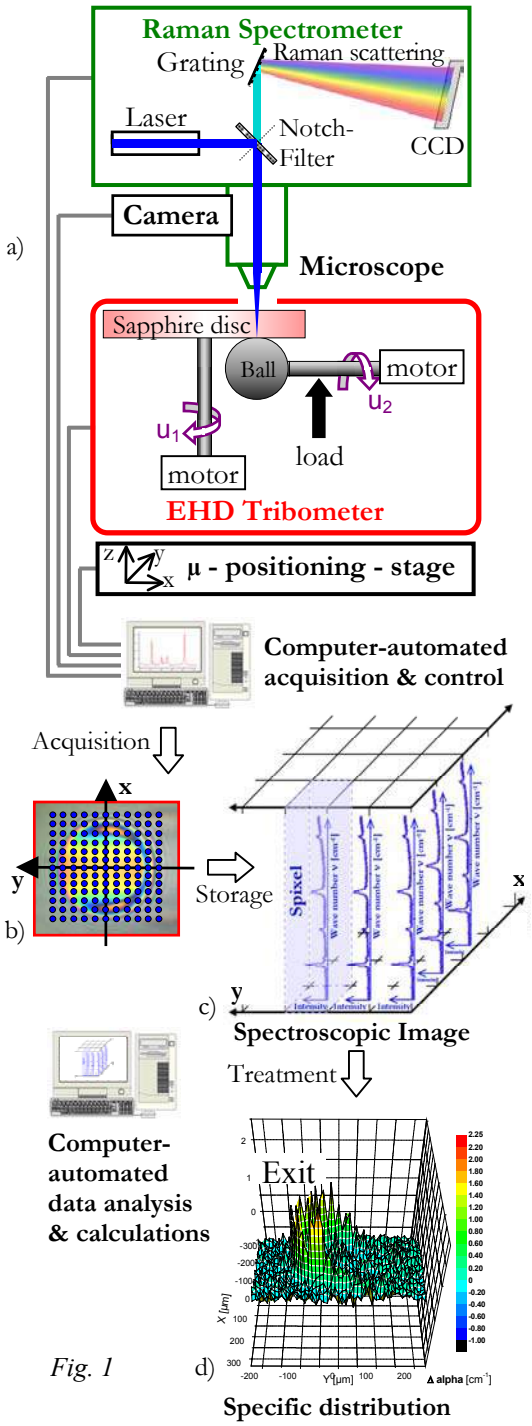

Fig. 1

The calibration and quantitative interpretation of Raman signals in terms of pressure [2-5] and lubricant film thickness allows us to obtain simultaneously high spatial resolution pressure and thickness distributions in pure rolling and rolling sliding conditions (Fig.2).

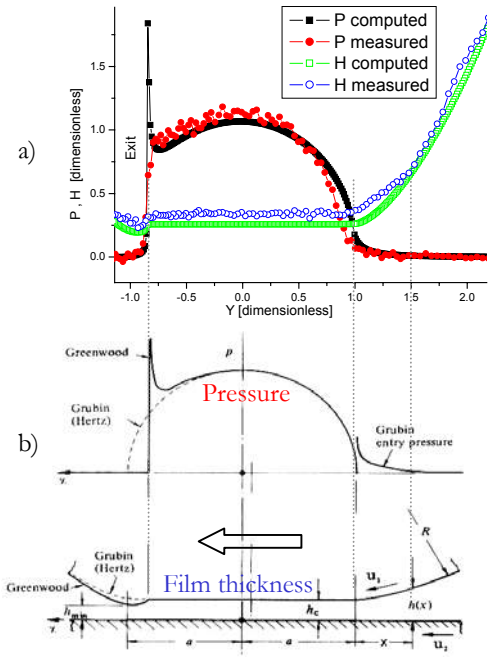

Fig.2
a) Pressure and Film thickness distributions simultaneously measured in an EHD-contact (load F_N=88 N, speed u_e=0,15 m/s , Lubricant entry Temperature T=39±1°C, pure rolling) compared to the distributions computed by Prof. A.A. Lubrecht for the dimensionless values M=127 and L=26.
b) Ideal pressure and film thickness distribution profiles by Hertz (1882) – Grubin (1949) - Greenwood (1972) after K.L. Johnson [6].

Acknowledgments

The authors acknowledge the CNRS, the Conseil Régional de la Guadeloupe and the Fond Social Européen for their financial supports.

References

[1] P. Dhamelincourt, "Developments and applications of the Laser Raman Microprobe MOLE", Proc. of the 14th Microbeam Analysis Society Conf., San Francisco Press (1979)

[2] J.L. Mansot, "Etude des pressions dans un interface sphère/plan en présence d'une couche mince organique", PhD Thesis, University of Lyon, France , n° 86.50 (1986)

[3] I. Jubault, J.L. Mansot, P. Vergne and D. Mazuyer, ASME Trans., J.of Tribology, vol.124, (2002) 114.

[4] Jubault, J. Molimard, A.A. Lubrecht, J.L. Mansot and Ph. Vergne, Tribology letters, v.15, n° 4, (2003) 421.

[5] Himmel D., PhD Thesis, (2005) Université des Antilles et de la Guyane

[6] JOHNSON, K.L. Contact Mechanics. London : Cambridge University Press, 1985

Chemistry / Physics of Materials

Band Structure Calculations Applied to Structural Determination of Graphite Intercalation Compounds: the Case of CaC_6

K. DELBÉ (1), PH. THOMAS (1), N. EMERY (2), C. HÉROLD (2), F. BOUCHER (3), J.-P. BUISSON (3), P. LAGRANGE (2) AND J.L. MANSOT (1)

(1) Groupe de Technologie des Surfaces et Interfaces, (GTSI E.A. 2432), Faculté des sciences Exactes et Naturelles, Université des Antilles et de la Guyane, 97159 Pointe-à-Pitre Cedex – kdelbe@univ-ag.fr
(2) Laboratoire de Chimie du Solide Minéral, UMR 7555, Université Henri Poincaré Nancy I, B.P. 239, 54506 Vandœuvre-lès-Nancy Cedex.
(3) Institut des Matériaux de Nantes Jean Rouxel, UMR CNRS 110, 2 rue de la Houssinière, 44072 Nantes cedex 03, France

Keywords: crystalline structure, band structure calculation, structure optimisation

Due to the presence of a Van der Waals gap in its structure, Graphite can undergo intercalation by electron donor or electron acceptor species [1]. Depending on the intercalated species and the intercalation processes various stoichiometries can be obtained.

In the case of stage one compounds, M representing the intercalated elements, MC_6 type compounds are obtained with Li, Sr, Ba and MC_8 with K, Rb and Cs. For the MC_6 compounds three possible crystalline structures were deduced from X-rays diffraction data: P6/mmm (LiC_6) [2], $P6_3/mmc$ (SrC_6, BaC_6) [3,4] and R-3m were proposed for the recently synthesized CaC_6 phase [5] (Fig.1).

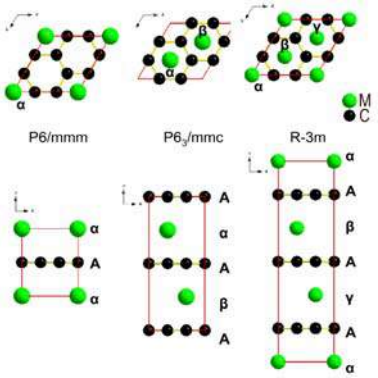

Fig.1 Representation of the three space groups observed for MC_6 compounds

In this work a band structure calculation approach is applied to the structural determination of the CaC_6 phase. In order to validate this theoretical approach, structural optimisations (VASP code) and total energy calculations (FLAPW method, Wien2k code) are carried out for the three well-known compounds (LiC_6, SrC_6, BaC_6) in the three possible structures (P6/mmm, $P6_3/mmc$, R-3m). It is demonstrated that in each case, the total energy is minimum for the experimentally deduced structure (see Tab.1).

The method is then applied to CaC_6 still presenting a structural ambiguity ($P6_3/mmc$ or R-3m).

The minimum energy is obtained for the R-3m structure strongly supporting the X rays data refinement results (see Tab.2).

	P6/mmm	$P6_3/mmc$	R-3m
LiC_6	**-57,292 eV** ΔE=0	-57,273 eV ΔE= 0,019 eV	-57,274 eV ΔE= 0,018 eV
SrC_6	-57,339 eV ΔE= 0,010	**-57,349** eV ΔE=0	-57,343 eV ΔE= 0,006 eV
BaC_6	-57,842 eV ΔE= 0,035 eV	**-57,877** eV ΔE=0	-57,867 eV ΔE= 0,020 eV

Tab.1 Total energy calculated for LiC_6, SrC_6 and BaC_6 for the 3 different space groups. ΔE is the difference between the total energy of a structure and the lowest one.

Symétrie	P6/mmm	$P6_3/mmc$	R-3m
Energie totale	-57,522 eV ΔE = 0,019 eV	-57,538 eV ΔE = 0,003 eV	**-57,541** eV ΔE=0

Tab.2 Total energy calculated for CaC_6 for the 3 different space groups.

Acknowledgements: The authors acknowledge the Conseil Régional de la Guadeloupe, the European Social Fund and the FEDER for their financial supports.

References

[1] M.Noel, R. Santhamam, Journal of Power Source, 72 (1998) 53-65.
[2] D. Guérard and A. Hérold, Carbon 13 (1975) 337-345.
[3] D. Guérard, M. Chaabouni, P. Lagrange, M. El Makrini and A. Hérold, Carbon 18 (1980) 257-264.
[4] D. Guérard and A. Hérold, C.R. Acad. Sc. Paris, t. 279 (1974) 455-456.
[5] N. Emery, C. Hérold, P. Lagrange, Solid State Chemistry, 178 (2005) 2947.

Chemistry / Physics of Materials

Development and Applications of a Flash Test Using High Powered Ultrasounds for the Fast Evaluation of the Durability of Painted Galvanized Steel Sheets

J. PIGERRE (1), P. RODRIGUEZ (1), Y. BERCION (2) AND J.L. MANSOT (2)

(1) Groupe de Technologie des Surfaces et Interfaces (GTSI EA 2432), Université des Antilles et de la Guyane, Institut d'Enseignement Supérieur de Guyane, Avenue d'Estrées Campus Saint-Denis BP 792, 97337 Cayenne Cedex, French Guyana.

jacques.pigerre@guyane.univ-ag.fr, - pablo.rodriguez @guyane.univ-ag.fr

(2) Groupe de Technologie des Surfaces et Interfaces (GTSI EA 2432), Université des Antilles et de la Guyane, Faculté des Sciences Exactes et Naturelles, Campus Fouillole, 97159 Pointe à Pitre cédex Guadeloupe (France). - Yves.bercion@univ-ag.fr, jean-louis.mansot@univ-ag.fr

Keywords : ultrasounds, cavitation, wet adhesion

Abstract

The present work is concerned with the development of a flash test using high-powered ultrasounds source in order to characterize the adhesion properties and long-term efficiency of mineral and organic coatings used for protection of steel sheets against corrosion. The examination of the damages processes of the protection coatings under ultrasonic solicitations allowed us to extract quantitative classification of behaviour in extremely good agreement with classical evaluation done on class 5 stand exposure.

Introduction

Steel sheets are extensively used in the Caribbean area for the roofing of houses and industrial walls buildings (figure 1 natural stand of exposure in Cayenne, French Guiana). Due to the high aggressiveness of the tropical climate, the protection against corrosion of such materials is done by application of galvanization coatings and further reinforced by various paint layers called "Paint Assembly" in the text [1].

The Paint Assemblies (PA1, to PA7) we studied were supposed to enhance the protection effect by addition of corrosion inhibitors in the primary layer and to reduce the intrusion of water to the paint/steel interface by the barrier effect of the finishing layer.

Figure 1 : stand of exposure located near the sea in Cayenne, French Guiana

The main problem encountered with these materials is the evaluation of their durability and long term efficiency. Up to now, the classical procedure used to evaluate these properties is the exposure in severe environmental conditions in order to accelerate the damage processes. This is done in stands where UV, moisture, temperature mechanical stresses can be applied simultaneously in a controlled manner. Such procedures need however long time experiments (up to ten years in natural exposure).

In this work, the developed flash test uses high power ultrasounds waves in aqueous medium in order to produce high mechanical stresses on the painted surface of the tested samples.

The samples

The schematic structure of the studied materials is presented in figure 2. The steel sheet is first covered by a zinc-based anodic layer of ten microns thickness [2]. Then a surface treatment based of chromates is applied to increase the adhesion of the paint. A primary layer of paint and a finishing one are then applied.

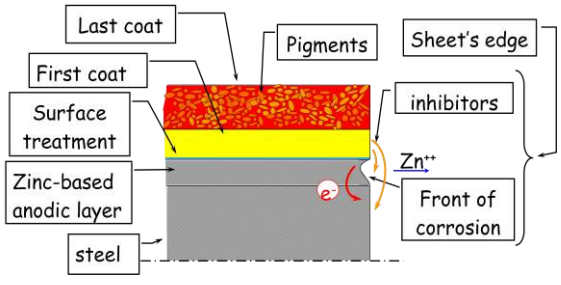

Figure 2 : strategy of protection in wet conditions[2]

Flash test set up

The experimental set up is presented in figure 3. 20 kHz ultrasounds are produced by means of piezoelectric ceramics generator [3].

The sample is glued on the tip of the generator and immersed in water. The displacement of the sample is controlled and the power is self adjusted to keep constant the amplitude of the movement of the sample. In our case the power was about 90 Watts.

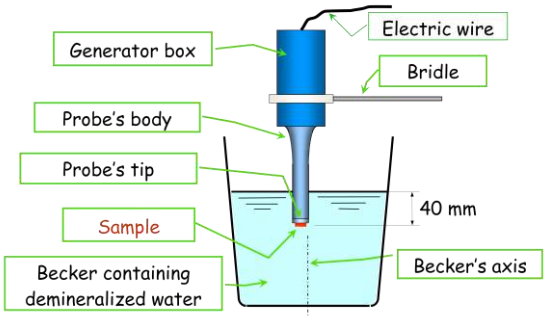

Figure 3: the "Flash test" device

The figure 4 shows a detail of the tip of the generator to show the sample fixing.
The sample is a small disk of eighteen millimetres and the studied paint coating is turned to the water.

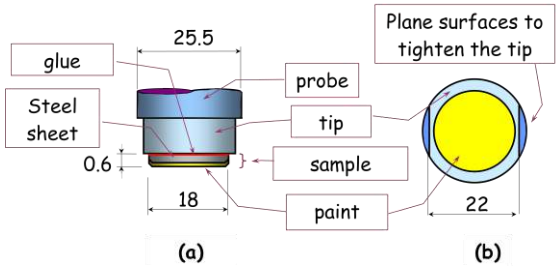

Figure 4 : probe's tip detail, (a) front view, (b) view from under

Outline on the mechanical effects of ultrasounds in water

As soon as the generator runs, a cloud of micro-scopic bubbles and water streams appears as schematically drawn in figure 5.

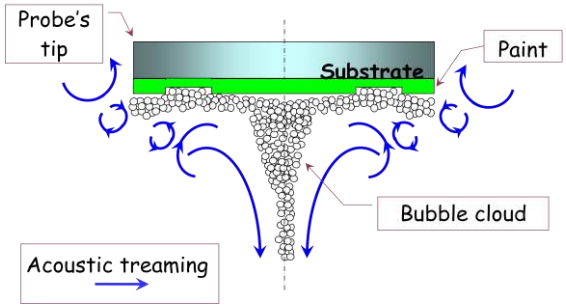

Figure 5: cavitation bubbles and acoustic streaming when the test is running

It has been previously shown that these cavitation bubbles are mainly composed of water vapour and some gas dissolved in the water. They are resulting from the fast movement of the solid surface [4].
The water streams increase the density of bubbles on a circular area on the sample. That can explain the distribution of the damages undergone by the samples during the test (figure 6).

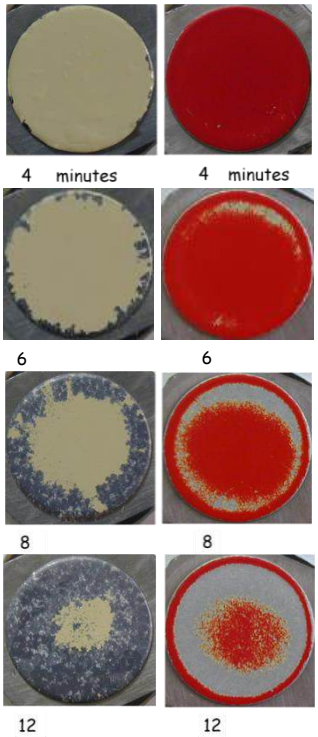

Figure 6 : successive aspects of 2 samples after 4, 6, 8 and 12 minutes of ultrasound solicitations

The numerical solving of the Rayleigh/Plesset equation allowed CHOUVELON et all [5] to deduce the evolution of bubble radius as a function of time for a 500 kHz ultrasonic source (figure 7).

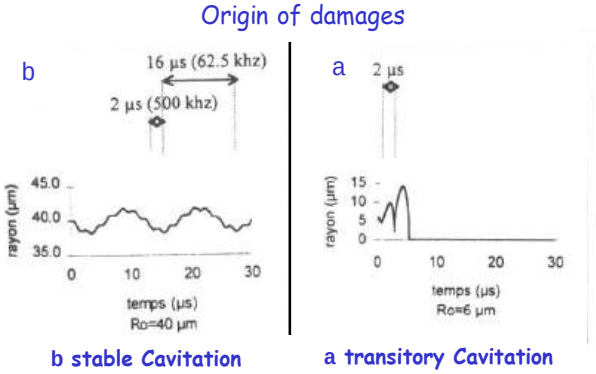

Figure 7 : evolution of the radius of two bubbles which have different initial sizes, according to M. CHOUVELON [5]

Two kinds of bubble are pointed out :
The figure 7a presents the evolution of the radius of a "transitory cavitation bubble". This kind of bubble is very small and resonates at the frequency of the ultrasonic waves. It rapidly collapses and disappears. During the collapse these bubbles are able to produce locally high pressures [6] (up to 100 MPa) by the so called "water hammer effect" simulated in figure 8.

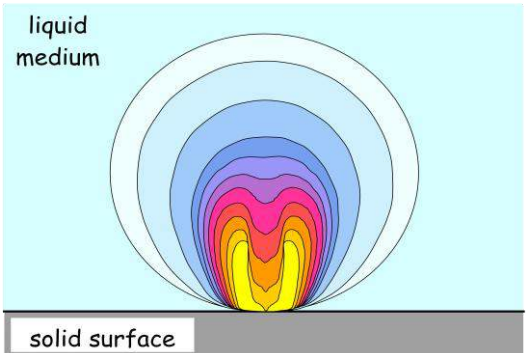

Figure 8 : evolution of a bubble shape during the collapse near a solid boundary, according to M. S. PLESSET [6]

The figure 7b shows the oscillations of the radius of a "stable cavitation bubble". The radius of such a bubble is larger than the transitory one and oscillates at a lower frequency. In our case (with an ultrasound source of 20 kHz), the frequency of the oscillations are in the hear able range (which explain the acoustic sound detected during the test).
The figure 9 illustrates the pilling process induced by the stable cavitation bubble oscillating near a paint boundary. In these case, water acts as a real lever and draw the paint away from the substrate during the bubble motion.

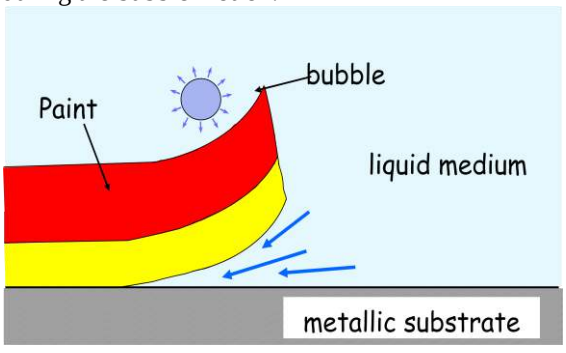

Figure 9 : oscillations of a stable cavitation bubble near a paint boundary

Damages generated by the two types of cavitation bubbles

Damages generated by the two kinds of cavitation bubbles are mainly pitting induced by the "water hammer effect" (figure 8) and pilling due to lever effect induced by the oscillations of stable cavitation bubbles (figure 9).

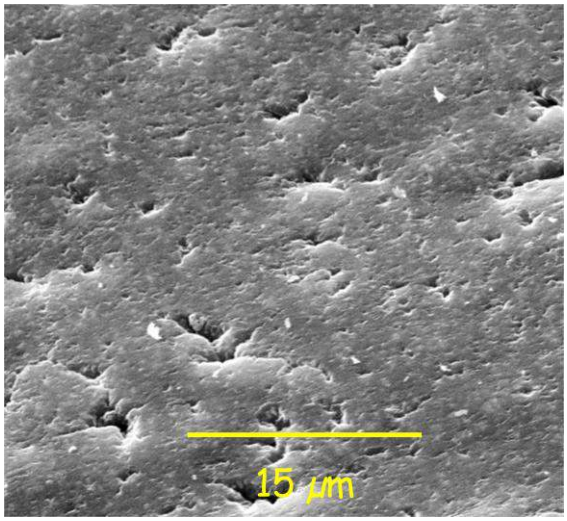

Figure 10: aspect of the surface damaged by water hammer effect, view by SEM

In figure 10, a lot of small cracks can be seen with a star shape, which are attributed to the action of collapsing bubbles. The extracted particles are small (few microns size).
Stable cavitation bubbles, on the other hand, when they are generated near the paint/metal interface (figure 11) are able to extract particles in large flakes (some tens of microns size).

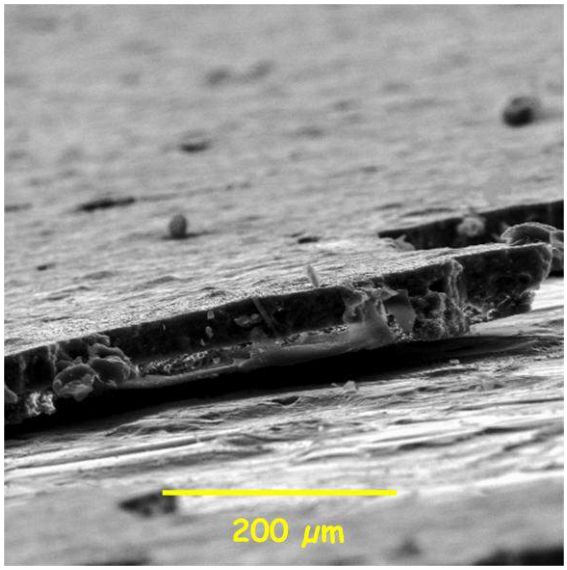

Figure 11: pilling effect due to oscillation of stable cavitation bubbles, view by SEM

Depending on the adhesion energy of the coatings on the substrate, one of the two mechanisms will be favoured : pitting in the case of high adhesion and pilling in the case of weak adhesion. These two

mechanisms lead to stripping kinetic curves which present small (pitting) or large (pilling) dispersions (figure 12).

Flash test procedure and data treatments

The sample glued at the tip of the ultrasounds generator is submitted to ultrasonic solicitations for fixed durations (30 s and 1 minute for example). At the end of the fixed solicitation period, an optical picture is recorded.
The procedure (solicitations/picture) is repeated up to the total stripping of the coating(s).
The images corresponding to 30s, 60s... of solicitations are then numerically analysed in order to estimate the area of remaining paint on the sample surface.

Results

Figure 12 shows the evolutions of the "undamaged surface" as a function of ultrasonic solicitation time for two material types. Six samples of each material are tested in order to evaluate the spreading of the stripping curves.
In order to evaluate adhesion, benefit is taken from the various dispersion of the stripping curves generated by our process.

A Flash Test Index (FTI) is calculated as the ratio :

$$FTI = \frac{area\ beetwen\ the\ two\ limit\ curves\ (min\ \%)}{total\ area\ of\ the\ graph\ (\text{min})}$$

As previously mentioned in the case of high adhesion of the coatings pitting damages will predominate leading to a weak dispersion of the stripping kinetic curves (figure 12 - PA7).
On the contrary, in the case of weak adhesion, pilling damages will be found inducing greater dispersion of the stripping curves (figure 12 - PA5).
The two cases will lead to two different flash test indexes : small for the high adherent coating (example PA1 : FTI = 6.5) and great for the weak adherent coating (example PA5 : FTI = 12.3).

Experiments carried out on 7 types of materials allowed us to deduce the Flash Test Index and correlate them to the long term efficiency of the coatings tested by 4 years natural exposure on our class 5 stand. The table 1 point clearly out that the best long term efficiencies are associated to the weakest Flash Test Indexes with PA1 as the best one and PA3 as the worse one.

Table 1 : Comparison between flash test and 4 years natural exposure results

Paint Assembly	Flash test damage process	Flash Test Index	Flash test classification	four years natural exposure behaviour
PA7	pitting	6,5	1	very good
PA6	pitting	8,0	2	good
PA1	pitting	8,6	3	good
PA2	pilling & pitting	9,1	4	medium
PA4	pilling	11,3	5	medium
PA5	pilling	12,3	6	bad
PA3	pilling	14,5	7	very bad

Conclusion

The use of ultrasonic solicitations as described in this paper represents an alternative mean of characterisation of long term efficiency of coatings used for steel sheets protection against corrosion. The main advantages of this test are its simplicity and its rapidity.
Outside of its predictive possibilities, this test can also be applied to follow in real time the quality of the finished product at the end of the production line.

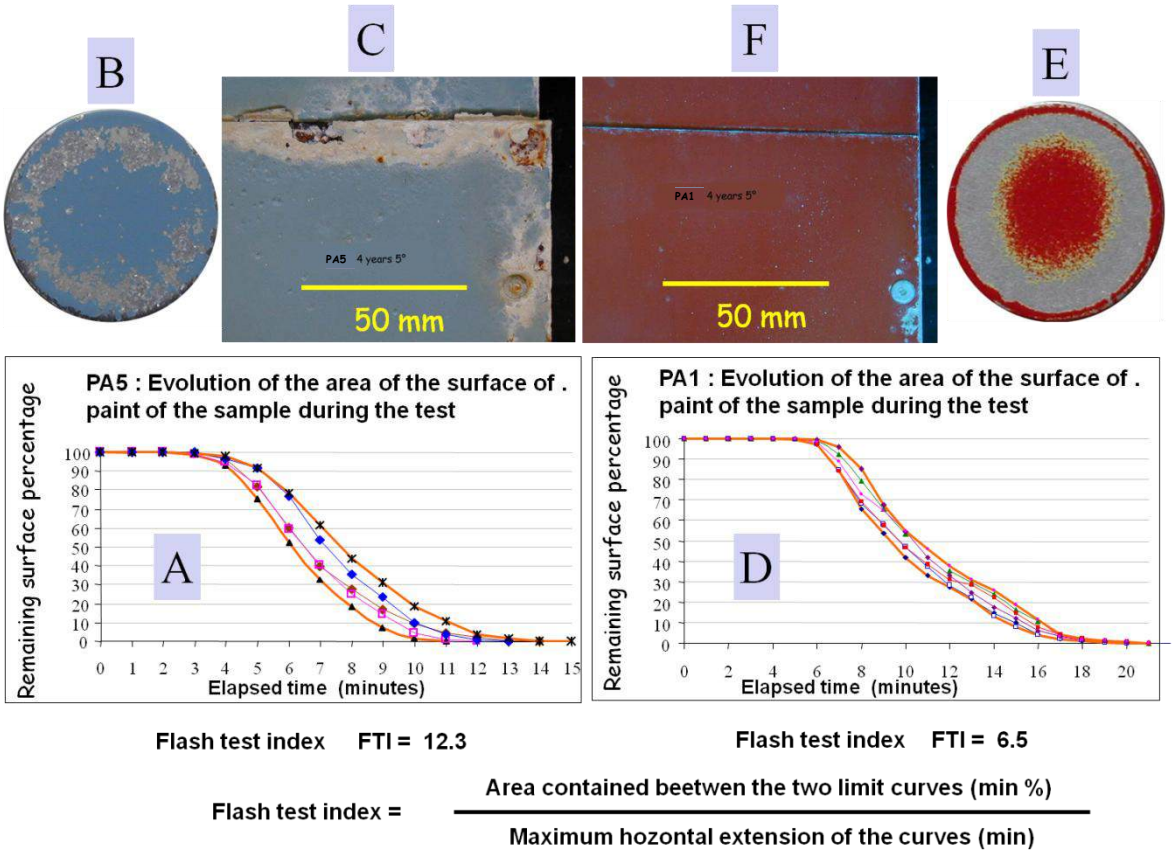

Figure 12 : results of Flash Test and natural exposure for two different samples: PA5 and PA1
A, D stripping kinetic curves
B, E aspects of sample surfaces after respectivly 6 and 12minutes of ultrasonic solicitations
C, F aspects of the sample surfaces after 4 years exposure on our class 5 Stand
Dispersion of the stripping curves allowed us to deduce the Flash Test Index.

[1] J. PIGERRE, *Ph. D. Thesis*, Université des Antilles et de la Guyane, Cayenne, 2002

[2] G. BERANGER, G. SANZ, G. HENRY (Eds.) *Le livre de l'acier* (1994).

[3] J. PIGERRE, P. RODRIGUEZ, T. MEHINTO, C. ROOS, J. L. MANSOT, C. BARREAU, « *An accelerated test using ultrasonics to qualify industrial organic coatings resistance Part I : methodological approach* », Prog. Org. Coat. , vol 50, p. 132 (2004).

[4] J. PIGERRE, P. RODRIGUEZ, T. MEHINTO, J. L. MANSOT, C. ROOS, « *Development of an ultrasonics-based flash test used for fast qualification of the mechanical resistance of industrial organic coatings Part II : Comparative results* », Prog. Org. Coat. , vol 54, p. 377-383 (2005)

[5] M. CHOUVELLON, T. FOURNEL, C. DUCOTTET "*Visualisation des bulles de cavitation"* , Revue de l'électricité et de l'électronique, vol. n° 3, pp. 63-66 (March 1999).

[6] M. S. PLESSET, R. B. CHAPMAN *Collapse of an initially spherical vapour cavity in the neighbourhood of a solid boundary*, J. Fluid Mech. Vol. 47, part 2, pp.283-290, (1971).

Acknowledgments: The authors acknowledge Arcelor, the Conseils Régionaux of Guadeloupe and Guyane and the Fond Social Européen for their financial supports.

Chemistry / Physics of Materials

Nano friction of low dimensional compounds using Atomic and Lateral Force Microscopy: toward an atomic interpretation.

P. BILAS, L. ROMANA, F. BADE*, K. DELBE, P. THOMAS AND J.L. MANSOT

Groupe de Technologie des Surfaces et des Interfaces (GTSI EA 2432)
** Groupe de Recherche sur les Energies Renouvelables (GRER EA 924)*
Université des Antilles et de la Guyane,
Campus de Fouillole, 97159 Pointe à Pitre Cédex Guadeloupe (France) - Philippe.Bilas@univ-ag.fr

Abstract :

Friction properties of molybdenum diselenide ($NbSe_2$) are studied at the nanometer scale by means of an Atomic and Lateral forces microscope. In order to investigate the influence of the interaction potential between the sliding surfaces, the experiments are carried out at two scan velocities (30 $nm.s^{-1}$ or 15 $\mu m.s^{-1}$). Comparison between the friction forces recorded at low and high speeds are discussed in term of atomic Tomlinson [1] or Postnikov theories [2].

Introduction:

The recent developments of atomic force microscopes [3] have provided a powerful tool to study the mechanisms of friction at the nanometer scale allowing experimental conditions closed to the single asperity contact context. At such scale, the variations of the friction force with load or scan speed are more complex than the one observed in multi-asperity contact experiments carried out in macro tribological tests [4].

In this paper we used an original calibration method developed in our laboratory and presented elsewhere [5-6] to study quantitatively the friction properties of $NbSe_2$ at two different scan speeds. Comparison between the friction forces and tip displacements recorded for these different experimental set-ups help us to better understand the energy dissipation processes which occur during friction.

Experimental set-up:

The nanotribological properties of $NbSe_2$ are investigated by means of an Atomic Friction Force Microscope (AFFM) from Molecular Imaging Corp. (PICOSPM). The cantilevers are rectangular shaped and made of silicon.

Calibration of the normal and lateral forces are performed using the method developed in references [5-6]. The friction force is deduced from the conventional friction loop and is defined as $F_F = \frac{F_{Lforth} + F_{LBack}}{2}$ where F_{Lforth} and F_{LBack} are the lateral forces recorded for the forth and back directions of the scan.

Normal stiffnesses calculated using the method developed by Sader et al.[7] range from 1 $N.m^{-1}$ to 5 $N.m^{-1}$ allowing us to apply normal load up to 120 nN.

The variation of the friction force as a function of the applied load F_N is investigated for two different scan velocities V=30 $nm.s^{-1}$ and V=15 $\mu m.s^{-1}$. Such speeds are reached by recording images of 5nm x 5nm and 5µm x 5µm sizes for the low and high scan velocities respectively. Experiments performed at low and high speeds are referred as atomic scale and meso scale experiments respectively.

In order to perform the AFFM tests on clean substrate, the $NbSe_2$ surface is cleaved with an adhesive tape just before the experiments.

All the data reported have been recorded under air atmosphere with 55% humidity.

Results and discussion

Numerical approach

In order to interpret our experimental data, we used a conventional model based on Tomlinson approach to describe the AFM tip motion of the surface sample. In this model, the motion equations of the tip can be described by the following equations:

$$m\ddot{x}_t = k_x(Vt - x_t) - \frac{\partial V_{ts}}{\partial x} - \gamma_x \dot{x}_t$$

$$m_y\ddot{y}_t = k_y(Vt - y_t) - \frac{\partial V_{ts}}{\partial y} - \gamma_y \dot{y}_t$$

Where m is the effective mass of the tip, k is the total stiffness of the tip/surface system, Vts is the interaction potential between the tip and the surface, γ is the damping term representing the energy dissipation during sliding. All the parameter values are extracted from the experimental data (mainly the friction force loop)

except for the effective mass and damping term. The chosen values are the ones generally reported in literature [8].

Experimental data and discussion

Figure 1 represents the lateral friction force images recorded on $NbSe_2$ surface for the two different speeds. At low speed (fig. 1a) the image clearly evidences the stick-slip motion of the tip. The distance between two patterns and the symmetry observed corresponds to those of $NbSe_2$ crystalline structure. The insert picture is the lateral force image simulated by the model previously described. A good agreement is observed between experimental and simulated data. The lateral image recorded at higher speed do not revealed any periodic pattern (fig. 1b).

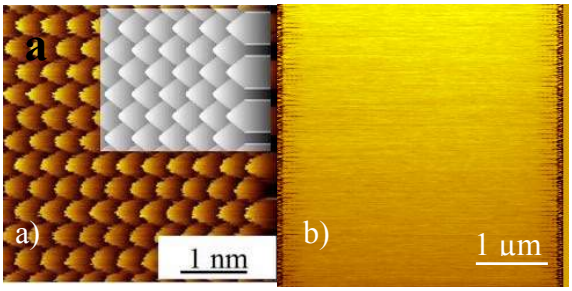

Fig. 1: Lateral force images recorded on NbSe2 surfaces for a scan speed of 30nms^{-1} (a) and 15µms^{-1} (b).

This figure did not allow us to determine if the tip undergoes a stick-slip motion since the spatial resolution is too small (for a 256x256 pixels images recorded for a scan of 5µm, each pixel corresponds to 20 nm).

However, numerical simulation performed with enough spatial resolution (0.02 nm/pixel) clearly evidences that the tip has a continuous motion on the surface samples (not shown in the paper).

The evolutions of the experimental friction forces as a function of the applied normal loads are shown in fig. 2 for the both scan speeds investigated. It has been shown previously from the $F_F(F_N)$ curve recorded at high speed (meso scale) that the $NbSe_2$ contact obeys the JKR theory with a shear stress at the sliding interface close to 20 MPa [6]. The main point deduced from figure 2 is the similitude values of the friction forces measured at high and low speed.

According to the simulated data the friction force at high speed should be one hundred time higher than the one measured at low speed.

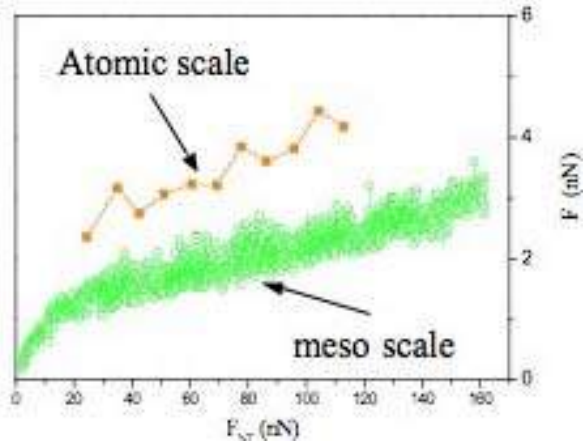

Fig 2: experimental friction force as a function of applied normal load. The curves are recorded at atomic scale (low speed) and meso scale (high speed).

This discrepancy between simulated and experimental data seems to indicate that energy dissipation process are different whether the tip is subject to a stick-slip motion (low speed) or moves continuously on the surface sample.

In the case stick-slip motion, energy dissipation process is expected to occur discontinuously (either by the shearing of the contact area join together during the sticking phase or by atomic vibrations during the slip phase) whereas at meso scale, energy dissipation is expected to be induced by continuous normal vibrations of the tip and substrate atoms due to the periodic interaction potential (as described by the Postnikov model).

Further investigations are in progress to elucidate this point.

Acknowledgements

The authors acknowledge Molecular Imaging Corp., Gatan Inc., the Conseil Régional de la Guadeloupe and the Fond Social Européen for their financial supports. The authors wish to thank the C3I for its technical support in collecting computational data.

Bibliography

[1] G.A. Tomlinson, Phil. Mag. Serie, 20 (1929), 905

[2] S. N. Postnikov, « Electrophysical and electrochemical phenomena in friction, cutting and lubrification » (1978)

[3] G. Binnig;C.F. Quate; Ch. Gerber; Phys.Rev. Lett. 56, (1986) p.930

[4] "Fundamentals of friction and wear on the nanoscale", Gnecco and E. Meyers Eds, Springer (2007)

[5] P. Bilas; L. Romana; B. Kraus ; Y. Bercion; J.L.Mansot, Review of Scientific Instrument, Vol 75, N°2, (2004); 1-7

[6] P. Bilas, PhD thesis, Université des Antilles et de la Guyane (2006)

[7] J.E. Sader, J. W. Chon, P. Mulvaney, Rev. Sci. Instrum., Vol. 70, (1999) 3967

[8] O. Zwörner, H. Hölsher, U. D.Schawrz and R. Wiesenger; Applied Physics A, 66, (1998), 263-267

Chemistry / Physics of Materials

Nanomechanical Characterizations of Submicrometer Thick-Tribologic Films

L. ROMANA, P. BILAS, V. GOLABKAN AND J.L. MANSOT

Groupe de Technologie des Surfaces et des Interfaces (GTSI EA 2432), Université des Antilles et de la Guyane, Campus de Fouillole, 97159 Pointe à Pitre Cédex Guadeloupe (France)
laurence.romana@univ-ag.fr

Abstract

Nanomechanical properties of tribological films are investigated at the nanometer scales by means of atomic force microscopy and nanoindentation. The studied tribological films are formed using an alternative macroscopic sphere/plan tribometer. Adherence of the tribofilm to the steel substrate is estimated by nanoscratch testing and the hardness and Young's modulus are measured by means of dynamic mechanical analyses. These characterisations are used to better understand the good anti-wear and anti friction properties of these films.

Introduction

Organometallic reverse micelles are well known to be multifunctional additives acting generally as detergent and anticorrosion agents in lubricants [1-2]. Recent studies have shown that Strontium and Calcium dimethyl-3,5-hexanoate micelles dispersed in dodecane can also be used as friction reducers and anti wear additives [3]. Their good tribological properties are supposed to be due to the micro-granular structure of the tribological films constituted of microcrystalline grains of strontianite embedded into an amorphous intergranular phase [4].
In this work, the nanomechanical properties of these tribological films are studied using a nanoindentor. The hardness and the Young's modulus are measured as a function of depth by means of dynamic mechanical analyses [4]. The data confirm the main role plays by the film microstructure on the tribological properties.

Experimental set-up

Tribological films are formed during alternative macroscopic sphere/plane tribologic tests in the presence of a 3% (weight/weight) colloidal dispersion of organometallic reverse micelles in dodecane. The amphiphilic molecules used to form the micelles are Calcium 3,5-dimethyl hexanoate. The ball and the plane are made of 52100 AISI steel and have a mirror polished surface (Ra≤ 10nm). A normal force of 10 N is applied while the ball scans the surface sample with 1 hertz frequency over a scan length of 2mm.

Prior to study the mechanical properties completely, the plane is rinsed in pentane in order to remove the lubricant solution. The film is characterized by means of a nanoindentor apparatus purchased from MTS. The nano-indentor is used for different purposes:
- Nanoscratch tester: The tip scans the surface across the film/plane interface with controlled normal load in order to investigate the film adherence onto the steel.
- Dynamical nanoindentor: The young's modulus and the hardness of the film are measured as a function of the depth [5].

All the experiments are done in air with 55% humidity.

Results and discussions

1- Tribological film

Figure 1 shows the evolution of the friction coefficient as a function of the scan cycles.

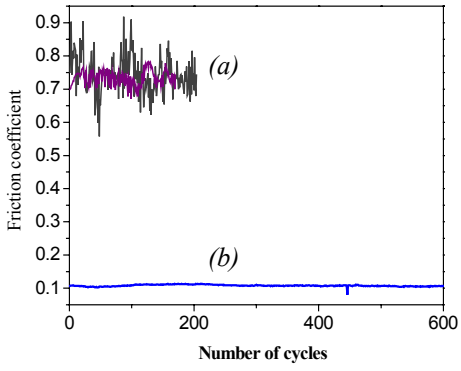

Figure 1: Evolution of the friction coefficient as a function of cycles a) in the presence of pure dodecane b) in the presence of a 3% Calcium hexanoate in dodecane.

As observed on the graph the tribological film builds-up immediately (no induction period is observed) and remains stable (around 0.1) during few thousands of cycles.

For indication the friction coefficient of steel/dodecane/steel interface is also reported. The measured value is close to 0.7 These results evidence the good properties of the additives as friction-reducer.

2- *Film topography*

Optical picture of the tribological film is shown in figure 2.

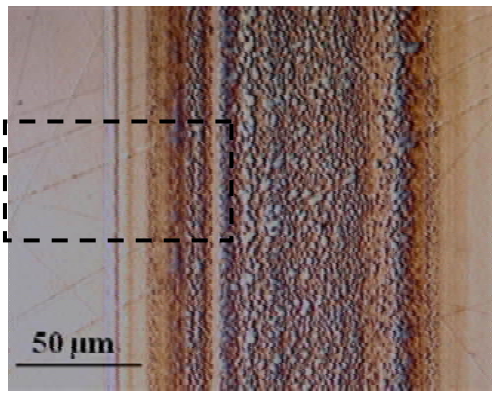

Figure 2: Optical micrograph recorded on the tribofilm at the end of the tribologic tests.

The film surface appears non uniform constituted of platelets of few micron sizes with an average height of 200 nm as measured by atomic force microscopy.

3- *Adherence*

Film/substrate adherence is evaluated by performing a scratch test (using the nanoindentor) across the trace as indicated by the dash line of figure 2.

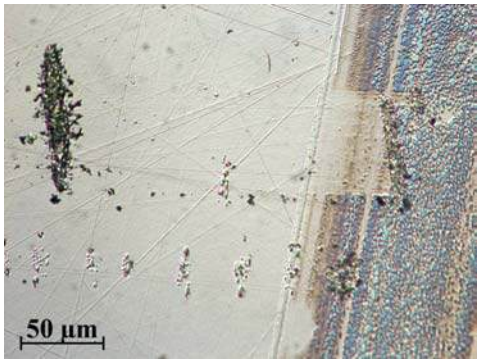

Figure 3: Optical micrograph of the tribological film after performing a scratch test with applied load lower than 1 µN.

For load lower than 1 µN, the film is easily removed by the indentor head as shown in figure 3 indicating a poor cohesive energy of the film and a probably a poor adhesion of the film onto the substrate.

4- *Mechanical Properties*

The mechanical properties of the tribological film are measured using the nanoindentor.

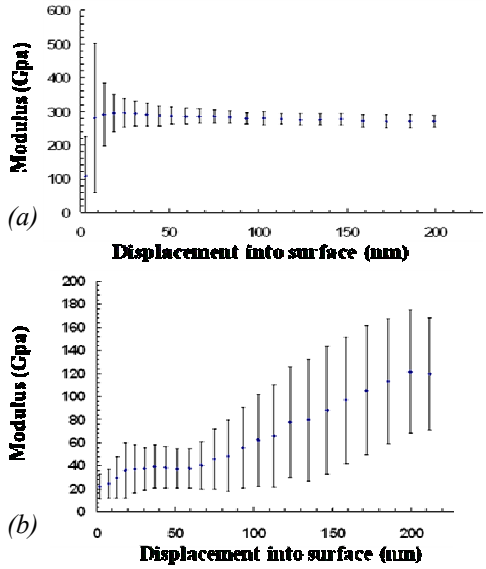

Figure 4: Reduced young's modulus as a function of depth indentation recorded on the wear track for uncovered substrate area (a) and area covered by the tribological film (b).

Figure 4 represents the reduced young's modulus as a function of the indentation depth. Each error bar corresponds to the different values recorded during 50 tests. Due to the patchy surface of the tribological film, two mechanical behaviours are observed depending on the indentation zone:

- For the set of data reported in figure 4a. the young's modulus measured is closed to the steel substrate one (300 GPa): these data are recorded on the wear track areas uncovered by the film.
- The set of data reported on figure 4b corresponds to indentation tests performed on area covered by the tribological film. The reduced Young's modulus of the tribological film is close to 20 GPa. As the indentation depth increases, the young's modulus value increases due to the substrate influence.

Same behaviour is observed for hardness measurements (figure 5). The data reported in

figure 5a quickly reaches the value of steel substrate (12 GPa). From figure 5b we can deduce that film hardness is around 0.5 GPa.

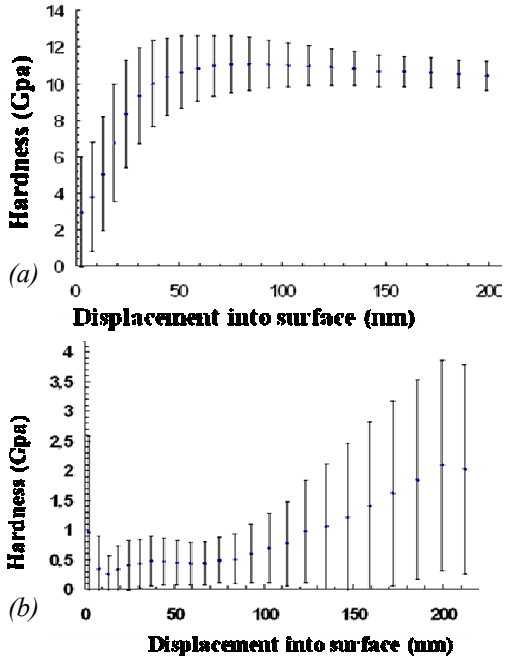

Figure 5: Hardness evolution as a function of depth indentation.

The high dispersion of the data reported on figure 4b and 5b can be attributed to the thickness variation of the tribological film.

5- Discussion

From previous works [3-4], it has been shown, using analytical electron transmission microscopy that:
- The anti wear film is composed of poly-crystalline calcite aggregated through an amorphous intergranular phase.
- The film builds -up without any reaction with the substrate.

These results are consistent with the ones reported in the present paper:
- The easy removal of the film during the scratch tests is attributed to the lack of chemical reaction between the film and the substrate and to the low cohesive energy between the calcite crystals.
- The low cohesive energy of the film induced by its granular structure results in an easy shearing of the film during the indent (similar to a footprint in the sand) and then leads to a high contact area. Since the hardness is defined as $\frac{F}{A}$, this surface increase leads to a low hardness value.

6- Conclusion

In the present work, the nanomechanical properties of tribological films formed during macro tribometer tests have been investigated. The low hardness and elastic modulus values measured have been attributed to the low cohesive energy of the film. This result is consistent with the low friction coefficient measured during classical alternative tribometer test, since easy shearing film will leads to good tribological properties. During the macro tribological test, the film is trapped inside the contact which explains its extended life time even if it adheres poorly to the substrate as shown in this study.

Acknowledgments

The authors acknowledge Molecular Imaging Corp., Gatan Inc., the Conseil Régional de la Guadeloupe and the Fond Social Européen for their financial supports.

Bibliography

[1] J.F. Marsh, Chem. Ind. 20 (1987) 470.
[2] J.M. Martin, J.L. Mansot, M. Hallouis, ultramicroscopy 30 (1989)321.
[3] J.L. Mansot, V. Golabkan, L. Romana and T. Cesaire, Journal of Microscopy, Vol.210 (2003), 110-118,
[4] J.L. Mansot, L. Romana, V. Golabkan, P. Bilas, E. Alleman, Journal of Colloids and Surfaces Vol.243 N°1-3, (2004), pp 67-77
[5] J.B. Pethica, R. Hutchings, W.C. Oliver, Philosophical Magazine, A48 (1983) 593

Theoretical Approach of Nanocristallized Graphite Phases: Influence of Cluster Size Electronic Band Structure–Correlation to EELS Near Edges Structures

T. CESAIRE (1), V. JEANNE-ROSE (2), L.LARGITTE (2) AND J.L. MANSOT (1)

(1) Groupe de Technologie des Surfaces et Interfaces (GTSI EA 2432) - Thierry.Cesaire@univ-ag.fr
(2) Chimie des Matériaux - Connaissance et Valorisation (COVACHIMM - EA 925)
Université des Antilles et de la Guyane, Campus Fouillole, 97159 Pointe à Pitre, Guadeloupe, France

Keywords: EELS, multiple scattering, band structure calculation, carbon

Carbonaceous materials are widely used for their tribological (friction and wear reducer) and adsorption properties (activated charcoal, NH3 adsorbent in freezing devices…). These carbonaceous phases can be obtained by chemical exfoliation or mechanical crushing of natural graphite or by high temperature pyrolysis of crushed organic compounds such as ligneous precursors [1,2]. In that last case, the final product can also be nano crystallized graphite. As it is commonly encountered, the physical and chemical properties of such materials are strongly related to the size of the clusters or crystallites.

The present work is a theoretical approach based on band structure calculation, using multiple scattering FEFF software [3], applied to polycrystalline graphite in order to study the evolution of electronic band structure as a function of the size and geometry of the graphite crystallites (fig 1).

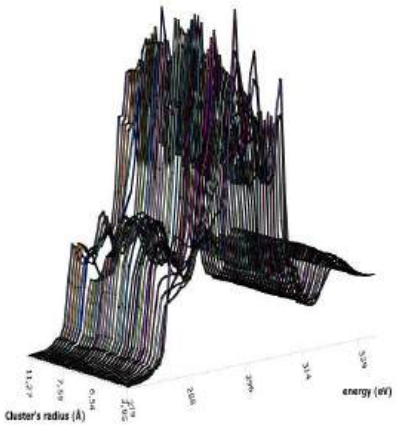

Fig 1: Evolution of calculated carbon K near edge features as function of cluster's radius.

The results obtained for various crystallite growth (spherical, cylindrical, planar growth), point out that electronic structure of such materials is strongly governed by the bi-dimensional character (size evolution of graphene planes, fig 2). The tri-dimensional evolution affects weakly the band structure, fig 3).
The theoretical calculations of the corresponding Electron Energy Loss Spectra (EELS) at Carbon Kedge [4], show that the extension of

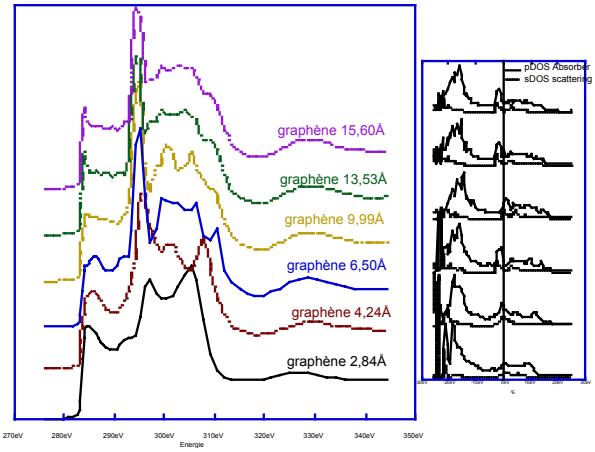

Fig 2 : Evolution of calculated carbon K near edge features as function of plane cluster radius correlate to the DOS calculations.

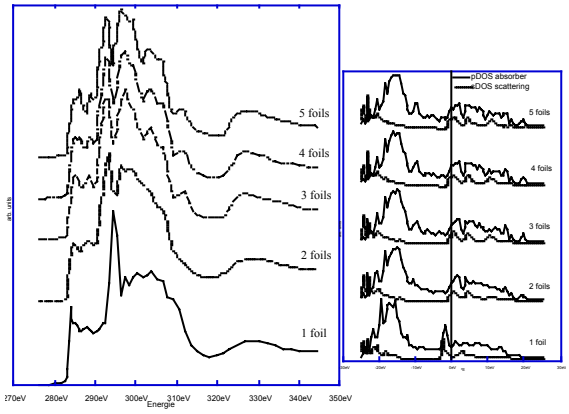

Fig 3 : Evolution of calculated carbon K near edge features as function of number of graphen's foils correlate to the DOS calculations.

bi-dimensional order generate a well defined Near Edge Feature related to 1s-> σ* dipole allowed transitions. The intensity of this feature seems strongly related to the size of the nano crystallites.

These theoretical results are supported by experimental EEL spectra collected on various carbonaceous compounds presenting increasing long range order.

The relationship between long range order and intensity of the well defined 1s ->σ* feature at carbon K edge could constitute an EELS experimental method to determine the graphite crystallites mean sizes in unknown carbonaceous compounds.

References

[1] V. Jeanne - Rose, V. Golabkan, J. L. Mansot, L. Largitte, T. Cesaire & A.Ouensanga, Journal of Microscopy, Vol. 210, (2003) 53-59.

[2] P.L. Gai, B.H.M.Billinge & A.M. Brown, Carbon,27, (1989) 41-53.

[3] J.J. Rehr, the feff Project, Department of Physics University of Washington (2002) Version 8.20

[4] Egerton R.F. Electron Energy loss Spectroscopy in the Electron Microscope, 2nd ed. Plenum Press, New York (1996).

Antiwear and Antifriction Action Mechanisms of Colloidal Lubricant Additives

V. GOLABKAN, P. BILAS, L. ROMANA, J. PIGERRE AND J.L. MANSOT

Groupe de Technologie des Surfaces et Interfaces (GTSI EA 2432), Université des Antilles et de la Guyane, Faculté des Sciences Exactes et Naturelles, Campus Fouillole, 97159 Pointe à Pitre cédex Guadeloupe (France) - vanyna.golabkan@univ-ag.fr

Keywords: Reverse micelles, Analytical Electron Microscopy, EELS, Tribology

Organometallic reverse micellar systems [1] are of great interest for industrial applications because such systems permit the formation of stable dispersions of small mineral particles in hydrocarbons. These systems have wide applications in various industries (painting, catalysis, anticorrosive, lubrication, etc…).

In this work the mechanism of action of overbased strontium cekanoate micelles in dodecane as lubricant base is investigated in the boundary lubrication regime.

For this purpose, tribologic experiments are carried out on an alternative sphere / plane tribometer the ball and the plane being made of 52100 AISI steel.

The tribologic results point out the extreme efficiency of these additives as friction and wear reducers as soon as the experiment started by the immediate built up of a tribofilm in the physical conditions of the sliding contact. This dielectric antiwear film is easily evidenced during the test by dynamic electrical contact measurements and at the end of the experiment by optical microscopy examinations of the tested surfaces.

The investigation of morphology, chemical composition and structure by means of Analytical Transmission Electron Microscopy (ATEM) [2, 3] allows us to identify that the tribofilm is constituted of polycrystalline strontium carbonate (strontianite).

Friction experiments carried out on the tribofilm alone, in order to investigate its intrinsic friction reducer properties, strongly point out that the main friction reduction action is due to adsorbed strontium cekanoate molecules on the surface of the film.

Lateral Force Microscopy [4] experiments carried out on freshly deposited strontium cekanoate film on freshly cleaved mica strongly confirm the high mobility and the good friction properties of these molecules.

Acknowledgments: The authors acknowledge EdF Archipel Guadeloupe and the French Research Department for their financial support and Exxon Chemical International Inc. which provides the micellar additives.

[1] K.L. Mittal , "Micellization, Solubilization and Microemulsions", Plenum Press, New York, (1977).

[2] V. Golabkan, J.L. Mansot, L. Romana, Ph. Bilas, E. Alleman, Y. Bercion, Coll. and Surf.A: Physicochem.Eng . Aspects 243 (2004) 67.

[3] V. Golabkan, PhD Thesis, Université des Antilles et de la Guyane (2005)

[4] Ph. Bilas, PhD Thesis, Université des Antilles et de la Guyane (2005)

Chemistry / Physics of Materials

Tribological properties of room temperature graphite fluorides heat-treated under fluorine atmosphere

P.THOMAS [1], K. DELBÉ [1], D. HIMMEL [1], J.L. MANSOT [1], C. DELABARRE [2], M. DUBOIS [2], K. GUÉRIN [2], A. HAMWI [2]

1 Groupe de Technologie des Surfaces et Interfaces (GTSI EA 2432) Université des Antilles et de la Guyane, 97159 Pointe a Pitre Cedex, FRANCE - pthomas@univ-ag.fr
2 Laboratoire des Materiaux Inorganiques, Universite Blaise Pascal de Clermont-Ferrand, UMR-CNRS 6002, 63177 Aubiere, FRANCE

Keywords: Fluorinated graphite compounds, Tribology, Raman spectroscopy

Introduction

Conventional graphite fluorides used as friction reducers are synthesized at temperatures ranging between 300°C and 600°C by direct reaction of fluorine gas over graphite. The resulting $(CF_x)_n$ compounds, present a lamellar chair type structure associated to a sp^3 hybridisation of carbon atoms. In this work, the lubricating performances of fluorinated phases obtained at room temperature are investigated. Special attention is paid to the evolution of the friction properties induced by a thermal post-treatment under fluorine atmosphere in correlation with the induced structural modifications of the compounds.

Experimental

The starting fluorinated materials, are obtained at room temperature by the reaction of natural graphite with a gaseous mixture F_2-HF-MF_n. Three volatile fluorides MF_n were chosen: IF_5, BF_3 and ClF_x. Thermal post-treatments are then performed under fluorine atmosphere at temperatures ranging from 100°C to 600°C [1,2].
The friction properties of the compounds are determined using a ball-on-plane tribometer. The ball and the plane are made of AISI 52100 steel, the sliding speed is 2 mm/s, the applied normal load is 10N leading to a mean contact pressure of 0.7 Gpa. The structure evolutions induced by friction are investigated by means of Raman spectroscopy.

Results

The tribological properties of the various starting materials at the beginning of the test (three first cycles) are presented in figure 1. For compounds prepared with ClF_x and BF_3 catalysts, the friction properties are similar and better than with IF_5 for the synthesis. This is attributed to the nature of the intercalated species inducing different interactions with the host structure (particularly the presence of HF).
The modification of the tribological performances observed for post-treated compounds

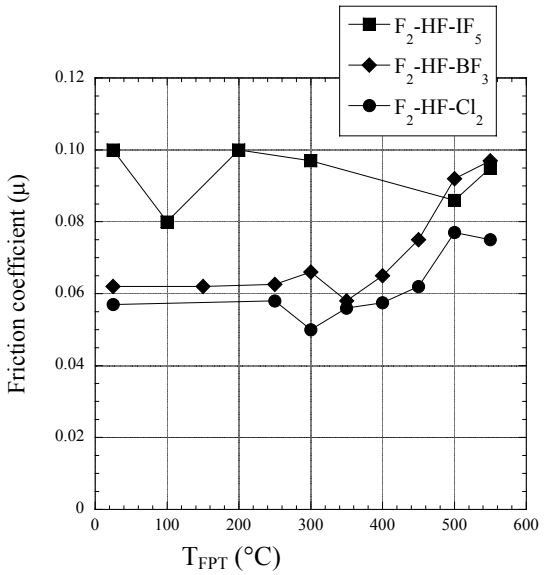

Fig.1: Evolution of the intrinsic friction coefficient (three first cycles) of the fluorinated materials as a function of the fluorination post-treatment temperature.

is due to the evolution of the nature and rates of the intercalated species (decrease of HF_n species content ; $IF_5 \rightarrow IF_6$- ; $BF_3 \rightarrow BF_4$-) modifying the interactions in the van der Waals gap. The progressive elimination of residual catalyst molecules leads to the appearance of sp^3 hybridization of the carbon atoms (chair-type configuration of the fluorocarbon layers) at 350°C < T_{FPT} < 500°C. The obtained

hybrid materials (coexistence of the planar and chair structures) present the best tribologic performances.The structure of the materials obtained for $T_{FPT} > 550°C$ is similar to the conventional commercial graphite fluoride one and the related friction coefficients are in good agreement with those of literature.

For $T_{FPT} > 500°C$, the fluorinated compounds do not contain any intercalated species so the increase of the friction can be related to the friction process. This phenomenon was evidenced by Raman spectroscopy in the case of IF_5 catalyst. The spectra presented in figure 2 recorded before and after friction, exhibit after the test drastic increases of the intensity of the D (1344 cm^{-1}) and G (1588 cm^{-1}) characteristic graphene bands implying loss of fluorine and partial rebuilding of graphene planes.

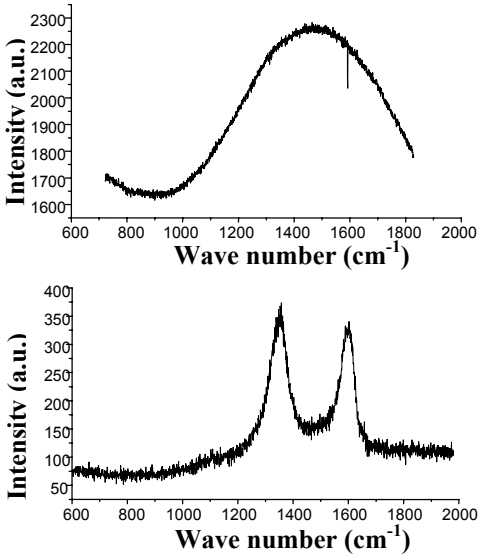

Fig.2: Raman spectra of the fluorinated phase obtained at T_{FPT}=500°C:
(a) before friction tests
(b) after friction tests (30 cycles)

Discussion

The increase of friction coefficient obtained for low temperature heated compounds during friction can be attributed to the release of HF molecules entrapped in the lamellar structure. This leads to severe corrosion of the metallic substrates probably at the origin of the bad tribologic behaviour of these compounds. Indeed, the wear scars show heavy corrosion and wear resulting from the reaction of HF molecules with the contacting iron substrates.

For intermediate T_{FPT}s, the stability or the improvement of the lubricating performances at a low value can be due to the elimination of HF molecules and the remaining of MF_n intercalated species at the origin of the weakening of the interplanar interactions.

In the case $T_{FPT} > 500°C$, the friction induced structural transformations lead to the partial rebuilding of graphene planes by loss of fluorine molecules. The resulting friction coefficient seems to asymptotically tend to the graphite one.

Conclusion

Low temperature graphite fluorides present very attractive lubrication properties. Moreover, the friction performances can be improved by modifying the nature of C-F bonds and residual intercalated species. The best results are obtained for samples presenting mainly semi-ionic C-F bonds and low content of HFn species, characterized by the conservation of the planar shape of the carbon layers stabilized by the presence of intercalated MFn species.

Acknowledgements

The authors acknowledge the Conseil Régional de la Guadeloupe and the Fond Social Européen for their financial supports.

References

[1] M. Dubois, K. Guérin, J.P. Pinheiro, Z. Fawal, F. Masin, A. Hamwi, Carbon, 42, [10], (2004), 1931-1940.

[2] C. Delabarre, K. Guérin, M. Dubois, J. Giraudet, Z. Fawal, A. Hamwi, J. of Fluorine Chemistry, 126, [7], (2005), 1078-1087.

Kinetic Study of Sulfation of Natural Limestones from Guadeloupe

PASSE-COUTRIN, N., OUENSANGA, A.,

Laboratoire COVACHIM M, Université des Antilles et de la Guyane, Pointe-à-Pitre (Guadeloupe) France - Nady.Passe-Coutrin@univ-ag.fr

The aim of this study is to propose a local limestone able to capture rapidly the larger quantity of sulphur dioxide SO2, by a dry process.

Samples Analysis

Four samples, each from a different morphological site of Grande-Terre are tested. The technical methods of analysis are XR diffraction, FTIR spectroscopy, Induced Coupled Plasma Atomic Emission Spectroscopy and BET measurements. We observed that the samples were 95 wt% CaCO3, with the calcitic allotropic form in major part but the NPC3 called sample contains 14 wt% of aragonite. They are not porous (fig. 1).

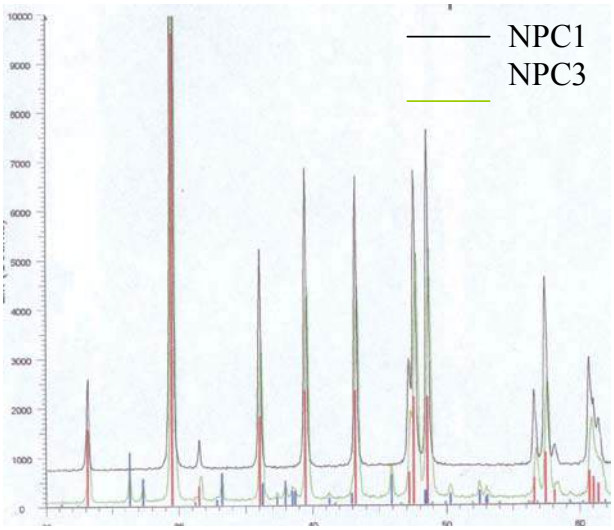

Fig.1: *XR diffraction of NPC1 and NPC3 samples compared with crystalline aragonite and calcite spectra.*

Apparatus

A flow of gas specially prepared and composed of 209 ppm SO_2, 6% O_2 and N_2 reached a 10 to 20 mg sample of limestone in a quartz crucible hung in a thermogravimetric analyser. The gas flow rate is 3 NLh^{-1}.

Thermogravimetric results

The mass decrease shows the decarbonation then the gas is sent (fig.2). The mass increase is the studied part. It shows sulfatation:

$CaO + SO_2 + ½ O_2 \rightarrow CaSO_4$

$850°C < T_{optimal} < 910°C$

Reaction is mainly a surfacic one. NPC2 has the maximum sulfation conversion. NPC1 has the maximum reaction rate.

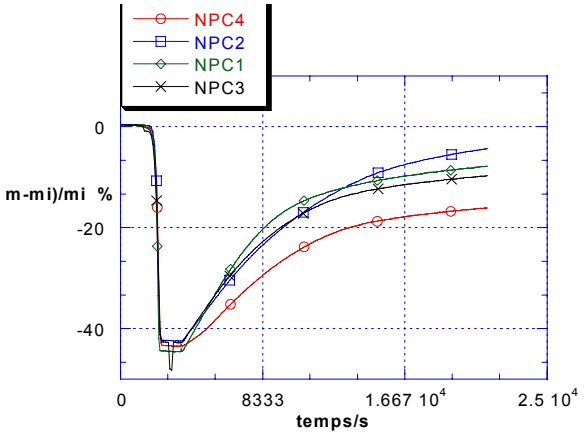

Fig.2: *Relative mass loss versus time for decarbonation then sulfatation of 3mg of the samples at 900°C.*

Modelling

Takes into account the following assumptions:
- Pseudo-steady state
- Isothermal process
- One size particles bed.

The gas transport around the sample bed is modelling by a CFD calculus code (fig.3).
Reaction and gas transport inside the sample bed are modeled using the Random Pore Model (Bhatia et al 1980).

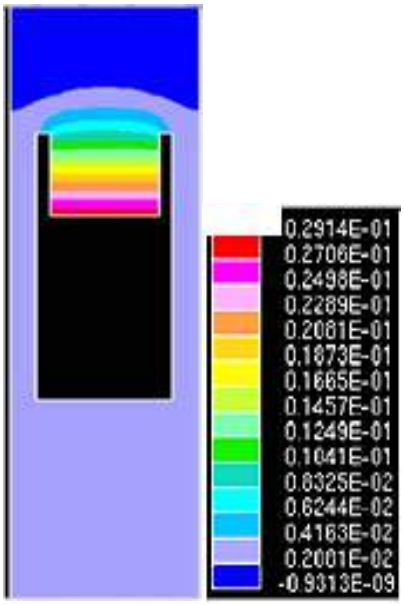

***Fig.3**: gas mass fractions round the sample in the crucible by the CFD calculus code.*

Results

ks: reaction rate constant.

$dr/dt = ks\ C_{SO2}$
r : reacting area radius around the pore
D_p diffusivity inside the pore
Eta: sulfatation reaction conversion.
ks and D_p are determined by fitting modelling to experiment (fig.4).

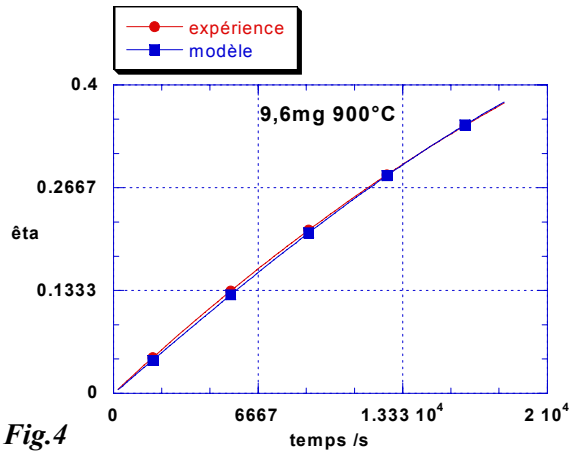

Fig.4

	Our study	**Borgwardt and Hartman studies**
Material	In situ calcined limestone	Non calcined limestone
SO_2 concentration(ppm)	209	3000
Gas flow	Diffusion and convection	Directly on particles
Rate limiting process	Inside pore diffusion	Diffusion through the product layer
ks ($m^4\ mol^{-1}\ s^{-1}$)	$1.4 * 10^{-8}$	$4.7 * 10^{-8}$
Dp ($m^2\ s^{-1}$)	$5 * 10^{-11}$	$1.9 * 10^{-11}$

References

Bhatia, S.K., Perlmutter, D.D., AIChE J. 26(3) 379,1980
Borgwardt,R.H., Environ. Sci. Technol. 4,59,1970
Hartman,M., Coughlin,R.W.,AIChE J., 22(3) 490,1976

Chemistry / Physics of Materials

Experimental Aqueous Phase Adsorbents from Purpleheart sawdust (*Peltogyne venosa*) and Rice husk

FOX, DAWN IONA & **SINGH,** RESHMA

Department of Chemistry, University of Guyana, Turkeyen Campus, Greater Georgetown, Guyana - dawniking@yahoo.com

Abstract

Two experimental aqueous phase adsorbents were prepared by acid pre-treatment of Purpleheart *(Peltogyne venosa)* sawdust and rice husk. The objective of the study was to employ appropriate technology to process local biomass waste into adsorbents for wastewater remediation. This will meet two needs in Guyana; consumption of waste materials currently posing solid waste management challenges to produce a material which will assist the local and regional water management and conservation drive.

The materials were characterised by iodine removal, copper (II) ion removal and methylene blue adsorption tests. For both rice husk and sawdust materials, increasing the level of acid pre-treatment resulted in increased methylene blue adsorption. Acid pre-treatment also improved iodine removal but had no effect on copper (II) removal. The adsorption performance was also affected by solution pH. Overall, the sawdust adsorbent was superior.

Introduction

Guyana has a predominantly agriculture-based economy with rice and timber being two important export products. Sawdust and rice husk, the main waste products of these industries, have been accumulating at sawmills and rice mills across the country posing waste management challenges. Converting these wastes into bioadsorbents not only provides a solution to this problem, but also to the wider problem of water resource management through wastewater remediation.

Plant based fabrics have long been shown to have a high affinity for dyes. As such, cellulosic plant materials have found natural applications as dye adsorbents. It is currently accepted that the hydroxyl (-OH) groups of cellulose, hemicellulose and lignin are the major adsorption sites (Kaewprasit, Hequet et al. 1998).

Several researchers have studied the adsorptive capacity of cellulosic biowastes including rice husk, sawdust, bagasse, and cotton (McKay et al, 1988; Yu et al, 2000; Ho & McKay, 2003; Garg *et al.*, 2003; Garg *et al.* 2004:a,b,c). Overall, materials that underwent simple pre-treatments (acid, formaldehyde) showed greater adsorptive capacity than the native materials. In this study, the adsorptive capacity of Purpleheart (*Peltogyne venosa*), a local hardwood used for construction, and that of rice husk were investigated by methylene blue iodine and copper (II) ion adsorption.

Materials and Methods

Material Preparation:

Purpleheart (*Peltogyne venosa*) sawdust was collected from several local sawmills in the West Coast Demerara area. Rice husk samples were collected from a rice mill located at Ruimzeigt, also on the West Coast. Both sawdust and rice husk were washed with distilled water and dried in sunlight. They were then ground in a laboratory mill and sieved to 1 mm. The materials were immersed in conc. H_2SO_4 (30%, 50% and 75%) for 24h then washed with 1% Na_2CO_3 and distilled water until the wash water was neutral. The adsorbents were then oven dried at 105 ^{O}C for 24h and sealed in airtight bags.

Material Characterisation:

The principal test was Methylene Blue ($C_{16}H_{18}N_3SCl$; MB) dye adsorption. Weighed adsorbent samples were introduced to 100 ml MB solutions of known concentration and shaken on a flatbed shaker for 3h. The adsorbents were separated by centrifugation at 4500 rpm for 5 min and the dye concentration remaining in solution was determined by UVVIS spectrophotometry (UVIKON 992, Kontron Instruments). Optimisation tests included varying the adsorbate concentration (50 – 250 ppm MB), the adsorbent mass (0.2 – 1.0 g) and the solution pH (4, 7 and 10).

Iodine adsorption tests were carried out using a modification of the standard iodine number test (Ahmedna, Johns et al, 1997). Copper (II) ion removal tests were also conducted; 0.5 g of adsorbent were weighed into 250 ml conical flasks and 100 ml 50 ppm $CuCl_2$ solution (buffered to pH 5) were added. The mixtures were shaken for 24h on a flatbed shaker, separated and the concentration of Cu^{2+} remaining in solution was determined by AAS (Varian Spectra AA 5). The mass of copper removed per gram of adsorbent was determined.

Results and Discussion

Methylene blue (MB) adsorption

At pH below 10, the sawdust adsorbents (SD) outperformed the rice husk (RH) adsorbents in MB adsorption (shown in Figure 1). Also, increasing acid dosage in the pre-treatment was shown to improve the adsorption capacity of both materials.

However, solution pH appeared more important than raw material composition as, with each material, MB adsorption increased with increasing solution pH. Interestingly, at pH 10 there was no significant difference in MB adsorption between the rice husk and sawdust materials.

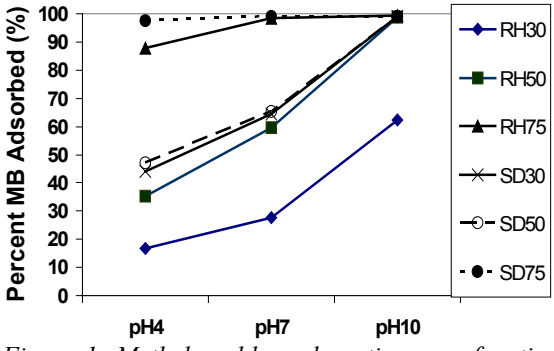

Figure 1: Methylene blue adsorption as a function of solution pH

The sawdust adsorbents with the higher cellulose content were expected to outperform the rice husk adsorbents; notably, the rice husk materials showed increased adsorptive capacity following pre-treatment.

The overall increase in adsorption capacity with increased acid dosage in the pre-treatment was also found by other researchers on similar materials (Garg *et al.*, 2003; Garg *et al*. 2004:a, 2004:c). This is thought to be a function of acid-induced cellulose hydrolysation; under acidic conditions cellulose fibres become hydrolysed exposing more reactive hydroxyl groups at the surface of the material, thus facilitating adsorption. Physical modification of the cellulose strands may have contributed to adsorption; further study of the surface with scanning electron microscopy (SEM) is recommended.

Increasing the solution pH to 10 appears to overcome adsorptive limitations in all the materials. This may be due to electrostatic attraction between the adsorbate and the surface of the adsorbent. It is proposed that in an alkaline medium, the surface of the adsorbents becomes negatively charged due to ionisation of the hydroxyl groups. These negative sites attract the positively charged dye molecule. Similar phenomena were observed with activated carbon adsorbents (Fox & Hyland, 2003). Percent iodine removal (PIR) is a test of microporosity (0 – 20 Å); the materials did not show appreciable micropore development; the maximum PIR observed was below 50% (refer to Figure 2). While acid pre-treatment level increased the microporosity of the native rice husk material (from 8% in the untreated material to 22% at 30% acid treatment), higher dosages appeared to have no further effect. The microporosity of the sawdust adsorbent increased with increasing acid pre-treatment level indicating some micropore development. These observations point to the surface being the more important adsorptive site in these materials.

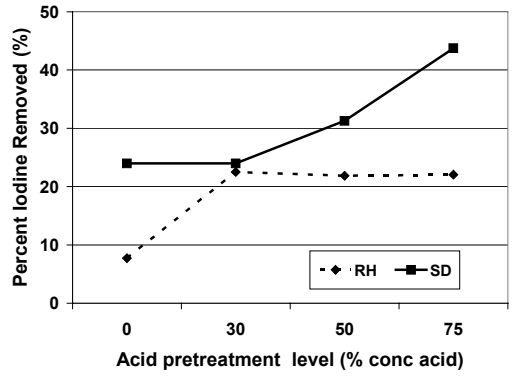

Figure 2: Percent Iodine Removal (PIR) by rice husk (RH) and sawdust (SD) adsorbents

Both materials showed poor copper (II) ion removal (less than 40%); moreover, acid pre-treatment appeared to have no effect on the materials' ability to adsorb Cu^{2+}. As such, the adsorbents show little potential as heavy metal ion adsorbers.

Conclusions

1. Acid pre-treatment improved the adsorptive capacity (methylene blue) of rice husk and sawdust adsorbents.
2. Acid-treated sawdust showed greater adsorptive capacity than the rice husk counterpart.
3. Solution pH affects the materials' ability to adsorb methylene blue with higher pH favouring adsorption.
4. The materials were not significantly microporous; the sawdust showed limited micropore development with acid treatment.
5. The materials were poor at removing Cu^{2+}; acid treatment had no effect on this characteristic.

Acknowledgements

The authors wish to thank Dr Faye Homer, Director of Guyana Sugar Corporation (GuySuCo) Central Analytical & Environment Monitoring Laboratories.

References:

1. Ahmedna M, Johns M, et al. Potential of agricultural by-product based activated carbons for use in raw sugar decolourisation. *Journal of Science of Food & Agriculture* **75**: 117-124
2. Fox D I, Hyland M M, (2003) Treatment of Iron Cyanides with activated carbon. *Chemistry at the interfaces: The 39th IUPAC Congress and the 86th Conference of the Canadian Society for Chemistry Abstracts, Ottawa, Canada (August 10-15)*
3. Garg V K, Amita M, et al. (2004:a) Basic dye (methylene blue) removal from simulated waste water by adsorption using Indian Rosewood sawdust: a timber industry waste. *Dyes and Pigments* **63**:243-250
4. Garg, V K, Gupta R, et al. (2003) Dye removal from aqueous solution by adsorption on treated sawdust. *Bioresource Technology* **89**: 121-124
5. Garg, V K, Gupta R, et al. (2004:b) Adsorption of chromium from aqueous solution on treated sawdust. *Bioresource Technology* **92**: 79-81
6. Garg, V K, Gupta R, et al. (2004:c) Removal of malachite green dye from aqueous solution by adsorption using agro-industry waste: a case of *Prosopis Cineraria*. *Dyes and Pigments* **62**: 1-10
7. Ho Y S & McKay, G, (2003) Sorption of dyes and copper ions onto biosorbents. *Process Biochemistry* **38**: 1047 – 1051
8. Kaewprasit C, Hequet E, et al. (1998) Application of methylene blue adsorption to cotton fibre specific surface area measurement: Part 1. Methodology. *The Journal of Cotton Science* **2**: 164 - 173
9. McKay G, et al. (1999) The removal of dye colours from aqueous solutions by adsorption on low cost materials. *Water Air & Soil Pollution* **114** (3-4): 423 - 438
10. Yu et al (2000) The removal of heavy metals from aqueous solutions by sawdust adsorption – removal of copper. *Journal of Hazardous Materials* **80** (1-3): 33-42

Chemistry / Physics of Materials

Organic Electronics: From Molecules to Devices

L. HIRSCH, G. WANTZ, N. HUBY, M. URIEN, L. VIGNAU AND J.P. PARNEIX

Fédération de Recherche SyMe CNRS FR2648 – Laboratoires PIOM & IXL, Ecole Nationale Supérieure de Chimie et de Physique de Bordeaux, 16 Av. Pey Berland 33607 Pessac Cedex, France hirsch@ixl.fr

Abstract

Since reports on efficient light emission from organic light-emitting (OLED) devices based on low molecular weight molecules and solution-processed conjugated polymers (PLED), the OLED field has gained great attention because of its applications in full-color flat-panel displays and lighting. OLED have several advantages, such as a wide viewing angle, low fabrication costs, as well as being light and thin. A large amount of dedicated research efforts has been expended in this field over the last decade. It is believed that the PLED technology has the potential to be economically applied to large-area, fine-pixel displays because the polymer film can be prepared by using a solution process such as spin-coating, screen printing, or ink-jet printing. The quantum efficiency of PLED light emission is, however, still below 5% and lifetimes still have to be improved.

Similar improvements are due to organic solar cells. The goal of solar cells is converting light energy to electrical power. Improving solar cells efficiency is improving the absorption coefficient, the exciton separation and charge collection at the electrodes. Within the different organic photovoltaic devices the conjugated polymer/fullerene bulk heterojunction approach is one of the foci of today's research interest. These devices are highly dependent on the solid state nanoscale morphology of the two components (donor/acceptor) in the photoactive layer.

The technological aspect for device fabrication will be presented. The influence of the substrate roughness will be discussed. The role of the molecular structure, the supramolecular organization and of the device architecture will be evoked. For instance, the control of substrate temperature during the OLED active layer deposition can lead to a lamellar structure which confines electron and holes in conjugated region. Other examples on OLEDs and organic solar cells will be presented.

Characterization of Vetiver Roots Activated Carbon and Absorption Of Phenolic Compounds

S. ALTENOR, B. CARENE, J. LAMBERT, J.J EHRHARDT, A. OUENSANGA AND S. GASPARD

Laboratoire COVACHIMM, EA 3592 . UFR des Sciences exactes et Naturelles. Université des Antilles et de la Guyane, Guadeloupe, France - sgaspard@univ-ag.fr

Abstract

Vetiver grass (*Vetiveria zizanioides*) roots are mainly used for industrial production of essential oil lead to huge quantities of lignocellulosic residues that can be used for activated carbon preparation. Sugar cane (*Saccharum spp.*) bagasse is the fibrous fraction that remains after the sugar milling of sugar cane plants. Approximately 47 000 tons of bagasse are produced in annually Guadeloupe and 10 000 tons of vetiver roots residues are produced in Haïti.

The conversion of that agriculture byproducts to activated carbons represents an opportunity to convert those under utilized lignocellulosic compounds to value-added materials. ACs have been prepared using vetiver roots and sugarcane bagasse by physical and chemical activation. Water steam and phosphoric acid (H_3PO_4) 85% ratios X_P: 0.5, 1 and 1.5 (g H_3PO_4 /g precursor); have been used as activating agents. ACs have been characterized. The specific surface area and the pore structure were evaluated from the results obtained by N_2 adsorption at 77 K. These results show that vetiver roots lead to both microporous and mesoporous ACs, while sugarcane bagasse provides mainly microporous ACs. The properties and chemical surface of these ACs were investigated by XPS (X-Ray Photoelectron Spectroscopy). Results of the adsorption tests with iodine, phenol, gallic acid and tannic acid show that, ACs with good adsorption properties can be obtained from vetiver roots and sugarcane bagasse. Their possible use for water treatment must be confirmed by attrition measurements.

Chemistry / Physics of Materials

A Comparative Study of Biological Indigenous Products Used to Increase Surface Hardness of Low Plain Carbon Steel

D. GOSSETT AND A. OLIVER

Faculty of Engineering & Computing, University of Technology, Jamaica, 237 Old Hope Road, Kingston 6, Jamaica - goliver@utech.edu.jm

Abstract

The use of indigenous plants containing nitrogen such as blue mountain coffee shells and cassava leaf were used to evaluate the possibility of case hardening plain low carbon steel by diffusion process. The comparative hardness of the plain low carbon steel of each product was studied as a function of time and temperature. For both plant products nine (9) plain carbon steel specimens were used at three (3) independent diffusion time and temperature.

The results indicate that both cassava and dry blue mountain coffee husk can be used for case hardening of plain low carbon steel. Peak hardness of 900 HV and case depth of 3mm with hardness values of 500 HV were obtained using blue mountain coffee shells as the case hardening medium.

The cassava leave showed peak hardness value of 800 HV. At a case depth of 3mm, the hardness value was 480 HV.

Industrial Production of Value-Added Chemicals From Sugarcane Bagasse

ISABELLE, GILLIAN B.

Edenscapes, Inc. Newton, MA 02459 U.S.A - gisabelle@edenscapes.com

Abstract

The Caribbean sugarcane industry will face intense pricing pressures within the next few years. While the industry is plagued by inefficiency (high costs and low productivity), it is one of the largest employers and agricultural producers in the region, and must therefore find a way to compete in the face of globalization. There is significant interest in diversifying into products of higher value which can command higher unit prices, broaden the region's manufacturing base and promote energy independence. In Jamaica, for example, in addition to the primary product, sugar, the one million tons of bagasse generated annually as a by-product may be converted by chemical and biochemical processes to create a diverse set of value-added products.

Edenscapes, Inc. is an industrial biotechnology company, focused on the production of value-added specialty chemicals and fuels using sugarcane and its by-products as raw materials. In order to be economically sustainable, production will depend on: (i) development of cost-effective manufacturing processes, so that the products can compete with those derived from fossil fuels; and (ii) the manufacture of a combination of products, such that no one product is required to cover the entire raw material cost.

In this presentation, issues surrounding the development of a commercial fermentation process for the conversion of bagasse into value-added products will be discussed, using xylitol as an example. As part of an ongoing collaboration with the Chemical and Biological Engineering Laboratory at MIT, xylitol is being prepared fermentatively from sugarcane bagasse hydrolysates by the yeast strain Candida guillermondii. Xylitol is a non-nutritive sweetener and an antibacterial which can be used by diabetics, a large and growing group. It is currently produced by an expensive chemical synthesis, leading to per kilogram selling prices up to 10 times those of sugar and other substitute sweeteners. An alternative production technique by yeast fermentation is being investigated, however, for an industrial fermentation process to be commercially successful, it is necessary to achieve high yields (efficient conversion of xylose into xylitol, in this case) at a high production rate. Preliminary data will be presented from this project.

Chemistry / Physics of Materials

Multi technique approach of chemical and mechanical properties of hot melts

N. NOMEDE MARTYR, A. GRUDA,S. RADEGONDE , T. CESAIRE, D. HIMMEL, J.L. MANSOT

Groupe de Technologie des Surfaces et Interfaces (GTSI EA 2432) - Université des Antilles et de la Guyane, Campus Fouillole, 97159 Pointe à Pitre, Guadeloupe (France) - nnomedem@univ-ag.fr

Hot melts used under environment conditions of equatorial/tropical climates, characterized by high humidity (98%), heavy rains (2 meters/year), high mean temperature (30°C) and high solar irradiation (2400 hours/year), undergo accelerated damage processes which limit their durability. The aim of the study under progress is the optimization of the formulas (type and relative proportion of mineral phases and binder) in order to improve their resistance to failures.
In order to achieve this goal, a multi-techniques approach of the hot melts and their components is developed. Mechanical properties (Elastic modulus, internal damping) of the hot melts are acquired by means of dynamical mechanical analysis and mechanical wave propagation in the media. Chemical information on the binders are obtained using classical selective extraction by solvents, in order to quantify the asphaltene / maltene proportion and residual solid (mineral) fraction. Analytical Scanning Electron Microscopy for elemental composition purpose. Vicoelasticity properties are acquired by mean of controlled temperature viscosimetry and DMA.
The communications presents first results obtained on various bitumens and manufactured hot melts.

Acknowledgments to Région Guadeloupe, Europe and Société Guadeloupéenne d'Enrobés à Chaud for their financial supports.

Table of contents

Energy / Environment / Pollution

A Day – Night Solar Air Dryer with the Temperature and Flow Rate Controls: Numérical Simulation and Experimental Results 75
O. Tamarin, J.L. Bernard, F. Dupont, H. Clergeot and M. Dupont

Lack of Significance of Usual Ecological Indicators in Predicting Pesticides Contamination: Specificities of Tropical Islands Freshwaters 79
S. Coat and D. Monti

A Reactor for the Decontamination of Water Using Titanium Dioxide Nanoparticles and Solar Energy 81
S. Ali Shah, R. Saunders and R. Clarke.

Metallic Contaminations in Two Bays of Guadeloupe - Set Up of a Biomonitoring Survey by Using a Biomarker of Genotoxicity on the Mangrove Oyster (*Crassostrea rhizophorae*) 85
G. Ramdine, D. Fichet and S. Lemoine

Short-Time Scales Variability of the Global Solar Radiation in Guadeloupe 87
T. Soubdhan, F. Dupont, R. Calif and B. Deshaies

Acceptance, Applicability and Efficiency of Batch Disinfection of Rainwater for Human Consumption in Rural Communities of Trinidad Using Solar Radiation 87
W.A. Mellowes and K.D. Thomas

Retrieval of Aerosol Optical Thickness from Solar Radiation Data: Study of a Saharan Dust Event In Guadeloupe 88
T. Feuillard, R. Bonhomme, J. Molinié, S. Jacoby-Koaly, R.H. Petit and F. Brute

High Particles Concentration Levels and Relationship with Air Conditioning: Study of Three Cases of Intoxication in Public Offices 89
J. Molinié, R.H. Petit, S. Jacoby-Koaly and A. Roussas

Measurement and Analysis of Wind Velocity and short Time Scale Wind Speed Forecast 89
R. Blonbou, R. Calif, F. Dupont, T. Soubdhan and B. Deshaies

Simulation of Rainfall Interception Processes for Pollution Hazards Estimation Under Banana Plants 90
C. Bassette and F. Bussière

Molasse Spentwash Treatment by Two Processes: Adsorption on AC and Biodegradation 90
S. Figaro, C. Jean-Marius, O. Gros, L. Farhasmane, B. Ganou, F. Bazile, W. Achouack, M.A. Roncato, A. Ouensanga and S. Gaspard

Measurement and Computer Representation of Banana Plants for Environmental Studies 91
S. Dufour-Kowalski, and F. Bussière

Energy Production and Pollutant Mitigation from Broiler Houses on Poultry Farms in Pennsylvania and Jamaica 92
N. M. Brown and C.E. Mortley

Root Growth Responses of a wheat Cropland Weed, *Melilotus indicus(L.) All.,* Papilionaceae to Air Pollution 93
Mohammad Saquib

Energy / Environment / Pollution

A day – night solar dryer with the temperature and the flow control: numerical simulation

OLLIVIER TAMARIN[1], JEAN LOUIS BERNARD[2], FRÉDERIC DUPONT[2], HENRI. CLERGEOT[1], MICHEL DUPONT[2]
Groupe de Recherche sur les Energies Renouvelables (GRER)
Université des Antilles et de la Guyane
[1]Campus de St Denis 97 300 Cayenne
[2]Campus de Fouiolle 97 157 Pointe à Pitre Cedex
ollivier.tamarin@guyane.univ-ag.fr

Abstract

A solar dryer working continuously during day and night had been experimented in Guadeloupe (FWI) and in French Guyana. To improve the prototype components size, a dynamic numerical simulation has been done in the electrical analogy scheme. Electrical tools, PSPICE / MATLAB and the thermal transient code TRNSYS has been used. The numerical results has been compared with the experimental data when the air temperature and (or) the air flow was controlled. A good agreement has been obtained.

Nomenclature

P_i	Solar Power, (W)
T_i	Temperature, (°C)
C_i	Thermal capacity, ($J.kg^{-1}.K^{-1}$)
R_i	Thermal resistance, ($° K.W^{-1}$)
C_{air}	Air thermal capacity , ($J.kg^{-1}.K^{-1}$)
I	Electrical current, (A)
V	Electrical potential, (V)
C	Electrical capacity, (F)
R	Electrical resistance, (Ω)
η	Optical efficiency of the solar panel

Introduction

Fruits production follows saisonnal cycle. In rural regions the overabundance followed with blackout periods is prevented by drying fruits exposed under the sun radiation [1]. Others more performant methods have been developed but they use energy sources such as gaz and electricity which are not disponible in isolated sites.

In regions where solar energy is abundant, the solar dryer is an adequate solution [2]. However the lack of sun during the night stop the drying process and could be responsible of the degradation of the product. To prevent this damage, a solar dryer has been completed with a solar hot water storage which is used during the night. A patent has been filed [3] in which a solar open cycle air dryer was included using a solid desiccant. When the air temperature is controlled, the drying process is more reproducible.

With the electrical analogy, complex systems can be represented with electrical circuits in place of differential equations.

In the following sections we will use this electrical analogy to modelize and to simulate our solar dryer and we propose to use the common electronics software (Orcad PSPICE) in order to make quantitative investigations of the solar dryer.

Both results from the well known TRNSYS software and the code used in the electrical engineering processes (Matlab-Simulink) has been compared with the experimental results.

Description of the solar dryer

On the figure 1 is given a synoptic diagram of the machine. The principal components of the dryer has been reported: the air solar collector and the drying room, the air water exchanger, the hot water storage. The electrical elements such as pump and fans could be supplied with photovoltaic panels. An automaton gave order to shut or open the valves introducing ambient air to be mixed with the hot air. A constant air flow is maintained in the drying room. Moreover, to manage a more reproducible drying process, a constant temperature with a constant air flow was necessary in the drying room. A PID controller was used for the regulation.

But, during the day, the air temperature depends of the solar collector temperature. During the night, a better temperature regulation could be obtained from the hot water storage temperature through the water-air heat exchanger

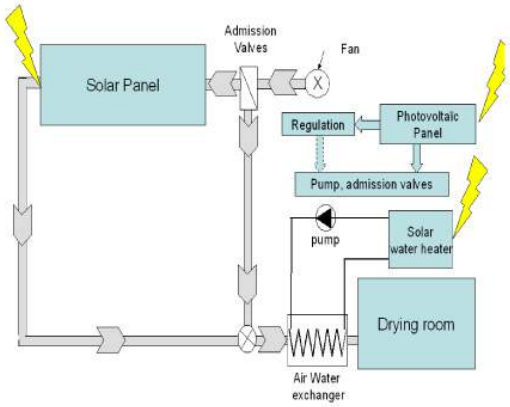

Figure 1. Synoptic diagram of the dryer

Modelisation

Solar collector :
On the table 1 has been given the analogy between electrical and thermal parameters and the relations between these parameters. the subscript i is a generic letter corresponding to a component of our solar dryer.

Thermal parameters	P_i	T_i	R_i	C_i	$T = R_i.P_i$	$P = C_i.\frac{dT}{dt}$
Electrical parameters	I	V	R	C	V= R.I	$I = C.\frac{dV}{dt}$

Table 1: Electrical and thermal parameters

The thermal power P_i is associated to the electrical current I as respectively the temperature T_i, the thermal capacity C_i, the thermal resistance R_i to the potential V, the electrical capacity C and the electrical resistance R.
In the model, T_e is the inlet and T_s is the outlet collector temperatures. T_a is the ambient air temperature. With a constant efficiency η the absorbed power by the collector P_R , the collector lost P_L and the power flow rate to the air P_g could be expressed with the followed equations:

$P_R = \eta.P_S$ (1)
$P_L = (T_S-T_e)/R_L$ (2)
$P_g = (T_S-T_e)/R_D$ (3)

where R_L is the collector thermal resistance and $R_D = 1 / (C_{air}.D)$ the thermal resistance of air through the collector. D was the mass flow rate and C_{air} the air thermal capacity.

The power balance gave the differential equation of the outlet air temperature where C_p is the thermal capacity of the collector:
$C_p.dT/dt = P_R - (T_S-T_e)/R_D-(T_S-T_a)/R_L$ (4)

The equation (4) gave the electric diagram of the solar collector reported in the figure 2.

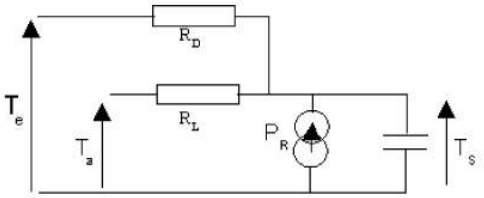

Figure 2. Equivalent circuit of the solar collector

The transfer function in Laplace space is: :

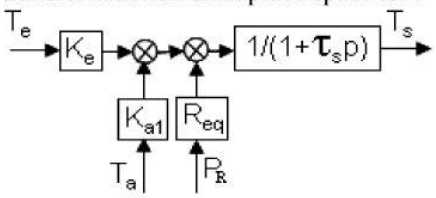

Figure 3: Transfer function of the solar collector.
$K_{a1} = R_{eq} / R_L$, $K_e = R_{eq} / R_D$, $\tau_s = R_{eq}.Cp$

Air temperature and flow rate regulation :
Control of the air mass flow rate and of the air temperature has been obtained with two valves. Their openings was ordered depending of the outlet air collector temperature and of the air flow rate D. The ratio x of new ambient air was mixed with (1-x) ratio from the solar collector. In final the regulation was controlled by the balance equation: $T_{mix}-T_e = x(T_S-T_e)$ with $0 \leq x \leq 1$. T_{mix} is the inlet temperature of the drying room.

Drying room:
The balance of the thermal flow rate entering and leaving the drying room leads to an equivalent circuit.

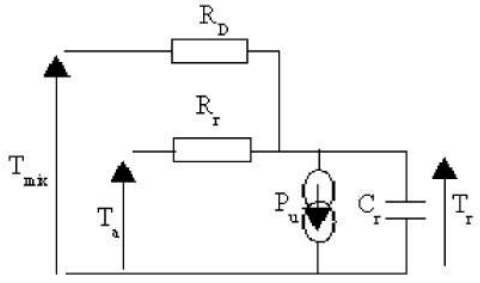

Figure 4: Equivalent circuit for the drying room.

R_r is the thermal resistance between the drying room and the ambient air, T_r is the room temperature. P_u is the thermal power needed for the dehydration process.

The whole transfer function is given on the figure 5. Both, the electric circuit (with Orcad PSPICE for example) and the transfer function (with Matlab Simulink) allowed to simulate the heat transfer in dynamic regime.

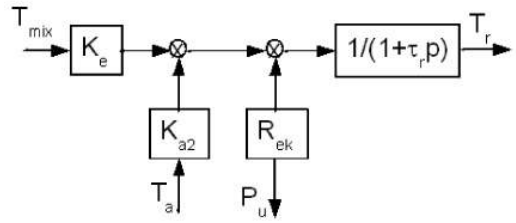

Figure 5 : Transfer function of the drying process.

$1/R_{ek} = 1/R_D + 1/R_r$, $K_{a2}=R_{ek}/R_r$, $K_e=R_{ek}/R_D$, $\tau_r = R_{ek}.C_r$

Simulation

The thermal resistances and the thermal capacities are reported on the table 2.
The values has been determined from the thermophysical parameters the masses, the thickness of the different pieces of the prototype built in our laboratory [3,4].

Solar collector	$C_P = 41.10^{3}$ J.°C^{-1}	$R_P = 29.10^{-3}$ C.°W^{-1}
Drying room	$C_r = 20.10^{3}$ J.°C^{-1}	$R_r = 0{,}50$ °C W^{-1}.

Table 2 : Values of the parameters used in the simulation

The figure 6 gives a Simulink diagram of the whole solar dryer using all the transfer functions. The regulation of the temperature used a PID controller coupled with the control flow rate.

Test of the solar dryer model

The simulation has been tested in comparing the calculation results with the experimental data. The outlet temperatures from the solar collector and the drying room compared on the figure 7 and 8 allowed a fitting of the thermal resistances of the collector and the drying room. No more then a 10% adjustment has been necessary.

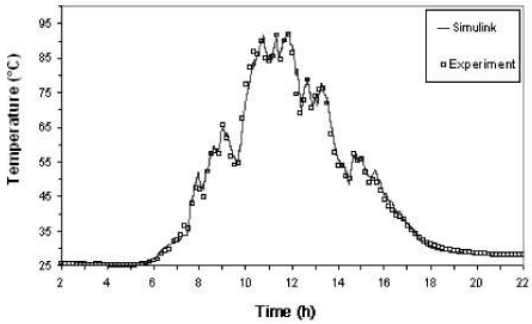

Figure 7. Outlet solar collector temperature.

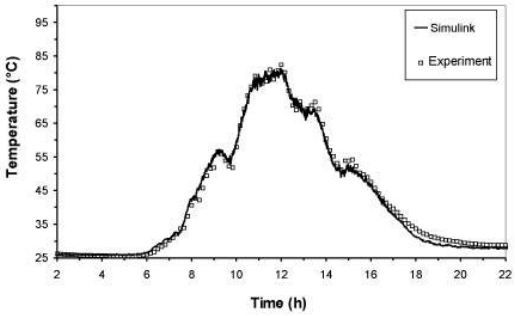

Figure 8 : Drying room temperature.

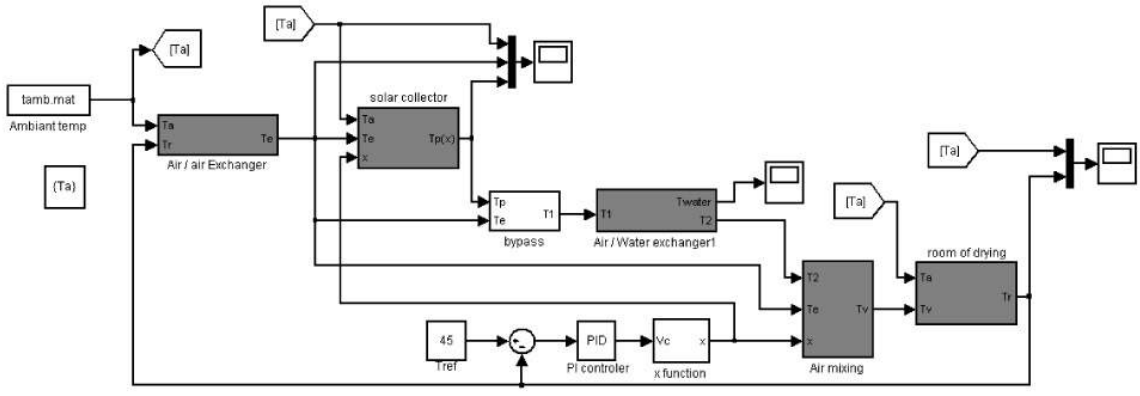

Figure 6: Simulink diagram of the regulated solar dryer

Comparison between Matlab-Simulink and TRNSYS simulations.

TRNSYS and Simulink simulations are compared on the figure 9 where the temperature of the drying room has been calculated for 25 $m^3.h^{-1}$ and 55 $m^3.h^{-1}$ flow rates:
These results show that the both approaches seemed equivalent. They give the same qualitative evolution of temperature as a function of the time in spite of some difference near the maximum.

.

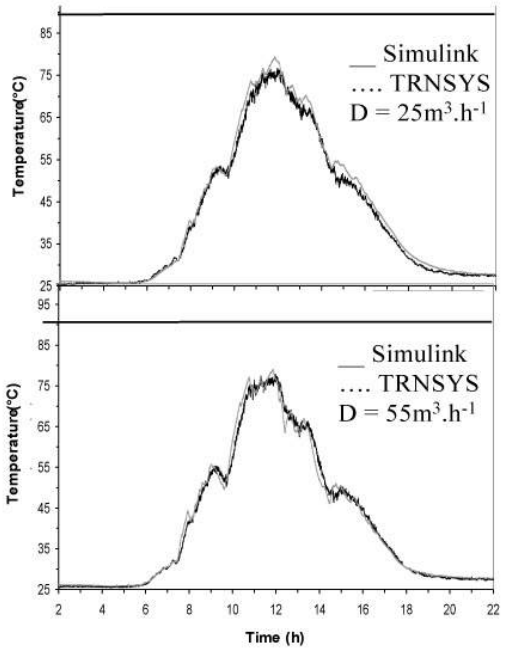

Figure 9 :Comparison of the TRNSYS and the Simulink calculated air temperatures in the drying room.

We concluded that it was possible to model a thermal system with electrical engineering software (Matlab/Simulink, Orcad Pspice). Indeed, these softwares allowed to model the behaviours of electrical devices (for example the control system) and to model the heat flow

Regulation of the drying room temperature.

The temperature of the drying room has been regulated with a constant flow rate

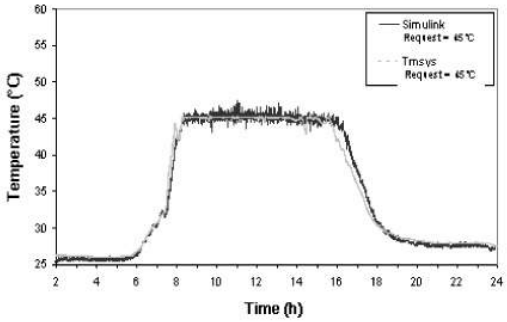

Figure 10 : Regulation of the drying temperature at 45°C.

During the night process with two intake valves and a PID control. The results from Matlab Simulink and TRNSYS are compared on the figure 10 when the drying temperature has been fixed at 45°C, the air flow rate at 55 $m^3.h^{-1}$. The temperature of the drying room has been regulated with a constant flow rate. Simulink and TRNSYS approaches gave the same evolution of the drying room: the beginning of the regulation near 8 am, low temperature variations near the requested value (45°C), decreasing of the temperature after 16 pm when the sun went down.

Conclusion

In this paper a simulation method of a thermal system like a solar dryer has been proposed using the electric analogy. The Matlab Simulink software has been used. The model has been validated with experimental data.
Such approach of the heat transfer simulation using the Matlab Simulink graphic tools, has been compared with TRNSYS code commonly used to describe thermal systems in dynamic regime. The two simulations are in good agreement and the electrical approach will make easier a rapid description of heat tranfer from an electrical scheme. The model will be completed to describe the whole system continuously during day and night.

Références

[1] A. Esper and W. Mühlbauer. Solar Drying. An Effective Means of Food Preservation. *Renewable Energy*, 15(1-4):95–100, Sept 1998.
[2] O. V. Ekechukwu and B. Norton. Review of Solar-Energy Drying System 2: An Overview of Solar Drying Technology. *Energy Conversion and Management*, 40(6):615–655, 1998.
[3] F. Dupont, L. Philis, M. Dupont, Dispositif solaire en production d'air chaud à température asservie en continu jour et nuit, *Brevet n° 0400385000,* 15 janvier 2004.
[4] F. Dupont, R. Blonbou, M. Dupont, Night and Day Solar Warm Air Production. Application to the Vegetable drying, *Proceedings of the Fourth European Thermal Conference 2004,* England, 29-31 Mars 2004.

Energy / Environment / Pollution

Lack of significance of usual ecological indicators in predicting pesticides contamination: specificities of tropical islands freshwaters

SOPHIE COAT AND DOMINIQUE MONTI

Laboratoire de Biologie Marine, UFR Sciences, Université des Antilles et de la Guyane, BP592, 97159 Pointe-à-Pitre cedex - sophie.coat@univ-ag.fr, dominique.monti@univ-ag.fr

Abstract

Residues of pesticides were measured in the freshwater fauna of five rivers situated in Basse-Terre, Guadeloupe (French West Indies). The results confirm the presence of pesticides at high levels in fish and crustaceans with four recurrent molecules : organochlorinated insecticides (chlordecone, β-HCH, dieldrin) and fungicides (dithiocarbamates). In the same locations, common ecological indicators were calculated but no link was detected between the biocontamination levels and these indicators usually used to express the environmental quality. This lack of significance is interpreted as the result of the strong originalities of tropical freshwater ecosystems that are pointed out.

Introduction

Most of the freshwaters ecosystems of Guadeloupe are affected by varying pollutions. Intensive agriculture led to the use of considerable amounts of pesticides which could contribute to the degradation of water quality and ecosystems. Organochlorinated insecticides (chlordecone/kepone, β-HCH and dieldrin) and fungicides (dithiocarbamates) were detected at high levels in some river mouths of the south of Basse-Terre (up to 3.2 µg/L of chlordecone (DIREN, 2004)). These chemicals, toxic and persistent, are usually considered as a threat for freshwater fauna.

This study was aimed at *i)* assessing the level of biocontamination of fish and crustacean species from the most contaminated area and *ii)* confronting these results with common ecological indicators used to evaluate quality in ecological surveys.

Materials and methods

Sampling : stratified sampling was performed in five rivers with various levels of pesticide contamination (Figure 1). Organisms collected by electrofishing were numbered, measured, weighed and returned alive to the river, except for a sample which was subjected to analyses of its pesticide content. Collected species belong to the three major groups of tropical freshwater organisms : the Fishes, the *Palaemonidae* shrimps (Ouassous) and the *Atyidae* shrimps (Cacadors).

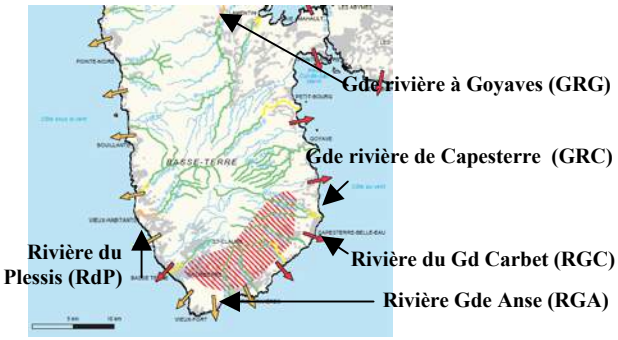

Figure 1 : Sampling stations in Basse-Terre island, Guadeloupe (Source: DIREN, 2001).

Chemical analysis : sample processing (extraction and purification) and measurement of pesticide concentrations were carried out at the Laboratoire Départemental d'Analyses de la Drôme (Valence, France). We checked for 126 pesticides in various tissues (muscle, liver, hepatopancreas or gonad).

Ecological indicators (species richness, total abundance, total biomass, diversities) were calculated for each river studied.

Results and Discussion

Whatever the species and the tissue analysed, all organisms collected were contamined by various and high levels of pesticides (Table 1). Four recurrent molecules were identified: three of them belonging to the organochlorinated

pesticides (chlordecone, β HCH, dieldrin) and the other pooled as a group, the dithiocarbamates. Chlordecone, an insecticide used during forty years and prohibited in 1993 in Guadeloupe, showed the highest concentrations in organisms, up to 39400 µg/kg wet weight in the liver of the fish *Gobiomorus Dormitor* at the Rivière Grande Anse (RGA).

Table 1 : Higher levels of pesticides detected in aquatic fauna of the freshwater contaminated area

Rivers	Pesticides detected in organisms	Bioconcentrations (µg/kg wet weight) in the most contaminated species
GRG	-chlordecone -dithiocarbamates	290 µg/kg chlordecone in liver of *Eleotris sp*.
RdP	-chlordecone -β HCH -dithiocarbamates	1 300 µg/kg chlordecone in gonad and hepatopancreas of *Macrobrachium carcinus*
RGC	-chlordecone -β HCH -dithiocarbamates	2 100 µg/kg chlordecone in muscle of *Macrobrachium faustinum*
GRC	-chlordecone -β HCH -dithiocarbamates	8 700 µg/kg chlordecone in gonad and hepatopancreas of *Macrobrachium faustinum*
RGA	-chlordecone -β HCH -dithiocarbamates -dieldrin	39 400 µg/kg chlordecone in liver of *Gobiomorus dormitor*

Ecological indicators, reported in Table 2, are calculated for the same surface unit (80 m^2) sampled in each river .

Table 2: Ecological indicators

Rivers	Species richness	Abundance	Biomass	Diversity index H'
GRG	10	869	1701 g	1.26
RdP	11	904	736 g	1.52
RGC	8	232	439 g	1.48
GRC	8	372	557 g	1.44
RGA	11	822	1715 g	1.66

Three of the best values for these synthetic indicators were found in the Rivière Grande Anse (RGA), where we detected the most contaminated organisms.

Conclusion

The incidence between pesticides contamination and perturbation of aquatic species equilibriums is well documented in the literature. However, our results do not reveals any link between the biocontamination levels and the ecological indicators usually used to express changes in environmental quality. This lack of significance is the result of the strong originalities of 90 % of the species living in our tropical freshwater ecosystems :

1. they are amphidromous species that spend their larval and juvenile stages elsewhere in saline waters or open sea,
2. every year, juveniles migrate upstream and colonize new biotopes,
3. at adult stage, individuals move regularly through altitude gradients.

These species finally never spend their entire life cycle in the same place and are poorly integrative of the ecosystem quality. These results emphasize the need of more accurate studies in order to set up physiological or ecological indicators of tropical freshwater ecosystems characteristics.

Acknowledgements

Financial support from the Direction Régionale de l'Environnement de Guadeloupe (DIREN) is gratefully acknowledged.

References :

DIREN, 2001. Schéma directeur d'aménagement et de gestion des eaux (SDAGE de la Guadeloupe).

DIREN, 2004. Suivi phytosanitaire sur les eaux superficielles en 2003 et 2004.

Energy / Environment / Pollution

A Reactor for the Decontamination of Water using Titanium Dioxide Nanoparticles and Solar Energy.

Shazaad Ali Shah, Ramsey Saunders, Ricardo Clarke. Department of Physics
The University of the West Indies, St Augustine, Trinidad. sali-shah@fsa.uwi.tt - rsaunders@fsa.uwi.tt

Abstract

In previous work using the solar disinfection (SODIS) method we have shown that a 99.9% deactivation of E.coli bacteria is achieved after four (4) hours of insulation and that with simple solar concentration techniques the decontamination time was reduced to one (1) hour. We have now built and successfully tested a photocatalytic reactor using TiO_2 nanoparticles immobilized on a glass plate. This reactor is capable of decontaminating water on a larger scale and in a shorter time than is possible with SODIS. A 1 m^2 glass plate on which TiO_2 is deposited forms the lower plate of a sealed double plate reactor. The top plate consists of glass which is not only protective but also serves as the window for infrared and ultra-violet light either from the sun or an artificial source (two 500 watt halogen lamps). The reactor can be tilted at angles in the range 0-30 degrees and can be rotated to track the sun if necessary. Initially it was oriented in a north-south direction on the roof of the Natural Science building at an inclination of 11 degrees to the horizontal consistent with the latitude of Trinidad and exposed to sunlight. Contaminated water is pumped from a reservoir to the top of the reactor and flows by gravity over the active surface back to the reservoir. Bacterial counts were carried out on samples of water from the reservoir at various intervals. Experiments were also carried out during nighttime as a control. While, under sunny conditions (1058Wh/m^2) complete disinfection occurred after thirty (30) minutes, under cloudy conditions (750.5Wh/m^2) the time required was sixty (60) minutes. There was no effect for runs carried out at night-times. This rapid sterilization of contaminated water is attributed to the production of highly reactive species of hydroxyl radicals produced by titanium dioxide in the presence of the UV component of sunlight.

Introduction

The availability of potable water is an important issue in the modern world. In the developed countries the purification and recycling of wastewater by modern technologies such as reverse osmosis have contributed significantly to improving the availability of potable water. Today, about two billion people in mainly in the developing world do not have a safe supply of drinking water (WHO Report, 1993). Diarrhea and the resulting body dehydration are respon-sible for about 2.5 million deaths annually in the third world. Additionally, fresh water avail-ability can become a life threatening issue as a result of natural disasters. The aftermath of the tsunami in South East Asia on December 26th 2004, and the effects of hurricane Katrina in the United States in August of 2005 are clear examples of the effect of disasters on the fresh water supplies. It is therefore important that simple technological methods be developed not only to satisfy the needs of poor communities in areas of the developing world such as Latin America and the Caribbean but also to address the immediate needs of people following natural disasters. In earlier publications we have shown that the solar disinfection (SODIS) method can be applied under the environmental conditions of Trinidad and Tobago. Water contaminated with E. coli bacteria can be purified in four hours by the SODIS method using PET bottles and in two hours using simple solar concen-tration techniques. In this paper we report on the disinfection of artificially contaminated water using solar energy together with a reactor with an active surface containing titanium dioxide nanoparticles.

Materials & Method

Figure (1) is a schematic view of the Titanium dioxide (TiO_2) reactor system.

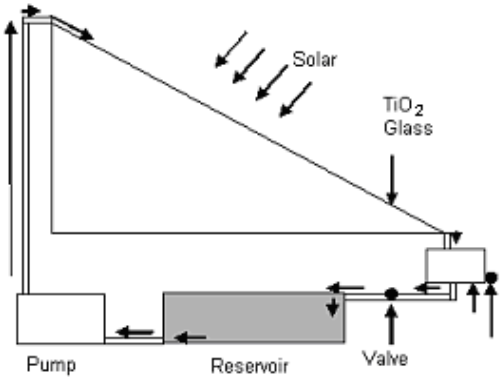

Figure (1) Schematic view of the Reactor

The reactor consists of two glass plates mounted in an aluminum frame. They are separated by about 8.0cm. TiO2 is deposited on the lower plate, which is made of frosted glass. This is the "active" surface of the reactor. The upper plate is protective and consists of normal transparent clear glass. Both plates are supported by "channelings" on the inner perimeter of the aluminum frame. The supporting base consists of three sections, which can be easily dismantled making it very portable. The upper section has a deep recessed area to accommodate the reactor and built in locks to firmly secure it. The middle section has adjustable stability pins at the corners to ensure stability of the entire structure. It has, in addition, two pivots at one end for attachment to the upper section and a centrally mounted car jack to permit elevation of the upper section, which carries the reactor. The lower section is the "foot" of the entire system. It contains a centrally mounted bearing to which the middle section is connected. This section permits rotation of the middle section about its axis for solar tracking. In operation the upper section forms a sealed chamber, which can be inclined at an appropriate angle. The peristaltic pump ensures a fixed flow rate of contaminated water to the top of the active reactor plate, which then flows under the influence of gravity to the collection point at the lower end of the plate. The flow rate can be varied to determine the optimum rate for photo-degradation. The stainless steel reservoir can be isolated from the main reservoir by a valve, which therefore permits single runs or multiple runs. The inlet port and both outlet ports are made of polyvinyl chloride (PVC). All areas with which the contaminated water will be in contact are constructed with either stainless steel, glass, PVC or non-reacting Tygon hosing. To coat the active reactor plate with TiO_2, the protective plate of the upper section was removed to expose the active reactor plate and the "sedimentation" method used. With this plate in a horizontal position, a suspension of 8gm of TiO_2 in two (2) litres of water was poured onto it. The TiO_2 in the suspension was deposited on the frosted glass plate in about twelve (12) hours and excess water removed by evaporation.

Contaminated water from a reservoir is pumped at a rate of 50 litres per hour into the reactor and allowed to flow by gravity over the active surface while being exposed to sunlight. Water collected from the reactor flows into the reservoir and is recycled. It is also tested for fecal coliform bacteria at intervals using the COLILERT 18 method.

This experiment was performed on four separate occasions as indicated in the results.

Results & Discussion

Sunday 12th June 2005, 11:10 am — 1:40 pm

This was a sunny day with mild cloud cover. The weather pattern changed however after forty minutes into the experiment. Increasing cloud cover caused the insulation to drop to values as low as 316Wh/m^2 for a short time duration. Subsequently the insulation values increased rapidly to yield a maximum value of 1.1kWh/m^2 for the latter part of the testing. The average insulation was 1058 Wh/m^2.

A maximum air temperature of 36^0 C was attained about thirty minutes (30) into the run. This fell with the increase in cloud cover to 30^0C but then increased to 32^0C. The inner layer (area between the both plates) temperature at the start was 42^0C and it remained at this temperature for 40 minutes. With the drop in insulation values,

the temperature also decreased. The reservoir temperature rose from 27.4^{0}C to 43.5^{0}C in 40 minutes. Again with the drop in insulation its characteristics were similar to that of the other parameters. Both the reservoir temperature and the inner layer temperature rose to a maximum of 48^{0}C after 150 minutes. Bacterial counts were down to measurable values within 10 minutes and all bacteria were totally destroyed after a further 15 minutes.

Thursday 23rd June 2005, 12:30 pm — 1:30 pm

There was more cloud cover than what was experienced on June 12th. A marked reduction in the insulation with an average value of 733 Wh/m^2 was observed.

A maximum air temperature of 34^{0}C was observed at the start but there was a gradual drop in value throughout the experiment with a minimum value of 27^{0}C being recorded. The reservoir temperature increased from 24.5^{0}C to a maximum of 41.7^{0}C. The inner layer however maintained an average temperature of 41^{0}C. Bacterial decrease was rapid. After 15 minutes the bacterial count per 100 ml was down to a measurable level and it fell to zero in a further 15 minutes.

Thursday 30th June, 2005, 2:10 pm – 3:10 pm

This day in comparison with the other days was overcast. There was a decrease in insulation from a maximum value of 820 Wh/m^2 to a minimum value of 645 Wh/m^2. The average insulation for the duration of the experiment was 750.5 Wh/m^2.

The air temperature was constant throughout the experiment with an average value of 34^0 C being observed. The reservoir temperature increased from 28.9^{0}C to 42.4^{0}C in just one hour.

Bacterial decrease was not as rapid as with the previous two days, however, after 45 minutes, the counts per 100 ml were down to a measurable level. Total degradation was achieved in a further 15 minutes.

Wednesday 6th July, 2005, 8:45 pm – 10:45 pm

The same procedure was followed as with the other days with one exception. This experiment was performed in the night. The insulation was zero throughout the experiment. The air temperature was at 28^{0}C at the start and it dropped to 27^{0}C for the balance of the experiment. At the start, the reservoir temperature was 25.4^{0}C and it decreased by 0.4^{0}C over the 2-hour duration of the testing. Bacterial counts were unaltered for the experiment.

For comparism purposes the insulation values are shown in Fig (2). As previously mentioned the average value of 1058 Wh/m^2 for June 12th was the highest.

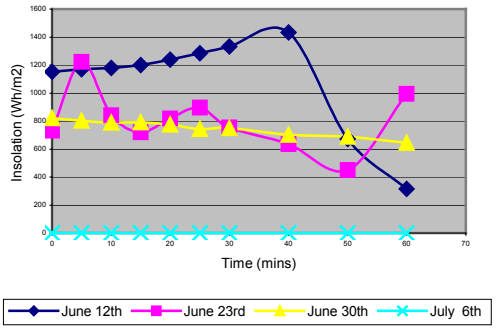

Figure (2) Insulation graphs for the 12th, 23rd and 30th of June and the 6th of July.

Except for the night run there was generally an increase in the temperature of the reservoir as well as the reactor with time. The final temperature of the reservoir after one hour in each case was 42 degrees Celsius as shown in figure (3). This increase in temperature will contribute to a reduction in the bacterial concentration (see Clarke et. al, 2005). However temperature increase cannot fully account for the data since SODIS must operate for about four hours for complete removal of E coli.

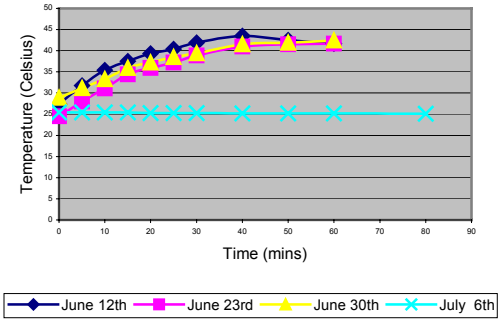

Figure (3) Reservoir temperatures for the 12th, 23rd and 30th of June and the 6th of July.

No heating effect was observed on the night of July 6th. The temperature recorded was the ambient temperature and this decreased by less than 1^0C as the night became cooler. There was no insulation also as expected. In our experiments complete disinfection was obtained after 30 minutes on two occasions and 60 minutes on another occasion as shown in figure (4).

We believe that the photo-catalytic effect of Titanium dioxide is the main contributor to the observed decrease in bacterial concentration with the assistance of ultraviolet light. TiO_2 is a photocatalyst, which absorbs ultraviolet light from short wavelengths up to 385nm and is known to be effective in solar detoxification (Pelizzetli et al, 1990; Linsebigler et al 1995).

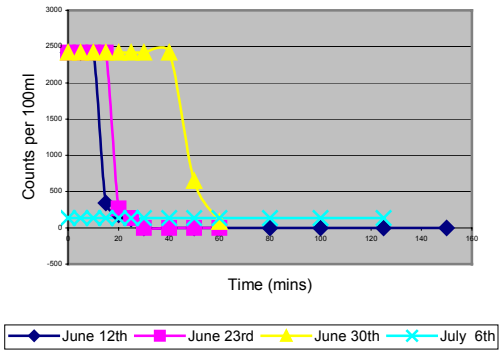

Figure (4) Bacterial decrease with time for the 12th, 23rd and 30th of June and the 6th of July.

Upon near UV irradiation, TiO_2 generates electron/hole (e^-/ h+) pairs, according to equation (1).

$$TiO_2 + hv \text{ ------ } TiO_2\ (e^- + h+) \text{ -------- } (1)$$

The latter can react with surface bound hydroxyl groups to generate hydroxyl radicals as shown in Equation (2).

$$TiO_2\ (h+) + OH^- \text{------ } \cdot OH + TiO_2 \text{ ------ } (2)$$

The hydroxyl radicals then attack the bacteria thereby disinfecting the water. It is perhaps significant to note that while the solar insulation on June 30th was about the same average value as on June 23rd, bacteria were totally eliminated in 60 minutes on June 30th but in 30 minutes on June 23rd. June 30th was however a cloudier day which suggests a reduced UV effect and consequently an increased time duration for complete disinfection. This also explains why no effect was obtained for the night run.

REFERENCES

Clarke R, Saunders R., Mellowes W., Kimkeram K., and Ali Shah S. (2005). Economic technologies for water disinfection in rural areas in Trinidad. APCSEET 2005, 116-122

Linsebigler A.L, Lu G, and Yates Jr.J. T. (1995). Photocatalysis in TiO2 surfaces: principles, mechanisms and selected results. Chem. Rev. ., 95, 735-758.

Pelizzetti E., Minor C and Maurino C. (1990) The role of colloidal particles in the photodegration of organic compounds of environmental concern in aquatic systems. Advances in Colloidal Interface Science, 32, 271-316.

WHO: Guidelines for drinking water quality (1993) 2nd Edition Vol. 1, Geneva

Raquel F.P. Nogueira and Wilson F. Jardim, 1996, "TiO2-fixed bed reactor for water decontamination using solar light," Solar energy, vol.56, No.5, pp. 471-477.

Metallic contaminations in two bays of Guadeloupe – Set up of a biomonitoring survey by using a biomarker of genotoxicity on the mangrove oyster (*Crassostrea rhizophorae*).

Gaëlle Ramdine [(1)], Denis Fichet [(2)], Soazig Lemoine [(1)]

(1) Laboratoire de Biologie Marine, DYNECAR, Université des Antilles et de la Guyane, Campus de Fouillole, BP 592, 97159 Pointe-à-Pitre cedex. (2) Laboratoire de Biologie et d'Environnement Marin, FRE CNRS 2727, Université de La Rochelle, Pôle Science, Avenue Michel Crépeau 17042 La Rochelle.
gaelle.ramdine@univ-ag.fr , denis.fichet@univ-lr.fr , soazig.lemoine@univ-ag.fr

Abstract

The pollution of coastal marine ecosystems has become an important concern for the Caribbean islands and especially in Guadeloupe (Lesser Antilles). In this island, many human activities are concentrated around two bays: the Grand Cul-de-Sac Marin and the Petit Cul-de-Sac Marin, and contribute to the contamination of the whole coastal ecosystems by polluting substances such as heavy metals. The present study aimed at assessing the metallic contamination of these two bays. Effects induced by the pollution in oysters were assessed by using a biomarker of genotoxicity in a "comet assay". Concentrations of three non-essential trace metals with toxicity (cadmium: Cd, mercury: Hg and Lead: Pb) were measured in fine sediment fraction (<63µm) and soft tissues of mangrove oysters (*Crassostrea rhizophorae*). Heavy metal concentrations recorded in Guadeloupe were generally lower than concentrations recorded in other Caribbean and South American countries. Nevertheless, stations localised within the Grand Cul-de-Sac Marin marine reserve, near the dump of Grand-Camp (Rivière Salée), exhibited high metallic concentrations. The comet assay underlined important induced effects on oysters coming from contaminated stations. Further investigations involving a wider range of indicators should be conducted to properly quantify the metallic contamination detected in these areas.

Introduction

The pollution of coastal marine ecosystems has become an important concern in a worldwide scale. In the Caribbean Islands, Guadeloupe (F.W.I.) is concerned by this problem as well. Indeed, many human activities are expanding on Guadeloupe's coastline. The main goals of the study are to establish an assessment of metallic contamination in two bays of Guadeloupe: the Grand Cul-de-Sac Marin and the Petit Cul-de-Sac Marin, and to evaluate the effects induced by pollution on the organisms.

Materials & Methods

Samples were taken in 22 stations around the Grand Cul-de-Sac Marin, the Rivière Salée and the Petit Cul-de-Sac Marin (Figure 1) from January to February 2005.

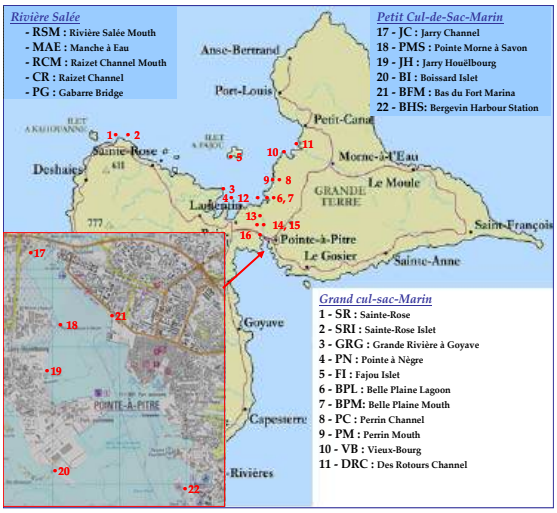

Figure 1: Location of the different stations in the study area

Samples of sediment and mangrove oysters were collected. Surface sediment samples were collected by core sampling and dried at 50°C. The fine fraction

(<63 µm) separated by nylon sieves was conserved to be analyzed. After 24 hours of depuration, mangrove oysters tissues were collected, pooled (10 individuals per lots) before homogenization and drying at 50°C.

For heavy metals analysis, sediment and oyster soft tissues were dissolved in concentrated nitric acid. Reagent blanks and standard reference materials were submitted to the same protocol as the samples. Atomic absorption spectrophotometry by flame or graphite furnace was used to analyze cadmium and lead. Total mercury was analyzed with an Automated Mercury Analysis system fit for solid sample.

For genotoxicity analysis, the Comet assay/Single Cell Gel (SCG) was used. It is a recent technique developed to detect DNA strand breaks (1). A suspension of oyster's gills single cells was included in agarose gel. Cells were lysed in an alkaline solution to liberate DNA, prior to be submitted to an electrophoresis. DNA was stained with ethidium bromide and then visualized by microscopy. Comets were classified into four categories based on the length of migration and/or the perceived relative proportion of DNA in the tail. By assigning a numerical value to each category, an average could be calculated. This test was realized on 11 individuals sampled in five stations.

Results

Concentrations of Cd, Hg and Pb in the sediment and mangrove oyster's soft tissues (*Crassostrea rhizophorae*)

The concentrations range from 0.059 to 0.764 mg/kg, dw for Cd; from 0.03 to 0.75 mg/kg, dw for Hg and from 4.88 to 465.9 mg/kg, dw for Pb (Figures 2a, 2b).

In the fine surface sediment, the highest concentrations of Cd, Hg and Pb are found in the site of Rivière Salée.
In oysters soft tissues, the concentrations range from 0.11 to 0.92 mg/kg, dw for Cd ; from 0.04 to 0.205 mg/kg, dw for Hg and from 0.072 to 1.47 mg/kg, dw for Pb (Figure 3).
In the soft tissues of oysters, the highest concentrations of Cd, Hg and Pb are found in the site of the Rivière Salée.

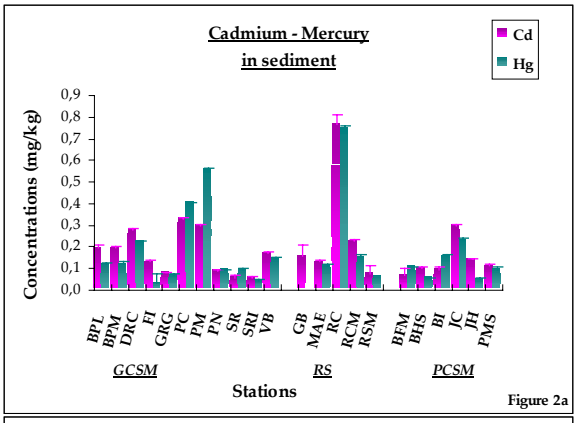

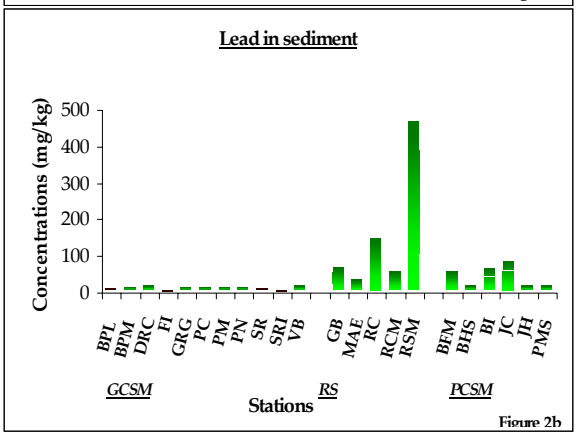

Figures 2: Average values of metallic concentrations (mg/kg, dry weight) into the sediments coming from the three sites of the study zone. GCSM: Grand Cul-de-Sac Marin; RS: Rivière Salée; PCSM: Petit cul-de-sac Marin.

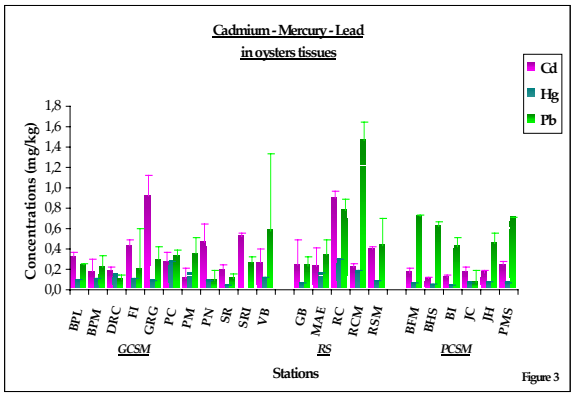

Figure 3: Concentration of Cd, Hg and Pb (mg/kg, dry weight) in the total soft tissues of mangrove oysters (*Crassostrea rhizophorae*) coming from the three sites in the study zone (value are expressed as means ± S.D). GCSM: Grand Cul-de-Sac Marin; RS: Rivière Salée; PCSM: Petit Cul-de-Sac Marin.

Genotoxicity analysis: results of the Comet assay
Stations GB, GRG and RC are not significantly different and show important mean scores, while RSM and FI mean scores are less important.

Discussion and Conclusion
In Guadeloupe, the concentrations recorded are generally lower than those recorded in other Caribbean and South American countries (2, 3).

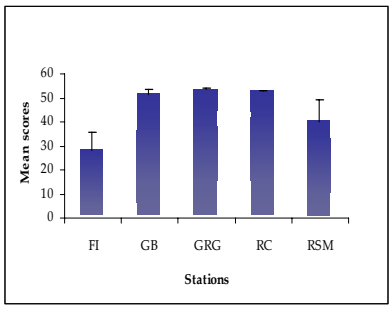

Figure 4: Mean scores (n = 11) for the five stations studied. FI: Fajou Islet; GB: Gabarre Bridge; GRG: Grande Rivière à Goyave; RC: Raizet Channel; RSM: Rivière Salée Mouth.

In the Rivière Salée site, the concentrations recorded into the sediment and the oyster' soft tissues are higher than the other sites. Into Rivière Salée site, the highest concentrations of cadmium, lead and mercury, three non-essential trace metals with high toxicity (4, 5) were recorded in Raizet Channel which receives all the lixiviation products of the intercommunal Grand-Camp dump (6).
These data suggest that Cd and Hg have a high bioavailability coupled with and eventual partial or non-existent regulation, contrary to Pb (Figures 2, 3).
The comet assay underlines important induced effects into contaminated stations. Nevertheless it only permits to evaluate the health level of oysters analyzed because this test is not specific to metals.

It would be advisable to continue these investigations in regular studies by using a wide range of bio-indicators, and metallic specific biomarkers like métalloamthionéines (7). Moreover, it would be interesting to keep Fajou Islet as a reference station for forthcoming studies.

References
(1) Tice *et al.*, 2000. Environmental and Molecular Mutagenesis 35, 206-221.

(2) Sbriz *et al.*, 1998. Marine Pollution Bulletin 36 (12), 971-979.

(3) Rojas de Astudillo *et al.*, 2002. Archives of Environmental Contamination and Toxicology 42, 410-415.

(4) Depledge, M.H., Rainbow, P.S., 1990. Models of regulation and accumulation of trace metals in marine invertebrates. Comp. Biochem. Physiol. 97C, (1) 1-7.

(5) Pruski, A.M., Dixon, D.R., 2002. Effects of cadmium on nuclear integrity and DNA repair efficiency in the gill cells of Mytilus edulis. Aquatic Toxicology 57, 127-137.

(6) DDE Guadeloupe, Mai 1995. Impact de la décharge publique de Grand-Camp sur la pollution de la Rivière Salée.

(7) Rebelo *et al.*, 2003. Aquatic Toxicology 64, 359-362.

Energy / Environment / Pollution

Short - Time Scales Variability of the Global Solar Radiation in Guadeloupe

T. SOUBDHAN, F. DUPONT, R. CALIF AND B. DESHAIES

Groupe de Recherche sur les Energies Renouvelables, Université des Antilles et de la Guyane
Campus de Fouillole, BP 592, 97157 Pointe à Pitre cedex - Ted.soubdhan@univ-ag.fr

Abstract

The amount of solar radiation arriving at a particular location varies greatly with time. A part from the astronomical and geographic factor, such as the day of the year, the time, latitude and surface geometry that constitute its deterministic component, the solar radiation also depends on the size, velocity and type of clouds, which is responsible of rapid stochastic irradiance variations. Thereby, as shown by a preliminary measurement campaign, these rapid stochastic variations at a given time can reach a significant amount (nearly 60%) of the expected clear sky irradiance. Moreover, these variations can occur on very short time scales (down to few seconds), a situation frequently observed in tropical climate.

The global solar irradiance variability at surface level is an important parameter in designing solar energy applications such as photovoltaic cells or energy efficient building design. For instance, this volatility of the solar radiation demands a specific adaptation of the electronics (regulator, UPS, ...) for grid connected photovoltaic systems, as it can initiate instabilities on the electrical utility network. Thus, managing the electrical network could benefit from short time scales probabilistic forecasting models.

This emphasizes the need for statistical and dynamical characterization of the short time scales solar radiation variability.

Following this goal, we are carrying out solar radiation measurements at two locations in Guadeloupe (FWI) with a 1 Hertz sampling frequency. The collected data are processed to identify and to classify the different time sequences not only from their mean irradiance but also from their stochastic variations characteristics.

The results will be conditioned so as to provide the tools necessary to build a synthetic solar radiation signal to test the effect of solar radiation variability on the overall solar energy system performance.

Acceptance, Applicability and Efficiency of Batch Disinfection of Rainwater for Human Consumption in Rural Communities of Trinidad Using Solar Radiation

W.A. MELLOWES AND K.D. THOMAS

Environmental Unit, Faculty of Engineering, The University of the West Indies, Trinidad & Tobago
wmellowe@eng.uwi.tt

Keywords: Trinidad, BOD, batch solar disinfection (SODIS), solar concentrators, natural ultraviolet radiation.

Abstract

This project sought to investigate probable solutions to the current problem of the lack of potable water in several rural villages throughout Trinidad. Attempts to attain this ultimate goal initiated the objectives of this study. This paper gives results of an investigation into the applicability of batch solar disinfection (SODIS) for the treatment rain and river water within five (5) rural areas in Trinidad: Caura, Cedros, Guayaguayare, Matura and Quinam. The assessment of SODIS' applicability incorporated a social survey of the ability of residents in the above-mentioned rural areas to conduct batch SODIS successfully after learning the method by demonstration.

SODIS was investigated by the use of plastic (i.e. polyethylene terephthalate) bottles - in both the half blackened (i.e. 1/2BB) and transparent (i.e. TB) states - that are typically discarded by most

Trinidadian households and natural ultraviolet radiation (i.e. from the sun). Bottle volumes of 650mL, 1L and 2L, in both 1/2BB and TB, were subjected to rainwater, river water and RBC effluent. Each filled bottle size was also subjected to four (4) solar concentrators: double parabola, galvanised sheet, square and rectangular. Faecal coliform and heterotrophic bacteria were used as the indicator organisms as to determine when SODIS was successful. As a result, water samples were taken from each test bottle every ten (10) minutes for indicator analyses to be done.
The use of all four (4) concentrators effected total inactivation of both faecal coliform and heterotrophic bacteria under sunny conditions. When effectiveness of reduction of faecal coliform and heterotrophic bacteria was based on the time for inactivation, for all sample types, the double parabola was found to be the best concentrator. Further, bottles in the 1/2BB state were found to give superior results than their volume-respective TB. In terms of container size, whether 1/2BB or not, it was determined that the smaller the container volume the quicker that SODIS is effected. When the effect of turbidity on SODIS was investigated it was found that only waters with turbidity less than 30 NTU could be successfully subjected to SODIS. Overall, it can be said that SODIS, by use of any concentrator, bottle state and bottle size investigated, can be effective in Trinidad for achieving potable water standards in terms of microbial count provided the water needing solar disinfection has a turbidity below 30 NTU.

Retrieval of Aerosol Optical Thickness from Solar Radiation Data: Study of a Saharan Dust Event In Guadeloupe

T. FEUILLARD, J. MOLINIÉ, S. JACOBY-KOALY, R.H. PETIT AND F. BRUTE

LPAT-GEOL, UFR Sciences Exactes et Naturelles, Campus de Fouillole, 97157 Pointe-à-Pitre, Université des Antilles et de la Guyane - jmolinie@univ-ag.fr

Abstract

Saharan dust outbreaks are often reported over Caribbean islands during the wet season, due to the long-range transport of air masses from African natural sources. From May to August 2005, several notable dust events were observed in Guadeloupe (French West Indies, 16.2°N, 61.5°W).
During this period, global and diffuse solar irradiance and downward infrared irradiance measurements respectively by two ground-based pyranometers and a pyrgeometer were collected at Petit Canal, at the same place as Aerosol Optical Thickness (AOT) measurements by a sun photometer, part of AERONET network. On this site, rainfall depth, relative humidity, ground temperature in the shade and horizontal velocity data from a meteorological station were also available during the experiment. About 30 kilometers far from that, horizontal visibility from Meteo France, and PM_{10} mean concentrations from Guadeloupe air quality network Gwad'air, allowed to attest high concentrations of dust in the air masses flying over the archipelago during the studied period.
In this paper, direct solar irradiance is calculated from global and diffuse irradiance and is compared to AOT data. A good correlation is found between these two quantities. The main difficulty of this study was to detect the fluctuations of irradiance signals due to the presence of clouds over the area of measurements and to eliminate the corresponding data from the study.
The observed agreement between AOT and direct irradiance allows to conclude that the climatology of Saharan dust incomings in Guadeloupe should be established from irradiance data, even in the absence of photometric measurements. AOT measurements began in Guadeloupe in 1993 whereas irradiance data are registered since several decades. Then, it will be possible to verify the assumption according to a greater and greater amount of dust is travelling between African and American continents in relation to global warming.

Energy / Environment / Pollution

High Particles Concentration Levels and Relationship with Air Conditioning: Study of Three Cases of Intoxication in Public Offices

J. MOLINIÉ, R.H. PETIT, S. JACOBY-KOALY AND A. ROUSSAS

LPAT-GEOL, UFR SEN, Campus de Fouillole, 97157 Pointe-à-Pitre. jmolinie@univ-ag.fr

Abstract

In recent years, scientists have noted a tremendous increase of problems in the working environment, due to limited natural ventilation in closed buildings.

In Guadeloupe, some cases of indoor pollution have been reported. During the last year, three public offices had to be cleared out because of respiratory and allergic troubles dramatically experimented by the employees.

Following these incidents, the LPAT (Laboratoire de Physique de l'Atmosphère Tropicale was asked for analyses of the indoor air composition. Particles were collected on filters with a 10 litters per minute airflow and analysed by gravimetric method. Parts of the filters were observed by electronic microscopy to investigate the sizes and composition of particles.

Results have put into evidence the presence of highly numerous very fine particles of respirable size (particles diameter lower than 2,5 μm). Previous studies have showed that these particles are the most hazardous for health. They were mainly composed of carbon coming from combustion of petrol derived released in the neighbouring outdoor air. Indoor air quality should be corrected by air filtration. This solution has an inconvenient since it could be incompatible with energy savings. The balance between health protection, energy savings and human comfort is an essential question to solve in our inter tropical countries.

Measurement and Analysis of Wind Velocity and short Time Scale Wind Speed Forecast

R. BLONBOU, R. CALIF, F. DUPONT, T. SOUBDHAN AND B. DESHAIES

Groupe de Recherche sur les Energies Renouvelables, Université des Antilles et de la Guyane, Campus de Fouillole, BP 592, 97157 Pointe à Pitre cedex. - rblonbou@univ-ag.fr

Abstract

Increasing the part of wind energy sources in a given electrical network needs the knowledge of not only the expected mean power but also of the variability of such a stochastic source. More precisely the choice of storage systems and/or of alternative conventional generators, as well as the development of forecasting tools devoted to the network management, require the determination of the statistical and dynamical properties of this variability. For instance, using thermal power stations, where combustion acts as the energy source, to palliate the shortcoming of wind energy could lead to starting times ranging from 10 to 60 minutes. Therefore as soon as wind power becomes a significant part of the electricity sources, as it could be in island network, efficient forecast tools for time scales smaller than one hour are needed. If meteorological offices provide forecast information and wind variability characteristics for times scales larger than one or a few hours, this is no longer the case when time scales smaller than one hour are considered.

The results of a six month campaign of 1hz velocity measurements, that we performed during the trade wind season in a Guadeloupe wind farm, are used to develop a statistical and dynamical analysis of the wind velocity. More precisely, we first proceed to a time scale separation of the wind speed signal to provide the main statistical characteristics of the wind fluctuations (probability density functions, first to fourth momentum, autocorrelation time, power density spectra….) on time scales ranging from ten minutes to one hour. The corresponding time series are than compared in order to proceed to a classification of the different possible time series. The results are then discussed from the point of view of wind speed forecast, for time scale smaller than one hour. Different strategies are envisaged to achieved such short time scales wind speed forecast.

Energy / Environment / Pollution

Simulation of Rainfall Interception Processes for Pollution Hazards Estimation Under Banana Plants

C. BASSETTE (1) AND F. BUSSIÈRE (2)

(1) LPAT, Université des Antilles et de la Guyane, Faculté SEN, Campus de Fouillole, Pointe-à-Pitre, Guadeloupe - Celine.Bassette@univ-ag.fr
(2) INRA, Unité Agropédoclimatique, Domaine Duclos, Petit-Bourg, Guadeloupe

Abstract

Rainfall interception by plant canopies varies according to the plant structure and raindrop physical properties. Banana plant architecture provides important rainfall redistribution as stemflow (water flux on the stem) and throughfall (water fluxes through the foliage). Experimental measurements of drop diameters under banana plants showed the plant structure affected the drop size distribution by generating large drip diameters. Large kinetic energies and dripping rates may affect soil erosion as well as location of fertilizers and pesticides spread to the soil near the plant collars and sprayed on the leaves. Theses agrochemicals can be leached and carried to surface or ground waters, threatening environment and human health.

In order to locate these hazard zones, we used the DROP (Distribution of Rainfall On Plants) model combining first 3-D representation of the plant architecture given by digitising and triangulation, second rainfall distribution simulation according to the plant physical properties. Firstly, thanks to experimental measurements we developed empirical laws describing splash and storage losses at the leaf surfaces. Secondly, we introduced these laws into the model to improve the simulation of rainfall distribution under the foliage. Thus, splash and storage amounts resulting from incident rainfall interception were evaluated according to leaf inclination, drop diameter and drop fall height.

Experimental results showed splash increased with fall height and decreased with leaf inclination. Storage was not affected by fall height, increased with drop diameter and decreased exponentially with leaf inclination. Interception lows inferred from these results improved significantly DROP water flux simulation which provided in agreement with measurements 1 mm interception losses on average per rainfall event. Moreover, high kinetic energies and rainfall rates were simulated in a ring comprised between ½ and ¾ of the maximum crown radius. In addition to stemflow area, this ring could be considered as a zone favouring agrochemicals leaching or run-off.

Molasse Spentwash Treatment by Two Processes: Adsorption on AC and Biodegradation

S. Figaro (1), C. Jean-Marius (1), O. Gros (2), L. Farhasmane (3), B. Ganou (3), F. Bazile (3), W. Achouack (4), M.A. Roncato (4), A. Ouensanga (1) and S. Gaspard (1)

(1) UAG- COVACHIM, Fouillole BP 250 Pointe-à-Pitre Cedex sfigaro@univ-ag.fr
(2) UAG- UFR Sciences Exactes et Naturelles – Département de biologie
(3) INRA Guadeloupe : URTPV, 97-170 Petit-Bourg
(4) CEA Cadarache: plate-forme Ecophysiologie végétale et Microbiologie, 13-108 St-Paul Les Durance Cedex

Abstract

Fermented molasses are used in order to produce ethanol in distilleries. After distillation of the fermented product, huge amount of wastewater (molasse spentwash) are generated. They have a dark brown color due to melanoidin and phenolics compounds. This coulored effluent is a major pollutant when it is discharged into natural waters because of its high organic content, it has approximately a Chemical Oxygen Demand (COD) ranging between 60 and 120 g/L. Anaerobic digestion is an

efficient process in order to treat them but only partially. The aim of this work is to set up a remediation procedure of digested molasse spentwash (DMS) from sugar cane industries.
First, the adsorption potential of different activated carbons for this effluent and its recalcitrant compounds has been studied. Adsorption kinetics and adsorption isotherms of (DMS) and its recalcitrant compounds (gallic acid, tannic acid, melanoidin and phenol) have been measured using three commercial carbons: PICACTIF TA50, PICACTIF TE60 and vegetal activated carbon (VAC). The adsorption kinetic of these compounds was determined at three differents pH (3, 7 and 10) and temperatures (20, 25 and 35 °C). Kinetic data were fitted using the pseudo- first order equation of Lagergren (log (qe – qt) = log qe – k1.t) or a pseudo- second order model (t/qt = 1/k2. 1/qe2 + t/qe). Isotherm adsorption data were fitted using the Freundlich model or a modified Freundlich model. Thermogravimetric study of the different activated carbons loaded with these compounds were performed in order to quantify the mass loss and to determine the adsorption energy.
Secondly, biodegradation of DMS and its recalcitrant compounds has been studied. In a first step, using Poly Chain Reaction (PCR) and sequencing techniques, Cirtobacter amanolaticus, a pure bacterial culture which may be able to use DMS as sole carbon source, has been identified. In a second step, aerobic degradation of these compounds by another pure bacterial culture of Burkholderia caribensis isolated in martinique's vertisols has been studied. Degradation study of DMS by Citrobacter amanolaticus will be studied in the near future.

Measurement and Computer Representation of Banana Plants for Environmental Studies

S. Dufour-Kowalski, and F. Bussière

Unité Agropédoclimatique de la zone Caraïbe, Institut National de la Recherche Agronomique, Petit Bourg - Guadeloupe - samuel.dufour-kowalski@antilles.inra.fr

Abstract

Plant computer models are increasingly used for entertainment and environmental studies. For example, energy and mass transfers between plants and the aerial environment can be simulated on 3D computerized plant mock-ups. The design of these mock-ups needed both detailed data acquisition and mathematical development for the geometrical representation of plants.
In order to evaluate environmental hazards due to rainfall interception in banana plantation, we had to examine water fluxes for several possible plant patterns. We then had to design a database of the 3D coordinates of several plants collected in the fields. For that purpose we developed data acquisition and plant rendering software.
Firstly, we evaluated and specified the use in the field of a long-range electromagnetic digitizer. We developed a computer software that drive the digitizing process and allow simultaneously data visualization and correction in order to ensure fast and accurate data collection. The digitalization process consisted in describing each leaf by series of ordered points on the leaf edges and on the midrib.
Secondly we developed a new method to represent complex plant leaves by meshes of triangles in the 3D space. Banana leaves are complex because they are large and occasionally torn by wind and rain. Usually, leaf triangulation algorithms were based on "Constrained Delaunay Triangulation" and were not adapted to these complex shapes.
Digitized banana leaves formed three dimensional polygons for which triangulation is a NP-complete problem. As surface meshing methods need 3D data projection on a plane, the problem leaded to the triangulation of non simple and self-intersecting polygons. We adapted existing robust methods (i. e. ear clipping and edge flipping methods) in order to obtain a sub-optimal but generic and satisfying triangulation of torn leafs. This algorithm could be used to process other complex leaf shapes. We used these data acquisition and triangulation algorithm to design a convivial graphical tool, using the DROP model to visualize rainfall interception and water transfers in heterogeneous plant patterns.

Energy / Environment / Pollution

Energy Production and Pollutant Mitigation from Broiler Houses on Poultry Farms in Pennsylvania and Jamaica

N. M. BROWN AND C. E.MORTLEY

Faculty of Engineering and Computing, University of Technology, Jamaica, Kingston Jamaica
nbrown@utech.edu.jm

Abstract

This proposal forms part of the development of a collaborative research and design program in the area of energy production for use in the agricultural sectors of both Jamaica and the United States, while addressing environmental concerns in each country.

While the underlying technology of bio-digestion is not new to Jamaica (introduced by the then Ministry of Mining and Energy in the late 1970s), the use of chicken litter as a feed material for digestion was viewed with scepticism. This is due to the fact that in Jamaica, poultry are fed with antibiotics to treat some of the common illnesses. These antibiotics are known to have adverse effect on the microorganisms required to carryout the digestion process, and ultimately negatively affect the gas generated by the process.

The project explores the economic viability of this technology by constructing and testing simple, inexpensive anaerobic biodigesters capable of producing methane gas from a variety of feed materials. The digesters were fed with pure chicken litter, a mixture of chicken and cow litter, a mixture of chicken and swine litter and a mixture of chicken litter and vegetable material. The quality and quantity of gas produced will be measured to determine the concentration of chicken litter required for optimum gas production.

Jamaica produces 6.1 million birds annually for broiler meat processing; these birds with an average life span of six weeks will produce 206.64 Giga-grams (206,640 tonnes) of litter annually. This waste can be digested to produce 57 million cubic meters of biogas, with the potential of producing 1200 Tera-Joules of energy, which is equivalent to 333.3 Gigawatt hours annually.

Focusing primarily on contract poultry operations the project will present a technological option, which will ultimately have two impacts. Firstly, the mitigation of environmental degradation caused by the release of high load of untreated phosphorus and nitrogen and secondly, a renewable energy source which will enhance the competitiveness of the industry.

Energy / Environment / Pollution

Root Growth Responses of a wheat Cropland Weed, Melilotus indicus(L.) All., Papilionaceae to Air Pollution

M. SAQUIB

Department of Biology, Faculty of Natural Sciences, University of Guyana, Georgetown, Guyana
mohammadaqib@hotmail.com

Abstract

The root length, root biomass and net primary productivity were studied at the monthly intervals on a wheat crop land weed, Melilotus indicus growing under the stress of air pollution caused by coal burning of a thermal power plant of Kasimpur (U.P, India). The daily average of sulphur rich bituminous type of coal consumption in the whole power plant complex during the winter season is about 3483 Metric tonnes. The rate of coal consumption and the amount of three major gases viz. oxides of Sulphur, Nitrogen and Carbon and particulate matters released from the power plant complex are 0.14Kg./hr, 2.58 Kg. /hr, 23.38Kg./hr and 32.2x 103 Kg. /hr respectively. Ten Plants of Melilotus indicus growing in a wheat crop land under almost similar edaphic factor as well as ecological and agricultural practices were collected randomly on monthly interval basis at the four selected sites situated at 0.5km, 2 Km, 4Km and 20 Km leeward from the source of pollution. The data indicates that the degree of response increased with decreasing distance from the source of pollution. The trend of loss in the root length and root biomass is similar in all the stages. The root length and root biomass affected significantly at the 0.5 Km. in the seedling stage while, in the middle stage and old stage the loss is significantly increased up to 4 Km. in comparison to the reference site situated at 20 Km. away from the source of pollution. However, the severity of loss was found to be higher at the vicinity that 0.5 Km. in comparison to the reference site. The root length, root biomass and net primary productivity were more affected by pollutants at the middle stage (60%, 87.2% and 95.6% respectively) followed by old stage (52.4%, 85.6% and 66.7% respectively) and seedling stage (27.7%, 70.4% and 71% respectively). The root length and root biomass showed a significant and positive relationship with the distance from the source. The degree of relationship, however, increased from seedling stage to middle stage and decline at the old stage. Root length showed 19.4 to 66% dependence on the distance from the source while, the root biomass exhibited a relatively greater degree of dependence and varied from 46.3% to 67.3%. The consumption rate at the power plant, relative humidity, wind direction and other environmental factor were found to influence the degree of growth response to air pollution. Losses in the root growth are also possible in the Caribbean countries that are emitting air pollutants from diesel generating power plant and other industries.

Environment / Climate / Naural Hazards / Simulation

Mathematical Tools for Modeling Natural Risks 97
M.F. Hasler
Climatological Analysis of Deep Convective Days in Guadeloupe 100
N. Nathou and E. Hicks
Modelling of The Wind Field Produced During a Hurricane Passage in the Vicinity of an Island. A Case Study: The Island of Guadeloupe (FWI) 104
K. Elise. and C. Asselin de Beauville
Behavioral Change: an Original Application of Health Belief Models for the Prevention of Natural Hazards 108
N. Michalon
Two Numerical Experiments for the Investigation of Possible Influences of a Climate Change on the Global Atmospheric Electrical Circuit 111
N. Michalon
Facing Natural Hazards: Policies, Strategies, role of Basic Sciences 114
L. Alvarez-Diaz
CDSA: A New Seismological Data Center for French West Indies 114
M. Bengoubou-Valérius, D. Bertil, S. Bazin, A. Bosson, F. Beauducel and A. Randrianasolo
Seismogenic Potential of Fore-Arc Tectonic Structures: Onshore - Offshore Geology Helps to Understand the Tectonic Activity at the Marie-Galante Basin - Lesser Antilles 115
J.F. Lebrun, J.L. Léticée, S. Bes de Berc, J.J. Cornée, P. Munch, A. Randrianasolo, I. Thinon and M. Villeneuve
Evaluation of the Tsunami Risk for Guadeloupe (Lesser Antilles) 116
N. Zahibo, E. Pelinovsky and I. Nikolkina
North Atlantic Hurricanes Trajectories; Important Forecast Parameters: a Case Study, 2006 Hurricane Season 116
G. Lequellec and C. Asselin de Beauville
A Method of Analysis and Identification of Clouds of Satellite Images Coming from GOES Satellite 117
J. Nagau and J-L Henry
Initialization of an Atmospheric Mesoscale Model for the Prediction of the Track and Intensity of Hurricanes 118
W. Sicot
Climatology of African Dust using Meteosat IR throughout the Period 1984-1998 118
M. Legrand, O. Pancrati, N. J. Brooks and L. J. Shipman
Evaluation of Rainfall Over Guadeloupe by Four Cumulus Parameterization Schemes: Case of the Tropical Depression Jeanne 119
C. Jean-Charles and C. Asselin De Beauville
Estimation of Downward Longwave Radiation in Guadeloupe 119
A. Fouéré, R. Bonhomme, F. Busière and S. Dufour-Kowalski
Early Observations of the Blazar OJ 287: Further Evidence for the Binary Black Hole Model 120
H. Rampadarath, M.J. Valtonen, R. Saunders and H.J. Lehto

Environment / Climate / Naural Hazards / Simulation

Mathematical Tools for Modeling Natural Risks

MAXIMILIAN F. HASLER

D.S.I., Laboratoire A.O.C., Université des Antilles et de la Guyane, B.P. 7209, F-97275 SCHOELCHER cedex, Martinique (F.W.I.), France - Maximilian.Hasler@martinique.univ-ag.fr

Abstract

Without attempting to give a complete overview of the rich knowledge existing in the field addressed by the title, we discuss several recent original and powerful, but not always very well known mathematical tools, which find their application in mathematical models of natural risks, with special emphasis on the description of singularities and their propagation, in particular in the context of shock waves, hurricanes and tsunami. We consider two categories of these tools: on one hand, theories from functional analysis designed to find solutions to partial differential equations with singularities of various types, and on the other hand, numerical methods which are useful when these models are applied in concrete calculations. As an illustration, we present an interesting mathematical model for the prediction of hurricane tracks.

Introduction

Through the past years, the need for precise mathematical models, describing natural phenomena potentially constituting a hazard for population and/or environment accurately enough to allow reliable predictions, has proved more and more evident. These models are usually made from three basic building blocks: heuristics based on experience, rigorous theory, and numerical calculations. The first leads to a system of equations reasonably well describing the phenomena, the second is necessary to ensure that manipulation of these equations will not introduce new (unrealistic) or exclude relevant existing solutions, and the third will allow to apply the model to reality, which usually requires treatment of a large amount of data in order to yield a realistic description. In this paper, we will discuss in how far these issues, in particular the second one, need to be reconsidered in the context we are interested in, where "classical" ideas, theories and well-established techniques become inadequate or even invalid.

Mathematical aspects of catastrophes

The violence of phenomena related to natural risks corresponds from a mathematical point of view to *singularities* of the functions describing the physical system. These range from insufficient smoothness through functions having jumps in their graph, up to objects which are so "rough" that they can no more be considered as functions in the usual sense. Still, they can be rigorously described and manipulated in the mathematical theory of Schwartz distributions, as long as only linear operations are involved.
Physical laws, especially equations of motion, usually involve differential operators that tend to increase irregularities of the initial data. However, if the latter are sufficiently smooth, irregularities will not be appear "out of nothing", as long as the laws respectively the associated operators remain *linear*.

Non-linearity as source of singularities

The key property responsible for the birth of natural catastrophes is thus the *non-linearity* of the physical laws describing these phenomena. This can be illustrated by considering Burger's equation

$$\partial_t u + u\, \partial_x u = 0$$

which can be seen as a simplified version of the more realistic Navier-Stokes equation from fluid dynamics we use later for modeling hurricanes. The presence of the non-linear term $u\ \partial_x\ u$ makes it impossible to treat this quite simple wave equation in the framework of Schwartz distributions (which cannot be multiplied among themselves). A solution to this equation, for initial data $u(0,x) = u_0(x)$, is given by

$$u(t,x) = u_0(x - t\, u(t,x)) = u_0(y) \quad \text{for} \quad x = y + t\, u_0(y)\ .$$

It is easy to see that a point (x, $u_0(x)$) will propagate to the left with speed $u_0(x)$. Thus, the negative slope to the right of a maximum of u_0 will tend to $-\infty$ in a finite time: a shock wave is born out of smooth initial data!

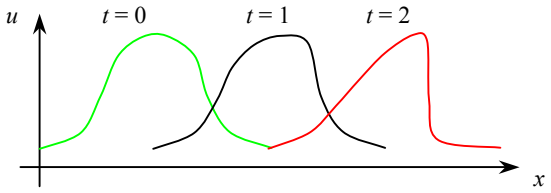

Fig. 1: formation of a shock wave from smooth initial data in Burger's nonlinear wave equation

Algebras of generalized functions

Since non-linearity and singularities are characteristic ingredients in realistic descriptions of natural risks, but the two cannot be combined in the classical theory, one needs (new) generalized functions which form *algebras*, i.e. which can be multiplied among themselves. Such a theory has been proposed by Colombeau in the 1980s, and has since then seen important developments, especially during the last decade. The idea is to take quotient spaces $G = E_M / E_N$ of "moderate" modulo "negligible" sequences of functions, where these properties refer to growth with respect to some regularization parameter ε. For example, E_M may contain sequences $(f_\varepsilon)_\varepsilon$ growing like *some* power ε^{-p} when $\varepsilon \to 0$, while the $(f_\varepsilon)_\varepsilon \in E_N$ will decrease to 0 faster than *any* power ε^p. The value of such generalized functions in a point are *generalized numbers*, which can represent "infinite" quantities in a precise manner.

Application: soliton waves

If we add an "infinitesimally small" term $[\varepsilon]\ \partial_x^3\ u$ to Burger's equation, where [ε] is a generalized number associated (i.e. in the "classical" limit equal) to zero, we get the Korteweg-deVries equation with small dispersion. It has as an exact solution the function

$$u(t,x) = 3\ c\ \cosh^{-2}(\ b\ (\ x - c\ t\ -\ x_0\ )/2)$$

for arbitrary (generalized!) numbers b and x_0, which represents a soliton wave moving with speed $c = [\varepsilon]\ b^2$ to the left. If b is a finite number, then the speed and the amplitude of the wave are infinitesimally small. But the speed can also be finite; then b is a infinitely large number, which means that classically the wave is zero in any point except $x_0 + c\ t$, where it has a finite value. In usual distribution theory, this object cannot be distinguished from the zero function. However, the derivative of u (which is related to the energy transported by the wave) is not bounded; it corresponds to the difference of two δ-distributions located at $x_0 + c\ t \pm \ln(2+\sqrt{3})/b$. One can also consider the case of a finite overall "mass" $\int\ u(x,t)\ dx = 12\ c/b = 12\ [\varepsilon]\ b$. Then the solution resembles to a δ-distribution moving with infinite speed, since c and b are both infinitely large.

Asymptotic expansions

A quite different approach from Colombeau's theory, which can also yield a differential algebra of generalized functions, is that of asymptotic expansions. Here one considers a collection of particular (non-smooth) generalized functions, which can be multiplied by smooth functions. According to the application, this collection might contain the Dirac distribution, and power series in a regularization parameter ε. In the sequel we describe a variant of this which has been used to develop a model for the prediction of hurricane tracks.

While shock waves, whose support is a hyperplane, have been studied since a long time, but only in the 1980s V.P. Maslov and collaborators started to study propagation of structurally stable *weak* singularities having a support of codimension > 1; examples have then been constructed in the setting of asymptotic expansions.

Application: dynamics of the hurricane's eye

The hurricane's eye is the typical example of a point-like weak singularity propagating in $D \geq 2$ dimensions. It can be described as follows: Starting from the full Navier-Stokes equations and conservation of mass,

$$\rho\ (\partial_t\ \mathbf{u} + \mathbf{u}\cdot\nabla\ \mathbf{u}) = -\nabla\ p + \eta\ \Delta\ \mathbf{u}\ ,\ \ \partial_t\ \rho + \mathrm{div}(\rho\ \mathbf{u}) = 0\ ,$$

which describes the flow $\mathbf{u}$ of a fluid with density ρ, pressure p, and viscosity η, we go into a coordinate system relative to a point $X(t)$, taken to be the position of the eye on the earth's surface, to which we restrict the dynamics, and whose rotation introduces Coriolis' acceleration $\mathbf{a}_C = 2\ \mathbf{u} \times \mathbf{\Omega}$ (depending on the latitude):

$$\rho\ (\partial_t\ \mathbf{U} + \mathbf{X''} + \mathbf{U}\cdot\nabla\ \mathbf{U} + 2\ (\mathbf{U} + \mathbf{X'}) \times \boldsymbol{\omega}\ ) = -\nabla\ p + \eta\ \Delta\ \mathbf{U}\ .$$

In this two dimensional approximation, the pressure is replaced by a function of the density, $p = k\ \rho^{2+\delta}$. Taking $\eta = 0$, one gets the so-called shallow water equations. Neglecting viscosity seems reasonable for air, but we keep in mind the big gradients of $\mathbf{u}$ expected near the eye, and that this term improves stability of the equations.

Decomposition into regular and singular part

Following seminal work by V. N. Zhikharev, we consider solutions of which each component is of the form

$$f(x) = f^0(x) + S(x)\ f^1(x)\ ,$$

where f^0 and f^1 are smooth functions, while S presents a weak singularity in one point (which will be the hurricane's position). Theoretical considerations by Zikharev, Maslov and others imply that $S(x)$ must be of the form $S(x) = \beta(x - X_0)^{1/2}$, where β is a positive quadratic form. This has as a consequence that the product of such functions will again be of the same type. We try to find solutions of this form to the above equations, which means that the density $\rho(t,x)$ and each of the three components of the flow $\mathbf{u}(t,x)$ are decomposed into a smooth part (ρ^0, $\mathbf{u}^0$) and a "singular" part (ρ^1,$\mathbf{u}^1$) which multiplies $S(x)$. One then finds that the equations allow themselves also for such a decomposition in a smooth and a singular part, symbolically

$$E(\rho,u) = 0 \quad \Leftrightarrow \quad E^0(\rho,u) + S\ E^1(\rho,u) = 0\ ,$$

while both parts involve as well the smooth as the singular components of the unknown functions.

The next crucial step is to show that these two parts of the equations can be considered independently. In fact, this is justified in an immediate neighborhood of the point $X(t)$ where the singularity is located. Roughly speaking, since the function $S(x)$ does not allow an asymptotic expansion around $x = X(t)$, the Taylor coefficients of the regular and singular part can be identified separately, order by order.

Truncation of the chain

By doing so, we obtain an *infinite* chain of equations for the Taylor coefficients $(\rho_{ij},\mathbf{u}_{ij})^{0,1}$, which are functions of time only. Thus, the system of PDE's has been reduced to a sequence of *ordinary* differential equations. Analyzing them order by order shows that many of the equations turn out to be purely algebraic, in virtue of preceding results. These allow to express "directly" some unknown components in terms of other ones. Of course, an infinite number of equations cannot be dealt with, so one must proceed to a truncation of the chain at some order. A thorough study concerning this truncation has been done for the model under investigation, but there still remain open theoretical questions concerning the general case of such developments. Using the computer algebra system Maple, we have pushed the calculation to include all terms up to the third order, while previous work only considered terms up to the second order. We also made all calculations for nonzero values of η and the parameter δ, which seems strongly motivated by phenomenological laws of state.

Numerical optimization

Now we are able to determine the trajectory $\mathbf{X}(t)$ of the singularity (among other information) by simply integrating the system of ODE's, for given initial data. However, the "correct" values of the latter are not directly known. We wish to determine the important number of these unknown initial data ξ for the coefficient functions, in such a way that the integral curve $\mathbf{X}(t;\xi)$ of the eye's track matches as well as possible a given collection $\{ \mathbf{X}(t_i) \}$ of already available measured points. Then we can assume that extrapolation to future times will give a reasonably good prediction of the track. Minimizing the error

$$E(\xi) = \sum_i \rho(t_i) \, \| \mathbf{X}(t_i;\xi) - \mathbf{X}(t_i) \|^2$$

(where ρ is a weight function) requires an efficient method of high-dimensional numerical optimization.

This takes us to another general and frequent problem arising in mathematical models of the reality, which nearly always involve a process of fitting parameters which cannot be determined from theory, to get a "best approximation". To find a sequence (ξ_k) converging to the optimal value ξ^*, we choose step by step a direction $\mathbf{d}_k$ and then perform a *linear search* to determine $\boldsymbol{\delta}_k = \alpha_k \mathbf{d}_k = \xi_{k+1} - \xi_k$ minimizing $E(\xi_{k+1})$.
The most naïve *steepest decent* method $\mathbf{d}_k = -\nabla E(\xi_k)$ is easily seen to be a bad choice in general, but also the rapidly converging *Newton's method* $\mathbf{d}_k = - \mathrm{B}(\xi_k) \nabla E(\xi_k)$, where B is the inverse matrix of the Hessian $\mathrm{H} = \mathrm{D}^2 E$, is inadequate since the calculation of H requires about n^2 evaluations of E (involving in our case numerical integration of $n = 15$ or 30 ODE's to calculate each $\mathbf{X}(t_i;\xi)$!), plus $\mathrm{O}(n^3)$ operations for the matrix inversion. This is avoided by *quasi-Newton methods*, where $\mathrm{B}(\xi_k)$ is replaced by an approximation B_k which can be calculated at low cost. The improved Broyden-Fletcher-Goldfarb-Shanno (BFGS) formula,

$$\mathrm{B}_{k+1} = \mathrm{B}_k + \gamma \, [(1 + \gamma \, \mathbf{y} \cdot \mathbf{b}) \, \boldsymbol{\delta}\boldsymbol{\delta}^{\mathrm{T}} - \mathbf{b}\boldsymbol{\delta}^{\mathrm{T}} - \boldsymbol{\delta}\mathbf{b}^{\mathrm{T}}],$$

where $\mathbf{y} = \nabla E(\xi_{k+1}) - \nabla E(\xi_k)$, $\mathbf{b} = \mathrm{B}_k \cdot \mathbf{y}^{\mathrm{T}}$, $\gamma = 1/\mathbf{y} \cdot \boldsymbol{\delta}$, is one of the most efficient implementations of this idea, avoiding any matrix inversion. Combined with heuristic rules for inexact line search (Armijo's rule, Wolfe conditions) this yields a very efficient all-purpose minimizing routine, which we tuned for our purpose by adding additional stopping criteria, among others for early detection of approaching irrelevant parameter domains. For numerical integration, we chose classical 4^{th}-5^{th} order Runge-Kutta routines, and sped up the (vector valued) function evaluation by methods of automatic code optimization, e.g. with respect to common subexpressions.

Discussion of results

Once the optimization procedure is "connected" to the function $\mathbf{X}(t;\xi)$ which corresponds to the numerical integration of the truncated chain of ODE's, we can predict, i.e. extrapolate a given trajectory to future times. A basic version of this model had already been proposed over 10 years ago. In spite of its simplicity, it already gave quite satisfactory predictions in generic situations. Using computer algebra systems, we could take into account the next order in the Hugoniot-Maslov chain and nonzero values for η and δ. This considerably complicates the (theoretical) calculations, but yields better numerical stability and a more realistic model, allowing finally even better long-term predictions than the already promising original model. However, new conceptual challenges arise with this extended model, for example concerning the choice of the starting point for the optimization procedure.

One of the important features of the model is the relatively low cost in calculation power, compared to traditional finite element methods, which still persists even if the equations become more complicated as the model gets refined. Another advantage lies in the fact that it can not only predict the hurricane's track, but also other relevant information, e.g. estimates for the wind strength near the hurricane's eye, and even information on *gradients* of data like the density of air.
Of course, the model can and should be refined in several ways to become more accurate from the phenomenological point of view. It could for example take into account external factors like the ocean's surface temperature (crucial for the hurricane's dynamics), geographical data, etc. Another improvement would be to use a multi–layer model, to take into account the different physical conditions, in particular temperature, at higher altitudes. Anyway, it should be obvious that this is more than just a toy model, and clearly deserves to be studied further.

However, the presentation of this model was not the only purpose of this paper. It rather served as a nice and interesting illustration of how recent theoretical advances from quite different domains come to a productive interplay in the context of nonlinear differential problems, which are typical for models describing natural risks, and where many well established classical methods can no more be used. This area of research is challenging for both practical and theoretical motivations. The former are evident, and concerning the latter, we hope that we could give enough insight into the generically new problems arising here, but also on the quite powerful recently developed tools which may used to tackle these problems, particularly relevant in our geographical context.

References

1. J.-F. Colombeau (1984), New generalized functions and multiplication of distributions, North Holland.
   A. Delcroix, M. F. Hasler, S. Pilipović and V. Valmorin (2004), *Proc. Amer. Math. Soc.* **132**:2031.
2. V. Butalov, Yu. Vladimirov, V. Danilov and S. Dobrokotov (1994), *Mathematical Notes* **55**(3):11.
   S. Yu. Dobrokhotov, K. V. Pankrashkin and E. S. Semenov (2001), *Russian J. of Math. Physics* **8**(1):25.
   S. Yu. Dobrokhotov, E. S. Semenov, B. Tirozzi (2004), *Theoretical & Mathematical Physics* **139**(1): 500.
   V. P. Maslov (1980), *Russ. Math. Surv.* **35**(2):252.
   V. N. Zhikharev (1986), Dep. VINITI, No. 8148-B86, Moscow.
3. C. G. Broyden (1970), *J. Inst. Math. Comput.* **6**:222.
   R. Fletcher (1970), *Comput. J.* **13**:317.
   D. Goldfarb (1970), *Math. Comput.* **24**:23.
   D.F. Shanno (1970), *Math. Comput.* **24**:647.
   H.Y. Huang (1970), *J. Opt. Theor. Applic.* **5**:405.
   J.C. Gilbert, C. Maréchal (1989), *Math. Progr.* **45**:407.
   W. H. Press, S. Teukolsky, W. Vetterling, B.P. Flannery (1992), Numerical recipes in C, Camb. Univ. Press.
   R. H. Byrd, P. Lu, J. Nocedal, C. Zhu (1995), *SIAM J. Sci. Comp.* **16**(5):1190.

Environment / Climate / Natural Hazards / Simulation

Climatological Analysis of Deep Convective Days in Guadeloupe

N. NATHOU, E. HICKS

Laboratoire de Physique de l'Atmosphère Tropicale, Université des Antilles et de la Guyane
BP 250, 97157 Pointe-à-Pitre Cedex, nnathou@univ-ag.fr

Abstract

The satellite lightning observations (LIS and OTD) clearly show a marked contrast between lightning activity over land and ocean. Two hypotheses have been formulated to explain the physical origin of this contrast: the thermal and the aerosol hypothesis. In this study, a climatological analysis on thunderstorm days over a period of 33 years has been carried out in order to test the role of the surface temperature on cloud electrification as supposed by the thermal hypothesis. In a second time, the dynamical characteristics (maximum cloud top height, vertical velocity, CAPE and CIN) in both the storm and deep convective clouds have been compared by using a 1D cloud model, initialized with the corresponding appropriate atmospheric sounding. According to the results, the clouds that have been observed on days with deep convection have dynamical characteristics as on storm days, but have not developed any significant electricity leading to lightning.

Introduction

The lightning production of thunderstorm clouds is of interest in different fields of research, engineering and civil protection. However, the mechanisms which govern the global atmospheric electrical circuit remain still badly known. This ignorance delays the development of certain applications such as reflection, refraction and diffusion of the radio waves by the ionized layers of the upper atmosphere among which telecommunications hold a significant part. Tropospheric storms are electric generators of current which bring electricity in altitude through the conductive atmosphere. Lightning discharges play a key role in the maintenance of the ionosphere to a potential of + 250 kV compared to the surface of the Earth. Ground based and satellite lightning observations (LIS and OTD), presented in Fig. 1, clearly show a marked contrast between lightning activity over land and ocean.

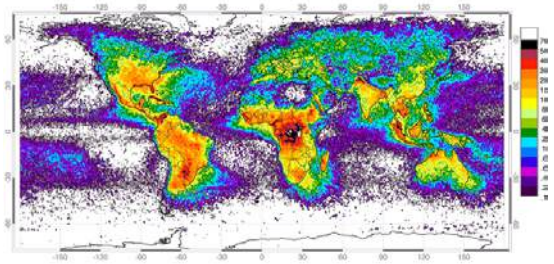

Figure 1 – Global annual flash rate distribution obtained from the combined NASA LIS and OTD observations.

Two hypotheses have been formulated to explain the physical origin of this contrast. The thermal hypothesis is based upon the contrast between oceanic and continental surface temperatures. It simply considers that land lightning is dominant because land is hotter than ocean [1]. This hypothesis considers that the temperature correlated to the CAPE and consequently to the dynamical characteristics of thunderclouds, is a preferential parameter for the evaluation of the change in thundercloud electrification. The aerosol hypothesis [2] is based upon the aerosol concentration differences in the sub-cloud layer. Low aerosol and condensation nuclei concentrations, as in the case of oceanic thunderclouds, lead to premature formation of warm precipitation. Vertical velocities are thus inhibited, the concentrations of cloud drops and ice crystals (essential for the electrification process) in the mixed phase region are low and the optimal conditions for cloud electrification are reduced.

The purpose of this work is to determine if the thermal hypothesis alone may explain the cloud electrification process that leads to lightning production. In this paper, section 1 presents some elements of the classical thunderstorm climatology in Guadeloupe. In the following section, the cloud dynamical characteristics during days characterized by deep convective events are examined.

Thunderstorm climatology in Guadeloupe

Data of thunderstorm occurrence reported by meteorological service (Météo-France Guadeloupe) have been collected for the 1973 - 2005 period. With 34 mean annual thunderstorm days, Guadeloupe is not one of the main tropical regions of occurrence of thunderstorm. Nevertheless, because of its geographical position which subjects it to an oceanic tropical climate, Guadeloupe becomes a place of interest to study the land-ocean contrast in lightning activity. Fig. 2 presents the annual thunderstorm day values and the yearly mean sunspot numbers [3] during the 1973-2005 period. One may note on one hand that for the first and the second cycle solar activity minima are back 2 or 3 years in comparison with thunderstorm activity minima. On the other hand, solar cycle peaks are relatively well correlated with the both first thunderstorm activity maxima. An inverse correlation between the decrease of solar activity in the last cycle and the two extreme values of thunderstorm activity in 2004 and 2005is also observed. However, the weak amount of data does not allow to make any conclusion in relation to the global change.

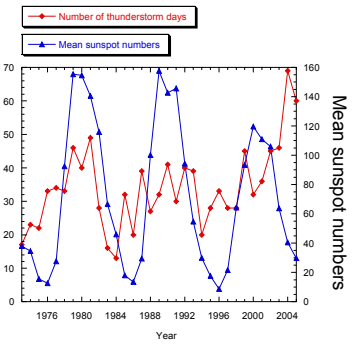

Figure 2 – Annual thunderstorm days and yearly mean sunspots numbers for the 1973-2005 period.

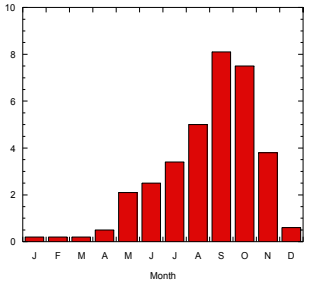

Figure 3 – Monthly average number of thunderstorm days.

The climatological analysis is pursued by plotting the monthly average number of thunderstorm days (Fig. 3). It clearly situates the thunderstorm season in Guadeloupe from May to November with a peak of activity during September-October and a period of no (or very weak) activity from December to April. One note that transition from low activity to the activity peak spreads out on 5 months. The faster inverse transition only lasts 2 months. Then thunderstorm events during the 1973-2005 period have been separated by time of occurrence and their average durations have been calculated for each month.

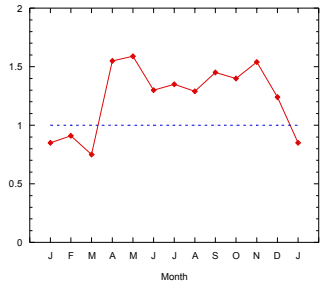

Figure 4 – Monthly average duration of thunderstorm events (in hours).

Fig. 4 reveals that average duration of thunderstorm is larger than 1 hour from April to December and the greatest values (more than 1.5 hour) are observed for April, May and November. The hourly distribution of total number of events from 1973 to 2005 (Fig. 5) plainly presents a first peak between 12 AM and 03 PM (local time). This first peak, well correlated to the maximum value of temperature during the diurnal cycle, indicates that temperature is indirectly a control parameter for thunderstorm activity. In contrast, the results do not show the expected drop of thunderstorm activity between 03 AM and 05 AM. One may note the existence of a weaker secondary peak of thunderstorm activity. The latter is in inverse correlation with the temperature. Further, both peaks are present independently of the monthly electrical activity. As an example, Figure 6 presents the hourly number of thunderstorm events for the months of May and September, months that are respectively representative of low and high electrical activity.

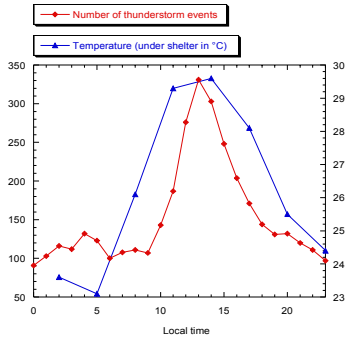

Figure 5 – Hourly total number of thunderstorms events and mean diurnal variation of temperature during the 1973-2005 period.

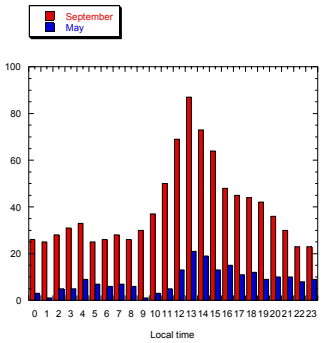

Figure 6 – Hourly total number of thunderstorms events during the 1973-2005 period for May and September.

Finally, as may be seen in Table 1, thunderstorm days for a 4 year period (2002 - 2005) have been classified in 5 categories according to the type of weather. Roughly half of the thunderstorm events occur in synoptic conditions (for example, the passage of tropical disturbance, the proximity of the ITCZ during its yearly cycle). One can assume that under these conditions they are unlikely influenced by the thermal instabilities. Furthermore, if 28.8% of thunderstorm days from 2002 to 2005 were characterized by trade wind breakdown or weak trade winds, 37.1% of these days were thunderstorm days. During the trade wind breakdown or weak trade wind days one may suppose that both local thermal and aerosol concentration conditions influence thunderstorm activity.

Table 1 – Percentage of thunderstorm days related to the type of weather from 2002 to 2005.

	Thunderstorm days (%)
Sustained or strong trade winds	0.0
Undisturbed trade winds	3.3
Moist and unstable trade winds	19.5
Trade wind Breakdown or weak trade winds	28.8
Synoptic conditions	48.4

Cloud dynamical characteristics of deep convective events

Values of the following dynamical parameters: maximum cloud top height, maximum vertical velocity, CAPE and CIN have been computed for both thunderstorm days and days characterized by deep convection without production of atmospheric electricity. Computations were carried out for a 33 years period (1973-2005) using a 1D cloud model initialized with the corresponding appropriate atmospheric sounding. Then all cases with cloud top heights equal or higher than 7000 meters have been selected for this study. This choice is equivalent to the assumption that ice crystals, supercooled water and water vapour coexist above this altitude. Thunderclouds (hereafter referred to as TH clouds) are in average higher (roughly 7% as reported in Table 2) than clouds occurring during days characterized by deep convection (hereafter referred to as DC clouds). The same trend is observed in the case of maximum vertical velocity and CAPE values.

With an average value of 38 m/s, TH clouds seem develop larger maximum vertical velocities than DC clouds, and correspond to air masses characterized by roughly 19% to 24%

Table 2 – Mean values of dynamical parameters for TH and DC days at 00 and 12UT

	Maximum cloud top height (m)		Maximum vertical velocity (m/s)		CAPE (J/kg)		CIN (J/kg)	
Type of day and UT	**Mean value**	**Standard deviation**	**Mean value**	**Standard deviation**	**Mean value**	**Standard deviation**	**Mean value**	**Standard deviation**
Thunderstorm days at 00UT	12 709,4	1 147,1	38,1	11,5	1 903,3	539,3	-468,3	301,3
Thunderstorm days at 12UT	12 621,5	1 291,6	38,4	12,2	1 926,1	595,5	-482,9	353,8
Days of deep convection at 00UT	11 919,7	1 663,6	31,8	12,9	1 593,6	632,8	-326,5	329,2
Days of deep convection at 12UT	11 730,3	1 722,8	31,8	12,7	1 559,3	632,0	-320,2	338,7

larger values of CAPE. In contrast, mean CIN values are widely weaker in the case of TH clouds. Nevertheless, the high values of standard deviation for all theses parameters lead to examine first the distribution of the maximum cloud top height in relation to the corresponding cloud type (TH, DC). Figure 7 suggests that both TH and DC clouds preferentially have their tops in the 10000-15000 m range independently of the sounding hour.

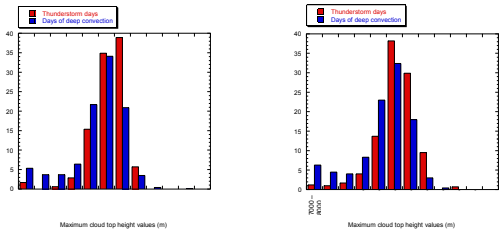

Figure 7 – Percentage of thunderstorm days and days of deep convection in relation to maximum cloud top heights values (A – 00h UT soundings, B – 12h UT soundings).

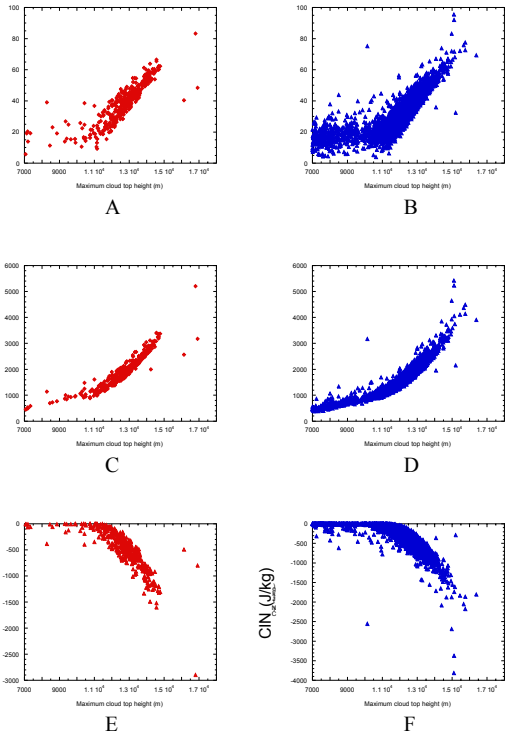

Figure 8 – Maximum vertical velocities (A, B), CAPE (C, D) and CIN (E, F) values in relation to maximum cloud top height values for 12UT soundings (A, C, and E – Thunderstorm days, B, D, and F – Days of deep convection).

Then, by representing maximum vertical velocity, CAPE and CIN values as a function of maximum cloud top height (Fig. 8), one can note that TH and DC clouds can clearly develop similar maximum vertical velocities, be characterized by similar CAPE and similar CIN in the 10000-15000 m range of maximum cloud top heights. The existence of deep convective clouds, with similar characteristics, that may or may not produce thunder, suggests that the dynamical indices studied in this work constitute deep convection indices and not cloud electrification indices. Obviously another parameter is most probably implicated in the cloud electrification process. This parameter could be the aerosol concentration in the subcloud layer.

Conclusion

In a first time a climatological analysis of thunderstorm events has showed that during the diurnal cycle it appears a thunderstorm peak of activity from 12 AM to 03 PM in local time which is well correlated with the maximum values of temperature as supposed by the thermal hypothesis. Conversely, this hypothesis can not explain the presence of a weaker secondary peak from 03 AM to 05 AM.

Furthermore, by using a 1D cloud model, it have been shown that dynamical parameters such as maximum cloud top height, maximum vertical velocity, CAPE and CIN can not be used as indices for cloud electrification. They have to be most probably considered as convection indices that inform on deep convective cloud development.

Thermal and aerosol hypotheses should be envisaged as complementary. However further investigations on the influence of aerosol on thundercloud electrification are necessary.

References

[1] E.Williams, S.Stanfill, The physical origin of the land-ocean contrast in lightning activity, C.R. Physique 3 (2002), 1277-1292.

[2] J.Molinié, C. Pontikis, A climatological study of tropical thunderstorm clouds and lightning frequencies on the French Guyana coast, Geophys. Res. Lett. 22 (1995) 1085-1088.

[3] ftp://ftp.ngdc.noaa.gov/STP/SOLAR_DATA/SUNSPOT_NUMBERS/

Environment / Climate / Natural Hazards / Simulation

Modelling of The Wind Field Produced During a Hurricane Passage In The Vicinity of An Island. A Case Study: The Island of Guadeloupe (FWI).

Kimathy ELISE
Université des Antilles et de la Guyane, faculté des sciences. LPAT-GEOL BP250
97157 Pointe-à-Pitre cedex, Guadeloupe - kimathy.elise@univ-ag.fr

Abstract

The hurricane wind impact may have dramatic consequences on life, property and infrastructures if the hurricane trajectory crosses inhabited island regions. Thus, during the pre-crisis phase, simulation of the wind field in the layer close to the surface may constitute a powerful tool for deciders in the taking of decisions. In this paper, the preliminary investigations, drawn by means of simulation techniques in order to determine the wind field established by the interaction of a hurricane with an island's relief, are presented.

In this work, the Oklahoma University mesoscale model ARPS (Advanced Regional Prediction System) has been used in relation to the numerical terrain model of the island of Guadeloupe and cyclonic vortex bogusing techniques in order to infer the island boundary layer wind field as organized during the hurricane HUGO's passage (1989).

Two different numerical experiments have been drawn by using a large scale domain and a smaller one, corresponding to the same number of integration point domain but two different grid element lengths with lengths ratio equal to ten. The model initialization was made by means of the Météo-France local atmospheric sounding, whereby the hurricane was simulated by implementing an artificial (bogus) Rankine type vortex at a characteristic HUGO's centre trajectory location when the hurricane was close to the island, 16,18° latitude, -60,67° longitude at 9:30pm. Note that during these runs, the organization of the wind field resulted under the influence of the implemented island's relief and maximum sustained wind velocity as produced by the initial bogus.

Further, since the damage degree is proportional to the sustained wind velocity, a potential damage distribution may be extracted from the calculated wind fields and compared to the real damage.

Based upon the above mentioned conclusions, future investigations will concern the improvement of the bogus vortex in order to increase the accuracy of the real wind field conditions as well as the pertinent improvement of the relation between damages and sustained wind velocity in order to adapt this relation to the objective conditions of the island of Guadeloupe.

1. Introduction

Guadeloupe and many other islands in the Caribbean are more and more at risk of severe damage and life threatening conditions from wind danger produced by tropical cyclones since the number and strength of the hurricanes has increased due to the global warming.

These phenomena cause human losses and create enormous material damages thus costing a lot to the states. These are, among others, the reasons why means are set to work to understand intrinsically these atmospheric disturbances as to predict their trajectory and impact so that the current losses are reduced. For example, hurricane Ivan, in 2004, crossed Grenada at category 3 on the Saffir-Simpson hurricane Scale causing catastrophic damages, 85% of the island was ruined and 39 people was killed. Hurricane Hugo was the last destructive one that struck Guadeloupe Island in the night of September 16 to 17 1989. As a direct result of it 60% of the sugar cane plantation were destroyed, 466 millions of francs was needed to restore the banana fields, 35 000 persons became homeless and 7 persons were killed. It was a hurricane with sustained wind of 144 mph and strong gust from 163 to 187 mph. Hugo is serving as reference for a hurricane impact simulation in the presented work.

Hurricane modelling has already been studied to know its impact, Gary Y.K. Chocka and Leighton Cochran modelled the topographic wind speed effects in Hawaii and applied it to hurricane Iniki.

In this paper a study is carried out to see how the implementation of a wind field close to a hurricane can lead to the creation of vulnerability maps toward wind with the threatening of a hurricane coming through Guadeloupe.

The bogus vortex implemented for this use describes the radial profile of the wind and sets the pressure difference between the eye and the periphery, the radius of maximum wind is set plus the pulsation frequency. To study the wind field of the vortex over a numerical terrain of Guadeloupe, the Oklahoma University Mesoscale model ARPS (Advanced Regional Prediction System) is used.

A few words about the ARPS description will be given (the model capabilities), also, the hurricane Hugo characteristics will be depicted. Afterwards, the structure of the vortex and the simulation experiments will be explained and the results will be exposed and shown.

2. Description of the ARPS model

During the past few years, a model known as the Advanced Regional Prediction System (ARPS) has been developed at the Center for Analysis and Prediction of Storms (ARPS, Xue *et al.*, 1995) at the University of Oklahoma.The model is a non-hydrostatic, compressible atmospheric prediction model in a terrain following coordinate with equal spacing in *x* and *y* directions and the grid stretching in the vertical direction. It is used for scales ranging from a few meters to hundreds of kilometers. The model can be run in 1D, 2D and 3D modes. The ARPS model solves prognostic equations for *u*, *v*, *and w*, the *x*, *y*, and *z* components of velocity, the perturbation potential temperature θ, and perturbation pressure *P*, sub-grid scale turbulent kinetic energy and the six categories of water variables such as water vapor, cloud water, rain water, cloud ice, snow and hail. Detailed description of the model, governing equations, the numerical methods, the physics parameterizations and computational implementation and configuration instruction are shown in the ARPS user's guide (Xue *et al* 1995).

3. Hurricane Hugo

According to Météo France information and data related by F.Pagney and E.Benito Espinal in "the hurricane Hugo", it arrived on the West-Indies with, in its centre, a minimum pressure of 942 hPa at the sea level, which is a low, but not extreme, value. In Raizet, Guadeloupe, it was 942hPA between & and 2am the 17 September. The anemometer was blocked shortly after the arrival but depicted maximum speed of 230 km/h (149 mph) at the eye approach and some wind gust from 26Okm/h to 300 km/h (162 to 186, 41 mph) affected the island. The active part of the hurricane spread over a 22Okm diameter, the spiral bands added 200km more of cloud clusters responsible of the persistent bad weather the whole day of 17 September The eye, that was really clear, seems to have had a diameter around 34 km. But this diameter was likely to have changed along the phenomenon way and the eye's shape seemed to be complex because it wasn't experienced the same way on the different locations where it passed. The radar of the meteorological service of Guadeloupe stopped to operate at 23 pm. The motion speed when it came to the eye island was 20 km/h (12,43 mph) which show some acceleration in some places, since on the sea, the speed was 19 km/h (11,81 mph). The first north wind started on the beginning of the evening and reached its peak from 11pm to 1:30 - 1:45am. The renewal of the strong wind where around 2:30-2:45 am, the wind was persistent until 4:30- 5am in the morning.

It is this persistence of violent wind that causes most of the damages, Hugo last ruthlessly a longer time than the previous hurricanes. The most ravaged disaster zone, in which the habitations were more damaged, follows a diagonal from St François, Ste Anne reaching to Petit Canal and Anse-Bertrand (Fig1). Désirade is included in this zone. This is also the area were the vegetation and the cultures were most affected.

Figure1. Geographical distribution of the damages estimation

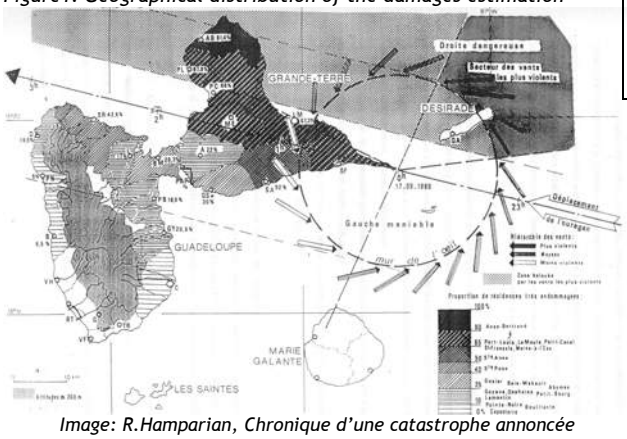

Image: R.Hamparian, Chronique d'une catastrophe annoncée

4. Simulation experiments

Tropical cyclones are one of the most difficult phenomena in the atmosphere to fully describe and predict even with access to highly sophisticated meso-scale models. Wind measurements from surface platforms, satellites, and aircraft reconnaissance may be available during and prior to landfall, but are seldom sufficient to describe the three-dimensional and constantly changing wind structures over the entire course of their existence. Engineers and scientists often resort to using parametric models to approximate the two-dimensional wind structure within a tropical cyclone in practical applications.

There are several parametric wind models, each of which has been shown to be valid and useful for at least one tropical cyclone event in a particular region. Essential to a parametric model is the representation of the wind flow in an idealized tropical cyclone by concentric circles. The wind speed is zero at the centre and increases rapidly to its maximum at the radius of maximum wind Rm and then decreases gradually to zero at large radii. This is the Rankine vortex in which the inner part turns as a disk and in the outer part the velocity is inversely proportional to the distance from the centre; i.e :

$v(r) = vm(r/ Rm)$ for $r \leq Rm$ (1)

$v(r) = vm/(r/ Rm)$ for $r \geq Rm$ (2)

where v_m is the tangential velocity at r=Rm. In a cyclone "Rm" would be the radius of the eye wall.

Here a modified Rankine vortex is used. It has the particularity of traducing the inner organization of a hurricane; we can distinguish the eye, its wall and the external part considered as the spiral. Concerning the equations, it is different from the real rankine one by the fact that the wind speed is calculated with the expression (1) only for the disk representing the eye wall, the speed corresponding to the part of the ratio within the eye is zero.

Tab1.Simulation initialisation

Simulation	EXP1	EXP2
Grid Centre	Lat: 16,18 Lon: -61,44	Lat: 16,20 Lon: -61,44
Resolution	1km	100m
Dimension	660x660x35	660x660x35
Modified Rankine Vortex	anr = 110.0, omegacyc = 0.00825, cyclat = 16.18, cyclon = -60.67, wvit = 1.0 u0 = -18.00 v0 = 6 autoconvnp = 0.0005 anre = 16.5 anrv = 56.0 dip = 70.0 ur = 0.5	

Anr: total hurricane ratio in *km*
Anre: eye ratio *in km*
Anrv: vortex ratio in km
Omegacyc: angular momentum
Cyclat: latitude of the vortex centre
Cyclon : longitude of the vortex centre
Wvit: vertical velocity inside the vortex
u0: translation speed E-W of the vortex *km/h*
v0: translation speed E-W of the vortex *km/h*! Autoconvnp: conversion rate of the cloud water in to rain water
dip: pressure difference between the centre and the periphery of the vortex
ur : radial velocity of the vortex

To know the impact of the wind of a hurricane it is important to study the phenomena at a good resolution to analyse the wind field over the Guadeloupe terrain. Thus, two different numerical experiments (Exp1, Exp2) have been drawn by using a 660x660x35 points integration domain. These experiments corresponded to two different grid element lengths of respectively **1**km and 100m). The model initialization was made by means of the Météo-France local atmospheric sounding, whereby the hurricane was simulated by implementing the modified Rankine type vortex at a characteristic Hugo's centre trajectory location when the hurricane

was close to the island, 16,18° latitude, -60,67° longitude at 9:30pm. At that time the wind speed was around 220km/h and progressively increase to 230km/h. The model results were taken after 1hour and 30 minutes of simulation at 11:00pm when the strong winds started in Pointe à Pitre.

The experiment Exp1 gives the wind parameter from the first coarse grid with 660km length and a 1km terrain resolution. These parameters are run in Exp2 in the fine grid with 66km length and 100m terrain resolution. Note that during these runs, the organization of the wind field resulted under the influence of the implemented island's relief and maximum sustained wind velocity as produced by the initial bogus vortex.

5. Results and Analyses

Results

Figure2.1 ***Exp1:***

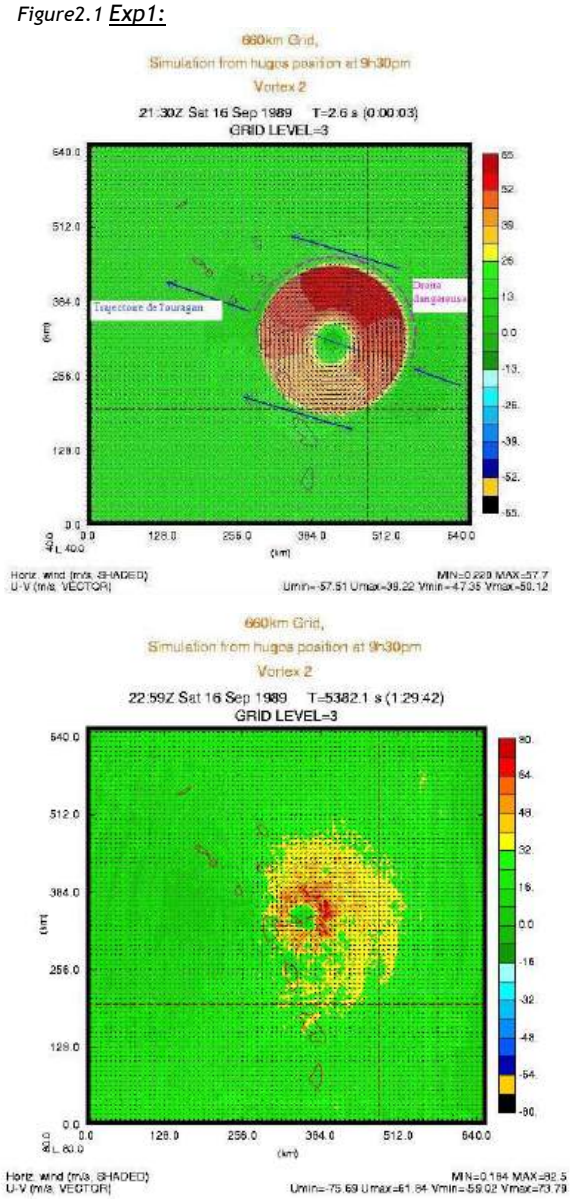

Figure2.2 ***Exp2:***

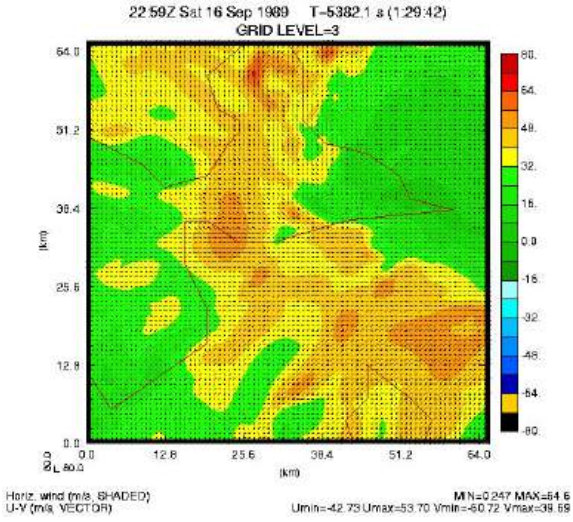

Tab2.1. Table of u v w values of wind velocities in Anse-Bertrand (Massioux) zone

Latitude	longitude	u_component	v_component	w_component	qr	hterain
16.403805	-61.471703	-0.924368	-50.334469	4.264474	0.001036	9.826756
16.412863	-61.471703	-5.882792	-52.663532	2.766037	0.001029	14.337385
16.421921	-61.471703	-6.073307	-52.436192	1.908681	0.001346	19.423969
16.430979	-61.471703	-1.275618	-51.857082	4.903445	0.001819	25.127672
16.440037	-61.471703	1.029837	-51.647030	9.215911	0.001791	31.453529
16.449095	-61.471703	-6.211184	-49.968559	8.407942	0.001201	34.982761
16.458153	-61.471703	-20.913389	-45.597721	1.105975	0.000975	37.342041
16.467211	-61.471703	-33.368221	-42.061317	-0.271710	0.001171	37.459557
16.476269	-61.471703	-34.549599	-43.735725	5.700829	0.001145	32.764809
16.485327	-61.471703	-25.691101	-47.825230	4.326044	0.001097	24.745712
16.494385	-61.471703	-19.126661	-47.576447	1.188165	0.001201	17.465893
16.503443	-61.471703	-19.099751	-42.433399	2.508601	0.001335	12.794712
16.512501	-61.471703	-20.084269	-38.608051	3.614814	0.001460	8.855769
16.521559	-61.471703	-18.226631	-38.815609	2.946603	0.001602	5.299107
16.530617	-61.471703	-13.918523	-39.309109	2.599587	0.001834	2.215637
16.539675	-61.471703	-10.731243	-37.957397	2.937972	0.002068	0.000000
16.548733	-61.471703	-11.612287	-36.910351	3.505904	0.002268	0.000000

Tab2.2 Table of u v w des values of wind velocities in Grands fond Ste Anne (Deshauteurs, St Protais zone).

Latitude	longitude	u_component	v_component	w_component	qr	hterain
16.213587	-61.426411	32.551445	3.324858	-1.986142	0.001245	0.000000
16.222645	-61.426411	31.313257	-0.243378	-2.795199	0.001149	6.851657
16.231703	-61.426411	25.755281	-7.816748	-2.476076	0.001247	25.328421
16.240761	-61.426411	26.607233	-13.771370	-2.316369	0.001403	51.459465
16.249819	-61.426411	33.603600	-17.870070	-2.400411	0.001370	71.706734
16.258877	-61.426411	34.111198	-25.670208	-3.074846	0.001018	88.296234
16.267935	-61.426411	29.290289	-34.735229	-4.652631	0.000487	102.617226
16.276993	-61.426411	17.729357	-38.288403	-3.721531	0.000262	107.079697
16.286051	-61.426411	11.674391	-34.552807	-1.924759	0.000634	105.397766
16.295109	-61.426411	21.527514	-32.046589	-1.805303	0.001152	97.128006
16.304167	-61.426411	26.519556	-33.860687	-0.642535	0.001244	81.486313
16.313225	-61.426411	19.041925	-35.351566	-0.238229	0.001061	58.956963
16.322283	-61.426411	12.708139	-35.234325	0.123919	0.001002	39.679840
16.331341	-61.426411	14.834063	-32.251419	-0.658161	0.001085	26.183043

Analyses

The simulation shows that there's a clear distinction between the wind velocities in the "lethal part" of the hurricane and the other part. The wind values are more important in this side at the right of the hurricane trajectory. We can see that the areas of Guadeloupe that was under this part during the trajectory suffered more damages (fig 1, fig2.1, fig2.2, fig3).

The comparison of importance of the calculated wind velocities (Tab2.1, Tab2.2) and the percentage of damages occurred at different locations (fig3) suggests a close relation. Following the meridian -61,47° of longitude that is passing trough "Massioux" plateau in Anse-Bertrand that suffered heavy damages, we can notice too that model retranscribe the increase of the wind velocities from the sea zone in the north at latitude 16,54° where the wind speed is less important than in the higher elevation terrain at latitude 16,46°.

Same results are observed in "Les Grands Fonds" zone in Ste Anne.
Further, since the damage degree is roughly proportional to the third power of the sustained wind velocity, a potential damage distribution may be easily extracted from the calculated wind fields and compared to the real damage distribution as inferred from the insurance and state archives.

Figure3. Damages Anse-Bertrand, Port-Louis, Petit-Canal
% of damaged habitations by zones + comparison

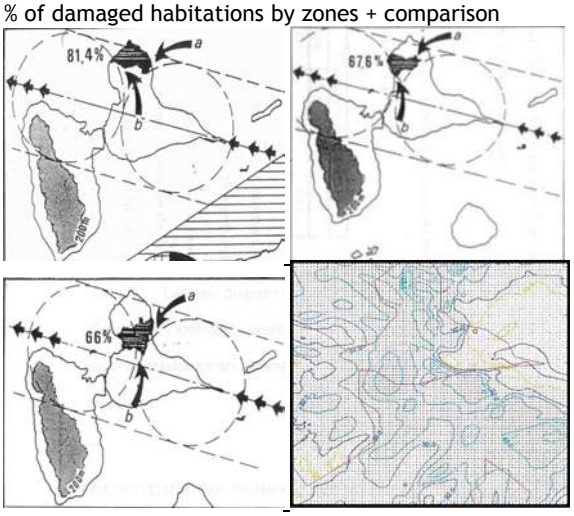

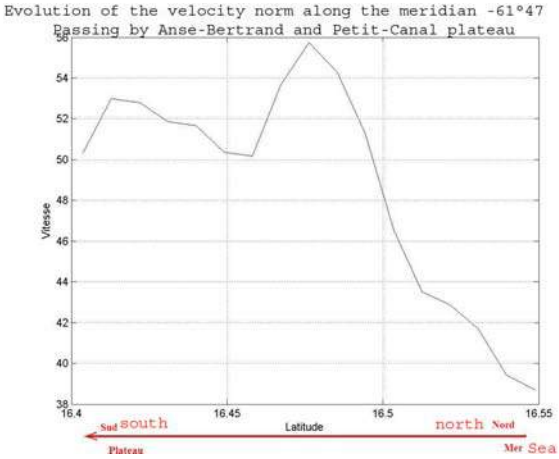

6. Conclusion

Based upon the above mentioned conclusions, future investigations will concern the improvement of the bogus vortex in order to increase the real wind field conditions as well as the pertinent improvement of the relation between damages and sustained wind velocity in order to adapt this relation to the objective conditions of the island of Guadeloupe. Thus, from modelling an up coming hurricane (the wind field and its trajectory), we can know the zone of the island that will be under danger. With a geographic study of the vulnerability factors and the vulnerable elements we can lastly make a vulnerability map towards a hurricane coming.

References

1. PAGNEY F. L'ouragan Hugo: genèse, incidences géographiques et écologiques sur la Guadeloupe, Ouvrage publié par le Parc National de la Guadeloupe, la DRAC de la Guadeloupe, le Parc Naturel Régional de la Martinique, 1992. L'Agence Guadeloupéenne de l'Environnement du Tourisme et des Loisirs, Fort-de-France. pp. 17-76.
2. Ming Xue, Kelvin K. Droegemeier, Vince Wong, Alan Sahpiro, Keith Brewster, (1995), ARPS Users's Guide, Center for Analysis and Prediction of Storms CAPS.
3. Gary Y.K. Chocka and Leighton Cochran. (2005) Modeling of topographic wind speed effects in Hawaii.
4. Robert Hamparian, Mémoire de Ter, (1994) université des Antilles et de la Guyane.
La Guadeloupe à l'épreuve de l'ouragan Hugo: *chronique d'une catastrophe annoncée*.
5. J. Thielen, A. Gadian
Influence of different wind directions in relation to topography on the outbreak of convection in Northern England, Ann. Geophysicae 14, 1078Ð1087 (1996) EGS Springer-Verlag 1996

Environment / Climate / Natural Hazards / Simulation

Behavioral Change : An Original Application Of Health Belief Models For The Prevention Of Natural Hazards

NATHALIE MICHALON

Département d'Anthropologie, Centre d'Etudes et de Recherche Caraïbes,
Université des Antilles et de la Guyane - nathalie.michalon@univ-ag.fr

Abstract

The Caribbean islands, located in a high potential seismic area with a great probability of volcanic eruptions, are moreover submitted to major meteorological phenomena. The prevention of these hazards, is vital for the entire populations of the Basin, where most of them use creole languages. The educational tools used in this domain must take into account the particular context in which each community lives, for a good understanding of the safety orders.

Lightning has shown to be harmful to both human and ecological life and can cause damage to the world's infrastructure. Through the lightning phenomenon narrative description, a practical and original method of behavioral change, using cognitive process based upon health belief models, is presented in this study.

Introduction

The Caribbean islands, located in a high potential seismic area with a great probability of volcanic eruptions, are moreover submitted to major meteorological phenomena. The prevention of these hazards, is vital for the entire populations of the Basin.

Most of the people which are living in these countries are descendants of the African deportees by the Triangular Trade and which have developed their own culture by creolization process. Tales have an important place in these cultures because they allowed to transmit a part of the ancestral cultures.

Lightning has shown to be harmful to both human and ecological life and can cause damage to the world's infrastructure. Using a tale which describes the lightning phenomenon, we propose an original educational tool for the prevention of this hazard. Moreover, the social learning theory embedded in the story can be detailed for educational use in the case of behavioral change experiments.

Connections between weather and disease are well established, with many diseases occurring during certain seasons or erupting from flood or drought conditions. Climate change is likely to have various potential impacts on human health. In tropical countries, rising temperatures and humidity have facilitated the spread of many vector borne infectious diseases including malaria, dengue, Nile fever and recently chikungunya in Reunion island, because their transmission vector is the mosquito, which is sensitive to weather conditions (Tsai and Liu, 2005). Perceiving the susceptibility of the climate change problem, related to its impact on the human health, can be the starting point of a behavioral change in front of this situation.

Materials & Methods

A narrative description of the lightning phenomenon, "From dust to lightning" (Michalon, 2005), had been elaborated in the form of a tale. During the travel inside a thundercloud, the readers are driven from a bubble in the ocean until the production of a lightning. For a best understanding for the creole speaking people from Haïti, Saint-Lucia, Dominica, Guadeloupe, Martinique and French Guyana, it was been translated in kréyòl, entitled "Kont a van é gout". Physics contained in the text are exact (McGorman and Rust, 1998; Pruppacher and Klett, 1978).

The 5 chapters present the following descriptions:

Chapter 1: the bubble burst mechanism

Chapter 2: the coagulation process and turbulent movements in the atmosphere

Chapter 3: the greenhouse effect and the buoyancy
Chapter 4: the rainfall formation process
Chapter 5: the freezing and crystallization process ; the sparks and lightning production.
Embedded in the story, a social learning theory which takes into account cognitive process, allow to memorize the stages of belief model used in behavioral change experiments.

Structure and cognitive process

The pivotal notion of "structure" is defined as a system of transformations which abides by certain laws and which sustains or enriches itself by a play of these transformations, which occur without the use of external factors (Piaget,1978). This auto-structuration of a complete whole is defined as "auto-regulation". In the individual, the latter is established by biological rhythms, biological and mental regulations and mental operations. These can be theoretically formalized.
The existence of all living substances begin with action and this is rooted in biological processes. Action implies the formation of cognitive structures which are at first exteriorized in coordinated external movements. After repeated actions, interiorization, permanency, invariant principles and imagination allow for the emergence of internal cognitive structures. So the following sequence appears :

1 external actions (system) and reactions (environment) ;
2 interiorization and permanency ;
3 internal cognitive structures and auto-regulation ;
4 novel external actions.

These internal cognitive structures are constantly being transformed and regulated in order to adapt the system to new situations. This process is recurrent and so always more complex cognitive structure emerge.

Health Belief Model and behavioral change

A Health Belief Model, developed in the 1990s by Prochaska and colleagues, holds that health behavior is a function of individual's socio-demographic characteristics, knowledge and attitudes (King, 1999). According to this model, individuals or groups pass through 6 stages in order to be able to change behavior. They are:
1) pre-contemplation (Perceiving susceptibility to a particular problem)
2) contemplation (Perceiving seriousness of the condition)
3) preparation (Belief in effectiveness of the new behavior)
4) action
5) maintenance (Perceiving benefits of preventive action)
6) relapse (Perceiving barriers to taking action)
In this model, promoting action to change behavior includes changing individual personal beliefs.
Individuals weigh the benefits against the perceived costs and barriers to change.

Results & Discussion

Historically, the tales were socially and psychologically best suited to the condition of the people in the Caribbean islands during the slavery period because they allowed them to express their fantasies and their deepest anxieties (Tiffin, 1982). Creolization is defined as " a cultural action, material, psychological and spiritual based upon the stimulus response of individuals to their environment" (Brathwaite, 1971). In that way, tales can act as creolization responses to a new environment, dramatizing efforts to manipulate it verbally and symbolically and they can become measures of self-reliance and self-affirmation (Tortello, 1991).
The continuous emancipation of the different cognitive forms of equilibrium (an always increasing cognition) is a pivotal notion in the behavioral change process. This increase is the natural result of successful re-equilibrations, in which logico-symbolical functions plays a major role. Auto-regulation is also the result of the interactions between the system and its environment. Hence, intersubjectivity is always essential in the construction of new and stronger cognitive structures. This implies that cognitive processes not only appear as resulting from organical auto-regulation of which they reflect

the essential mechanisms, but also emerge as differentiated organs of this regulation in the arena of interactions with the environment. Cognition is the most differentiated biological organ of survival human beings have. Social cognitive or social learning theory states that new behaviors are learned either by modeling the behavior of others or by direct experience. It focuses on the important roles played by vicarious, symbolic, and self-regulatory processes in psychological functioning and looks at human behavior as a continuous interaction between cognitive, behavioral and environmental determinants (Bandura, 1977). In order for an intervention to be successful, the model must target the appropriate stage of the individual or group which pass through all stages, but do not necessarily move in a linear fashion (Prochaska, 1994). The stages of change model emphasizes the importance of cognitive processes and movement between stages depends on cognitive-behavioral processes.

Consequently, the tale "From dust to lightning", which includes recent social learning theory for behavioral change, can be used for the prevention of natural hazards, particularly for the electrical risks related to lightning struck and for the climate change prevention, and as well in several domains which need educational tools for behavioral change (health problem and HIV/AIDS prevention, industrial risks prevention, etc.). Moreover, in the Caribbean islands, the illiteracy is a major problem for the prevention programs. Translations in creole languages would allow to transmit safety orders with a better understanding from creole speaking people.

References

1. Bandura A., (1977). Social learning theory. Prentice-Hall, Inc., Englewood Cliffs, New Jersey 07632.

2. Brathwaite, E. K. (1971). The Development of Creole society in Jamaica. Oxford: Clarendon Press.

3. King R. (1999). Sexual behavioural change for HIV: where have theories taken us?, Joint United Nations Program on HIV/AIDS, UNAIDS Best Practice Collection.

4. MacGorman, D.R., and W.D. Rust (1998). The Electrical Nature of Storms, Oxford University Press.

5. Michalon N. (2005). From dust to lightning, Paljor Publications Ltd.

6. Piaget J. (1978). Le structuralisme, Que sais-je ?, éditions PUF, 12ème édition (1996).

7. Prochaska J., Redding C., Harlow L., Rossi J., Velicer W. (1994). The transtheoretical model of change an HIV prevention: a review, Health Ed Quartely 21 (4) , 471-486.

8. Pruppacher H.D. and J.D. Klett (1978). Microphysics of cloud and precipitation, D. Reidel Edition , Higham, USA.

9. Tiffin, H. (1982). "The metaphor of Anancy in Caribbean literature" in Sellick, R. (Ed). Myth and metaphor.
Adelaide: Centre for Research in New Literatures in England

10. Tortello, R. (1991). "The Magical spider-man: The Metaphormoses of Bredda Anansi." Diss. Harvard University.

11. Tsai H.T., Liu T.M. (2005). Effects of global climate change on disease epidemics and social instability around the world, Human Security and Climate Change, International Workshop, Asker (Oslo), 21-23 June.

Environment / Climate / Natural Hazards / Simulation

Two Numerical Experiments For The Investigation Of Possible Influences Of A Climate Change On The Global Atmospheric Electrical Circuit

NATHALIE MICHALON

Agence KaNNH, Saint-Joseph, Martinique - nathalie_michalon@yahoo.fr

Abstract

Evidence is emerging for physical links among clouds, global temperatures, the global atmospheric electrical circuit and cosmic ionization. Atmospheric electrical modification of cloud properties may have significant global implications for climate, via changes in the atmospheric energy balance. Likewise, global temperature changes have been suggested as a source of variability in the global atmospheric electrical circuit.

In this study, in order to infer the impact of a global climate change on the atmospheric electrical circuit, two numerical climate change experiments with respectively doubled CO2 concentration and a 3% continental cloud cover decrease have been made.

Both numerical experiments lead to a roughly 10% increase of the mean global annual flash frequency, that corresponds to a mean global surface warming of 1.92 K.

Introduction

The lightning production of thunderstorm clouds is of interest in different fields of research, engineering and civil protection. It is usually expressed in terms of lightning frequency F which is a function of the thunderstorm cloud electrification degree and is related to the dynamical and microphysical cloud characteristics (Price and Rind, 1992; Rutledge et al., 1992; Molinié and Pontikis, 1995; 1996; Michalon et al., 1999). It has been suggested that lightning activity might be used as a sensitive indicator of changes in climate (Williams, 1992; 1994; Reeve and Toumi, 1999).

Moreover, recent observations indicate electromagnetic waves association with earthquake. The emission of these waves as a result of electric charge redistribution is one of the main hypothesis regarding the waves generation mechanism (Singh et al., 2002).

In this study, in order to infer the impact of a global climate change on the atmospheric electrical circuit, two numerical climate change experiments with respectively doubled CO2 concentration and a 3% continental cloud cover decrease have been made.

Materials & Methods

The Michalon et al. (1999) flash frequency parameterization has been obtained by combining the

Price and Rind (1992) analysis results, the Molinié and Pontikis (1995) conclusions suggesting that the cloud droplet concentration is a key parameter for cloud electrification, and simple dimensional arguments. It may be written as

$$F = 4.392 \times 10^{-7} N^{2/3} H^{4.9}$$

where H is the cloud height and N the cloud droplet concentration.

In the numerical experiments, we use two "standard" droplet concentration values (Nc = 600 cm-3 and Nm = 50 cm-3) respectively valid for continental and maritime clouds.

The determination of the relative proportion of cloud-to-ground flashes uses the empirically derived formulation (Price and Rind, 1994):

$$P = 1/ (aD^4 + bD^3 + cD^2 + dD + e)$$

where a, b, c, d and e are the appropriate coefficients, and D the cold cloud thickness.

An analysis by Marsh and Svensmark (2000), shows that cosmic rays and low (i.e. with altitudes less than about 3 km) clouds observed by global satellites are strongly correlated around the cosmic ray minimum of 1990. The correlation was originally presented in 1997 (Svensmark and Friis-Christensen, 1997) and the

limitations of the data analysis and acquisition have been the subject of considerable discussion (Kernthaler et al., 1999; Kristjánsson and Kristiansen, 2000). There is no correlation with high clouds (Kristjánsson and Kristiansen, 2000). However, variations in the ionospheric potential has been linked to cosmic ray variations arising from the solar cycle (Markson, 1981).

The "ARPEGE-IFS-cycle 14" GCM used for the numerical experiments has been developed jointly by Meteo- France and the European Center for Medium Range Weather Forecasts (ECMWF) and has been adapted by Déqué et al. (1994) for climate purposes. The model has been validated at various horizontal resolutions in 10-year integrations using prescribed monthly mean sea-surface temperatures observed between 1979 and 1988 (Déqué et al., 1994). The cloud top heights used to infer the flash frequencies are obtained from two different numerical experiments hereafter referred to as 1×CO2 (control simulation) and 2×CO2 (global warming simulation) concerning the time period between the 28 October 1998 (0.00 UT) and 27 October 1998 (24.00 UT). As the model is purely atmospheric, the sea surface temperatures (SSTs) are prescribed as external boundary conditions, whereby the methodology known as "time-slice simulations" (Mahfouf et al., 1994; Timbal et al., 1997) is used. In 2×CO2 experiment, the ocean response to increased greenhouse warming is taken into account by adding to the climatological SSTs of 1×CO2 experiment, the ocean warming simulated at the time of CO2 doubling in a fully coupled transient scenario performed with the Hamburg ocean-atmosphere coupled model (Cubasch et al., 1992).

In order to infer the influence of the solar cycle on the climate, the second experiment is a rough test of the impact of a 3% continental cloud convective cover decrease on the global electrical circuit, whatever the cause of the cloud cover change.

Results & Discussion

The global circuit consists of the ionosphere, Earth's surface, fair-weather current and thunderstorm current. Within the ionosphere, the positive charge is carried to areas of fair weather, and small currents flows vertically. In order for the spherical capacitor to remain charged, there must be a mechanism that acts to re-supply the charge to close the electrical circuit. Thunderstorms are the most common forms of disturbed weather that cause local electric fields to be produced and cause positive charge to move upwards toward the ionosphere and negative charge to move to the surface (Wilson, 1920).

The fair-weather current is the flow of current from the positively charged ionosphere to the negatively charged Earth's surface in regions of fair-weather. The vertical atmospheric electric field E(z) is derived from the measured potential V at a height z. The ionospheric potential VI which is obtained from vertical sounding of the variation of E(z) with height, is the potential of the lowest conducting regions of the ionosphere, reckoned with respect to a zero potential at the surface.

The control simulation (1×CO2) results are in good agreement with the recent observations of the lightning frequency distributions (Christian et al., 2003). The variation of the global diurnal lightning cycle obtained from the numerical control experiment are in good agreement with the variation of the measured fair-weather potential.

The 2×CO2 experiment shows a 9.8% increase of the mean global flash frequency which corresponds to a mean global surface warming of 1.92 K. The experiment of a decrease of the convective cloud cover shows a 12.9 % increase of the global flash frequency. Both experiments show similar variations of the flash frequency distribution.

Changes in thunderstorms caused by surface temperature changes would cause modulations on the global atmospheric electrical circuit. Increases in surface temperature leading to more vigorous convection have been quantitatively linked with increases in VI (Price, 1993), offering a possible indirect method of monitoring surface temperatures. A positive correlation between global temperature datasets and VI was observed, supporting a relationship

between warmer temperatures and an increased VI (Markson and Price, 1999). A global increase of the ionospheric potential VI linked with increases in global surface temperature would change the charging of the global electric circuit. A small observed modulation in VI has been linked to cosmic ray variations arising from the solar cycle (Markson, 1981) : cosmic ray ionization modifies the atmosphere's columnar resistance. VI increased when an increase in cosmic rays occurred. Markson (1981) showed that, for the increase in cosmic rays to increase VI , the change has to influence the charging part of the global electrical circuit.

Although the effects of electric fields on cloud physical processes are not well understood, an increase of the cloud electrification would result from an amplified fair-weather current or an enhanced conductivity in the lower stratosphere (Markson and Muir, 1980). Flash frequency lightning distributions and particularly the diurnal lightning cycle which follows the fair-weather current variation, would be interesting parameters to estimate the earth's electric field evolution, linked or not to a global warming.

Acknowledgements

The results of climate modeling used in this study are issued from the work made in the Laboratoire de Physique de l'Atmosphère Tropicale, Université des Antilles et de la Guyane, in the frame of my PhD thesis. I thank all the LPAT's members for their support and their hospitality.

References

Christian H.G. et al. (2003). Global frequency and distribution of lightning as observed from space by the Optical Transient Detector, J. Geophys. Res., 108(D1), 4005, doi:10.1029/2002JD002347.

Cubash U., Hasselman K., Höck H., Maier-Reimer E., Mikolajewicz U., Santer B.D., Sausen R. (1992). Timedependent greenhouse warming computations with a coupled atmosphere-ocean model, Climate Dyn., 8, 55-69.

Kernthaler S.C., Toumi R. and Haigh J.D. (1999). Some doubts concerning a link between cosmic ray fluxes and global cloudiness, Geophys. Res. Lett., 26, 7, 863-865.

Kristjánsson J.E. and Kristiansen J. (2000). Is there a cosmic ray signal in recent variations in global cloud cover and cloud radiative forcing? J. Geophys. Res., 105, 11851-11863.

Mahfouf J.F., Cariolle D., Royer J.F., Geleyn J.F., Timbal B. (1994). Response of the Météo-France climate model to changes in CO2 and sea surface temperature, Climate Dyn., 9, 345-362.

Markson R. and Muir M. , 1980 : Solar wind control of the Earth's electric field, Science, 208 (4447), 979-990.

Markson R. (1981). Modulation of the earth's electric field by cosmic radiation, Nature, 291, 304-308.

Markson R. and Price C. (1999) Ionospheric potential as a proxy index for global temperature, Atmos. Res., 51, 315-321.

Marsh N. and Svensmark H. (2000). Low Cloud Properties influenced by Cosmic Rays, Phys. Rev. Lett., 85, 23, 5004-5007.

Michalon N., Nassif, A., Saouri, T., Royer, J. F., Pontikis C., 1999: Contribution to the climatological study of lightning ,Geophys. Res. Let., 26(20), 3097-3100.

Molinié J. and Pontikis C.A. (1995). A climatological study of tropical thunderstorm clouds and lightning frequencies on the French Guyana coast, Geophys. Res. Lett., 22(9), 1085-1088.

Molinié J. and Pontikis C.A. (1996) Reply, Geophys. Res. Lett., 23(13), 1703-1704.

Price C. (1993). Global surface temperatures and the atmospheric electrical circuit, Geophys. Res. Lett., 20 (13), 1363-1366.

Price C., Rind D. (1992). A simple lightning parameterization for calculating global lightning distributions, J. Geophys. Res., 97, 9919-9933.

Price C., Rind D. (1994). Modeling global lightning distributions in a general distribution model, Mon. Wea. Rev., 122, 1930-1939.

Reeve N. and Toumi R. (1999).Lightning activity as an indicator of climate change, Q. J. R. Meteor. Soc., 125, 893-903.

Rutledge, S.A., Williams E.R., and Kennan T.D. (1992). The down under Doppler and electricity experiment (DUNDEE): Overview and preliminary results. Bull. Amer. Meteor. Soc., 73, 3-16.

Singh R.P., Patel R.P., Ashok K Singh (2002). Lightning generated ELF, VLF, optical waves and their diagnostic features, Indian J. Phys., 76B (3), 235-249.

Svensmark H. and Friis-Christensen E. (1997). Variations of cosmic ray flux and global cloud coverage - a missing link in solar-climate relationships, J. Atmos Sol.-Terr. Phys., 59, 1225 - 1232.

Williams E.R. (1992) The Schumann Resonance: a global thermometer. Science, 256, 1184-1187.

Williams E.R. (1994) Global circuit response to seasonal variations in a global surface air temperature. Mon. Wea. Rev., 122 , 1917-1929.

Wilson C.T.R. (1920). Investigations on lightning discharges and on the electric field of thunderstorms, Phil. Trans. Roy. Soc. Lond., A221, 73-115.

Environment / Climate / Natural Hazard / Simulation

Facing Natural Hazards: Policies, Strategies, role of Basic Sciences

LILLIAM ALVAREZ DIAZ,

Director of Sciences, Ministery of Science, Technology and Environment of Cuba - lilliam@citma.cu

Abstract

The lecture will include some historical review of natural hazards in the island, comments and reflections of the social and governmental organization, civil defence, political strategies and policy of science and technology for facing mainly, tropical hurricanes.

Effective R&D systems to mobilize science and technology for sustainable development is not an impossible to design and implement, if the countries start for *a political will* to face, in first place the natural hazards. The Cuban experience has proved this.

Cuba has made many in implementing integrated Strategies and System of S&T and Environment, problem-driven, capacity building, place-based research and applications Programs in support of sustainability.

Some practical experiences, data, figures, indicators will be posed in the lecture and also methodologies and practical measures to minimize the impact of tropical organisms in general.

The importance of having human resources well prepared, educated, and a "critical mass" of scientists, engineers, modest infrastructures in R&D centers, programs and projects, including capacities in basic sciences, as Physics, Mathematics and Computational sciences, besides, good meteorologists, will be discussed.

The role of the media, the effective, real and veridical information by radio, newspapers, e-mails, internet, TV and different ways of preparation and social communication of the measures previous, during and after the disaster also will be a topic for the debate.

CDSA: A New Seismological Data Center for French Lesser Antilles

M. BENGOUBOU-VALÉRIUS (1), D. BERTIL (2), S. BAZIN (3), A. BOSSON (4), F. BEAUDUCEL (4) and A. RANDRIANASOLO (1)

(1)EA921 LPAT-GEOL, Université Antilles-Guyane, Guadeloupe - bengoubou@yahoo.fr

(2) Service géologique régional, BRGM, Guadeloupe

(3)OVSM, IPGP, Martinique - (4)OVSG, IPGP, Guadeloupe

Abstract

The Lesser Antilles is an area of high volcanic and earthquake activity, characterized by a 1000 km convergence zone resulting from the Atlantic plate subduction under the Caribbean plate with a slow convergent motion (2 cm/year). This arc has a specific regional setting with important structural heterogeneities which can affect seismic characteristics: oblique subduction in the North, large accretion prism in the South, aseismic ridge sinking in subduction, shallow intraplate active faults close to the volcanic arc. In 2000, the "*Centre des Données Sismologiques des Antilles*" (CDSA) was created, with the purpose to provide seismological data at public disposal for multiple applications: research, earthquake engineering, and pedagogic. To reach this objective, it is necessary to gather all Martinique and Guadeloupe seismological data, presently scattered between several institutions and in different numerical formats; then, to process data to make them compatible and produce more accurate information on regional and local seismic activity. Numerical signal records and phases arrival times bulletins come mainly from permanent volcanic and seismologic survey networks managed by IPGP Observatories and several accelerometric networks. More than 120 stations from 10 networks with short period, broadband or accelerometric sensors are concerned. With five years of available data, the

CDSA data base presents a more homogeneous vision of Lesser Antilles arc seismicity and allows detecting low seismic activity zones, in the north near the Virgin Islands, and in the south between St-Lucia and Grenada. The accuracy improvements of CDSA location, evidenced by the study case of Les Saintes 2004 swarm, is used to better study the relationship between tectonic structures and seismicity around Guadeloupe and Martinique islands, and to better define the subduction slab geometry. Cross-sections perpendicular to the arc reveal that the slab has a nearly constant, 50° dip angle, from St-Lucia to Nevis. As seismic hazard assessment depends from strong ground motion generated by earthquakes, the CDSA data base also includes strong motion records of the region. The underestimation of the peak acceleration values by standard attenuation laws at large distances shows the need to develop new formulae adapted to the Lesser Antilles context.

References: F.W.Klein, 2002, U.S.G.S. Openfile report 02-171.

Seismogenic Potential of Fore-Arc Tectonic Structures: Onshore - Offshore Geology Helps to Understand the Tectonic Activity at the Marie-Galante Basin - Lesser Antilles

J.F. LEBRUN (1), J.L. LÉTICÉE (1), S. BES DE BERC (2), J.J. CORNÉE (3), P. MUNCH (4), A. RANDRIANASOLO (1), I. THINON and M. VILLENEUVE (1)

(1) EA 923 LPAT-GEOL, Université des Antilles et de la Guyane, Pointe à Pitre, FWI - jflebrun@univ-ag.fr
(2) BRGM, Le Houëlmont, Gourbeyre, FWI
(3) UMR 5125 PEPS, Université de C. Bernard - Lyon 1, Villeurbanne, France
(4) FRE 2167 GSC, Université de Provence - Marseille, France

Abstract

Estimating seismogenic potential of active faults is a challenge that requires short and long term evaluation of faults activity. Therefore, the planform of fault systems as well as average velocity of deformation over periods ranging from 102, 106-7 years are key parameters to estimate magnitude and return period of earthquakes.

The Marie-Galante basin is a tectonic graben transverse to the lesser-Antilles fore-arc that accommodates the N-S extension of the fore-arc in response to oblique subduction. The graben abuts the Soufrière Volcano (Guadeloupe) to the west, and it is bounded along both sides by normal faults with clear morphological expression. These faults were identified onshore and offshore. Recent estimates of vertical displacement along one onshore segments of a fault at the southern border of the basin provides slip rates of 0.5 ± 0.2 cm/year over the last ca. 330Ma. A rough estimation of the maximum earthquake magnitude the fault can generate gives $M = 6.5$ with a recurrence time of 1400-3300 years (Feuillet et al, 2004). More precise estimates of earthquakes hazard require to investigate the exact 3D geometry of fault systems in the graben, and to quantify the evolution and propagation of the faults through time.

We newly interpreted seismic reflection profiles in the offshore basin to constrain the geometry, the timing and the evolution of the fault systems in the graben. This study permits to sort out the active faults and to identify several incipient structures. We also identified inactive faults systems and established a relative chronology of the fault propagation. We highlight the total amount of displacement accommodated along the various faults. Onshore our description of the stratigraphic records of the carbonate platform in Marie-Galante and Grande Terre (Guadeloupe) in terms of paleo-environment and paleo-bathymetry reveals the influence the glacio-eustatic variations versus the tectonic contribution. Our study helps to constrain the age of the tectonic inception in the Marie-Galante Basin. Offshore sampling of geological series, due in late 2006 and 2007, will allow us to date the tectonic activity along the faults and, eventually, will lead to a quantification of the deformation and a more precise estimation of earthquakes hazard.

Environment / Climate / Natural Hazard / Simulation

Evaluation of the Tsunami Risk for Guadeloupe (Lesser Antilles)

N. ZAHIBO (1), E. PELINOVSKY (2) and I. NIKOLKINA (3)

(1) Laboratoire de Physique Atmosphérique et Tropicale, Département de Physique, Université Antilles Guyane, Pointe-a-Pitre, France - narcisse.zahibo@univ-ag.fr
(2) Laboratory of Hydrophysics, Institute of Applied Physics, Nizhny Novgorod, Russia Pelinovsky@hydro.appl.sci-nnov.ru
(3) Department of Applied Mathematics, Nizhny Novgorod State Technical University, Nizhny Novgorod, Russia - inikolkina@mail.ru

Abstract

Available data of tsunami manifestation in Guadeloupe (Lesser Antilles) for 500 years is analysed and discussed. Highest values of the tsunami heights have been recorded in the northern Guadeloupe (Basse-Terra Island). Numerical simulation of the wave height distribution along the coast of Guadeloupe is performed in the framework of shallow water theory for several possible locations of the tsunami sources, and also for historic 1867 and 2003 events. Results of the numerical simulations confirm that tsunami waves approached to Guadeloupe have large values in its northern part.

North Atlantic Hurricanes Trajectories; Important Forecast Parameters: a Case Study, 2006 Hurricane Season

G. LEQUELLEC, C. ASSELIN DE BEAUVILLE

Laboratoire L.PA.T/G.EO.L, Université des Antilles et de la Guyane, 97159 Pointe à Pitre Guadeloupe - christian.asselin@univ-ag.fr

Abstract

The poster presented is based on reseach from data of LPAT laboratory collected from 1996 to now. These data include photographies of GOES 12 satellite and A.V.N. model output. A.V.N models maps starts only in 2000. First we define the characteristic of hurricane track in Atlantic Ocean. All the tracks can be represented by three mean groups that is to say, extreme North paths in atlantic ocean, mid North which can reach the U.S coasts and South which can go accross the Lesser antilles Archipelago.

Next we study the influence of lower and higher pressures centers. The major influence of low-pressure center is to attract, while high-pressure systems makes curvatures. Recent cases are showed. Localisation of high-pressure centers are a crucial factor. Their evolution can be linked to N.A.O (North Atlantic Oscillations) as S.O.I. (South Oscillations Index) in Pacific Ocean. N.A.O index is necessary to determine the intensity of winter in Europe. This index associated with S.O.I. index may be useful to try to forecast the crossing of Lesser Antilles Archipelago; if not, the tracks recurve to the North. A data table for the past twenty years is showed. El nino phenomena as a inhibitive role. When la Nina phenomena is present and NA.O. index is negative, this is factor of risk for our Archipelago.
At last we show the predictors for 2006 season. The lack of El Nino can contribute to the crossing of a intense hurricane through or near the Lesser Antilles Archipelago.

Environment / Climate / Natural Hazard / Simulation

A Method of Analysis and Identification of Clouds of Satellite Images Coming from GOES Satellite

J. NAGAU AND J-L HENRY

Laboratoire GRIMAAG , Université des Antilles et de la Guyane, Département Mathématiques et Informatique, B.P. 592, 97159 Pointe-à-Pitre Cedex - jnagau@univ-ag.fr, jlhenry@univ-ag.fr

Keywords
Image analysis, pattern recognition, classifier systems, classification, supervised training, database knowledge.

Abstract

The purpose of our work is to provide physicists and meteorologists with an application capable of determining from satellite pictures taken in the field of visible and infrared lights the types and percentages of clouds present [1] to establish a climatic cartography of the Caribbean area. We take into account three types of clouds : the cirrus situated in the superior layer in approximately six kilometers in height, the cumulus in the lower layer than five hundred kilometers in height and the stratus which can be observed in the intermediate layer in two kilometers in heights. Our method consists by extracting discriminating characteristics of the various types of cloud heaps discovered on the images to make a classification. We carry out a sequence of operations appropriate for the theory of shape recognition [2] which, at first enables to track down the pixels which belong to clouds [3] and then, to extract information from the aggregates of points found. The image taken in the field of visible light enables to know if we are dealing with thick clouds or about thin cloud layers. Indeed, the thin layers of clouds are not detectable in the image taken in the visible light whereas the thick clouds appear clearly. This phenomenon is due to the fact that the very thin layers do not reflect the light. The elements we exploit are : the shapes of the cloudy heaps, the variations of pixels belonging to clouds, the clouds brightness. These values are coded in binary and concatenated with a view to achieving an interpretation from LCS (Learning Classifier Systems) type systems [4]. Every cloud is represented by a binary chain will be associated with one of the three classes. Before becoming autonomous, the system will need a supervised training period to set up its base of knowledge and correct the classification errors [5].

References

[1] Weather satellites: systems, data, and environmental applications, P. Krishna Rao, Susan J. Holmes, Ralph K. Anderson, Jay S. Winston, and Paul E. Lehr, American meteorological society.
[2] Reconnaissance des formes, Méthodes et applications, Abdel et Yolande Belaïd, Inter Editions.
[3] Analyse d'images: filtrage et segmentation, J.P. Cocquerez, S. Philippe, Masson.
[4] Evolution d'entités virtuelles coopératives par système de classifieurs, C. Sanza Thèse de doctorat, Université Paul Sabatier, Toulouse, juin 2001.
[5] Reconnaissance et contexte : une approche coopérative pour la lecture de textes imprimés, J.L. Henry Thèse de doctorat, institut des sciences appliquées de Lyon. Lyon, mars 1996.

Environment / Climate / Natural Hazard / Simulation

Initialization of an Atmospheric Mesoscale Model for the Prediction of the Track and Intensity of Hurricanes

W. SICOT

LPAT, Université des Antilles et de la Guyane, Faculté SEN, Campus de Fouillole, Pointe-à-Pitre, Guadeloupe wsicot@univ-ag.fr

Abstract

A bogus vortex method in order to initialise the Oklahoma University mesoscale model ARPS (Advanced Regional Prediction System) for the prediction of track and intensity of hurricanes on a 24 hours base is presented in this paper. The atmospheric fields issued from the Global Forecasting System (GFS) analysis are used for the model initialization. The approach adopted here consists of modifying the initial GFS pressure analysis field by implementing an axi-symetric pressure distribution. The latter is elaborated by using observed pressure values in the neighbourhood of the eye and the corresponding characteristic cyclonic vortex radii data. The resulting pressure field is used for the ARPS initialization. After a first six hours run (including the model spin-up time), a cyclonic vortex formation is observed. The resulting atmospheric fields are then used in a second run in order to determine the vortex trajectory and corresponding strength during a 24 hour period. In order to test this method, a numerical experiment has been drawn by using the data related to the evolution of hurricane Ivan (2004) from the 07 September 2004 12UTC to 08 September 2004 12 UTC. Starting with an initial minimal pressure equal to 963 hPa, the maximum surface wind value increases up to 185 km/h, thus conferring to the vortex the strength of a category 3 hurricane. The comparison between predicted and observed tracks after a 24 hour simulation leads to an 84 km forecast error. This is roughly 8% lower than the 95 km error associated to the NCEP (National Center for Environmental Prediction) prediction for the same time laps.

Climatology of African Dust using Meteosat IR throughout the Period 1984-1998

M. LEGRAND, O. PANCRATI, N. J. BROOKS AND L. J. SHIPMAN

Michel Legrand and Ovidiu Pancrati (LOA, Université de Lille-1, 59655 Villeneuve d'Ascq cedex, France). legrand@loa.univ-lille1.fr - ovidiu@loa.univ-lille1.fr
J. Brooks and Lisa J. Shipman (CRU, School of Environmental Sciences, University of East Anglia, Norwich NR4 7TJ, U.K.). n.brooks@uea.ac.uk - l.shipman@uea.ac.uk

Abstract

The infrared method enables the monitoring of the desert aerosol plumes over the African continent (and the Middle East), using Meteosat observations of the middle of the day. The method is based on the strong dust forcing in the thermal IR, involving the additive effects of the radiative cooling of the ground surface and of the upward infrared radiance extinction through the dust layer. Remote sensing of dust plumes is achieved through an algorithm operating on the Meteosat IR imagery. As a result, daily images of Infrared Difference Dust Index (IDDI) are obtained. The method is applied to the series of B2-ISCCP-formatted images covering the period 1984-1998. The resulting dataset constitutes the basis of a climatology 15-year long of the Saharan, Sahelian, Somalian, Arabian and South African dust events. Such a climatology consists of monthly means of IDDI (brightness temperature) and monthly frequencies of dust occurrence, computed for 1° square pixels. The dust distribution is observed to obey a marked annual cycle alternating turbid and comparatively cleaner periods. The year-to-year variability as well as the long term trend are analysed. The sources of dust emission are identified and their seasonal cycle of activity is described.

Environment / Climate / Natural Hazard / Simulation

Evaluation of Rainfall Over Guadeloupe by Four Cumulus Parameterization Schemes: Case of the Tropical Depression Jeanne

C. JEAN-CHARLES, ASSELIN DE BEAUVILLE

Université des Antilles et de la Guyane, faculté des sciences, Laboratoire de Physique de l'Atmosphère LPAT-GEOLBP250 - 97157 Pointe-à-Pitre cedex, Guadeloupe - cedric.jean-charles@univ-ag.fr

Abstract

Evaluation of rainfall over Guadeloupe by four cumulus parameterization schemes:
Case of the tropical depression Jeanne.

As it approaches the Lesser Antilles, a tropical wave presents signs of organization. It becomes a tropical depression (n 11) on Monday, September 13, 2004 at the end of the afternoon. The centre of the depression passes over Guadeloupe in the course of the night (minimal atmospheric pressure: 1009.1 hPa at 02. 03 local time). The continuous precipitations increase a lot during the night and storms burst out on the coast down-wind of the island of Basse-Terre. Very important rain intensities are observed in this region.

The frame of this study is the forecast of precipitation in the case of a cyclonic phenomenon, with great potential precipitation, during the warm season. We compare the results of precipitation simulations of this phenomenon obtained by using four different cumulus parameterization schemes in ARPS (Advanced Regional Prevision System), a meso-scale model of atmospheric forecast. The four schemes are: Kuo and Kessler's warm rain microphysics, Kaint and Fritsch's cumulus parameterization, Betts-Miller-Janjic's cumulus parameterization and finally the new Kaint-Fritsch's scheme (1994). The model has a 2 km grid resolution because of the exiguous character of the Guadeloupe archipelago and the variability of the relief. We initialize the model (already containing the vortex that represents the depression) with data from the AVN global file corresponding to September 13, 2004 at 00 hr UT and make 24 hour simulations. The precipitation obtained with the model and its different parameterizations is then compared to the maximum observed values, throughout the island's rain gauge network.

The parameterization of Kuo and Kessler overestimates the quantities of fallen precipitation but represents quite well the major part of the flooded zones. The other parameterizations underestimate the quantities of precipitation, whether it is in the accumulated value or the hourly one, and have trouble in representing effectively the zones of strong precipitation. Our results are in good agreement with Yang and Tung's (2003) results, for whom the Kaint-Fritsch and Betts-Miller schemes gave interesting results for the cold season events but underestimated the precipitation values for the warm season.

Estimation of Downward Longwave Radiation in Guadeloupe

A. FOUERE, R. BONHOMME, F. BUSIERE AND S. DUFOUR-KOWALSKYS

Unité APC, INRA, Domaine Duclos, 97170 Petit-Bourg, Guadeloupe, France
Alain.Fouere@antilles.inra.fr

Abstract

The downward longwave radiation (Rld), thermal infrared radiation emitted by atmospheric constituents is a main component of the radiative budget at the soil surface. The estimation of Rld is required in many domains of human activity like energy management for buildings or natural environment or in climate modelling. An accurate estimate of Rld is particularly required in agronomy and forestry sciences for the estimation of soil and plant canopies temperature and evaporation.

However measurements of Rld are quite rare in temperate countries and nearly inexistent in the humid tropics because of the cost of the sensors and the complex routine operation required by these radiometers.

We measured hourly Rld in Guadeloupe over several months with an Eppley pyrgeometer, a radiative sensor using a KRS 5 filter that is transparent to thermal infrared radiation and was periodically carefully calibrated with a black body emitter

The mean annual downward long wave radiation in Guadeloupe was high in comparison to existing estimates in temperate continental situations (412 ± 19 Wm-2). Such fluxes prevent night radiative cooling and explains the rather high nocturnal minimal temperatures observed in humid tropics. The lowest Rld measured in our conditions were about 350 Wm-2, that corresponded to a 7°C radiative sky temperature. This lowest sky temperature was high when compared to negative sky temperature classically recorded during clear nights in temperate latitudes. The daily and annual variability of our measurements for three years was only 100 Wm-2. This variability was low in comparison with the range 162-250 found in published large data series. These Rld behaviour confirmed the great influence of the constant high water content of the tropical atmosphere.
We then discussed the influences of air temperature and atmospheric vapour pressure in order to propose empirical formulae for tropical Rld estimate.

Early Observations of the Blazar OJ 287: Further Evidence for the Binary Black Hole Model

H. RAMPADARATH (1) , M.J. VALTONEN (2), R. SAUNDERS (1) and H.J. LEHTO (1)

(1) Physics Department, University of the West Indies, St. Augustine Campus, Trinidad
rsaunders@fsa.uwi.tt
(2) Tuorla Observatory, Turku University, Piikkiö, Finland

Abstract

OJ 287 is one of the most active blazars, and with an optical light curve covering over 100 years, it is the most observed. The observations after 1972 are quite dense, from which the optical behaviour is clear, but prior to 1972 data are scarce. These data are of great scientific value, as there are hints for the periodicity in the historical light curve, which could be used to definitely confirm the binary black hole nature of this object. In this study, the optical behaviour of OJ 287 during the years 1957-1965 was analyzed using digitally scanned photographic plates. Given that photographic plates are non-linear detectors, each scanned plate must be individually calibrated. The method of analysis was adapted from Innis et al (2004), in which a transformation equation relating instrumental magnitudes, Mi and B magnitude was derived for each plate. The method employed aperture photometry to obtain Mi, and the singular value decomposition (SVD) least squares method (Press et al 1992) to determine the calibration equations.
The new data collected from the scanned plates, were plotted with the previous data. This time period provides a unique study, since there are three disc crossings very close; 1956, 1959 and 1963, with a tidal outburst in 1960. The results show evidence that a disc impact outburst occurred around 1963.31-1963.41. The results favor the 'active disc' model of Sundelius et al (1997), which predicts the outburst to occur in 1963.21. In this model, the accretion disc of the primary black hole moves to meet the incoming secondary black hole causing the impact to occur earlier, this is shown by the results of this study. The predicted time of the 1963 outburst without the active disc is given by the Lehto and Valtonen (1996) binary black hole model, as 1963.59. The time of the 1963 outburst is approximately 4.1 yrs after the primary impact in 1959.2, the other well observed outbursts' secondary follows within 1-2 years. This result supports the precessing orbit of the binary black hole models of both Lehto and Valtonen (1996) and Sundelius et al (1997).

References

Lehto H.J., and Valtonen M.J. 1996. OJ 287 Outburst Structure and a Binary Black Hole Model. The Astrophysical Journal 460, 207-213
Sundelius B., Wahde M., Lehto H.J., and Valtonen M.J. 1997. A Numerical Simulation of the Brightness Variations of OJ 287. The Astrophysical Journal 484, 180-185
Innis J.L., Borisova A.P., Coates D.W., and Tsvetkov M.K. 2004. Archival lightcurves from the Bamberg Sky Patrol; CF Octantis, 1964 – 76.
Press W.H., Teukolsky S.A., Vetterling W.T., Flannery B.P., 1992 Numerical Recipies in Fortran. Cambridge University Press, Cambridge

Table of contents

Agriculture / Plant Biology

Statistical Study of Spatio-Temporal Evolution of Plant Infection by SCYLV in a Disease Free Plot 123
O. Jacquet, C. Edon, J. Vaillant and J.H. Daugrois

Tentative Estimates of Carbon Storage Ability Within Coastal Forested Wetlands in The Caribbean 125
J.M. Flower

Evaluation of a Direct Field Method of Soil Salinity Appraisal 127
G. Eudoxie

Paddy Cultivation in Sodic Soil through Vermitech 131
A. A. Ansari

Soil Texture and Organic Matter Effects on Structural Stability, Infiltration, Runoff and Seal Formation 134
M.N. Wuddivira, R.J. Stone and E.I. Ekwue

Effects Of *Musa x paradisiaca* Plant Extracts on the Digestive Parasitic Nematode *Haemonchus contortus* in the French West Indies 136
C. Marie-Magdeleine, M. Mahieu, H. Hoste and H. Archimède

The Ectomycorrhizal Fungus *Scleroderma bermudense* Improves Water Status and Limits Sodium and Chloride in Seagrape (*Coccoloba uvifera* L.) Seedlings 138
E. Bandou, F. Lebailly, F. Muller, M. Dulormne, A. Toribio, J. Chabrol, R. Courtecuisse, Y. Prin, B. Dreyfus and A. Bâ

Leaf Allometry in Long and Short Shoots of *Betula papyrifera* 138
J. C. Caesar

Biodiversity in Rain Forests of the Lesser Antilles 139
E. Ingadassamy and A. Rousteau

Agriculture / Plant Biology

Statistical study of spatio-temporal evolution of plant infection by SCYLV in a disease free plot

OLIVIER JACQUET[1], CARINE EDON[1, 2] JEAN VAILLANT[1], AND JEAN HEINRICH DAUGROIS[2]

[1]*GRIMAAG, UFR SEN, Université des Antilles et de la Guyane, 97159 Pointe-à-Pitre*
[2]*CIRAD-CA, Station de Roujol, 97170 Petit Bourg, Guadeloupe, French West Indies*
olivier.jacquet@univ-ag.fr, carine.edon@cirad.fr, jean.vaillant@univ-ag.fr, jean-heinrich.daugrois@cirad.fr

Abstract

In the framework of studying the evolution of infection by SCYLV (Sugarcane Yellow Leaf Virus) in the caribbean islands, we used a spatio-temporal model. This model was based on conditional intensities to investigate the infection evolution with respect to environmental heterogeneity. Since alate aphids may prefer some areas in a culture plot rather than others in relation with the variability in plant growth, wind direction, tree-shaded areas, primary and secondary infections were taken into account as in Gottwald *et al,* (1999). Different conditional intensities were considered and simulations were carried out with gradient effects.

Introduction

Statistical studies of spatio-temporal spread of viral diseases often require spatial and temporal modeling (Zhang *et al*., 2000). This is the case of plant viruses because most of them are transmitted by vectors. Thus, for investigating the evolution of infection by SCYLV in sugarcane fields, we used a spatio-temporal model based on conditional intensities. Since alate aphids may prefer some areas in a culture plot rather than others in relation with the variability in plant growth, wind direction, tree-shaded areas, primary and secondary infections were taken into account as in Gottwald *et al.* (1999). Different conditional intensities were considered and simulations were carried out. R packages for spatial dependence were also used to process the observed data.

Materials and methods

Sampling: several observations were carried out in Guadeloupe in 2004. A sugarcane trial (17 rows of 55m each) was established with 1,745 disease-free plants of cultivar SP71-6163. The number of SCYLV-infected plants was monitored on the whole plot, on weeks 6, 10, 14, 19 and 23 after transferring plants to the field, by tissue blot immunoassay (TBIA). Colonization of disease-free plants by aphid vector was monitored in plant cane and aphid population structure was estimated from 40 random identified plants on plant crop.

Statistical methods: We carried out Monte Carlo statistical tests based on the variance-mean ratio at several spatial scales of the observed plot. Similarly, we tested spatial autocorrelation at several scales based on Moran index (Celini and Vaillant, 1999) with neighbor-hood defined from a given distance between plants.

Stochastic modeling: the proposed model is such that during a first phase infections occur independently of each other. Then, there are local transmissions by apterous aphids which could move from one plant to another at a certain phenological stage of the sugarcane plants. The conditional intensity of infection at date t on plant x is denoted by $\lambda(x,t)$ and is such that $\lambda(x,t)dt$ is the probability that plant x is infected between dates t and $t+dt$.

For a non infected plant x at date t, we wrote:

$$\lambda(x,t) = (a + I(t)\sum \exp(-b.d(x,x_t)).h(t)$$

where a is the background infection parameter, b is the local interaction parameter, $I(t) = 0$ if date t belongs to the first phenological stage, $I(t) = 1$ if not.
$h(t)$ is the infective capacity at date t, $d(x,x_k)$ is the distance between plants x and x_k. $\sum$ indicates the sum over the whole set of infected plants x_k prior to date t.

Results and Discussion

We calculated the dispersion and Moran indexes for the number of SCYLV infected plants per quadrat. Different quadrat sizes were considered for each observation periods. The associated p-values clearly indicate that significant aggregation appears only from week 19. The hypothesis of completely random infection locations is rejected from week 19. Tables 1 and 2 show the results obtained for the smallest quadrat size (3m x 3m) considered in the analysis. After week 14, there exists a mechanism of local infection spread from infected plants to virus-free plants due to possibility for the infected apterous aphids to move easier from one plant to another. This was confirmed by calculating frequencies of infected nearest neighbors for both virus-free and infected plants (Fig. 1).

Week 14		Week 19		Week 23	
DI	P	DI	P	DI	P
1.155	0.111	1.152	0.115	1.281	0.018

Table 1. *Dispersion index (DI) and its p-value (P) for some observation dates.*

Week 14		Week 19		Week 23	
MI	P	MI	P	MI	P
0.040	0.153	0.169	0.001	0.198	0.000

Table 2. *Spatial Moran index (MI) and its p-value (P) for some observation dates.*

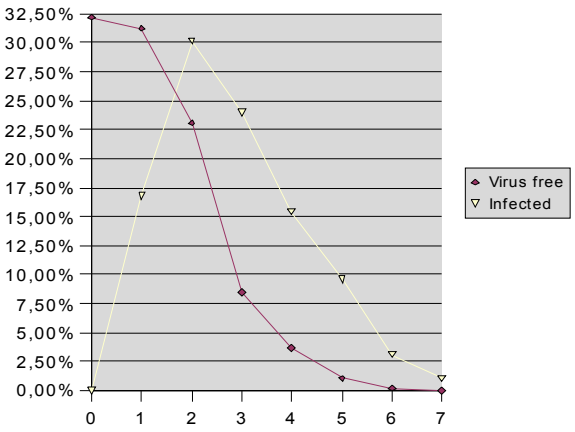

Figure 1. *Distribution of number of infected or non infected neighbors inside a circle of radius 1.5 m.*

The second phase of the stochastic model is described in figure. 2.

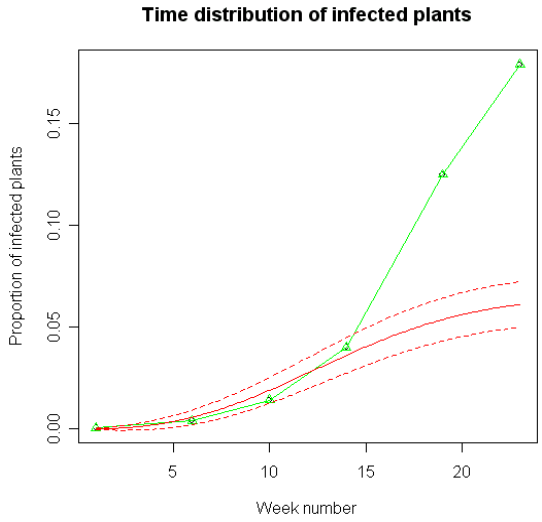

Figure 2. *Time distribution of infected plants. The green line corresponds to the observed proportions. The red lines correspond to the expected proportion in absence of spatio-temporal structure.*

Before week 14, the proportion of infected plants is inside the 95% confidence interval whereas after week 14, this proportion is much higher than the expected value under the hypothesis of completely random distribution of infections.

Conclusion

The early phenological stage of sugar cane fields corresponds to arrivals of alate aphids on the plot and first generations of apterous aphids. The statistical tests of dispersion and spatial structure are not significant before week 14. This suggests that SCYLV infections are completely randomly distributed due to non capacity of apterous aphids to move from one plant to another. From week 14, this moving is possible and local transmissions occur. This explains the significant overdispersion and aggregation observed at weeks 19 and 23.

References:

Celini L. and Vaillant J. (1999). *Répartition spatio-temporelle des presences d'ailés d'Aphis Gossipii (Hemiptera, Aphididae) en culture cotonnière.* Can. Entomol., 131, 813-824.

Gottwald T.R., Gibson G.J., Garnsey S.M., and Irey M. (1999). *Examination of the effect of Aphid vector population composition on the spatial dynamics of Citrus Tristeza Virus spread by stochastic modeling*. Phytopatology, 89, 603-608.

Zhang X.-S., Holt J., and Colvin J. (2000). *A general model of plant-virus disease infection incorporating vector aggregation.* Plant Pathology, 49, 435-444.

Agriculture / Plant Biology

Tentative Estimates Of Carbon Storage Ability Within Coastal Forested Wetlands In The Caribbean

JEAN-MARIE FLOWER

DACRYODES Environment, rés. L'Habitation, Apt D 525, Blachon, 97129 Lamentin, Guadeloupe
jean-marie.flower@wanadoo.fr

Abstract

Since the beginning of Holocene, relative sea level variations along caribbean coasts have significantly impacted coastal wetland ecosystems at various spatio-temporal scales, either in terms of structure, functioning, dynamics, or evolution.

Several soil core samples (Martinique, Guadeloupe, Saint-Martin, Haïti) were studied and analyzed in order to reconstruct the main steps which led to the current organisation of forested coastal wetlands within the Caribbean region, and to assess the amount of carbon stored in their soils.

In the years or decades to come, several indicators (temperatures, rainfall variability, frequency and intensity of hurricanes…) might confirm a sharp shift of the disturbance regime to which some coastal forested wetlands would be especially sensitive because of the celerity of the processes involved. Nevertheless, it seems likely that the overall "carbon sink" function could hardly be outweighted.

Introduction

Since the beginning of Holocene, relative sea level variations along caribbean coasts have significantly impacted coastal wetland ecosystems, in terms of structure, functioning, dynamics, and evolution.

Evidences of these changes have been progressively included within the peculiar organo-minéral sediments of these ecotone environments which contain most of their carbon stock.

In this study, we combine the use of field data with interpretation of previous multidisciplinary literature data to evaluate to what extent caribbean mangroves and their associated wetlands can act as net "carbon sinks".

Materials & Methods

Several soil core samples (Martinique, Guadeloupe, Saint-Martin, Haïti) were drilled until the bottom of the soil's organic layer, using a 10 cm-diameter Edelman auger. They were compared and interpreted in order to reconstruct the main steps which led to the current organisation of forested coastal wetlands within the Caribbean region.

These soil samples were also used to assess their amount of carbon stored in caribbean coastal wetlands. They were classified within 3 classes of organic richness (0-33%, 33-67% and 67-100%) which accounted for 3 distinct water contents (respectively 80%, 250% and 500% of dry weight). Then, their estimated carbon stock was computed assuming that most organic compounds were cellulose and lignin.

Estimates of past and current sea-level rise drawn from photointerpretation and vegetation inventories [1,2] allowed us to propose a range of possible future carbon storage by coastal caribbean wetlands for the next few decades.

Results & Discussion

The core samples ranged from 0.8m to 7.0m in depth, averaging 3.0m (n = 63). Irrespective of their location (Guadeloupe, n=50; Martinique, n=8; Haïti, n=3; Saint-Martin, n=2), they had a very similar structure showing a clayey / muddy base underlying an organo-mineral layer itself topped by a typical highly organic mangrove peat.

On average, each core had a dry weight of 130g which contained 60g of organic matter, accounting for 24g of carbon. These estimates lead to an amount of 305 t C/ha within caribbean coastal wetlands.

Radiocarbon datings performed on control core samples (Guadeloupe and Saint-Martin) showed that the lower mangrove sediments were approximately 3,000 yrs old [3,4]. Therefore, the swamps have stored a little more than 100 kg C / ha per year up to now.

Based on photo-interpretation spanning the last 50 years, the landward shift of the inner mangrove border has ranged from 100 to 300m, which indicates a relative sea-level rise of between 5 and 15cm since 1950. Meanwhile, the

marine border has been quite steady, accounting for the rather good mangrove adaptability to this rise. However, recent satellite estimates of sea-level rise during the last decade [5] seem to show an additional increase in the speed of the rise that challenges mangrove's ability to cope with such a rise.

Thus, caribbean coastal wetlands may be able to store at least 200kg C/ha/yr in the next decades. Given that methane emissions from wetlands are about 2 orders of magnitude lower than C uptake, it seems that mangroves will still remain "carbon sinks" for a while.

During the last five centuries, regional changes resulting from growing human impacts upon native ecosystems have been superimposed to these sea-level driven landscape evolutions that had occurred up to then and had resulted in net below-ground accumulation of carbon.

However, recent and current vegetation dynamics, assessed either through successional photo-interpretation or forest inventories, seems to reveal a dramatic increase of both pace and magnitude of environmental changes related to the rise of sea-level, that might locally modify carbon cycle patterns both qualitatively and quantitatively.

Although it is still to be confirmed at a wider scale, this acceleration remains comparable with other recent environmental shifts, either within or outside the intertropical zone. Moreover, the changes that have occurred throughout the last decades are remarkably consistent with numerous expected consequences related to the regional impacts of Climate Change, most probably driven by excessive greenhouse gas emissions from the consumption of fossil energy resources.

In the years or decades to come, several climate indicators (temperatures, rainfall variability, frequency and intensity of hurricanes…) might confirm a sharp shift of the disturbance regime to which some coastal forested wetlands would be especially sensitive because of the celerity of the processes involved [6]. Nevertheless, it seems likely that the overall "carbon sink" function could hardly be outweighted.

As it seems unlikely that we achieve to limit the worsening of the disturbance applied to the climatic system by a significant, long-term downturn of our energy consumption, it appears more and more useful, and even vital for us to be efficiently prepared to cope with the consequences of the climate's increasing instability [7]. In that perspective, preservation and restoration of coastal forested wetlands [8] are precious allies, and even unbeatable in terms of ratio quality / price, for us as well as for them.

Acknowledgements

A part of this research was financed by the French Ministry of Education, Research and Technology. I would like to thank Dr Daniel Imbert, Senior Lecturer at the University of French West Indies and French Guiana, for his invaluable help throughout many key aspects of this study.

References:

1. FLOWER, J.-M., Structure et dynamique de la mangrove dans la baie du Grand Cul-de-sac Marin (Guadeloupe, FWI) : Impact des cyclones sur l'évolution du milieu. Mémoire de DESU, UPS, Toulouse III, France. pp.50 (in french) (1997)
2. FLOWER, J.-M., Dynamique de la végétation dans la mangrove en Guadeloupe : Etude des cas de dépérissement massif et durable, Mémoire de DEA, Université des Antilles et de la Guyane, Pointe-à-Pitre, Guadeloupe. pp.51 (in french). (1999)
3. FELLER, C., M. FOURNIER, D. IMBERT, C. CARATINI, and L. MARTIN. Datations 14C et palynologie d'un sédiment tourbeux continu (0-7m) dans la mangrove de Guadeloupe (FWI) ; résultats préliminaires. Colloques et Séminaires ORSTOM: 193-202. (1992)
4. DELSANTI, F. Reconstitution des paléofaciès d'une mangrove de Guadeloupe grâce à l'étude comparative de différents descripteurs issus du sol. Mémoire de DESS. Pointe-à-Pitre, Université Pascal Paoli - Université des Antilles et de la Guyane. pp.51. (in french) (1999)
5. LOMBARD A., C. CABANES, A. CAZENAVE and F. REMY. 2,8 mm par an. Les Dossiers de La Recherche 17: 46-51 (in french) (2004)
6. FLOWER J.-M. and D. IMBERT. Recovery failure following massive tree mortality in mangroves of Caribbean islands: general assessment and classification. Wetl. Ecol. Manag. (2005, in press).
7. FLOWER J.-M. Dérèglements durables de la dynamique de la végétation dans les mangroves des Petites Antilles: problèmes de régénération forestière après mortalité massive liée à des perturbations naturelles. PhD thesis, Université des Antilles et de la Guyane, Pointe-à-Pitre, Guadeloupe. pp.209 (in french).
8. FLOWER J.-M. Semis expérimentaux dans deux sites de mangrove dépérissante : intérêt pour les aires protégées de Guadeloupe. Revue d'Ecologie (la Terre et la Vie) 59: 171-180 (in french) (2004).

Agriculture / Plant Biology

Evaluation of a Direct Field Method of Soil Salinity Appraisal

EUDOXIE, G.D. AND CARTER, N

Faculty of Science and Agriculture, University of the West Indies, St. Augustine Campus, Trinidad - geudoxie@fsa.uwi.tt

Abstract

Soil salinity strongly influences land productivity and its assessment is a routine practice for land evaluation. Traditional techniques to characterize salinity employed very dilute soil to water suspensions (1: 5). These suspensions do not simulate typical soil conditions and as such leads to erroneous data. Two methods, varying widely in approach were used to characterize salinity in a range of Trinidadian soils, with the intention of evaluating data accuracy. Both the field technique and the saturated paste extract resulted in electrical conductivities greater than the 1: 5 ratio. This resulted in variations in the classification of soils among the three methods. Although significant correlations existed among the methods the correlation coefficient was strongest between the field technique and the saturated paste. A strong significant relationship was observed between the saturated paste and the 1: 5 ratio, which allows for conversions of older reported salinity indicators and their use in land appraisal.

Introduction

Land evaluation provides the basis for planning and decision making leading to appropriate land management and use. Physical assessment of soil attributes represents an integral aspect of this process. Salinity assessment bears significance as it indicates the influence of ions in solution on soil and vegetative degradation with concomitant contamination of water sources (Dasberg and Nadler, 1988).

Regionally, salinity is associated with poor irrigation practices, salt water intrusion, effluent discharge from petroleum production and natural earth phenomenon (mud volcanoes). Shaw (1982) examined the dependency of soil salinization on the quality of the irrigation water for two southern coastal soils in Jamaica. Salt water intrusion and possible sea blast are chiefly responsible for salinity of coastal, swamp land soils through out the region (Brown and Bally, 1966). Impending sea level rise associated with global climate change seeks only to aggravate this situation (Trotz et al., 2001). Petroleum based produced waters (containing brine) will often cause "salt-scars" or areas of high salinity leading to degradation of soil structure and alteration of the osmotic gradient between plant roots and the soil (Holliday and Deuel, 1997). Land based oil exploration has been on the increase in Trinidad, which intensifies the need to assess and monitor salinity. Environmental regulations in Trinidad (WPR, 2000) do not include electrical conductivity (EC) or other indicator analyte for salinity, which indicates a lack of awareness and the need for correction.

Indicators of salinity in Trinidad were described by Brown and Bally (1966). Electrical conductivity was measured as part of the detailed soil survey using an extraction method, with a large soil to water ratio (1: 5). Dasberg and Nadler (1988) and Zhang et al. (2005) have shown this method to deviate from conditions normally present in the soil, but offer the user ease of determination. The preferred method adopted by the US salinity Laboratory (1954) uses a saturated extract and strongly represents the actual soil solution (Zhang et al., 2005). Because soil assessments and/or remediation recommendations are based on soil salt concentrations, soil salinity testing methods must be capable of providing accurate and precise results in a timely manner. The advent of electrical methods now allows for direct "in situ" soil measurements of EC.

The objectives of this study were to (i) validate the use of a salinity sensor (1401 EC-probe) over a range of Trinidad soils and (ii) to develop empirical relationships between EC determined by saturated extract and a 1: 5 soil: water suspension.

Materials and Methods

Soil samples were collected to provide a wide range of salinity levels based on previous work (Brown and Bally, 1966). Samples were taken at 0 - 25 cm and 50 - 75 cm depths, air-dried and ground to pass a 2 mm sieve prior to analysis.

Soil salinity was determined by the saturated paste extract method (Rhoades, 1996) and by the 1: 5 (soil: H_2O) method. For the 1: 5 methods the samples were stirred with a spatula for 1h and extracts were obtained by gravity filtration. Electrical conductivity of the saturated paste extract along with the 1: 5 extract was measured with dip-type conductivity cell. The concentration of Na+ in the extracts was determined using flame photometry. pH was measured in a 1:2.5 (soil/H_2O) suspension with a glass electrode. Cation exchange capacity (CEC) was determined using the unbuffered salt extraction method (Sumner and Miller, 1996). Direct measurement of apparent electrical conductivity (ECa) was determined using a four electrode probe (1401 EC-Probe, manufacturer) in the field at the two depth following methods described by Rhoades and Ingvalson (1971) and Nadler and Frenkel (1980).

Descriptive statistics were used to estimate precision, whilst comparisons of methods gave indications of accuracy. Correlation and regression analysis was used to determine the influence of other parameters on soil EC and the significance of the relationship between saturated extracts and soil water suspensions.

Results and Discussion

Brady and Weil (2006) and Shaninberg and Levy (2005) characterize salt affected soils based on pH, EC and Na content expressed as either Exchangeable Sodium Percentage (ESP) or Sodium Absorption Ratio (SAR). From the data presented in Table 1, all soils except Frederick and Piparo belonged to the category of normal soils. Frederick was categorized as a saline-sodic soil based on EC values from both the saturated paste and probe methods. Piparo was classed as a sodic soil. Using the suspension (1: 5 soil-water) extraction resulted in both soils being grouped as sodic soils. This indicates limitations in accuracy resulting from this procedure. Brown and Bally (1966) characterized soils throughout the Caribbean (English speaking) using this methodology, grossing underestimating true EC (Dasberg and Nadler, 1988) and in some cases falsely categorization. Based on their characterization Frederick clay (4000 ac) is characterized as a normal soil. Geomorphology provides an explanation for these two soils inherent salt affliction.

Soil	Lithology†	pH	EC			Na	CEC	ESP‡
			Paste	1: 5	Probe			
			dS m^{-1}			cmol kg^{-1}		%
Cacandee	Typic Pelluderts	4.05	0.26	0.10	0.39	0.65	18.28	3.56
Montserrat	Typic Tropudolls	5.9	0.21	0.08	0.67	0.59	35.97	1.64
Frederick	Vertic Tropaquolls	5.87	9.1	3.64	7.29	7.83	21.9	35.8
Piparo	Vertis Eutropets	9.35	2.82	1.09	2.59	3.91	4.57	85.6
Godineau	Thapto-Histic Sulfic Tropic Fluvaquents	4.01	0.32	0.13	0.58	0.72	41.15	1.75
River Estate	Fluventic Eutropepts	5.63	0.14	0.10	0.12	0.46	12.95	3.56
St.Augustine	Orthoxic Tropudults	5.27	0.28	0.07	0.08	0.72	8.89	8.10

† *Lithology extracted from Smith (1983)* ‡ *ESP calculated as Na/CEC * 100*

Table 1 Lithology, pH, EC and ESP for test soils at 0 - 25 cm

Frederick soil occurs below sea level, bordering the Caroni Swamp and is seasonally inundated with brackish water. Land use changes through development have resulted in contamination further inland. The Cacandee series which borders the Frederick series, but at a slightly higher elevation (Brown and Bally, 1966) was tested to determine the extent of exposure. Results indicate that this series has not been significantly influenced by salt water intrusion. Contrastingly, Piparo soil is associated with mud volcanoes (GSTT, 2007) which periodically erupt and deposit parent material (clay shale) rich in Na and other metals. The high pH (> 9) indicates the presence of Na which is associated with strongly alkaline soil conditions.

EC values determined by saturated extract ranged from 0.14 - 9.1 dS m^{-1}. The corresponding values for the 1: 5 extracts were proportionally lower in all instances, indicating a dilution effect with increased water content (Zhang et al., 2005). Electrical conductivity of saturation paste (EC_{SP}) was highly correlated with $EC_{1:5}$ for all the study soils ($r^2 = 0.99$, $P < 0.001$) (Fig. 1). The results of this study were similar to those of reported by other researchers (Zhang et al., 2005, Shirokova et al., 2000) who also found significant relationships between these variables. The slope of the relationship (3.03) is similar to that reported by Franzen (2003) but differs from that reported by Zhang (2005). Linear regression allows for accurate estimation of EC_{SP} from suspension extractions. This is favourable since the $EC_{1:5}$ or $EC_{1:1}$ provides a more efficient methodology with greater throughput. Secondly, data already present in reports and other publications where EC_{SP} was use can be mathematically converted to better represent soil conditions.

Apparent EC (EC_a) measured "in situ" showed similar variations among the soils (Table 1), but trends were different from laboratory methods. Values ranges from 0.08 dS m^{-1} for St.Augustine to 7.29 dS m^{-1} for Frederick. The significance of these differences was minor, as it did not affect soil characterization. A very strong correlation ($r^2 = 0.99$, $P < 0.001$) was also observed between the EC_a and EC_{SP} among test soils (Fig. 2). This data confirms the use direct EC measuring devices in providing accurate salinity data. Corwin and Lesch (2005) indicated that this technique is well suited for field scale application due to the ability of large volumes of measurement, which reduces local-scale variability.

However, they caution its use in soils where probe contact may be hindered.

Sodium concentrations and its derivative ESP were low (< 1 cmol kg^{-1}) for all soils except Frederick and Piparo, the latter soil

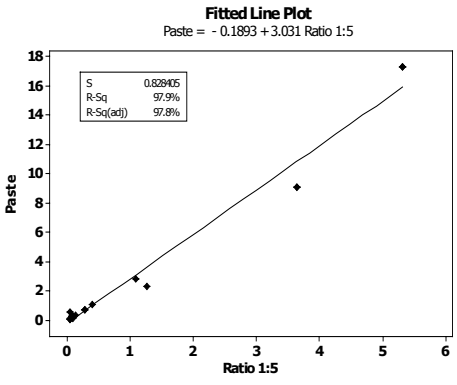

Figure 1. Relationship between electrical conductivity (EC) of saturated paste and 1: 5 soil/water extracts for 14 study soils. P < 0.001.

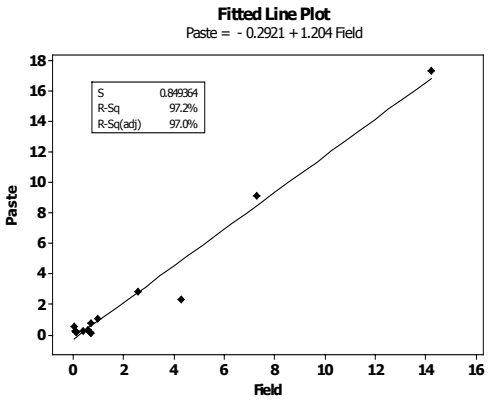

Figure 2. Relationship between electrical conductivity (EC) of saturated paste and apparent EC for 14 study soils. P < 0.001.

showing sodic properties. Exchangeable sodium percentage showed strong correlations with pH supporting the relationship between Na and alkalinity.

Trends among all variables were similar for samples at 50 - 75 cm (Table 2). pH decreased for all acidic soils except River Estate, whilst it increased for Piparo indicating increased Na and parent material with depth. Saturated paste EC increased with depth, doubling for Frederick, alluding to possible leaching of soluble ions to lower depth during periods of flooding. Although Na concentration increased with depth, especially for the salt-affected soils, this did not result in an increase in ESP as the CEC increased correspondingly.

Soil	pH	EC			Na	CEC	ESP
		Paste	1: 5	Probe			
		dS m^{-1}			cmol kg^{-1}		%
Cacandee	3.92	0.75	0.28	0.71	0.91	29.0	3.14
Montserrat	5.4	0.09	0.04	0.70	1.04	40.7	2.56
Frederick	3.77	17.3	5.32	14.2	11.09	36.0	30.8
Piparo	9.68	2.32	1.27	4.30	4.43	12.2	36.3
Godineau	3.69	1.09	0.40	0.98	0.72	42.7	1.69
River Estate	6.13	0.16	0.05	0.13	0.46	11.0	4.21
St.Augustine	4.9	0.57	0.04	0.04	0.52	25.4	2.05

Table 2 pH, EC and ESP for test soils at 50 - 75 cm

Conclusion

It is possible to achieve a satisfactory degree of precision and accuracy from utilizing field based methods of salinity assessment, namely EC_a. For large scale characterization studies this option offers many advantages, primarily taking account of present field conditions. Mathematically relationships established between $EC_{1:5}$ and EC_{SP} allow for conversion of older literature to be precisely describe soil salinity. Although the relationships established by this study was done on varied soil conditions, derived equations should be used with caution and appropriateness for local conditions evaluated.

References

Brown C B, and Bally G S (1966). Land Capability Survey of Trinidad and Tobago, No. 3. Port-of-Spain, Government Printery, Trinidad

Corwin D L, and Lesch S M (2005). Apparent soil electrical conductivity measurement in agriculture. Computers and Electronica in Agriculture 46, 11-43.

Dasberg S, and Nadler A (1988). Soil salinity measurements. Soil Use and Management, 4 (4) 127-133.

Franzen, D (2003). Managing saline soils in North Dakoda. Available online at http://www.ext.nodak.edu/extpubs/plantsci/soilfert/sf1087-1.htm.

Geologic Society of Trinidad and Tobago (2006). Mud volcanoes. Available online at http://www.gstt.org/teaching/mud%20volcanoes.htm.

Holiday G, and Deuel Jr. L E (1997) Soil Remediation for the Petroeum Extraction Industry. 2nd ed. PennWell Publishing Co., Tulsa, OK.

Nadler A, and Frenkel H (1980). Determining of soil solution electrical conductivity from bulk soil electrical conductivity measurements by the four-electrode measurements. Soil Sci. Soc. Am. J. 44 , 1216-1221.

Rhoades, J D (1996). Salinity: Electrical Conductivity and Total Dissolved Solids. In *Methods of Soil Analysis. Part 3. Chemical Methods,* Sparks D L, Ed. SSSA, ASA: Madison, WI, pp. 417-437.

Shainberg I, and Levy G J (2005). Salination Process. In: *Encyclopedia of Soil Science*, Lal R, Ed. Elsevier Ltd. Pp. 429-435.

Shaw M E A (1982). Aspects of the management of salinity on swelling clay soil in Jamaica. Trop. Agric. (Trinidad), 59 (2) 167-172.

Shirokova Y, Forkutsa I, and Sharafutdinova N (2000). Use of electrical conductivity insteat of soluble slats for soil salinity monitoring in Central Asia. Irrig. Drain. Syst. 14, 199-205.

Sumner M E, and Miller, W P (1996). Cation Exchange Capacity and Exchange Coefficients. In *Methods of Soil Analysis. Part 3. Chemical Methods,* Sparks D L, Ed. SSSA, ASA: Madison, WI, pp. 1185-1200.

Trotz U, Trotman A, and Narayan K (2001). Climate change impacts on Agriculture, Water Resources and Coastal Environments in the Caribbean. In: *Land and Water Resources of the Caribbean*, Paul C L and Opadeyi J, Eds. CARDI, CTA, Wageningen, The Netherlands, pp. 73-108.

U.S. Salinity Laboratory Staff, (1954). U.S.D.A. Handbook 60 - Diagnosis and Improvement of Saline and Alkali Soils. U.S. Government Printing Office, Washington, DC.

The Environmental Management Act, (2000). The Water Pollution Rules, (2001). Available online at http://faolex.fao.org/docs/pdf/tri36380.pdf.

Zhang H, Schroder J L, Pitman J J, Wang J J, and Payton M E (2005). Soil salinity using saturated paste and 1: 1 soil to water extracts. Soil Sci. Sci. Am. J. 69, 1146-1151.

Paddy cultivation in Sodic Soil through Vermitech

Abdullah ADIL ANSARI

Department of Biology, Faculty of Natural Sciences, University of Guyana, Turkeyen campus, Georgetown, Guyana, South America, Tel: 592-2266576, 592-6284007 - ansari_adil@hotmail.com
Department of Biology, Faculty of Natural Sciences, University of Guyana, Turkeyen campus, Georgetown, Guyana, South America, Tel: 592-2266576, 592-6284007 - ansari_adil@hotmail.com

Introduction

Soils in India are affected by problems like salinity, alkalinity (sodicity) and water logging. Alkaline or sodic soil predominates in the northern plains of India characterised by pH greater than 8.5 and higher quantity of active sodium. Such soils have been deterred by human interference by way of inappropriate tillage and cropping practices, improper fertiliser application and water management. It is therefore necessary to use suitable organic amendments for proper soil management.

There are a number of organic amendments like bio-solids, straw, sawdust, manures including farm yard manure (FYM) and crop residues which have been used for bio-remediation of sodic soil but the most important among them is the compost. Addition of compost to soil results in the improvement of physical, chemical and biological characteristics of soil with increased crop production (Pera *et al.,* 1983).Vermicompost has been found to have a favourable influence on yield parameters of paddy, sugarcane and vegetables like, tomato, brinjal and okra (Ismail, 1997).

Material and Methods

Experiments have been conducted at the Shivri farm of Uttar Pradesh Bhumi Sudhar Nigam, Lucknow during the kharif season (1998-99), to assess the impact of organic amendment i.e, vermicompost compared to chemical fertilisers on paddy (variety-*Sarju*-52) in relation to sodic soil bio-remediation, fertility, plant growth, yield parameters and economics.

Plots each 250m^2 (20m x 12.5m) were marked for trial (in triplicate), during 1998 (Kharif) at the Shivri farm of the Uttar Pradesh Bhumi Sudhar Nigam, Lucknow.

Composite soil samples were taken from the trial plots at pre-transplanting and post-harvesting stage and were subjected to chemical analysis [pH, electrical conductivity, organic matter, organic carbon and available nitrogen available phosphorus, available potassium, sodium and calcium ions and exchangeable sodium percentage (ESP)].

Plot-A was amended using vermicompost and vermiwash produced at Shivri farm of UPBSN, Lucknow, using Vermitech (Ismail, 1993).Vermicompost and vermiwash used for the experiments, were analysed for the nutrient quality (pH, EC, organic carbon, total nitrogen, total phosphorus, total potassium, ferrous ions, zinc ions, copper ions). Plot-B was amended with chemical fertilisers according to standard recommendations prevalent there. Paddy (*Sarju*-52) was transplanted in experimental plots A and B in July 1998 in Randomised Block Design (RBD) with sub-plot size of 250m^2.

Following crop data were recorded after 95 days of transplanting, before harvest: plant height (cm), number of tillers, number of panicles per hill, length of panicle (cm).

On harvest of crop, after 100 days, the following data were recorded: total yield (kg/ha), grain yield (kg/ha), weight of 1000 grains (grams).

Results

It is evident that there is an increase in organic matter content from 0.38 to 0.96 %, organic carbon from 0.22 to 0.96 %, available nitrogen from 499.52 to 1245.44 kg/ha, carbonate ions from 0.20 to 0.23 meq/100 g of soil, calcium ions from 0.89 to 1.09 meq/100 g of soil and decrease in pH from 8.74 to 8.25, EC from 0.86 to 0.69 dSm^{-1}, sodium ions from 1.85 to 1.47 meq/100 g of soil and ESP from 67.51 to 57.42, suggesting bio-remediation and qualitative improvement of sodic soil, in plot-A, amended with vermicompost. There is reduction in pH by 5.61% and ESP by 14.95% in plot-A (vermicompost) while in plot-B (chemical) on the contrary there is an increase by 0.81% and 2.75% respectively. Organic carbon and available nitrogen increased by 154.55% and 149.33% in plot-A while in plot-B it was reduced by 40.74% and 41.82%.

The nutrient composition of vermicompost in comparison to FYM showed moderate percentage increase of organic carbon and nitrogen confirming a better C: N ratio of 16.35.

Vermicompost has been found to have profound effect on plant parameters like height, number of tillers, panicles per hill, grain weight, total yield and grain yield in comparison to chemical fertilisers .

Paddy yield of 4975 kg per hectare was recorded from plot-A amended with vermincompost and 4900 kg per hectare from plot-B amended with chemical fertilisers. Weight of grains from plot-A (vermincompost) compared to plot-B (chemical), suggested, better quality, in case of paddy grown through Vermitech.

Total cost of cultivation of paddy per hectare through conventional farming applying chemical fertilisers and pesticides was Rs 16,900, while the cost of cultivation of paddy through vermitech was Rs 18,100.

Net income per hectare from
plot-A (vermicompost) = Rs 4492.50
plot-B (chemical) = Rs 2970.00

Cost benefit ratio for
plot-A = 1: 1.30
Plot-B = 1: 1.16

Economics of paddy cultivation suggest that practising organic cultivation through vermitech could reduce the cost of production.

Discussion

The high organic matter content of vermin-compost (19.3%) promotes humification, increased microbial activity and enzyme production, which in turn increases aggregate stability of soil particles, resulting in better aeration (Haynes and Swift, 1990; Perucci, 1990).

Increase in soil nitrogen after harvest from plot-A (vermicompost) is likely to be due to an increase in the presence of nitrogen-fixing microbes through application of compost. Reduction in pH and increase in humus content of the sodic soils are observed due to the production of humic acid during decomposition thereby, reducing soil alkalinity in terms of pH, as also observed by Patcharapreecha *et al.,* (1990). The effectiveness of compost in sodic soil is due to the production of carbondioxide, humic acid, drop in redox potential and replacement of exchangeable Na^{+} ions by Ca^{+2} ions leaching out of the root zone, thus reducing the ESP (Dagar, 1995).

The higher yield, reduced cost of cultivation, less cost benefit ratio and higher net income from paddy cultivation through vermitech compared to the use of chemical fertilisers correlates with the earlier works on economics of crops by organic methods (Ismail, 1997).

Conclusion

Organic amendments like vermicompost facilitates humus formation and prevents leaching of nutrients from the soil by their slow release compared to the conventional farming by the use of chemical fertilisers (Thampan, 1995; Kale, 1996). Considering all the aspects such as soil studies, production and cost effectiveness, from the above investigations, vermitech could be applied in farming practices for sustainable bio-remediation of sodic soil.

Acknowledgement

Authors duly acknowledge the facilities provided by UPBSN, Lucknow and The New College, Chennai.

References

Dagar, J. C., 1995. 0rganic amendments in the reclamation and management of problem soils. In: Thampan, P. K. (Eds.), Organic agriculture, Peekay Tree Crops Development Foundation, Cochin. pp. 145-171.

Haynes, R. J., Swift, R. S., 1990. Stability of soil aggregates in relation to organic constituents and soil water content. J. Soil Sci. 41, 73.

Ismail, S. A., 1993. Keynote Papers and Extended Abstracts. Congress on traditional sciences and technologies of India, I.I.T., Bombay. pp. 10, 27-30.

Ismail, S. A., 1997. Experiments from the Field. In: Ismail, S. A. (Eds.), Vermicology, Orient longman Press, Hyderabad. 92 pp.

Kale Radha, D., 1996. Earthworms- The significant contribution to organic farming and sustainable agriculture. Proc. Nat. Sem. Org. Fmg. and Sust. Agric. pp. 52-57.

Patcharapreecha, P., Toparak- Ngarm, B., Goto, I., Kinura, M., 1990. Studies on saline soils in Khonkaen region, Northeast Thailand. III. Effects of amelioration treatments on physical and chemical properties of the saline soils. Soil Sci. Plant Nutr. 36 (3), 363-374.

Pera, A., Valini, G., Sireno, I., Bianchin, M. L., De Bertoldi, M., 1983. Effect of organic matter on rhizosphere microorganisms and root development of Sorgum plants in two different soils. Plant Soil 74, 3.

Perucci, P., 1990. Effect of the addition of municipal solid-waste compost on microbial biomass and enzyme activities in soil. Biol. Fertil. Soils. 10(3), 221.

Thampan, P. K., 1995. Perspectives on organic agriculture. In: Thampan, P. K. (Eds.), Organic agriculture, Peekay Tree Crops Development Foundation, Cochin, pp. 1-38.

Agriculture / Plant Biology

Soil texture and organic matter effects on structural stability, infiltration, runoff and seal formation

M.N. WUDDIVIRA[1], R.J. STONE[1] AND E.I. EKWUE[2]

[1]*Department of Food Production, Faculty of Science and Agriculture and*
[2] *Department of Mechanical and Manufacturing Engineering*
The University of the West Indies, St.Augustine, Trinidad, West Indies.
wuravnakka@yahoo.com.

Abstract

Previous studies have shown that increasing clay concentration can increase aggregate stability on the one hand and on the other hand it can reinforce disruptive forces during wetting resulting in aggregate slaking, low infiltration rate, extensive seal formation, high runoff and the likelihood of erosion. In this study, the significantly higher water stable aggregates (WSA) and final infiltration rate of medium clay-high organic matter sample over its high clay-low organic matter counterpart under simulated rainfall suggests that the medium level (20-45 %) is the threshold clay level beyond which organic matter content must be high or disruptive forces will be strengthened during fast wetting leading to significant loss in aggregation and extensive seal formation.

Introduction

Aggregate stability is crucial for the maintenance of adequate pore space for infiltration and soil hydraulic properties. Maintenance of structural integrity under continuous wetting and raindrop impact is therefore important, particularly in the rainfall rich humid tropics.

The Caribbean region is characterised, by high rainfall amounts and intensities (Gumbs, 1982). The soils are of medium to heavy textures with low organic matter and low free iron oxides (Ahmad and Roblins, 1971). Under these conditions, the susceptibility of soils to structural breakdown with attendant runoff generation and soil loss are increased (Idowu, 2003).

Clay and organic matter have cementing and binding abilities which hold particles together in the aggregate and thus protects aggregates against disruptive forces. This paper test the hypothesis that increase in clay content if accompanied by an appropriate increase in organic matter content will suppress the extent of differential swelling and the volume of entrapped air thereby decreasing aggregate slaking during wetting.

Materials and Methods

Soils

Soil samples were taken from the top 0-10 cm of six agricultural soil series in Trinidad. Water stable aggregates were assessed using single sieve apparatus. Infiltration rate, time and infiltration depth prior to ponding, runoff and seal formation were assessed using a rainfall simulator in samples with three clay levels (low, <20 %; medium, 20-45 % and high, >45 %) and two organic matter levels (low, ≤3.0 % and high, ≥3.0 %). Analysis of variance was used to determine significance of treatments by comparing main effect and interaction means. Tukey's honestly significant difference test was used to discriminate among significant treatment means.

Results and Discussions

Aggregate stability

In both low- and high- organic matter soils, aggregate stability increased with increasing clay content.

Aggregate stability under fast prewetting increased in this order; Low clay-low organic matter (LL) < low clay-high organic matter (LH) < medium clay-low organic matter (ML) < high clay-low organic matter (HL) < medium clay-high organic matter (MH) < high clay-high organic matter (HH). This sequence illustrates that aggregate stability increases with increase in clay content up to the medium level after which increase in clay without accompanying increase in organic matter resulted in significant reduction in stability. This is shown by the signifycantly higher WSAf in the MH samples over their HL counterparts (Table 1). From a practical standpoint, this suggest that under disruptive forces of fast wetting which is common in humid tropics characterized by aggressive climatic conditions (Kral and Hawkins 1982), increasing and maintaining the organic matter concentration of medium clay soils that are often prone to disaggregation by fast wetting from low to high level may confer high aggregation and infiltration rate by increasing the amount of air encapsulation within soil aggregates during fast wetting sufficient to prevent slaking (Zaher et al., 2005). This also suggest that a threshold clay content exist above which high organic matter content is required to provide the cohesive force necessary to

protect the soil aggregates against disruptive forces during the wetting process.

Soil sample	WSAf‡	WSAs	FIR mm/h	Ip Mm	Tp h	Q mm
LL†	5.3aA††	18.9aB	5.7a	6.0a	0.05a	95.0de
LH	28.6bA	56.4bB	16.3b	7.3a	0.06a	86.3cd
ML	46.1cA	88.3cB	20.8b	15.5b	0.13b	77.3c
MH	61.5eA	94.1cB	109.9d	119.5d	1.00d	6.3a
HL	56.5dA	89.6cB	3.2a	4.7a	0.04a	100.6e
HH	68.8eA	93.8cB	60.7c	75.7c	0.63c	41.3b

WSAf Ratio (High-OM/Low-OM

Low clay (<20 %)	Medium clay (20-45 %)	High clay (>45 %)
5.4	1.3	1.2

Table1. Water stable Aggregate (WSA), final infiltration rate (FIR), time (Tp) and infiltration depth (Ip) prior to ponding, and runoff for studied samples.

†† Means followed by the same lowercase letter in the column, or same upper case letter in the row are not significantly different by Tukey's honestly significant difference test (P = 0.05)

†LL, low clay–low organic matter; LH, low clay–high organic matter; ML, medium clay–low organic matter; MH, medium clay–high organic matter; HL, high clay–low organic matter; HH, high clay–high organic matter.

‡ f (fast prewet); s (slow prewet).

Infiltration rate, seal formation and Runoff

In all the treatments, infiltration rate decreased with increase in cumulative rainfall until the attainment of a final infiltration rate (FIR) (Fig. 1). This decrease in infiltration rate with increase cumulative rainfall (Fig. 1) is an indication of increasing soil structural degradation caused by slaking due to fast wetting and the destructive impact of raindrops on soil aggregates. The destruction, led to aggregate breakdown and generation of finer particles that became substrate for seal formation. Once a seal was formed at the soil surface, the hydraulic conductivity of the soil layer was decreased leading to low infiltration and high runoff. The faster a seal was formed the lower the cumulative amount of water infiltrated until the attainment of FIR. Seal formation rate was slowest in MH and fastest in HL indicating that aggregate slaking and seal formation intensified with increase in clay when not accompanied with an appropriate increase in organic matter. Organic matter demonstrated its ability to reduce pressure buildup by reducing the rate of water entry into individual aggregates, lowering the potential at the wetting front and reducing the hydraulic conductivity of the aggregates (Zaher et al., 2005) during fast wetting. Thus, high stability and high infiltration rate are sustained when increase in clay is accompanied by increase in organic matter.

In a practical sense, cultivation of clay soils will be more effective if organic matter is high. Aggregates in these soils will remain stable and maintain a relatively high infiltration rate under continuous wetting and high-intense rainfall during the rainy season. On the other hand, high clay-low organic matter soils will easily succumb to aggregate slaking leading to seal formation and extremely low infiltration rate during the first few showers at the beginning of the rainy season. Although organic matter is most effective in stabilizing low clay soils (Table 1), soils with high clay soils must have high organic matter contents to avoid considerable slaking, dispersion and breakdown under rainfall effects.

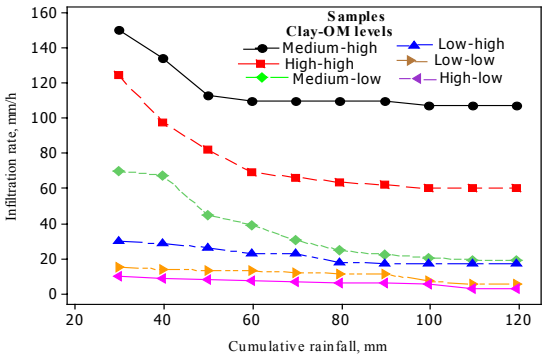

Fig. 1. Infiltration rate as a function of cumulative rainfall for low, medium and high clay samples at low and high organic matter (OM) levels.

References

1. Ahmad, N., and Roblins, A.J. (1971). Crusting of River Estate soil, Trinidad, and its effect on gaseous diffusion, percolation, and seedling emergence. *Journal of Soil Science* **22,** 23-31.
2. Gumbs, F.A. (1982). Soil and water management features in Trinidad and Guyana. *Tropical Agriculture (Trinidad)* **59.** 76-81.
3. Idowu, O.J. (2003). Relationship between aggregate stability and selected soil properties in a humid tropical environment. *Communucations in Soil Science and Plant Analysis* **34,** 695-708.
4. Kral, D. M. and S. Hawkins. (eds.) (1982). Soil Erosion and Conservation in the Tropics. *ASA Special Publications 43*.
5. Zaher, H., Caron, J. and Ouaki, B. (2005). Modeling aggregate internal pressure evolution following immersion to quantify mechanisms of structural stability. *Soil Science Society of America Journal* **69,** 1-12.

Agriculture / Plant Biology

Effects Of *Musa x paradisiaca* Plant Extracts On The Digestive Parasitic Nematode *Haemonchus contortus* In The French West Indies

MARIE-MAGDELEINE CARINE [A], MAHIEU MAURICE [A], HOSTE HERVE [B], ARCHIMEDE HARRY [A]

[A] *Unité de Recherches Zootechniques, Institut National de la Recherche Agronomique, Domaine de Duclos, 97170 Prise d'eau PETIT-BOURG, Guadeloupe (FWI)- marie@antilles.inra.fr*
[B] *UMR 1225 IHAP-INRA-DGER, 23 chemin des Capelles, 31076 Toulouse*

Abstract

Plants containing condensed tannins can represent a way of natural struggle to decrease the worm burden. The present study is aimed at testing the anti-parasitic potential of stem and leaf extracts (water, methanol end dichloromethane) of *Musa x paradisiaca*, a plant containing tannins. Water stem extract, dichloromethane and methanol leaf extracts had efficiency over 90%. Methanol stem extract had an efficiency of 79.5%. Water extract of leaves had the best efficiency on L3 migration inhibition (56%). Methanol stem extract had efficiency over 60% on adult worm motility. The results clearly indicate the anthelmintic properties of this plant extracts. Further researches into chemical compounds are necessary to seek whether the potential activity is due to tannin, other secondary metabolites, or to synergy between two or several compounds.

Introduction

Digestive parasitoses are the major pathologies of small ruminants in the Caribbean area. They are essentially due to the nematode *Haemonchus contortus*. For example, in Guadeloupe (French.West.Indies), the prevalence of this parasite varies between 80 and 100%. More than ¾ of mortality before weaning (that is to say 40%) is linked to gastro-intestinal strongylosis (Aumont et al, 1997). The control of parasites relies mainly on chemical anthelmintics. However, the frequent use of anthelmintics led to apparition of *Haemonchus contortus* strains resisting to benzimidazoles and avermectines in Guadeloupe and Martinique as everywhere in the tropics. Facing such a zootechnical deadlock, it seems urgent to search for alternative methods in order to decrease the parasite burden. Among these methods, figures phytotherapy. Indeed, cares by plants can represent a way of natural struggle to minimize the ailment and find new anthelmintic molecules.
Recent studies have shown that often, plants containing condensed tannins have anthelmintic properties. The present study is aimed at testing the anti-parasitic potential of banana tree (*Musa x paradisiaca)*, a plant containing tannins.

Materials and Methods

Banana tree material was collected in Guadeloupe (F.W.I). Fresh plant material was used for extraction. Three extracts (water, methanol and dichloromethane) of stem and leaves were prepared, in order to test a large range of compounds. The water extract decoction was filtered and lyophilised to obtain a powdered extract. To prepare the other extracts, fresh plant organs were lixiviated by solvents (methanol or dichloromethane) during 3h sheltered from light. The filtrates were collected and evaporated under low pressure at 40°C.

The extracts were tested *in vitro* on four different development stages of the nematode: eggs hatching, L1-L2 larval development, L3 migration and adult worm motility. Different doses of extracts were tested in five replicates for the three first assays and in three replicates for the last one. Negative controls (PBS or DMSO if used for extracts solution) were used. Parasite materials (eggs and adult worms) were obtained from Black belly donor lambs experimentally infected by *H. contortus* (Hubert and Kerboeuf, 1984).

The egg hatch assay was realised according to a modification of the method used for testing anthelmintic resistance (Assis et al., 2003).
The larval development assay was derived from the technique described by Hubert and Kerbouef (1992), (*in* Assis et al., 2003).
The L3 migration assay was performed according to Rabel et al. method (1994), (*in* Hounzangbe-Adote et al., 2005).
The adult worm motility assay was performed according to Hounzangbe-Adote et al. (2005).

The data were analysed by using the general linear model (GLM) procedure (Minitab® Release 14 software). The model took to account the nature of the extract and the dose response.

Results and Discussion

Egg hatch assay
No significant difference between the negative control and the extracts was observed. Banana tree extracts seemed to have no effect on egg hatching.

Larval development assay
Compared to the negative controls, the results of the assay showed that several extracts stopped

efficiently the larval development. Water stem extract, dichloromethane and methanol leaf extracts had efficiency over 90%. Methanol stem extract had an efficiency of 79.5%.

L3 mobility assay
Water extract of leaves had the best efficiency on L3 migration inhibition (56%).

Adult worm motility assay
Methanol stem extract had efficiency over 60%.

Stem and leaves extracts of Banana tree had a significant *in vitro* anthelmintic effect on three development stages of the parasite: larval development, L3 and adult stages. No effect was observed on eggs. These results showed that the extracts had specific targets.
Banana tree is known to contain tannins. The anthelmintic effect of the extracts could be due to the presence of these phenolic molecules. The variability of secondary metabolites present in the extracts could also explain the variability of efficiency on the four development stages according to anatomo-physiological particularity of the parasite.
Concerning the other suspected compounds, the efficiency of the three different extracts (water, methanol and dichloromethane) allows to imagine that several molecules could be responsible for the anthelmintic activity. In the banana tree, the suspected compounds are: terpens, carbohydrates, flavonoids and polyphenolics.
Studies on anthelmintic vegetal compounds showed that condensed tannins had activity against *Haemonchus contortus* (Paolini, 2004, Athanasiaodou et al, 2001). Water or methanol extracts of Banana tree could contain these compounds.
Several action modes could explain the direct *in vitro* effect on the parasite. The adult cuticule as the L3 sheath contain proteins with proline. These proteins have a high affinity for condensed tannins. The fixation of these two compounds could affect the normal moulting of the L3 or adulteration of adult worm cuticule. Enzymatic processes could be spoiled by linking between tannins and enzymes responsible for essential functions of the parasite like motility.
Concerning other secondary metabolites, the action mode could be classical anthelmintic-like. A study showed that Banana tree juice induced twitch augmentation in skeletal muscles of mice (Singh et al, 1990). This mechanism looks like Imidothiazoles action mode. Such compounds could also spoil nervous system by acting on synaptic functions.

Conclusion

These results clearly indicate the anthelmintic properties of *Musa x paradisiaca* extracts. However, further researches into chemical compounds are necessary to seek whether the potential activity is due to tannin, other secondary metabolites, or to synergy between two or several compounds.

Acknowledgements
The authors would like to thank “la Région Guadeloupe” and “The European Social funds” FSE for research financial support.

References:

1. Assis L.M., Bevilaqua C.M.L., Morais S.M., Vieira LS., Costa C.T.C., Souza J.A.L. (2003), Ovicidal and larvicidal activity *in vitro* of *Spigela anthelmia Linn*. Extracts on *Haemonchus contortus*. *Veterinary. Parasitology* **117**, 43-49.

2. Athanasiadou S., Kyria Zakis I., Jackson F., Coop R.L. (2001). Direct anthelminthic effects of condensed tannins towards different gastrointestinal nematodes of sheep : in vitro and in vivo studies. *Veterinary Parasitology* **99**, 205-219

3. Aumont G., Pouillot R., Simon R., Hostache G., Varo H., Barre N. (1997). Parasitisme digestif des petits ruminants d’élevage dans les Antilles françaises. *INRA Productions. Animales* **10-1**, 79-89.

4. Hounzangbe-Adote M.S., Paolini V., Fouraste I., Moutairou K., Hoste H. (2005). In vitro effects of four tropical plants on three life-cycle stages of the parasitic nematode *Haemonchus Contortus*. *Research in Veterinary Science* **78-2**, 155-160.

5. Hubert J., Kerboeuf D. (1984). A new method for culture of larvae used in diagnosis of ruminant gastrointestinal strongylosis: comparaison with fecal cultures. *Canadian Journal of comp Medicine* **48**, 63-71.

6. Paolini V. (2004). Effets des tanins condensés sur le parasitisme par les nématodes gastro-intestinaux chez la chèvre. Thèse Parasitologie. Université de Perpignan.

7. Singh Y.N., Dryden W.F. (1990). The augmentating action of banana tree juice on skeletal muscle contraction. *Toxicon* **28-10**, 1229-1236.

Agriculture / Plant Biology

The Ectomycorrhizal Fungus *Scleroderma bermudense* Improves Water Status and Limits Sodium and Chloride in Seagrape (*Coccoloba uvifera* L.) Seedlings

E. Bandou (1), F. Lebailly (1), F. Muller (1), M. Dulormne (1), A. Toribio (2), J. Chabrol (1), R. Courtecuisse (3), Y. Prin (4), B. Dreyfus (4) and A. Bâ (1,4)

(1) Laboratoire de biologie et physiologie végétales, UFR Sciences exactes et naturelles, BP. 592, Université Antilles et Guyane, 97159 Pointe-à-Pitre, Guadeloupe, France;
(2) Laboratoire de mycologie-flore pathogène du sol, Unité de recherches en productions végétales, Domaine de Duclos, 97170 Petit-Bourg, INRA centre Antilles-Guyane, Guadeloupe, France;
(3) Département de botanique, Faculté des sciences pharmaceutiques et biologiques, Université de Lille, BP. 83, F-59006 Lille Cedex;
(4) Laboratoire des symbioses tropicales et méditerranéennes, UMR 113 IRD/INRA/AGRO-M/CIRAD/UM2, TA10/J, Campus international de Baillarguet, 34398 Montpellier cedex, France

Keywords: Ectomycorrhiza, *Coccoloba uvifera*, *Scleroderma bermudense*, Ectomycorrhizal dependency, Salt stress

Abstract

Coccoloba uvifera (L.) L. (Polygonaceae), also named seagrape, is a small tree widely distributed along Altlantic, Caribbean and Pacific coasts of the American tropics and subtropics. It is an important tree for edible fruits, ornemental plantings and coastal windbreaks along Caribbean's Beach and Roadside. *C. uvifera* is considered as a drought-hardy and non-halophytic woody plant relatively tolerant to salt, growing often in pure stands within well-drained sandy soils that are slightly to moderately alkaline.

The purpose of this study was to test the hypothesis that the ectomycorrhizal (ECM) fungus, *Scleroderma bermudense*, have a high capacity to alleviate the saline stress in *Coccoloba uvifera* (L.) L. seedlings. Plants were grown over a range (0, 200, 350 and 500 mM) of NaCl levels for 12 weeks, following 4 weeks of non-saline pre-treatment under greenhouse condition. The *C. uvifera* seedlings growth and nutrition were stimulated by *S. bermudense* regardless of salt stress. Although ECM colonization was reduced with increasing NaCl levels, ECM dependency on *C. uvifera* seedlings was increased. The number of leaves and leaf area were significantly higher in ECM than non-ECM plants. ECM plant tissue had significantly increased concentrations of P and K but lower Na and Cl concentrations than non-ECM plants. Higher K concentrations in ECM plants suggest a higher osmoregulating capacity of these plants. In this respect, the water status of ECM plants was improved despite their higher evaporative leaf surface. The results suggest that the reduction in Na and Cl uptake together with a concomitant increase in P and K absorption and a high water status in ECM plants may be important salt-alleviating mechanisms for *C. uvifera* seedlings growing in saline soils.

Leaf Allometry in Long and Short Shoots Betula papyrifera

J. C. CAESAR

Department of Biology, Faculty of Natural Sciences, University of Guyana, Box 10-1110, Georgetown, Guyana - jccaesar@yahoo.com

Abstract

The morphology and developmental characteristics of shoot dimorphism in paper birch (*Betula papyrifera* Marsh.) has been well documented [1-3]. However, the allometric relationships (from the basic allometric equation $y = b \times x^{K}$; where **K** is the allometric coefficient of the relative growth rates of y and x) of leaf morphological attributes in the long and short shoot types have not been examined in those reports. Here we present data on the allometric parameters influenced by the dimorphic

development of shoots by comparing allometry of leaf lamina length versus width, lamina length versus petiole length and leaf dry weight versus leaf size. Calculated allometric coefficients, **K**, for the early leaf parameters indicates short shoot early leaves have ontogenetic tendency for increased rate of growth of lamina width faster than lamina length resulting in lower lamina length to width ratios. Long shoots, on the other hand, tend to have reduced tendency leading to higher lamina length to width ratios. The photosynthetic attributes of the two shoot types in relation to shoot distribution within the canopy will be briefly discussed.

References

[1] Caesar, JC and Macdonald, AD 1983. Shoot development in *Betula papyrifera*. 2. Comparison of vegetative and reproductive short shoot growth. *Canadian Journal of Botany* **61** pp 3066 – 3071.
[2] Caesar, JC and Macdonald, AD 1984. Shoot development in *Betula papyrifera.* 4. Comparisons between growth characteristics and expression of vegetative long and short shoots. *Canadian Journal of Botany* **62**: 446-453
[3] Macdonald, AD, Mothersill, DH & Caesar, JC. 1984. Shoot development in *Betula papyrifera*. 3. Long–shoot organogenesis. *Canadian Journal of Botany* 62:437 – 445.

Biodiversity in Rain Forests of the Lesser Antilles

E. Ingadassamy and A. Rousteau

Laboratoire de biologie et de physiologie végétales, Unversité des Antilles et de la Guyane 97159 Pointe-à-Pitre cedex - alain.rousteau@univ-ag.fr

Abstract

The diversity of the tree communities reaches very high levels in the forests of the Lesser Antilles. The Archipelago is thus included in one of the 34 hot spots of the biodiversity of the world. Clearly the number of native tree species depends: 1) on the land area but also 2) on the landscape diversity (diversity of the ecological conditions). So the volcanic islands with high elevation biota, usually posses more tree species than low islands without montane habitat.

Large parts of the primary vegetation were modified for human uses. In the volcanic islands however, rain forest were partly saved because of the soils and climates are not proper to crop production. In Guadeloupe for example, 40% of the rain forests are yet not far from their natural condition. Such formations exhibit the major part of the Lesser Antilles flora and their functions show a great concern with soils conservation, water resources sustainability or natural risks prevention.

The tree diversity of rain forest stands may be appreciated at the local scale as well as at the ecosystem one.

When considering 800m^2 plots, the richest forest stands lies at middle elevation on the leeward slopes of volcanic hills. Beside this particularity, both the forest richness (number of tree species in a plot) and the equitability of Shannon-Weaver, decreases as the elevation increases. These altitudinal trends suggest that the environmental conditions at high elevation act as a selective filter and limit the plant diversity. The montane rain forest thus exhibits the smallest local (or α) biodiversity.

At the ecosystem scale however, the montane rain forest seems to be as rich as the others forest types. In addition, the montane rain forest posses the highest endemism since no less than ¼ of its tree species are endemic of the Lesser Antilles archipelago.

We conclude that the montane tree stands, because of combining high ecosystem (or β) diversity with low local (or α) one, exhibits inhomogeneous spatial organisation. Such an organisation could be an adaptative response to montane constraints and disturbance regime.

The understanding of the dynamical process that generate such spatial organisation could be essential for the conservation biology in the tropical islands and for the restoration of the disturbed mountain areas.

Agriculture / Animal Biology

A Low Cost Mechanism for Restraint and Handling of the Collared Peccary (*Tayassu tajacu; Pecari tajacu*), **applied in Kourou, French Guiana** 143
G. Young, A. Steil and G. Garcia

The Ability of Near Infrared Reflectance Spectroscopy (NIRS) to Assess Quality and Level of Tropical Grass Intake by Creole Sheep 145
A. Fanchone, M. Boval, P. Lecomte and H. Archimede

Influence of a Sugar Cane Diet on Growth Performance, Carcass Traits and Meat Quality in Creole Growing Pigs 148
X. Xandé, D. Renaudeau, E. Despois, M. Giorgi and B. Bocage

How to Produce Heavy Goat Carcass With Lean Meat? 150
L. Limea, G. Alexandre, R. Arquet, G. Gravillon, B. Bocage

Agriculture / Animal Biology

A Low Cost Mechanism for Restraint and Handling of the Collared Peccary (*Tayassu tajacu; Pecari tajacu*), applied in Kourou, French Guiana

GAIL G.M. YOUNG (1), GARY W. GARCIA (1), ARNAUD STEIL (2)

(1) Department of Food Production, Faculty of Science and Agriculture The University of the West Indies, St. Augustine Campus, Republic of Trinidad and Tobago,
(2) SUA-TI, Chambre d'Agriculture de la Guyane, BP 544, 97333 Cayenne cedex, France.
GYoung@fsa.uwi.tt, garygwg1@gmail.com,
massalal01@yahoo.co.uk, chambre.agriculture.973@wanadoo.fr

Abstract

In order to reduce production costs attached to peccary farming, a low cost mechanism for restraint and handling was tested. Eighteen (18) collared peccaries were handled and restrained by three (3) personnel of the Kourou Experimental Station in French Guiana. Seven (7) wooden transport cages and one (1) restraining cage were used to carry out the procedure. In approximately three (3) hours all of the animals were identified with ear tags, weighed and any general maintenance and grooming applied. The methodology which is cost effective on labour, time, tranquilliser, space utilisation and functionality, can be used by farmers desirous of pursuing peccary farming.

Introduction

Extensive Peccary farming has been firmly established for years in Latin America, and is rapidly developing in other Neo-tropical countries. The costs attached to this farming system can be high, so low cost mechanisms can be useful in alleviating them. Handling, as part of peccary production is also of particular concern from a security standpoint, when one considers the animals' well-known aggressive comportments. The problem is one of achieving these goals in a cost-effective manner. The method described hereunder is an attempt to address this concern, and, as an example, the production system under which the method was tested is a semi-extensive one.

Materials and Methods

Eighteen (18) collared peccaries were stocked in a 25m x 25m enclosure located at the Soucoumou Experimental Station in Kourou, French Guiana. Three employees (a "Technicienne, Faune Sauvage" (TFS), providing technical guidance for the CAG-UWI project entitled *"Connaissance de la Faune Sauvage de la Guyane: Possibilités de Gestion et de Domestication"*; an "Agent, Faune Sauvage" (AFS), her Assistant; and a "CIA", one of the General Farm Assistants) of the "Service d'Utilité Agricole de Technologie et d'Innovation (SUA-TI), Chambre d'Agriculture de la Guyane (CAG)", entered the enclosure for the purposes of manipulating the animals.

Expanding on the restraint and handling technology used in Brazil by Nogueira (1999) and Neto (personal communication, 2003), the following manipulation steps were carried out:

a) the animals were enclosed in a small corral located within the enclosure; this being done to protect the personnel and to reduce stress on the animals;
b) seven (7) transport cages were assembled to form a corridor, and the restraining cage was placed at the end of this corridor;
c) the first set of animals were run through the corridor where they were held, immediately preceding their manipulation. The first animal went directly into the restraining cage;
d) the CIA then immobilised the animal in the restraining cage by pressing it between the side of the cage and the plywood sheet mounted to the handles;
e) the AFS next administered 1.5ml of the tranquiliser Zoletil 100®, i.m. to the animal at the level of its thigh using a 5ml syringe;
f) the animal was then released for the tranquiliser to take effect, while the animal next in line entered the restraining cage where steps (d) and (e) were repeated;
g) once the animal fell asleep, it was positioned on its side on the scale, using the pig lasso to secure its mouth shut. It was then weighed in this position;
h) length and width measurements, were taken by the AFS with a wooden folding tape measure. Measurements of the animal's length spanned the tip of the snout to the rump, while the width measurements began and ended at the top of the back to the bottom of the stomach respectively. Ear-tags on which the animal's identification number was written with a marker were fitted into the appropriate space

in the ear-tag punch and the male and female tags rejoined by piercing the animal's ear. The puncture on the newly-tagged animal was disinfected with AluSpray®, to reduce any possible incidence of infection (Fig. 1).

Figure 1: Disinfecting a freshly ear tagged, tranquilised Collared Peccary using the pig lasso for added security. (Source Author, 2004)

Other general maintenance and grooming activities (e.g. nail clipping), were also performed on the animal. All data were noted by the TFS on a datasheet developed for this purpose, and were then inputted into the Microsoft Excel programme;

i) after the completed operation, the sleeping animal was placed in a shaded recovery area;
j) different aspects of the operation were photographed by the TFS.

Results and Discussion

The entire operation lasted approximately 3 hours, and all 18 animals were manipulated in the described manner. An approximate completion time per 'sub-activity' is as follows: (a) weighing – ~5-7 minutes (time allotted for accurate positioning of the animal); (b) measurements – 5 minutes; (c) ear tagging – 1-2 minutes; and (d) disinfecting < 1 minute. Some 15 minutes/animal were used for each manipulation therefore. In a previous attempt on the station some 15-20 minutes were required to administer the tranquiliser by gun. A maximum of 3 persons were used, so that the manpower demand is not particularly high. In other commonly practised methods, upwards of 4 persons are needed. Other advantages include its cost-effectiveness on space – as it can be quickly dismantled and reassembled, as needed so that the enclosure need not have the corridor as a permanent fixture; and functionality – as the cages can also be used to transport the animals. The proximity of this method has also effectively decreased the quantity of tranquiliser used during one manipulation operation (Fig. 2), compared to using a tranquiliser gun to administer it.

Figure 2: A demonstration of an administration of the tranquiliser i.m., to an restrained Collared Peccary. (Source, Author, 2004)

Cautions to note however: (a) reduced cage usefulness and security over time (> 1 year) as animals may gnaw at the wood and create gaps for possible escape; (b) heaviness of the wooden cages especially when carrying animals can cause injury to handlers.

Conclusion

Based on the result of this trial, future manipulations should be less time-consuming, but it is dependent on the time initially taken to herd the animals and enter them into the corridor. It is therefore suggested that for a resource-challenged farming operation whether sole or integrated, and interested in peccary farming, this methodology can be incorporated with little extra time and labour demands.

Further research would more fully exploit the advantages of the methodology in a cash-strapped environment.

Acknowledgements

Financial support from "le Conseil Régional de la Guyane (CG); Fonds de Coopération Régionale de la Préfecture (FCR)" and the "Centre Nationale pour d'Etudes Spatiales (CNES)" under the project « Connaissance de la Faune Sauvage de la Guyane : Possibilités de Gestion et de Domestication » is gratefully acknowledged.

The technical assistance of Messrs. Patrick Francis (AFS) and Richard Pruyckemaker (CIA) and Bruno Brevet (Technicien, Aquacole) of SUA-TI, CAG is gratefully acknowledged. Mr. Terry Sampson's, and Dr. Marlon Knight's, Mr. Michael Joseph's and Dr. Neela Badrie's (Departments of Agricultural Economics and Extension, and Food Production, Faculty of Science and Agriculture, The UWI) communication expertise and comments on the content and assistance with the poster's presentation, are also much appreciated.

References

Nogueira-Filho, S. 1999. Criação de Cateto e Queixada. Viçosa, CPT. 70 pages.

Barreto, B. 2003. Personal Communication, July 2003.

Agriculture / Animal Biology

The ability of Near Infrared reflectance spectroscopy (NIRS) to assess quality and level of topical grass intake by creole sheep.

AUDREY FANCHONE[1], MARYLINE BOVAL[1], PHILIPPE LECOMTE[2], HARRY ARCHIMEDE[1].

[1]Unité de Recherches Zootechniques, Institut National de la Recherche Agronomique, Domaine de Duclos, 97170 Prise d'eau PETIT-BOURG, Guadeloupe (FWI),
[2]Pole élevage, Coopération International en Recherches Agronomiques pour le Développement. 7, Chemin Irat - Ligne Paradis, 97410 Saint-Pierre. Martinique (FWI)
Audrey.Fanchone@antilles.inra.fr

Abstract

Near infrared spectroscopy is increasingly use as an alternative to classical analytical method to evaluate quality and functional properties animal feeds and human food. This method provides a rapid, clean and green, and accurate measure of chemical composition of diet. At the same time, attempts to evaluate these parameters in grazing systems are laborious, time consuming, costly and introduce bias in parameter estimation. The aim of this study is to evaluate the potential of faecal and forage NIRS to assess functional properties of diet ingested by Creole sheep. Derived standard errors of cross validation (SECV) and coefficient of determination using faecal spectra were 2.18 % and 0.70 for organic matter digestibility, 9.27 g/kg$P^{0.75}$ and 0.28 for organic matter intake and 6.76 g/kg$P^{0.75}$ and 0.27 for digestible organic matter intake. Association of faecal and herbage spectra lead to increase of prediction accuracy of 17.4, 7.4 and 7.2 % for organic matter digestibility, organic matter intake and digestible organic matter intake respectively. These results clearly indicate that near infrared reflectance spectroscopy represent a new tool to study and monitor breeding systems.

Introduction

Amongst parameters contributing to ruminant production from forage, intake is the more important (Minson, 1990) but also the most variable and the most difficult to measure accurately. In pen fed experiments, measure of intake is laborious, costly, and time consuming. In grazing systems, voluntary intake can only be estimated by indirect methods requiring estimation of both total faecal excretion and digestibility. If several indirect methods allow estimations of digestibility (in vitro digestibility (Tilley and Terry, 1963, in sacco degradability (Demarquilly and Chenost, 1969), or method based on faecal index (Boval, 2003), they can introduce bias in intake estimation. At the same time, near infrared spectroscopy (NIRS) is increasingly used in agro industry to evaluate nutritional quality of animal and human foods. The aim of this study is to determine the potential NIRS to predict quality and quantity of diet ingested by martnik ewes.

Materiel & Method

The experiment was carried out at the experimental station of the National Agronomic Research Institute (INRA) in Guadeloupe.

Twelve martnik ewes weighing 44 (± 10 kg) were employed in this study. Each ewe was individually housed in metabolism cage to be fed fresh forage harvested from plot of Digitaria decumbens (Pangola). Grass was cut daily early in the morning and chopped (5 cm length) before being offered. Animals received amount of forage 1.1 times greater than their voluntary intake. Fresh weight of forage offered, forage refusals and faeces excreted were measured. Sub-samples at approximately 300 and 200 g fresh weight were collected for dry matter (DM) determination for forage and faeces respectively. Forage and faeces sub-samples were pooled within week and ewe before further processing and analysis. Organic matter intake (OMI), organic matter digestibility (OMD) and resultant digestible organic matter intake (DOMI) were calculated for each ewe per each week. Absorbance spectra (log 1/R) of samples were recorded using a Foss NIRSystem 6500 mono-

chromator. Samples were scanned at 2 nm intervals over the wavelength range 700-1100 and 1100-2500. Spectrums were subsequently reduced over the NIR region. Spectral data were processed using ISI software (Infrasoft international; Shenk, 1992). Calibration of dietary composition, OMI and OMD were developed using Modified Partial Least Square procedure (MPLS) as this technique has been proven to be superior in earlier research (Shenk and Westerhaus, 1993; Park et al., 1997, 1998).

Results & Discussion

Calibrations statistics for OMD obtained in our study (Table 1) using faecal NIRS compare favourably with those reported by Boval et al (2004) with steers fed with Digitaria decumbens or Dichatium sp (SEC-V = 2.0; $R^2 = 0.69$). Coates (1998) develop faecal NIRS equation for predicting DM digestibility (DMD) using data from 54 in vivo trials covering a wide range of pasture grass and legume hay and the author obtains a SEC of 2.5 % and R^2 of 89.0 (n = 187). Faecal NIRS equation for predicting OMD developed by Lyons and Stuth (1992) and Leite and Stuth (1995) used *in vitro* estimates of digestibility determined on oesophageal fistula sample as reference values. The resultants SEC value of 1.66 and 2.01 %, respectively were comparable with the 1.88 % from this study despite the fact that we used *in vivo* digestibility as reference value. Indeed, *in vivo* digestibility introduces an "animal factor" into the calibration process which is not taking into account in *in vitro* digestibility.

Variable	*n*	SEC	SEC-V	R^2_{CV}
OMD (%)	82	18.8	2.18	70.7
OMI ($g/kg^{0.75}$)	82	6.13	6.76	28.5
DOMI ($g/kg^{0.75}$)	82	6.03	9.27	27.3

There was a deterioration in cross validation statistics for intake (Table 1) as reported by Boval et al (2004). This is consistent with previous reports based on forage NIRS predictions of OMI where SECs (and R^2) for OMI of 9.6 (72.0), 7.3 (71.0) and 3.4 (90.0) $g/kgBW^{0.75}$ were reported for cattle consuming arid and semi-arid forages (Ward et al., 1982), temperate grasses and legumes (Redshaw at al., 1986), and silage (Park et al., 1987), respectively. Comparatively with OMD, *in vivo* OMI is subject to further "animal factors" such as rumen size or physiological stage. Moreover it is also affected by "forage factors" (forage digestibility, dietary chemical content …).

Since digestible organic matter intake is the resultant of digestibility and intake processes, it would allow intermediate statistics. Nevertheless, with SEC-V of 6.76 and R^2 of 27.31 % (Table 1) and taking into account the standard deviation of the reference value (SD = 7.69), calibration of DOMI in as poor as intake calibration. To how knowledge, no published reports of faecal NIRS calibration for predicting DOMI were found with which to make a real comparison.

Association of faecal and herbage spectra lead to increase of prediction accuracy (SECV = 1.80 and $R^2 = 0.79$, SECV = 8.58 and $R^2 = 0.46$ and SECV = 6.27 and $R^2 = 0.51$) for OMD, MOI and DOMI respectively. Requirement of software (Dardene, unpublished data) to associate faecal and forage spectrum makes this technique difficult to implement in breeding systems. Moreover, in grazing systems sampling of diet ingested are laborious and supply variable results.

Conclusion

These results clearly indicate the potential of near infrared spectroscopy to assess intake and digestibility of ruminants. Although precision obtained in intake prediction are lowest than digestibility prediction, it remain acceptable compared with those usually used in grazing system. Association of faecal and forage spectrums offers a new tool of research of diet quality in grazing system.

Acknowledgements

We gratefully acknowledge E. Ortega for technical participation. This study has been supported by the "Region Guadeloupe" and "The European Social Funds" FSE.

References:

1. Boval M., Archimède H., Fleury J., Xandé A., (2003). The ability of faecal nitrogen to predict digestibility for goats and sheep fed with tropical herbage. Journal of agricultural Science. 140, 443-450.

2. Boval M., Coates D.B., Lecomte P., Decruyenaere V., Archimède H. (2004). Faecal near infrared reflectance spectroscopy (NIRS) to assess chemical composition, in vivo digestibility and intake of tropical grass by Creole cattle. Animal Feed Science and technology. 114, 19-29.

3. Demarquilly C., Chenost M., 1969. Etude de la digestion des fourrages dans le rumen par la méthode des sachets de nylon, liaison avec la valeur alimentaire. Annale de Zootechnie., 18, 419-436

4. Leite E. R., and Stuth J. W. (1995). Fecal NIRS equation to assess diet quality of free-ranging cattle. Small Ruminant research. 15, 223-230.

5. Lyons R. K. and Stuth J. W. (1992). Fecal NIRS equations for predicting diet quality of free-ranging cattle. Journal of range management. 45, 238-244.

6. Minson D. J. (1990). Forage in Ruminant Nutrition. 483. Academic Press, San Diego, CA.

7. Park R. S., Gordon F. J., Agnew é R. E. Barnes R.J., Steen R. W. J. (1997). The use of near infrared reflectance spectroscopy on dried sample to predict chemical composition and digestibility parameters. Animal Feed Science and Technology (68). 155-167.

8. Redshaw E. L., Mathison G. W. Weisenburger R. D. (1986). Near infrared refelctance spectroscopy for predicting forage composition and voluntary consumption and digestibility in cattle and sheep. Canadian journal of Animal Science. 66, 103-115.

9. TilleyJ. M. A. and Terry R. A. (1963) A two-stage technique for in vitro digestion of forage crops. Journal of the BritishGrassland Society. 18, 104-111.

Agriculture / Animal Biology

Influence of a sugar cane diet on growth performance, carcass traits and meat quality in Creole growing pigs

XAVIER XANDÉ, DAVID RENAUDEAU, EDOUARD DESPOIS, MARIO GIORGI, BRUNO BOCAGE

INRA, Unité de Recherches Zootechniques, 97 170 Petit-Bourg, Guadeloupe (F.W.I)
xavier.xande@antilles.inra.fr

Abstract

The aim of this study was to evaluate a feeding system based on the use of sugar cane on growth performance and meat quality on local Creole breed (CR). Over the 30 to 65 kg body weight range, 3 groups of 12 CR pigs were fed with a control Soya meal-corn diet (C group), with sugar cane fresh juice (SCJ group) or with ground cane stalks (GCS group). Both SCJ and GCS were supplemented with Soya bean meal complement (45.8% crude protein diet).
Growth performance were significantly (P<0.001) affected by treatment. The average daily BW gain was threefold lower in GCS group than in C and SCJ groups. Fatty carcasses were found in C and SCJ diets which contrasted with GCS carcasses. However, the dressing percentage was significantly lower in GCS than C or SCJ groups. According to the indicators of meat quality measured on *longissimus dorsi* muscle, our results suggested a sensitive and technological superiority in C and GCS than in SCJ group.
In conclusion, this study suggests CR pig's ability to reach good growth performance and technological meat quality with a well-formulated sugar cane meal.

Introduction

The potential feed resources for pigs in the tropics are different from those traditionally used in temperate latitudes. Sugar cane is a crop with very high potential for biomass production. It is traditionally cultivated and processed for sugar production. However it can be envisaged as a multipurpose crop with an important role in animal production as non conventional feed resource.
The technology for using sugar cane as the basis of pig feeding is now employed commercially in several tropical country, specially in juice or molasses form (Preston, 1980; Mena, 1981). Nevertheless, there is very little information concerning the use of whole or ground sugar cane stalks for feeding pigs.
The present study was therefore designed to examine the influence of a sugar cane diet on growth performance, carcass traits and meat quality in Creole growing pigs. In fact, according to its low nutritional requirements, it would be assumed that CR pigs might be use in extensive production system, inside a mixed crop farm system, with sugar cane as feeding resource to provide high taste quality niche product to the market.

Materials and Methods

Experimental design and animal management
The effects of dietary treatment based on the use of sugar cane were studied on a total of 36 CR pigs (18 females and 18 castrated males) between 30 to 65 kg BW. This trail was performed at the experimental facilities of INRA in Guadeloupe, a French Caribbean island characterized by a humid tropical climate. Blocks (n=12) were initially composed of 3 littermates and moved at about 20 kg in an open concrete floor experimental room. At the end of the adaptation period, i.e., when animals weighed about 30 kg, one pig per block was randomly assigned to one of the 3 different dietary treatments: a control Soya meal-corn diet containing 15% crude protein and 14.2 MJ DE/kg (C group), a sugar cane fresh juice diet (SCJ group) or a ground cane stalks diet (GCS group). Both SCJ and GCS diets were supplemented with Soya bean meal complement (400 g/d of a 45.8% crude protein diet). Pigs were assumed to be fed close to the ad libitum level and had free access to water.

Measurements
The pigs were weighed every two weeks. Monthly, backfat thickness was measured ultrasonically (Agroscan, E.C.M., Angoulême, France) at the last rib at 45 mm from midline. Average daily feed intake was measured daily for each group as the difference between allowed and refused feed. The brix value and the DM content of sugar cane were measured weekly and the values averaged over monthly periods. Samples of allowed and refused feed were analyzed for dry matter (DM) by drying to constant weight at 65°C in a forced draught oven during 4 days. Dried samples were ground through a 0.75 mm screen before standard chemical analysis.
At about 65 kg, all pigs were slaughtered by electric stunning after a 24-h fasting period. Empty gastrointestinal tract, internal organs and carcass were also weighed. After cooling for 24-h period at 3°C, the carcass was weighed and the left half was dissected according to the normalized European procedure. The carcass lean content was estimated from ham and loin weights, whereas carcass fat content was estimated from leaf fat and backfat weights.
Regarding meat quality parameters, ultimate pH was measured in the *longissimus dorsi* (LD) 6th rib muscle, the day after slaughter. Colour parameters were also measured on LD muscle using a Minolta chromameter CR300 (Minolta, Tokyo, Japan) with reference to reflectance (L*: 0= black, 100 = white) and two colour coordinates, a* (redness) and b* (yellowness).

Statistical analysis
Growth performance, carcass and meat quality traits were submitted to an analysis of variance (GLM procedure, Statistical Analysis Institute, 1997) including the effect of feed, block, sex and their interaction. Means comparison was performed according to the pdiff option of GLM procedure of SAS.

Results and Discussion

The growth performance were significantly (P<0.001) affected by dietary treatment (Table 1). Length of growth period was 52, 65, and 190 days for C, SCJ, and GCS group, respectively. In consequence, the average daily BW gain was significantly lower (P<0.001) GCS group (200 vs. 671 and 557 g/d respectively for C and SCJ pigs).

Table 1: Effect of dietary treatment on growth performance in Creole pigs (least square means)

Treatments	C	SCJ	GCS	RSD	Statistical Analysis
Nb. of pigs	12	12	12	-	-
Duration, d	52.1[a]	64.9[b]	190[c]	14.1	F***
Body weight, kg					
Initial	30.8[a]	29.4[a]	26.2[b]	4.1	F*
Final	64.8	64.6	64.1	2.2	NS
Average daily gain, g/d	671[a]	557[b]	200[c]	61.1	F***

C = soya meal-corn diet; SCJ = sugar cane juice diet; GSC = ground cane stalks diet.
F: effect of feed.
NS: not significant; * P< 0.05, ** P< 0.01, *** P< 0.001.
[a, b, c] Means without common letter differ significantly.

The reduced growth performance recorded in pigs fed with GCS diet resulted from its low energetic level due to the high level of fiber content (i.e., NDF content: 40.8 vs 15.6 and 5.6 g/100g DM GCS vs C and JSC groups, respectively). However, energetic cost at extracting juice (and energy) from GCS diet might be involved in a low efficiency for energy utilization in such diet and then in the low ADG of GCS pigs (table 2). Subsequently, the daily DM intake is reduced in GCS diet in relation with an increase of time dedicated to consumption of GCS diet. On average, daily DM were 1.2, 1.8 and 2.2 kg/day/pigs for GCS, C and SCJ, respectively. To sum up, the low growth performance for the GCS group of pigs was a consequence of a concomitant reduction of the average daily fed intake and dietary energy content.

Carcass performance were also affected by treatment (Table 2). Expressed in g/kg of left carcass weight, fat cuts weight (backfat + leaf fat) was significantly lower in GCS than in other groups (49.6 vs 76.3 g/kg; P<0.001). In contrast, lean cuts weight (ham + loin) was significantly higher in GCS group (282 vs 265, 258 g/kg, GCS vs C, and SCJ respectively; P<0.001). Regarding the carcass drip loss, there were no significant difference between the dietary treatments studied.

Table 2: Effect of dietary treatment on carcass performance in CR pigs (least square means)

Treatments	C	SCJ	GCS	RSD	Statistical Analysis
Slaughter BW, kg	64.8	64.6	64.1	2.2	NS
Dressing percentage, %	80.9[a]	81.1[a]	79.2[b]	1.1	F***
Digestive tract, g/kg	66.1	65.5	68.6	4.6	NS
Internal organs, g/kg	36.4[a]	36.6[a]	32.9[b]	2.7	F***
Carcass drip loss, g/kg	23.0	23.1	27.2	0.3	NS
Lean content, g/kg of left carcass weigh	265[a]	258[b]	282[c]	7.6	F***, S**
Fat content, g/kg of left carcass weigh	74.7[a]	77.8[a]	49.6[b]	10.3	F***
Backfat thickness, mm	37.2[a]	40.6[a]	24.6[b]	6.4	F***

Legend: see table 1.
S: effect of sex.

Our results showed that C and SCJ had fatter carcasses than GCS groups of pigs (Table 2). In fact, the C diet was initially formulated for Large White pigs with higher nutritional requirements than CR pigs (Renaudeau et al., 2005). According to its low growth potential, the high adiposity of CR pigs fed with C diet was related to an increase of extra energy and protein available for lipid synthesis. The high adiposity of SCJ carcasses could be explained by an excess of energy which increase fat deposition. The dressing percentage was significantly lower in GCS than in others groups (79.2 vs 81.0%; P<0.001). This result was mainly related to the higher relative weight of digestive tract in the GCS group due to the high dietary fiber content in the diet.

Whatever dietary treatment, the common indicators of meat quality measured on LD rib muscle, revealed a good quality of the CR pig meat. These results are in accordance with previous trials carried out in our experimental station (Deprès et al., 1992; Renaudeau et al., 2005). Nevertheless, ultimate pH was lower in SCJ group than in GCS and C group (Table 3). Regarding to the colour parameters, SCJ meat was lighter than GSC meat (L* value: 70.5 vs. 62.6, SCJ vs. GCS, respectively). These results suggest that SCJ technological meat quality is not as good as the GCS and C groups. Indeed, a low ultimate pH result in muscle protein denaturation and diminish technological quality of meat (Henckel et al., 2000).

Table 3: Effect of dietary treatment on meat quality in CR pigs measured on LD muscle (least square means)

Treatments	C	SCJ	GCS	RSD	Statistical Analysis
Ultimate pH	5.72[a]	5.45[b]	5.60[c]	0.1	F**, FxS*
Lightness, L*	66.8[ab]	70.5[b]	62.6[a]	5.4	F**
Redness, a*	8.8	8.0	7.0	1.9	NS
Yellowness, b*	6.9	7.1	5.4	1.8	NS

Legend: see table 1.
S: effect of sex.
L* = greater L* value indicates a lighter colour.
a* = greater a* value indicates a redder colour.
b* = greater b* value indicates a more yellow colour.

Conclusion

This study suggests that good growth performance and technological meat quality can be obtained with a well-formulated sugar cane meal. The GSC treatment significantly reduces growth performance but increases carcass lean content and meat quality. In contrast, rather good performances are measured in pigs fed with SCJ but this treatment has detrimental consequences in carcass and meat quality. Further researches are required to elaborate the dietary approach based on use of sugar cane with the aim to find the best compromise between growth performance and meat quality criteria.

References

1. Deprés E., Tamisier F., Naves M., and Rinaldo D. (1992). Comparaison de porcs Créole et Large White pour les performances de croissance et la qualité de la viande en fonction de l'âge d'abattage. *Journées de la Recherche Porcine en France*. **24**, 17-24.

2. Henckel P., Karlsson A., Oksbjerg N., and Petersen J.S. (2000). Control of post mortem pH decrease in pig muscle: Experimental designe and testing of animal models. *Meat Sci*. **55**, 131-138.

3. Mena A., Elliott R., Preston T.R. (1981). Sugar cane juice as an energy source for fattening pigs. *Tropical Animal Production*. **6**, 338-344.

4. Preston T.R. (1980). A model for converting biomass (sugar cane) in animal feed and fuel. *Animal production systems for the tropics*. International Foundation for Science, Stockholm: Pub. No. 8.

5. Renaudeau D., Hilaire M., and Mourot J. (2005). A comparison of growth performance, carcass and meat quality of Creole and Large White pigs slaughtered at 150 days of age. *Animal Research* **54**, 43-54

Agriculture / Animal Biology

How to produce heavy goat carcass with lean meat in Guadeloupe ?

LETICIA LIMEA, GISELE ALEXANDRE, REMY ARQUET, GERARD GRAVILLON, BRUNO BOCAGE

Unité de Recherches Zootechniques
INRA Antilles-Guyane, Duclos 97170 Petit-Bourg, Guadeloupe (F.W.I), France
Leticia.Limea@antilles.inra.fr

Abstract

The objective of the present study was to determine in the Creole goat the effects of an energy-rich diet on the carcass characteristics. Two groups were determined according to the % of concentrate (C) in the diet: C0% and C50%. The chilled carcass yield reached 66 % and 68 % for C0 and C50 animals. The proportion of muscles reached 70 vs 72 %, respectively. Values of the muscle to bone ratio were high: 3.3 vs. 3.7, respectively. Regarding proportions of fat tissues, both groups deposited less subcutaneous than visceral fat. C50 animals deposited more omental fat tissue (3.3 against 1.5 % of carcass weight) than C0 and their fat cover scores were 3 vs. 2 (scale from 1 to 5). The proportion of intermuscular fat did not differ between groups and was around only 8%. From these first results, it seems possible to produce heavy carcass while maintaining low proportions of fat in the meat or low fat cover score. Creole goats exhibits a good potential as meat producer in our region.

Introduction

From a health point of view, ruminant carcass has two major defects: it contains too much fat and the fat is mainly satured or mono-satured with a possible influence on cardiovascular disease in man. Consuming lean meat with low cholesterol content is an important issue for the consumer. Therefore, goats may offer an attractive alternative because they are leaner than cattle and sheep. The Creole goat of Guadeloupe is a small-sized meat breed which is mostly reared on pasture allover the year and produces light (6 to 10 kg) but lean carcass. Although it is a meat breed, very few studies give informations on carcass characteristics of Creole goats (Alexandre, 1987). The objective of the study was to determine the effects of an energy-rich diet on the carcass characteristics of Creole goat.

Materials & Methods

One hundred and forty eight intact male goats from Creole genotype were used in this study. After weaning at 3 months, two groups were determined according to their feeding system. In the first group (C0, n= 106), animals received tropical forage *ad libitum*. In the second (C50, n = 42), they received the same basal diet with commercial pellets (50% of diet DM), composed of maize (68%), soya bean meal (24%), wheat issues (6%) and minerals (2%). The goats were weighed twice a month from weaning to slaughter.

The animals were slaughtered at the end of either 4, 8 or 11 months of growth. The goats were weighed before slaughter (SW). Slaughtering was made following commercial procedures. The main body components were weighed: head, feet, skin, full and empty gastrointestinal tract, intestinal and mesenteric fats, and red organs. The carcass (including kidney and kidney fat) was weighed before and after cooling (at 4°C during 24h). Then the chilled carcass was graded according to conformation, colour of the meat and fat cover scores (3 different scales of 5 points). The left half carcass was used for carcass cutting according to standard methods and procedures (Colomer-Rocher et al. 1987), and for dissection of the shoulder.

The chilled carcass yield was calculated as cold carcass weight related to empty body weight (slaughter weight subtracted by the value of full gastrointestinal tract).

After the dissection of the shoulder of the half left carcass, the muscles, the bone and the intermuscular fat were weighed. The proportion of muscles, returned to the weight of the shoulder and the ratio of muscle weight to bone weight were then calculated .

Results & Discussion

1. Variation of slaughter weight

The slaughter weights varied from 13.5 to 42.0 kg according to the diet and the fattening duration. The heavier SW were observed with the energy-rich diet (45 % of C50 goats weighing 31 kg or more) while the lighter for the forage diet (50 % of C0 weighing 19 kg or less). For both groups, 24 kg of SW seemed to be an interesting alternative (45 % of animals reaching this weight whatever the diet). The three intermediate SW were taken into account for comparisons.

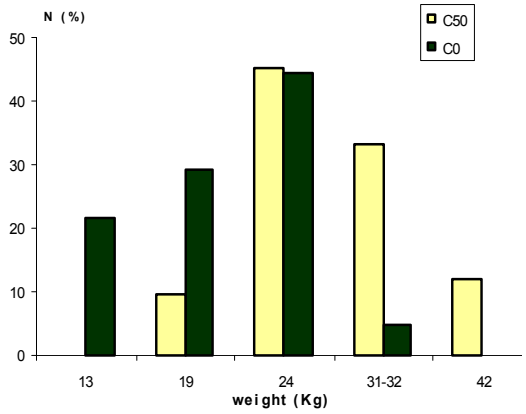

Figure 1: 1: Proportion of goats according to slaughter weight and diet

2. *Carcass yields and characteristics*

At 24 kg, the chilled carcass yield were similar and were around, 64 % and 66 % for C0 and C50 groups. However, the cold carcass weights were different: 9.2 vs. 11.4 kg, respectively (table 2). These results are in agreement with the effect of a diet rich in energy and proteins that generated higher growth and heavier carcasses. The notes of conformation (on a scale of 1 to 5) were on average 3.6 ± 0.6 for the C0 group and 4.2 ± 0.5 for the C50.

slaughter weights (Kg)	C0		C50	
	CCW (Kg)	Muscles (%)	CCW (Kg)	Muscles (%)
19	7.1	68.9	9.1	70.0
	±0.9	±2.4	±0.6	±1.5
24	9.2	71.8	11.4	72.3
	±0.9	±3.0	±1.0	±2.7
31-32	12.1	69.0	15.5	72.8
	±1.7	±6.4	±1.4	±4.0

Table 2: Cold carcass weights (CCW) and proportion of muscles (mean ± S.D) at 19, 24 and 32 kg of SW in Creole bucks according to the diet.

3. *Proportion of muscles and the muscle to bone ratio*

At 24 kg SW, the proportion of muscles (table 2) was 70 % for the C0 and the muscle to bone ratio was 3.4. Same traits for the C50 were 72 % and 3.7, respectively. Values for the other SW (19 and 31 kg) are reported in table 2. These results shown that the quantity of meat varies slightly from a diet to another and is high comparing to other breeds (Alexandre 1987; Warmington and Kirton , 1990).

4. *Proportion of fat tissues*

Regarding proportions of fat tissues, both groups deposited less subcutaneous than visceral fat. The fat cover scores (scale from 1 to 5) varied from 1.2 to 2.4 for C0 and from 2.8 to 3.6 for C50 (table 3). The subcutaneous fat cover is thin and poorly developed as reported by many researchers that have studied different breeds or management (see review of Warmington and Kirton ,1990). The weights of omental fat tissue varied from 39 to 206 g for the C0 group and from 267 to 1068 g for the C50. Thus, an energetic diet seemed to encourage the synthesis of fat by the animal. However the fat is deposited at higher rates in the abdominal area than as as body fat reserves (Colomer-Rocher et al.,1992). The proportion of intermuscular fat (IF) did not differ between groups and was low. Values of IF according to SW, were around 5.4 to 10.9 for the group fed only with forage, and 6.5 to 8.1 for the group receiving supplements.

Leanness is a common feature of goat carcasses (Warmington and Kirton, 1990, Gallo et al.,1996) and was also observed in this study on Creole goat of Guadeloupe.

slaughter weights (Kg)	C0		C50	
	FCS	OF/CCW(%)	FCS	OF/CCW(%)
19	2.1	1.3	3.3	2.9
	±0.7	±0.8	±1.0	±0.2
24	2.4	1.5	2.8	2.5
	±0.8	±0.8	±0.9	±1.1
31-32	2.0	1.7	3.1	4.3
	±0.0	±1.0	±1.1	±1.8

Table 3: Fat cover scores (FCS) and ratio of omental fat (OF) on cold carcass weights (CCW) (mean ± S.D) at 19, 24 and 32 kg of SW.

Conclusions

In view of all these first results, an energy-rich diet allows high carcass weights and yields. The feeding mode influences the carcass quality of the Creole goat. While becoming heavy, the proportions in muscles therefore in meat improve. The fat tissues that accumulate, essentially localized in the visceral area, doesn't alter the quality of the commercial carcass. It seems possible to produce heavy carcass while maintaining low proportions of fat in the meat. Creole goats exhibits a good potential as meat producer in our region. Assuming that the diet influences the fatty acid profiles of caprines further studies are required to characterise the fatty acid profile of this breed and to assess the diet influence.

References:

1. Alexandre, G. (1987). The production of goat meat and carcass quality in humid tropics. *In 4th IGC*, 195-209.

2. Colomer-Rocher, F., Morand-Fehr, P. and Kirton, A.H. (1987). Standard methods and procedures for goat carcass evaluation, jointing and tissue separation. *Livestock Production of Science,* **17**, 149–159.

3. Colomer-Rocher, F., Kirton, A.H., Merces, G.J.K. and Duganzich, D.M. (1992). Carcass composition of New Zealand Saanen goats slaughtered at differents weights. *Small Ruminant Research,* **7**, 161–173.

4. Gallo, C., Le Breton, Y., Wainnright, I. and Berkhoff, M. (1996). Body and carcass composition of male and female Criollo goats in the South of Chile . *Small Ruminant Research,* **23**, 163–169.

5. Warmington, B.G. & Kirton, A.H. 1990. Genetic and non-genetic influence on growth and carcass traits of goats. Small Ruminants Research. 3, 147-165.

Table of contents

Marine Biology / Bacteriology

Marine Biotechnology in the Caribbean: Study of *Codakia orbicularis* Gill Proteins 155
J.P.F. Gourdine and E.J. Smith-Ravin
The Post Larval Settlement of Fishes on a Coral Reef of Guadeloupe (FWI) 157
Y. Frejaville, Y. Bouchon-Navaro, M. Louis and C. Bouchon
Antimicrobial Substances from Marine Bacteria 159
C. Walters
The CHALOUPE Project: Global Change, Dynamics of Exploited Marine Diversity, and Viability of Fisheries 161
F. Blanchard and O. Thèbaud
A Spatial and Temporal Study of the Benthic Communities in the Coral Reefs of the Bay Islands, Honduras 163
P. Portillo, Y. Bouchon-Navaro, M. Louis and C. Bouchon
Significance of Environmental Variables for the Structure of Fish Assemblages in the Lagoon of the Grand Cul-De-Sac Marin (Guadeloupe – FWI) 165
A. Vaslet, C. Bouchon, Y. Bouchon-Navarro and M. Louis
Seagrass Beds as Important Habitats for Juvenile Fishes in the Bay of the Grand Cul-De-Sac Marin (Guadeloupe, F.W.I.) 167
D. Kopp, Y. Bouchon-Navarro, C. Bouchon and M. Louis
Colonization of Sunken Wood in the Caribbean Area: Influence of the Environment 169
M.C.Z. Laurent and O. Gros
Bacterial Symbiosis in Wood Fall Bivalves 169
M.C.Z. Laurent and O. Gros
Description of the Extracellular Bacterial Interactions in Marine Nematodes From t*halassia testudinum* Environment 170
L.C. Maurin and O. Gros
Observation of Marine Nematodes Along a Transect Beach-Seagrass Beds of t*halassia testudinum*: a SEM Analysis 170
L.C. Maurin, C. Grateloup, M. Delannay and O. Gros

Marine Biology / Bacteriology

Marine Biotechnology In The Caribbean: Study Of *Codakia orbicularis* Gill Proteins

Jean-Philippe F. GOURDINE, Emilie Juliette SMITH-RAVIN

Université Antilles Guyane, Pointe à Pitre, 97159 GUADELOUPE - jsmithra@univ-ag.fr

Abstract

The white clam, *Codakia orbicularis* (Linné, 1758), a tropical bivalve widely consumed in the Caribbean, inhabits the sulphur-containing sediments inherent to phanerogam seagrass beds. It possesses sulfur-oxidizing endosymbiontic bacteria localized in specialized cells in its gills. We presumed the existence of gill proteins of interest which would be required for adaptation to the stressful environmental conditions, particularly to the presence of sulphur and of sulfo-oxidizing bacteria. The full-length cDNA of its major gill protein had been successfully recovered using molecular biology techniques. This protein, named Codakine, is a dimeric mannose binding C-type lectin which might be involved in symbiosis process and immune defense. Future prospective work will involve the use of codakine against pathogenic organisms and symbiotic bacteria. These results reinforce the interest which should be put in marine biotechnology research in the Caribbean.

Introduction

The Caribbean islands and Brazil are the fourth biodiversity hotspot in the world concerning terrestrial or marine fauna and flora. Marine environments present a great genetic diversity and a number of ecosystems scarcely known *(Myers et al. 2000)*. This important biodiversity and the potential activities of isolated compounds should aim to the development of fundamental and practical research in marine biotechnology. This development is necessary in order to value the potential applications of the isolated products in health and environmental areas. Consequently our studies were carried out on the white clam *Codakia orbicularis* (Linné, 1758). This bivalve lives in sandy sulfured sediments of phanerogam-based ecosystems (*Thalassia testidunum*). Considering the stressful conditions of its habitat, presence of hydrogen sulfide and the symbiotic sulfo-oxidizing bacteria living in its gills, we might expect to isolate compounds of biotechnological interest *(Berg and Alatalo 1984)*. Studies on gill proteins of *C. orbicularis* on sodium dodecyl sulfate polyacrylamide gel electrophoresis (SDS-PAGE) in presence of DTT and lectin blotting assay, show a prominent weakly glycosylated protein of about 14 kDa on which we decided to focus our attention *(Gourdine and Smith-Ravin 2002)*.

Materials & Methods

From the 14kDa band, a partial peptide sequence were deduced using matrix assisted laser ionisation/desorption time of flight mass spectrometry (MALDI-TOF MS/MS). Polymerase chain reaction (PCR) was used on clones derived from a cDNA library of *C. orbicularis* and degenerate oligonucleotides in order to isolate the corresponding gene *(Gourdine and Smith-Ravin 2006)*. Bioinformatics softwares (BLAST, CLUSTALW, Rosetta software, etc.) were used to establish first, second and tertiary structures of the 14 kDa protein. According to bioinformatics analysis, we have decided to purify the protein, to perform chromatography on mannose-agarose column. *(Gourdine and Smith-Ravin 2006)*.

Results & Discussion

Electrophoretic profile of total gills protein of C. orbicularis is presented in figure 1. All the extraction buffers used show the presence of the major 14 kDa protein. The cDNA sequence of the major protein named codakine (Genbank AAX19697) is of 447 base pairs corresponding to 135 aminoacids (Fig.2).

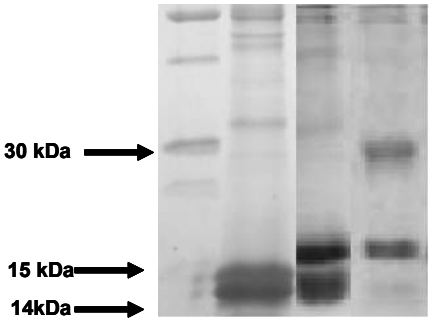

Fig. 1 : 18 % SDS-PAGE of total gill proteins of C. orbicularis ;
Lane 1 standard molecular weight markers.
Lane 2 CHAPS extraction buffer plus DTT ;
Lane 3 : Tris-HCl extraction buffer plus DTT ;
Lane 4 : Tris-HCl extraction buffer minus DTT

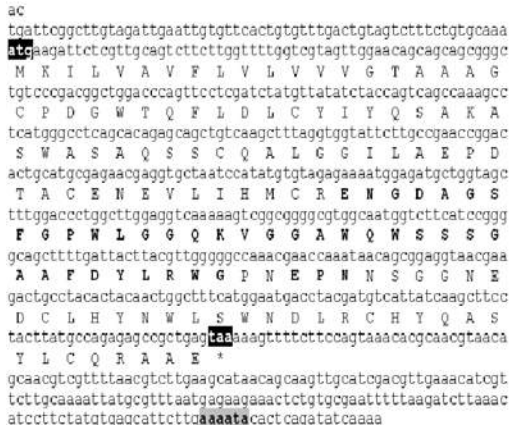

Fig.2 : cDNA derived aminoacid sequence of Codakine (Genbank AAX19697). Initial aminoacid sequence found by MALDI-TOF MS/MS is indicated in bold. The initiator and stop codons are shaded in black, and a potential polyadenylation signal is shown in bold and shaded in grey.

Theoretical isoelectric point and molecular weight confirmed the previous work (16.087 kDa, pI 4.72) peptide *(Gourdine and Smith-Ravin 2006)*. Bioinformatics analysis of cDNA sequence showed Codakine as a mannose-binding C-type lectin. Affinity chromatography on mannose-agarose column confirmed that Codakine is a homodimeric calcium-dependant mannose-binding lectin (14 kDa for each monomer) which contains a 2 kDa signal peptide *(Gourdine et al. 2006a)*. Codakine presents homologies with vertebrates and invertebrate lectins involved in immune system, cellular mediation and sulphur-oxidizing bacterial symbiont mediation (Gourdine et al. 2006b). Research works are underway to define the role and action of codakine *in vivo* and *in vitro* experiments.

Acknowledgements

We are grateful to Dr Nick TOTTY from Cancer Research Council (United Kingdom), Dr P. GREENWELL, Dr M. DWEK, Dr S. RUGOOPUTH and A. MARKIV (University of Westminster,London) for their supports.

References:

Berg, C.J., and Alatalo, P. 1984. Potential of chemosynthesis in molluscan mariculture. *Aquaculture* **39:** 165-179.

Gourdine, J.-P., Markiv, A., Rugooputh, S., Greenwell, P., Dwek, M.V., and Smith-Ravin, E.J. 2006a. Characterization of Codakine, a new Mannose-Binding Lectin from the gills of the tropical clam *Codakia orbicularis in preparation*.

Gourdine, J.-P., Markiv, A., and Smith-Ravin, E.J. 2006b. Computational analysis of Codakine and marine related homologues, reveals a common C-Type lectin folding *unpublished data*.

Gourdine, J.-P., and Smith-Ravin, E.J. 2002. Electrophoretic separation of gill proteins of the clam *Codakia orbicularis*. *Prep. Biochem. Biotechnol.* **32:** 341-353.

Gourdine, J.-P., and Smith-Ravin, E.J. 2006. Analysis of a cDNA-derived sequence of a novel mannose-binding lectin, codakine, from the tropical clam Codakia orbicularis. *Fish and Shellfish Immunology, submitted*.

Myers, N., Mittermeier, R.A., Mittermeier, C.G., da Fonseca, G.A., and Kent, J. 2000. Biodiversity hotspots for conservation priorities. *Nature* **403:** 853-858.

Marine Biology / Bacteriology

The Post-Larval Settlement Of Fishes On a Coral Reef Of Guadeloupe (FWI)

Y. FREJAVILLE, Y.BOUCHON-NAVARO, M. LOUIS, C. BOUCHON

Laboratoire de Biologie Marine – DYNECAR, Université des Antilles et de la Guyane
Campus de Fouillole, B.P. 592, 97159 Pointe-à-Pitre, Guadeloupe - Yann.Frejaville@univ-ag.fr

Abstract

In order to study qualitatively and quantitatively the specific phase of settlement of coral reef fishes, 18 monthly samplings of 24h were carried out on a coral reef located in the southeast coast of Guadeloupe. A total of 3 867 fishes representing 50 families were sampled. Redundancy analysis showed that settlement occurred almost only at night, preferably during the new moon phase; strong winds pushing the large pelagic patches of post larvae in direction of the coast, associated with high swells and current speeds carrying them on the reef were also very favourable to settlement.

Introduction

The early life of most coral reef fishes is pelagic, from the egg to the post larval stage. At the end of this stage that can last from 2 to 12 weeks, the fishes must find a coral reef to settle (Doherty, 1982). Then the fishes will quickly loose their pelagic adaptations to become juveniles, very similar to the adult form and begin their demersal life on the reef.

The interannual variations of the size of exploitable coral fish stocks is mainly governed by the quantity of fishes settling on the reefs each year, then by the mortality rate affecting them after their settlement (Shima, 1999).

The coral reef fishes represent an extremely important food resource for the countries of the intertropical zone. However, this crucial phase of the life cycle of reef fishes, conditioning the dynamics of exploited stocks, has never been studied in the Lesser Antilles. It thus seemed important to carry out a study of the flow of post-larvae settling on the reefs of Guadeloupe in order to know better their abundance, taxonomy and the environmental factors influencing their settlement.

Materials & Methods

From October 2003 to December 2004, 18 monthly samplings of fish post-larvae were conducted at different moon phases, on the coral reef of a small islet (îlet Gosier) located in southeast coast of Guadeloupe. During each field trip, fishes were sampled every 2 hours during 24 hours.

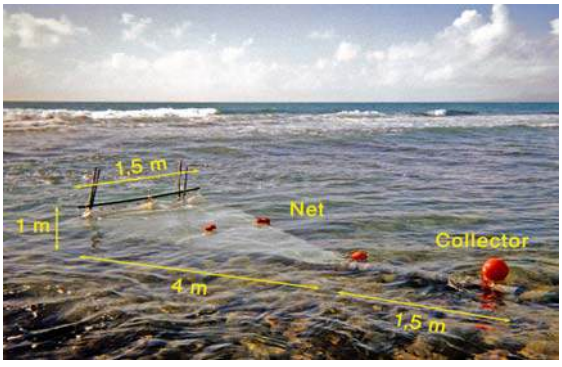

Fig. 1 : the sampling device.

The sampling device used was a crest net of pyramidal shape (fig. 1) fixed on the reef flat, facing the surge at approximately 50m of the reef crest. The drifting vegetal material (leaves of marine Phanerogams mostly) and the post larval fishes (Fig. 2) trapped by the net were retained in a tubular collector. Every 2 hours, the sample was collected and fixed with a 5% formalin solution for later identification and treatment.

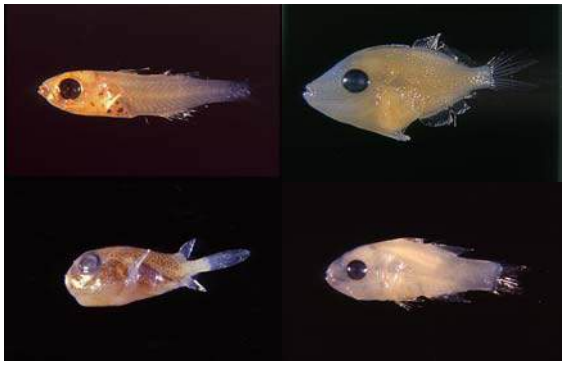

Fig. 2 : Post-larval specimens of Gerreidae, Monacanthidae, Diodontidae and Apogonidae.

In the same time, several environmental factors were measured: current speed, swell, nebulosity, rainfalls, speed and direction of the wind, state of the tide, state of the nycthemeral cycle, presence of the moon and moon phase, weight of drifted vegetal material, physicochemical parameters of the sea water.

In order to relate the characteristics of the incoming flow of settling post-larvae (numerical abundance, number of families, species diversity and equitability) with the environmental factors measured, the redundancy analysis (RDA) was used (software: CANOCO).

Results & Discussion

A total of 3 867 fishes representing 50 families were sampled. The most abundant families were represented by Gobidae (over 50% of the total captures), Clinidae, Scaridae, Clupeidae, Labridae and Gerreidae (Fig. 3). The most frequently captured families are the Gobidae (present in 43% of the samples), Scaridae (24,5%), Gerreidae (23,6%), Labridae (16,6%) and Clinidae (16,2%).

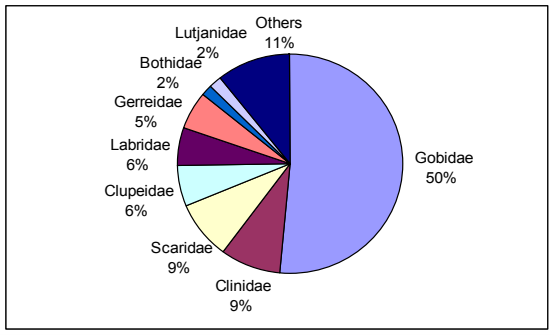

Fig. 3 : relative taxonomic composition of the settlers.

As it was observed in similar studies carried out in the Pacific (Dufour and Galzin, 1992), the post-larval settlement occurred almost exclusively at night (88,5% of the total captures). The intensity of settlement (expressed in individual per thousand cubic meter of filtered water) increased after dusk (fig. 4), then showed a peak during the second part of the night, and decreased at dawn. On the other hand, between 10 a.m. and 2 p.m., when sunlight is maximal, the settlement rate was very low (0.9% of the total captures).

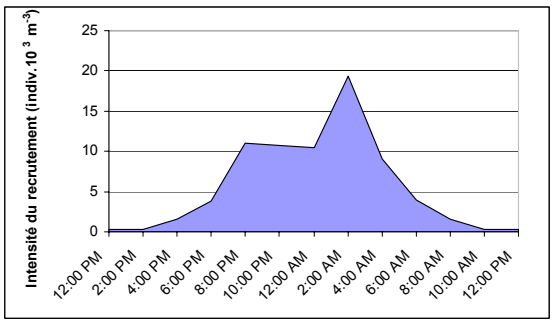

Fig. 4 : nycthemeral variations of the settlement intensity.

Among the 23 environmental variables introduced in the RDA, five had a significant statistical influence on the fish settlement (fig. 5), two were quantitative and three qualitative. They explained 38.6% of the total variance.
Axis 1 was correlated to the variable "swell" (r = 0.75), "daylight" (r = 0.58) and "current" (r = 0.59). Numerical abundance, family richness, diversity and equitability of the settlers were positively related to swell and current and negatively related to daylight on this axis.
Axis 2 was correlated to the variable "south wind" (r = 0.68), which was opposed to the variable "full moon". Abundance of the fishes was positively correlated to "south wind" and negatively related to the "full moon" on axis 2. But, the canonical coefficients are very low on this axis.
The predominant nocturnal settlement and the negative effects of sunlight and full moon on the abundance of post-larvae traduce an important negative phototropism of the settlers. This is probably intended to reduce their vulnerability to the predators hunting by sight that abound on the reefs.
The results of the RDA also showed that strong south winds played an important role in settlement by pushing the large pelagic patches of post-larvae in direction of the coast, when they come back to the surface during the night.
Moreover, high swells and currents carrying the settlers on the reef are also important factors explaining the variability of settlement. Strong hydrodynamic conditions, unfavourable to predation, may provide additive protection to the settlers.

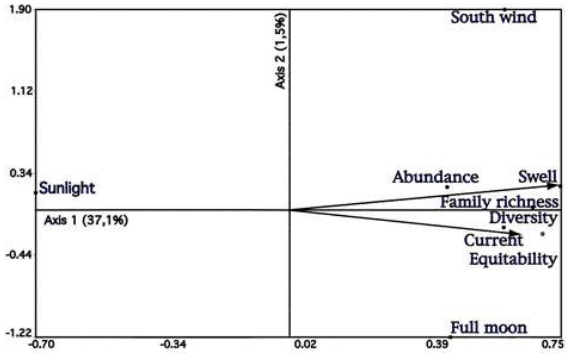

Fig. 5 : projection (biplot) of the redundancy analysis.

The average settlement rate calculated for the studied reef was 9 fishes per linear meter of reef front and per hour, representing around 80 000 settlers per meter and per year. However, in order to extrapolate those results to the whole island of Guadeloupe and thus to estimate the recruitment of fish in exploitable stocks, it would be necessary to undergo similar studies on various coasts of the island, under various influences of the trade winds and during several years (Robertson and Kaufmann, 1998) because of the importance of inter-annual variability in settlement rates.

References:

1. Doherty, P.J., (1982). Some effects of density of the juveniles of two species of tropical territorial damselfishes.
J. Exp. Mar. Biol. Ecol. 65, 249-261

2. Shima, J., (1999). Variability in relative importance of determinants of reef fish recruitment.
Ecol. Lett. 2, 304-310.

3. Dufour, V., Galzin, R., (1992). Le recrutement des poissons récifaux de Polynésie française, impact sur la dynamique des peuplements et conséquences sur la gestion des stocks.
Cybium 16 (4), 267-277.

4. Robertson, D., Kaufmann, K. (1998) Assessing early recruitment dynamics and its demographic consequences among tropical reef fishes: Accommodating variation in recruitment seasonality and longevity.
Australian Journal of ecology 23, 226-233.

Marine Biology / Bacteriology

Antimicrobial Substances From Marine Bacteria

CARL WALTERS, MARILAINE MOTA-MEIRA AND MARC LAVOIE
Department of Biological and Chemical Sciences, The University of the West Indies, Cave Hill Campus P. O. Box 64, Bridgetown BB 11000 Barbados
cwalters582@yahoo.com, motameira@yahoo.com , mlavoie@uwichill.edu.bb

Abstract

The arsenal of effective antibiotics used in clinical medicine is decreasing in the face of emerging antimicrobial resistance mechanisms. Thus, there is increasing need to find new sources of inhibitory substances. One such source is the marine environment, with its abundance of organisms that would undoubtedly have developed unique metabolic and physiological capabilities that ensure survival in diverse habitats. These capabilities offer the potential to produce metabolites that would not be observed from terrestrial microorganisms. A total of 373 isolates obtained from marine samples (sea weed, sea water, coral and sponge) were screened and of these isolates, 55 (15%) produce an inhibitory substance active against at least one indicator microorganism (*Micrococcus luteus, Staphylococcus aureus, Escherichia coli, Salmonella enteritidis, Enterococcus faecalis* and *Candida albicans*). However, only 5 (9%) isolates produce their inhibitory substance in liquid medium. These results clearly show the marine environment to be a source worth investigating for potentially novel inhibitory substances.

Introduction

The most important medicines and antibiotics in use today were obtained from terrestrial microorganisms. However, the arsenal of effective antibiotics used in clinical medicine is decreasing with the increased antimicrobial resistance among microorganisms. Thus, there is a need to find new sources of inhibitory substances. One such source is the marine environment. Work carried out by Rosenfeld and Zobell in 1947, showed that marine microorganisms are capable of producing antibacterial substances. More recent work include bacterial isolates that show fungicidal activity (1,6). Further more, marine invertebrates have also been shown to produce substances that are antagonistic towards clinically isolated antibiotic-resistant bacteria (3) as well as terrestrial bacteria (8).

The aims of this study are to *i)* to detect bacterial antagonistic substances among marine isolates, *ii)* to assess the activity spectra of these substances against different bacterial pathogens, *iii)* to optimize the production of these antibacterial agents in liquid media, *iv)* to purify them and *v)* to determine their chemical nature.

Materials and Methods

Marine samples were collected and screened for presence of bacterial isolates. Afterwards, the deferred antagonism assay was carried out to determine whether they produce an antimicrobial substance. Isolates producing inhibitory substances were preliminary identified and stocked in the isolation medium with 20 % glycerol at -20^{o}C and -80^{o}C. Subsequently, the production of the antimicrobial substance in broth culture was carried out.

Results and Discussion

The marine environment and the bacteria therein is becoming an important source for microbial products due to the likelihood that they would possess a greater molecular diversity than do their terrestrial counterparts (2). Thus the high number of antimicrobial substance producing strains observed (15%) is of particular importance (Table 1).

Table 1: Number of producing isolates from different sources.

Source	# of isolates obtained	# of isolates producing an inhibiton zone	% of isolates producing an inhibition zone
Sea weed	134	17	13
Sea water	65	6	9
Coral	34	0	0
Sponge	141	32	23
Total	373	55	15

The inhibitory isolates were more active against *M. luteus* and two were active against yeasts (Table 2).

Table 2: Inhibition of indicator strains by marine isolates.

Indicator Strain	# of isolates producing an inhibiton zone
Gram positive bacteria	
M. luteus	45
S. aureus	1
M. luteus and *S. aureus*	4
M. luteus, S. aureus and *E. faecalis*	2
Gram negative bacteria: *E. coli* and *S. enteritidis*	1
Yeast: *C. albicans*	2

Most of these producing isolates were from sponges (Table 1). Metabolites previously ascribed to sponges have been recently demonstrated to be synthesised by microbial symbionts of sponges (5). Sponges are also one of the richest sources of both biologically active secondary metabolites and chemical diversity (4, 7). The high percentage of isolates producing their inhibitors in liquid medium (9%) will permit an easier purification.

Of the isolates producing in liquid medium, only one gave clear inhibition zones. This isolate was identified as being a member of the genus *Staphylococcus*. Two other isolates (an *Actinomycete* and a *Bacillus*) produced their antagonistic substance in liquid medium. Bacteria from these genera are know to produce clinically important medicines.

Conclusion

There is a high rate of marine bacteria (especially from sponges) that are capable of producing microbial inhibitors. Also, an important proportion of these inhibitors are produced in liquid cultures and further work is needed to characterise these inhibitory substances.

Acknowledgements

Thanks to the Caribbean Health Research Council for funding the project, the Department of Biological and Chemical Sciences of the University of the West Indies, Cave Hill Campus and Renata Goodridge for collecting the samples used in this project.

References

1. Buck, J. D. *et al*. 1962. Inhibition of Yeast by a Marine Bacterium. J. Bacteriol. 85: 1132-1135
2. Belarbi, E. H. *et al.* 2003. Producing Drugs from Marine Sponges. Biotechnology Advances. 21: 585-598
3. Jang, W. S. *et al.* 2003. Biological Activities of Synthetic Analogs of Halocidin, an Antimicrobial Peptide from the Tunicate *Halocynthia aurantium*. Antimicrobial Agents and Chemotherapy. 47: 2481–2486
4. Kijjoa, A and P. Sawangwong. 2004. Drugs and Cosmetics from the Sea. *Mar. Drugs*. *2*: 73-82
5. Lee, Y. K. *et al.* 2001. Microbial Symbiosis in Marine Sponges. The Journal of Microbiology. 39: 254-264
6. Oleinikova, G. K. *et al*. 2001. Cyclic lipopeptides with fungicidal activity from the sea isolate of the bacterium *Bacillus subtilis.* Russ. Chem. Bull., Int. Ed., 50: 2231-2235
7. Proksch, P. *et* al. 2003. Drugs from the Sea - Opportunities and Obstacles. Mar. Drugs. 1: 5-17
8. Zheng. L. *et al*. 2005. Antimicrobial screening and active compound isolation from marine bacterium NJ6-3-1 associated with the sponge *Hymeniacidon perleve*. World Journal of Microbiology and Biotechnology. 21: 201-206

Marine Biology / Bacteriology

The CHALOUPE project: global change, dynamics of exploited marine biodiversity, and viability of fisheries.

Fabian Blanchard and Olivier Thébaud
1 Ifremer, Fisheries Resources laboratory of French Guyana, BP 477, 97331 Cayenne, French Guyana.
2 Ifremer, Marine Economy Department, BP 70, 29280 Plouzane Cedex, France.
Fabian.Blanchard@Ifremer.fr

Abstract

The CHALOUPE project, global change, dynamics of exploited marine biodiversity, and viability of fisheries, is a multidisciplinary research programme which objective is to provide a diagnostic on the bio-economic factors that lead major changes observed in the fisheries in three different types of ecosystems at the scale of the last decades.

Three case studies are the basis of the study : the up-welling system of south Morocco, the open temperate continental shelf of the Bay of Biscay (France) and the tropical continental shelf of French Guyana under Amazonian influence. The main factors driving changes differed among ecosystems : climate change (or variability), overexploitation and impact of fishing on biodiversity, globalisation of the seafood market, incentives.

In French Guyana, the objectives will focus on the impact of trawling shrimp fisheries and of climate change on the biological communities, the effects of the "El Niño"/"La Niña" events on shrimp recruitment and the economic consequences of measures to mitigate biodiversity impact through bio-economic modelling.

Introduction

Major changes are currently being observed in marine ecosystems and in the human activities, particularly fishing, that depend upon them. If the ecosystems are sustainable naturally, the observed changes raise growing concerns, both in terms of the loss of biodiversity of marine populations, and in the capacity of the communities to absorb these changes without being radically transformed. These worries apply to the sustainability of fisheries.

The effects of fishing and of climate change have by now been identified as key factors in the evolution of marine populations and communities. The effect of this evolution on fisheries specifically has been that its development operates in a context of failed regulations on access to resources. The extent of these changes and the relative weight of different factors on a regional scale have yet to be quantified. This is the principal objective of the CHALOUPE Project.

The anticipated output of the project is an assessment of the observed changes, evolutionary factors, and the sustainability of communities/ fisheries systems in three types of regional ecosystem : the temperate continental shelf of the Bay of Biscay, the tropical shelf of French Guyana, and the up-welling ecosystem of Morocco. The Chaloupe projet will be presented here focusing on the French Guyana case study.

The output is dependent upon the compilation and combined analysis of chronological series data related to environmental conditions, character-istics of populations and fisheries, fisheries econo-mics, and the evolution of governance, as well as system modelling.

The project, which will last three years (2006-8), benefits from financing by the National Research Agency (France), obtained under the framework of the 'Biodiversity 2005' call for appeals, and put together by teams working on fisheries ecology, economy, and modelling. It is coordinated by Ifremer (F. Blanchard and O. Thébaud), the French research institute for the exploitation of the sea.

Material and Methods

Two complementary approach are developed within Chaloupe : statistical analyses of biological and economic data sets and modelling of the bio-economic systems. Hence four work-packages (WP) were designed :

WP1) ecological dynamics : analyses of the temporal variations of environmental factors (sea surface temperatures, bottom temperatures, salinity, up-welling index…), analyses of the community changes from trawling sampling survey data

WP2) economic dynamics : description of the institutional and management context of fisheries, analyses of the temporal changes of the fisheries landings in biomass and monetary value, analyses of the changes in price of the seafood products…

WP3) integrated sets of multi-disciplinary indicators for state diagnostic of the ecosystem and fisheries: implement a

methodology of economic and bio-ecological indicator boards that summarized the knowledge on the state diagnostic as short reports

WP4) modelling of the functioning of the biological community/exploited resource/fishery taking into account driving factors (such as climate change and/or market changes for example)

Preliminary results in the French Guyana case study

WP1) Environmental data analysed were mainly SST (sea surface temperatures) collected from the ICOADS data set available from internet. The data showed a significant increase of the SST occurring from 1994-1995 of about 0.6°C (Figure 1). This increase can be locally greater than 1°C.

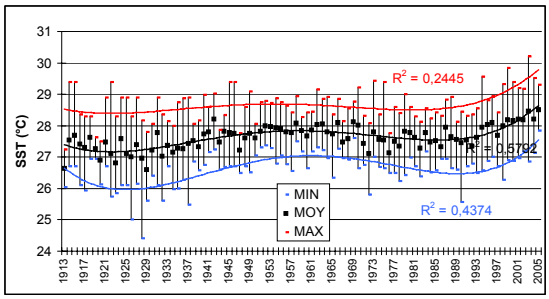

Figure 1. Temporal variations of the yearly averaged sea surface temperatures (SST in °C) in black squares, the minimal and maximal monthly value observed in the year and polynomial fit of these 3 variables with the r-squared value.

According to low seasonal variability, this could have impact on the fish community composition as compared to the situation of the Bay of Biscay where the most sub-tropical species became dominant (Blanchard and Vandermeirsch, 2005; Poulard and Blanchard, 2005). The analyses of community changes will be carried out using data from demersal trawling surveys carried out during the wet and dry season in 1992, 1993 and 1994 in French Guyana. Three new surveys will be then carried out according to the same sampling scheme.

WP2) The economic analyses will be focused on the shrimp fishery. Surveys will be made by inquiring the directors of the companies. Decrease of the shrimp price since 2000-2001 due to the arrival of shrimps from farming on the market as well as the increase of oil seems to be the most important factors.

WP3) Bio-economic indicators will then be choose to characterise the state of the system.

WP4) The bio-economic model of the shrimp fishery developed by C. Chaboud (IRD-France) in Madagascar will be modified and adapted to the Guianese case. Data from field get by Ifremer since three decades will be used to the parameterisation and build environmental scenarios as well as mitigation measures to avoid biodiversity impacts (turtle excluding device, by-catch reducing device, interaction with frigatebirds feeding on discards).

Discussion

These works will contribute to a more holistic approach of the fishery management. It is usually call the ecosystem approach to fisheries and is in fact the applying of the principle of sustainable development : social equity and welfare, environment friendly and economic efficiency. However, according to this principle the human aspect remain here poorly known and studied; one more next step (among other possible) would be to integrate social sciences to be able to get also a diagnostic on the fishermen communities.

References

Poulard, J-C., and Blanchard, F. (2005). The impact of climate change on the fish community structure of the eastern continental shelf of the Bay of Biscay. *ICES Journal of Marine Science* **62**, 1436-1443.

Blanchard, F., and Vandermeirsch, F. (2005). Warming and exponential abundance increase of the subtropical fish *Capros aper* in the Bay of Biscay (1973–2002). *Comptes-Rendus Académie des Sciences, série Biologies* **328**, 505-509.

Marine Biology / Bacteriology

A Spatial and Temporal Study of the Benthic Communities in the Coral Reefs of the Bay Islands, Honduras

PEDRO PORTILLO, YOLANDE BOUCHON-NAVARO, MAX LOUIS, CLAUDE BOUCHON

Laboratoire de Biologie Marine-DYNECAR, Université des Antilles et de la Guyane,
BP 592, 97159 Pointe-à-Pitre, Guadeloupe, France
pportill@univ-ag.fr

Abstract

A study was conducted on the benthic communities of the coral reefs of the Bay Islands of Honduras (Utila, Roatán and Guanaja) with the objectives to describe in what way coral communities are organized and to identify the factors that influence the coral distribution around the Bay Islands. A total of 92 sites was surveyed qualitatively on the reefs according to different depths, reef geomorphological units, geographical location and different sectors of local pollution pressure. Data were analyzed by a canonical correspondence analysis in which species composition surveys were correlated to geomorphological, geographical and pollution factors used as ecological and anthropogenic explanatory variables. Three different coral communities were identified. Their distribution is explained in 21 % by reef geomorphological factors, 7 % by bacterial and chemical pollution pressure and 4 % by a latitudinal gradient. A total of 50 coral species was found. No differences were found for coral species richness and community distribution between the three islands. Species richness varied from 10 to 34 species according to the stations and increased from the reef flats toward the fore reefs with a maximum of species richness between 10 to 25 m. The average number of species was 17.5 (±0.9) on the reef flats, 20.8 (±1.8) on the upper part of the fore reefs and 23,9 (±1.6) on the lower part between 10 to 25 m.

Introduction

The Bay Islands of Honduras are located in the south western part of the Caribbean Sea 40 to 50 kilometers off the Honduran north coast by 16° to 16°30' N and 85°50' to 87° W extended within a southwest-northeast axis. It is an archipelago composed of three major reef islands (Utila, Roatán and Guanaja), three minor islands and about 65 coral cays (Fig. 1).

The Bay Islands have a highly developed coral reef system composed of fringing reefs around the island of Utila and on the south coast of Roatán and Guanaja. Barrier reefs are found mostly on the north coasts of Roatán and Guanaja. Extended reef flats characterize the windward side of the islands in contrast to the leeward side where the reef flats are narrower and where the outer reef slope drop abruptly to a depth of 30 m.

Due to their close distance from the continent, the Bay Islands are influenced by direct discharges from the major rivers located in the north coast of Honduras. These islands are also submitted to different local pollution pressures due to the discharge of non-treated sewage and industrial wastewaters to the ocean. This is enhanced by the improper disposal of solid wastes and increasing deforestation as well as by the modification of littoral zones due to a rapid touristic development.
The present study describes in what way coral communities are organized and identifies the different factors that influence the coral distribution in the Bay Islands.

Materials and Methods

Underwater qualitative reef surveys were carried out according to different depths, reef geomorphological units, geographical location and different sectors under local pollution pressure.

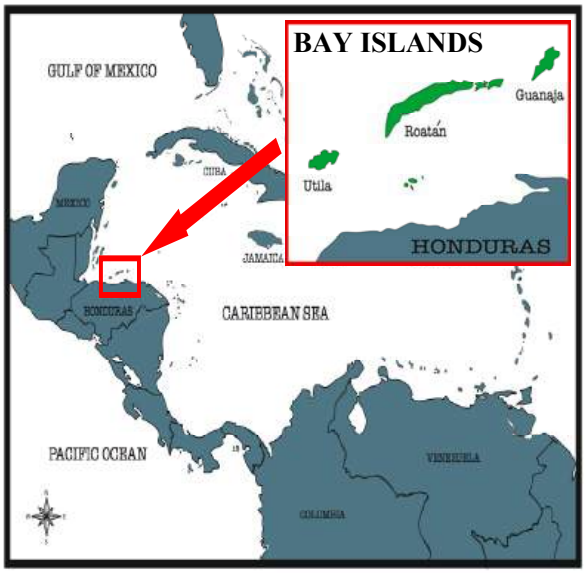

Figure 1: Location of the Bay Islands of Honduras in the Caribbean.

A total of 92 stations were studied: 24 in Utila, 50 in Roatán and 18 in Guanaja. Around the islands, different sectors corresponding to various local pollution pressure were delimited from a study on the quality of the coastal waters done by Lafforgue *et al.* (2001), in parallel to the present study.
Presence-absence data from the 92 sites were analyzed by a canonical correspondence analysis (ter Braak, 1988). Six pollution indices and a latitudinal and a longitudinal gradient constituted the quantitative variables. Qualitative descriptors corresponding to two main geographical locations (windward and leeward side of the islands) and 12 reef geomorphological units were also used as explanatory variables in the analysis.

Results and Discussion

A total of 50 coral species including three species of hydrocorals were identified. This can be compared to the latest species revision in the Caribbean done by Cairns (1999), in which 73 coral species were observed. It shows that the Bay Islands have very high coral species diversity.

No differences were found for coral species richness and community distribution between the three islands. Species richness varied from 10 to 34 species according to the stations and increased from the reef flats towards the fore reefs with a maximum of biodiversity between 10 to 25 m. This has been already observed in the Caribbean (Bouchon and Laborel, 1986,1990) and in the Indo-pacific region (Bouchon, 1996). The average number of species was 17.5 (±0.9) on the reef flats, 20,8 (±1,8) on the upper part of the fore reefs and 23.9 (±1.6) on the lower part between 10 to 25 m.

The canonical correspondence analysis revealed that the corals species in the Bay Islands are distributed in three major groups: corals of the reef flats, corals of the shallow outer reef slopes from 1 to 5 m and corals from the deeper outer reef slopes from 5 to 25 m (Fig.2).

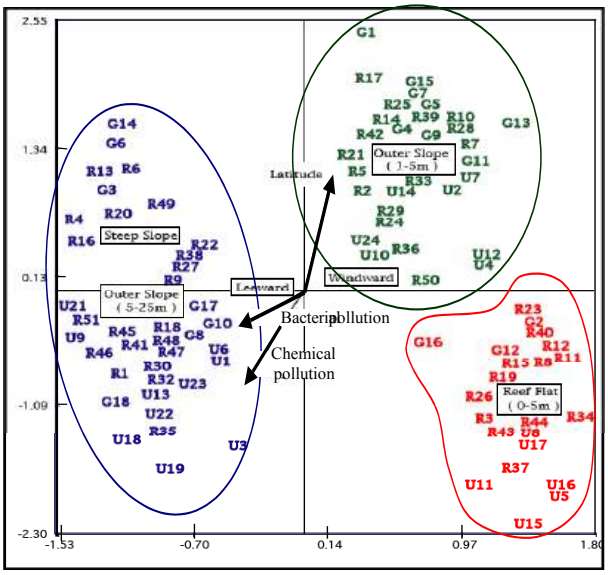

Figure 2: Canonical correspondence analysis biplot of sampling stations and ecological and anthropogenic descriptors.

Variance partitioning showed that 9 variables out of the 24 variables tested explained 32 % the coral distribution around the islands: 21 % is explained by geomorphological factors, 7 % by bacterial and chemical pollution pressure and 4 % by a latitudinal gradient. Among these factors coral communities are mainly controlled by depth. In fact, depth gathers two major ecological factors, which are light and water agitation. Water agitation is stronger in the shallow water areas and moderate in the outer slopes from 5 to 25 m. Both indices influence the development of corals and the species composition of the zone.

Corals from the deeper outer slopes from 5 to 25 m are the group mostly affected by bacterial and chemical pollution. The bacterial pollution index consisted simultaneously of total coliforms and fecal coliforms counts strictly referring to *Eschericia coli* as a direct indicator of human fecal pollution. Fecal pollution can be related to various coral diseases and the presence of organic matter and nutrient discharges that enhance the euthrophication of the coastal waters and increase the competition for space between corals and macro algae. The chemical pollution index concerned mainly heavy metals such as copper, zinc, cadmium and lead associated with anticorrosive or antifouling paints and additives in the gasoline. Other compounds found in pesticides also composed this index. Chemical pollution threatens the corals reproductive physiology, which limits its population dynamics.

The existence of a significant impact of the latitudinal position of the stations confirms that there is a continental influence over the coral community. The river plumes originated from the continent that reach the Bay Islands carries organic matter, nutrients and particles in suspension. This also participates to the euthrophication of the island coastal waters and limits the penetration of light.

Coral communities in the Bay Islands are organized according to depth and reef morphological zones. Moreover, the distribution of coral species is influenced by a latitudinal gradient, which highlights a continental influence and is also sensitive to local bacterial and chemical pressure.

References:

1. **Bouchon C.,** 1996. Recherches sur des peuplements de Sclératiniaires Indo-Pacifiques (mer Rouge, océan Indien, océan Pacifique). Thèse doctorat ès Sciences, Univ. Aix-Marseille II : 338 pp.
2. **Bouchon C., Laborel J.,** 1986. Les peuplements coralliens des côtes de la Martinique. *Ann. Inst. Oceanogr*. Paris, 62 (1) : 251-289.
3. **Bouchon C., Laborel J.,** 1990. Les peuplements coralliens du Grand Cul-de-Sac Marin de Guadeloupe (Antilles Françaises). *Ann. Inst. Oceanogr*. Paris, 66 (1-2) : 19-36.
4. **Cairns S.D.,** 1999. Species richness on recent Scleratinia. *Atoll Res. Bull.*, 459: 1-46.
5. **Lafforgue M., Pateron C., Ricard M.,** 2001. Informe complementario al diagnóstico de la calidad de las aguas de las Islas de la Bahía. Informe técnico No. CAC 04. Subprograma Manejo Integral de los Recursos Naturales. Proyecto de Manejo Ambiental de las Islas de la Bahía, Honduras: 194 pp.
6. **ter Braak C.J.F.**, 1988. A FORTRAN program for canonical community ordination by (partial) (extended) (canonical) correspondence analysis, principal components analysis (version 2.1) Agricultural Mathematics Group, report LWA-88-02, Wageningen.

Marine Biology / Bacteriology

Significance of environmental variables for the structure of fish assemblages in the lagoon of the Grand Cul-de-Sac Marin (Guadeloupe, F.W.I.)

Amandine VASLET, Yolande BOUCHON-NAVARO, Claude BOUCHON and Max LOUIS
Laboratoire de biologie marine – DYNECAR
Campus de Fouillole, Université des Antilles et de la Guyane, 97167 Pointe à Pitre, Guadeloupe, France
amandine.vaslet@univ-ag.fr

Abstract

The aim of the study is to describe the spatial patterns of the mangrove shoreline fish assemblages in the lagoon of the Grand Cul-de-Sac Marin of Guadeloupe and to try to understand the processes affecting this distribution. For that, fishes were collected at 32 stations and 18 environmental variables were simultaneously measured. Canonical correspondence analyses and hierarchical clusterings revealed the existence of two geographical gradients controlling the fish distribution. The first one is a "coast-seawards" gradient which opposes stations located near river mouths to stations under coral reef influence. The second gradient corresponds to an "east-west" axis in the lagoon which could be interpreted as an enrichment of coral formations in the western part of the lagoon.

Introduction

Mangrove ecosystems are known to play an important ecological role for fish communities. They provide a shelter, a source of food and a nursery ground for numerous fish species (Ley, et al., 1999; Sheridan, Hays, 2003; Hindell, Jenkins, 2004). The mangroves of Guadeloupe have been studied since 1974 (Louis et Lasserre, 1982; Louis et Baelde, 1987; François-Lubin, 2005; Vaslet, 2005). Louis (1983) identified three systems which composed the mangrove ecosystem: the channel system, the mangrove lagoon system and the mangrove shoreline system. This research is undertaken in order to study the relationships between fish spatial distribution and environmental variables in this last system.

Materials and Methods

The Grand Cul-de-Sac Marin is a lagoon of 11 000 hectares limited along the coast by a mangrove fringe and seawards by a barrier reef. A total of 32 stations were sampled along the mangrove fringe of the lagoon and around several islets. The sampling area spread from Sainte Rose on the west to the Rotour's channel on the east including Carénage, Fajou and Macou's islets (Fig.1).

Fish were sampled using a hoop net called "capéchade" which was settled during 24 hours at fence net (35 m long, 2 cm mesh size) which deviated fish migrating along the shore into three hoop nets. The sampling period took place from February to April 2005, during the dry season. The fish were brought back to the laboratory where they were identified, counted, measured and weighed.

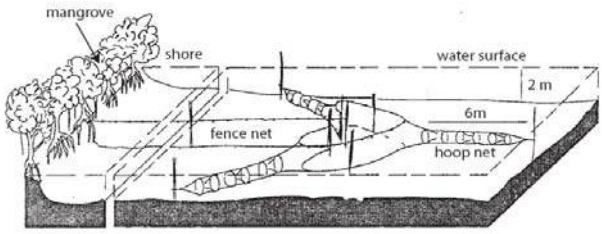

Figure 2: The fish hoop net called "capéchade" used to sample in the mangrove.

At each station, 16 quantitative environmental descriptors were measured: latitude, longitude, temperature, salinity, pH, dissolved oxygen, nitrate and phosphate concentrations, turbidity, depth, chlorophyll a, pheophytin a, suspended materials, organic materials present in sediment, reef and river proximity. Two qualitative variables were also

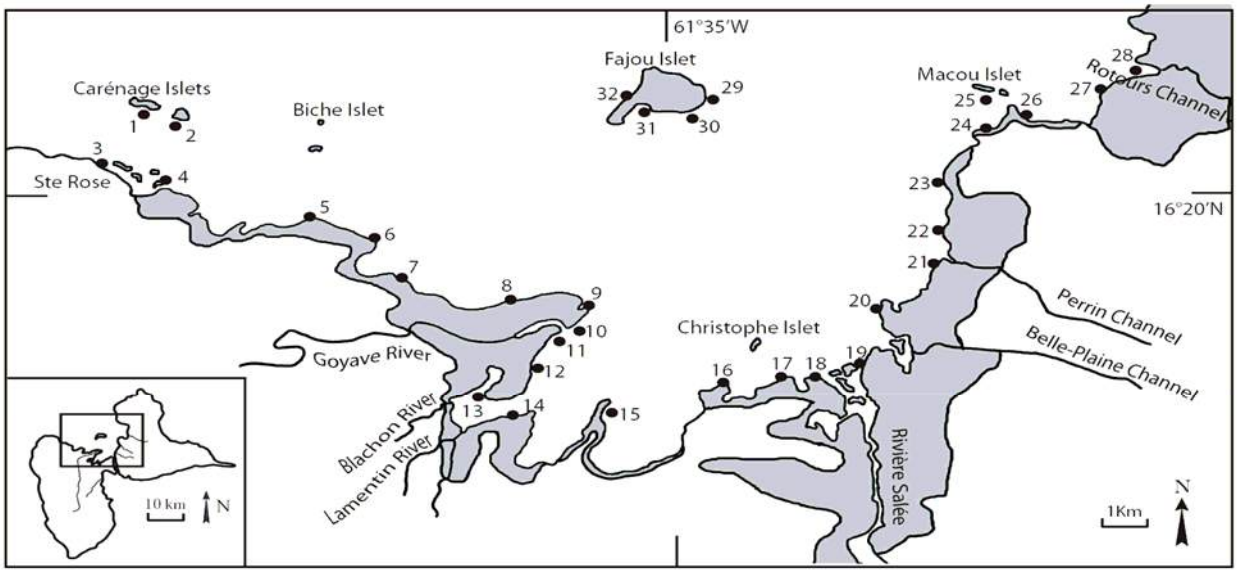

Figure 1: Location of sampling stations in the lagoon of the Grand Cul-de-Sac Marin in Guadeloupe.

indicated such as the water motion (calm or turbulent) and the presence or absence of seagrass beds.

Statistical analyses like canonical correspondence analyses (ter Braak, 1994) and hierarchical clusterings were performed on the data calculated from fish abundance, biomass and presence-absence.

Results and Discussion

A total of, 89 fish species belonging to 37 families were identified. Rare species (only one specimen per species) were not included in the analyses. Statistical analyses were performed on fish abundance, fish biomass and fish presence-absence data and gave similar results. Thus, only those obtained with fish abundance are described.

CCA analyses revealed and explained relationships between environmental descriptors and fish abundance. The biplot built with axis 1 and axis 2 showed a Guttman effect due to a quadratic relation between the two axes (Legendre et Legendre, 1998). Thus, the final factorial plan was plotted using axes 1 and 3. This projection reveals higher canonical correlations with environmental descriptors (Fig.3). Hierarchical classification was performed on fish abundance and divided the stations into four groups. Those groups are also represented on the plan and revealed the existence of several assemblages in the fish community (Fig.3).

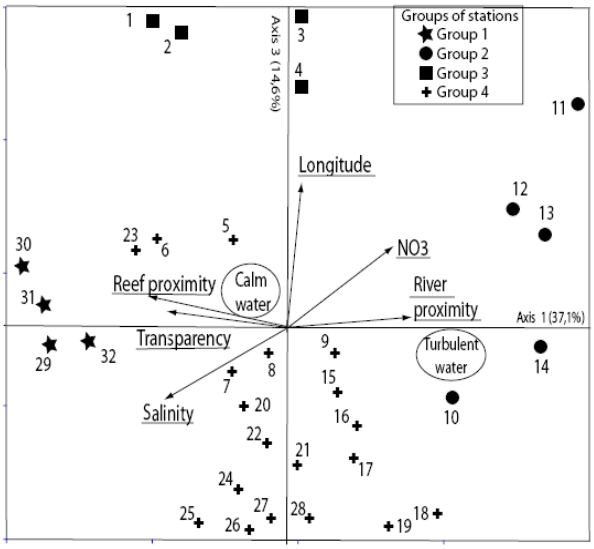

Figure 3: Canonical correspondence analyse biplot of sampling stations and environmental descriptors.

On the CCA biplot (Fig.3), only statistical significant descriptors are indicated. The two axes explained 51,7% of the canonical analysis (axis 1: 37,1%; axis 3: 14,6%). On axis 1, the first group of stations is correlated to water transparency, salinity, reef proximity and calm water (Fig.3). On the other side of this axis, stations of group 2 are linked to nitrate concentrations, river proximity and rough water. Thus, those stations are opposed along a "coast-seawards" gradient. On the third axis of the CCA biplot, a correlation was found with the factor "Longitude" which could be linked to an "east-west" separation of the lagoon fish assemblages. On the west part of the lagoon, the seagrass beds include coral heads whereas these are absent in the eastern part. This second gradient separates the stations of groups 3 and 4.

Statistical analyses have demonstrated the existence of two geographical gradients controlling the fish distribution. The first gradient is a "coast-seawards" gradient which opposed stations under coral reef influence to stations located near river's mouth. This gradient is characterized by six environmental descriptors: salinity, reef proximity, river proximity, nitrate concentrations, water transparency and water motion. The second gradient was correlated to the variables "Longitude" corresponding to an "east-west" separation in the lagoon. This gradient could be also interpreted as a westward decreasing terrestrial influence revealed by an enrichment of the western part of the lagoon with coral formations. That explains the presence of reef fish species mixed to the typical mangrove fish community. To complete the present study, further investigations have been undertaken concerning the temporal variation of the fish assemblages of the mangrove shoreline system.

Acknowledgements

Thanks are expressed to the Parc National de la Guadeloupe for the support of this study.

References

François-Lubin V., 2005. Les peuplements de poissons des canaux et des rivières: "Le cas du canal Belle-Plaine" (Guadeloupe). Thèse de doctorat. Université des Antilles et de la Guyane: 350 pp.

Hindell J. S., Jenkins G. P., 2004. Spatial and temporal variability in the assemblage structure of fishes associated with mangroves (Avicennia marina) and intertidal mudflats in temperate Australian embayments. Marine Biology. 144: 385-
395.

Legendre L., Legendre P., 1998. Numerical ecology. 2nd English edition. Elsevier Science BV, Amsterdam: vx + 853 pp.

Ley J. A., McIvor C. C., Montague C. L., 1999. Fishes in mangrove prop-root habitats of notheastern Florida Bay: distinct assemblages across an estuarine gradient. Estuarine, Coastal and Shelf Science. 48: 701-723.

Louis M., 1983. Biologie, écologie et dynamique des populations de poissons dans les mangroves de Guadeloupe (Antilles Françaises). Thèse de doctorat, Université de Montpellier II: 275 pp.

Louis M., Baelde P., 1987. Fish communities in Guadeloupe mangroves. Proc. V Congr. europ. Ichtyol. Stockholm 1985. 175-180.

Louis M., Lasserre G., 1982. Etude du peuplement de poissons dans les lagunes des mangroves de Guadeloupe (Antilles Françaises). Symposium International sur les lagunes côtières, Bordeaux (France). Oceanologica Acta. N°SP Septembre. 333-338.

Sheridan P., Hays C., 2003. Are mangroves nursery habitat for transient fishes and decapods? Wetlands. 23: 449-458.

ter Braak C. J. F., 1994. Canonical community ordination. Part I: Basic theory and linear methods. Ecoscience. 1: 127-140.

Vaslet A., 2005. Dynamique spatiale des peuplements ichtyologiques de la bordure lagonaire du Grand Cul-de-Sac Marin en Guadeloupe (Antilles Françaises). Rapport de stage de DEA, Université des Antilles et de la Guyane : 40 pp.

Marine Biology / Bacteriology

Seagrass Beds As Important Habitats For Juvenile Fishes In The Bay Of The Grand Cul-De-Sac Marin (Guadeloupe, F.W.I.)

Dorothée Kopp, Yolande Bouchon-Navaro, Claude Bouchon, Max Louis
Laboratoire de Biologie Marine, DYNECAR, Université Antilles-Guyane, Campus de Fouillole
97159 Pointe-à-Pitre Cedex, Guadeloupe - France - dkopp@univ-ag.fr

Abstract

In Guadeloupe, seagrass beds of *Thalassia testudinum* occupy important areas in the lagoon of the bay of the Grand Cul-de-Sac Marin. To examine the influence of adjacent shallow water habitats like coral reefs and mangroves on the seagrass juvenile fish assemblages, two seagrass beds were studied: one located near a coral reef, and one near coastal mangroves. Both habitats were sampled using a seine-net and a trap net.

The examination of minimal and maximum lengths for each species of the two sites revealed that the majority of the fishes caught in the samplings are of small size. The mean size of a fish was found to be 7.9 ± 0.2 cm in the coastal seagrass beds and 7.5 ± 0.2 cm in the seaward ones. Individuals less than 8 cm represented 70% of the fish population near the reef and 59% close to mangroves. Both types of seagrass beds function as an important nursery habitat for juveniles since an equivalent number of fishes with a size inferior to 6 cm was found in both sites. The examination of the faunistic list revealed that near the reef, the recruitment of juveniles was due to coral-reef fishes in addition to the typical seagrass species. Near mangroves, seagrass beds represent a good recruitment area for species from different origins (mangrove, seagrass and reefs).

Introduction

The role of seagrass beds as nursery and feeding grounds for fishes is widely recognized (Parrish 1989, Yañez-Arancibia et al. 1994, Jackson et al. 2001). In tropical areas, the seagrass beds are often adjacent to coral reefs and mangroves and offer an opportunity to study the ecological interactions between these ecosystems. In the Grand Cul-de-Sac Marin bay in Guadeloupe, the ichtyofauna has already been studied in mangroves (Louis and Guyard 1982), in seagrass beds (Bouchon-Navaro et al. 2004) and in coral reefs (Bouchon-Navaro 1997) but the linkage of fishes between these biotopes remain largely unknown. The aim of this study was to examine if two seagrass beds, either associated with mangroves or coral reefs, were used as equivalent nursery grounds for juvenile fishes.

Materials and Methods

Two sampling sites were chosen in the Grand Cul-de-Sac Marin bay (Figure 1), one located near the fringing mangroves (seagrass-mangrove) and one located close to the reef crest (seagrass-reef). Both seagrass beds consist of *Thalassia testudinum* intermingled with sparse *Syringodium filiforme*.

Two fishing gears were used: a seine-net (Figure 2) and a trap net called "capéchade" (Figure 3).

To determine if the fishes were on juvenile stage, we decided to consider as juvenile all the fishes which are smaller than the minimum maturation size L_m determined with the equation of Froese and Binohlan (2000).

Results and Discussion

A total of 98 fish species belonging to 36 families were collected in the two seagrass beds. 71 were observed in the seagrass - reef, 50 species in the seagrass - mangrove and 23 species were observed at both sites.

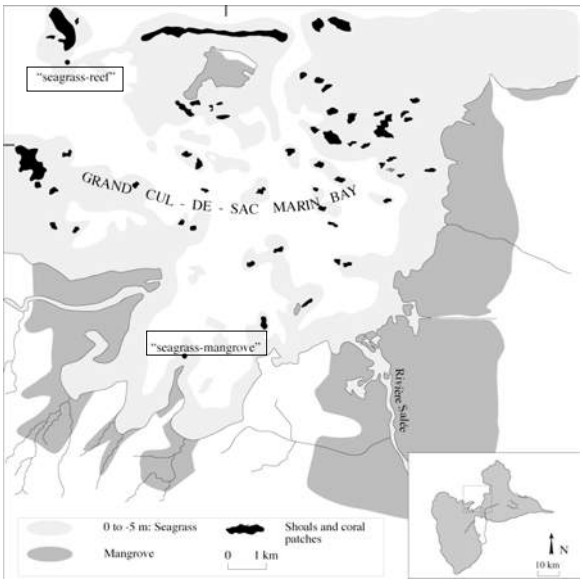

Figure 1: The Grand Cul-de-Sac Marin bay

According to the calculated L_m, 74 species were represented only by juvenile fishes, 20 species present juvenile and adult fishes and four species were represented only by adult fishes.

A total of 21 442 fish was collected in the two sites. In the seagrass-reef, 9 555 fishes were collected and 87.7% of the fishes were juveniles. In the seagrass-mangrove, a total of 11 887 fishes were captured and 98.3% of the fishes collected were under the size of maturity. Concerning biomass, the data showed that in the seagrass-reef the juveniles represented respectively 73.6% and 97.4% of the total biomass collected in the seagrass-reef (44.4 kg) and in the seagrass-mangrove (65 kg).

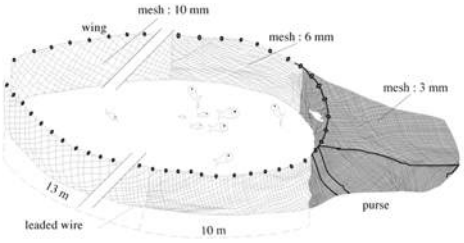

Figure 2: The seine-net

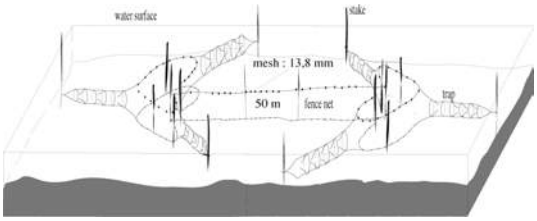

Figure 3: The "capéchade"

The examination of minimal and maximum lengths for each species of the 2 sites reveals that the majority of the species captured in the samplings are of small size. The mean size of a fish in the seagrass meadows was found to be 7.7 ± 0.12 cm (7.9 ± 0.16 cm in the coastal seagrass beds and 7.5 ± 0.20 cm in the seaward ones). Examination of the distribution of size-classes for all the collected fishes shows that small-sized individuals formed the majority of the fish community. Individuals less than 8 cm represent 70% of the fish population near the reef and 59% close to mangroves. Figure 4 shows that both seagrass beds function as important nursery habitats for juvenile fishes since an equivalent number of individuals between 0 and 6 cm was found in the 2 sites. Seagrass beds close to mangroves shelter more medium-sized fishes (6 to 14 cm) than those close to the reef. A Kolmogorov-Smirnov test shows that there is no significant difference between the two size distributions ($p>0.99$). The modal class for the two distributions is 4-6 cm.

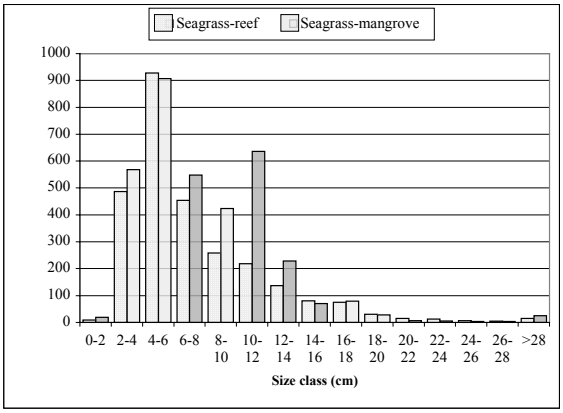

Figure 4: Distributions of size classes for seagrass fish communities

After considering all the individuals, the distribution of size classes was analysed for some species for which enough data were available. Examination of the histograms for the common species shows that juvenile fishes seem to be more abundant near the coast than near the reef. The fishes of big size are mainly observed in the seagrass-reef while the small-sized fishes of the same species are mainly found in the seagrass-mangrove. The histograms concerning mangrove species reflect the tendency observed on Figure 4. A first peak is observed between 2 and 4 cm and a second one between 12 and 14 cm. This higher abundance of medium sized fishes is only observed for the fish populations near mangroves.

The results of the present study highlight the fundamental role of *Thalassia testudinum* seagrass beds for the juvenile fish assemblages and the importance of the location of the seagrass beds, either near the reefs or near mangroves. This study confirms with quantitative data the role of these seagrass beds as nurseries and recruitment areas in Guadeloupe as it has already been reported in the Caribbean region. Moreover, seagrass beds harbour a lot of juveniles of commercially valuable species and their protection will be necessary for a sustainable management of resources for coastal fisheries. They must be included in the marine protected areas as coral reefs and mangroves.

References:

1. Bouchon-Navaro Y. (1997). Les peuplements ichtyologiques récifaux des Antilles. Distribution spatiale et dynamique temporelle. *PhD Thesis*, Université Antilles-Guyane, 242 pp.

2. Bouchon-Navaro Y., Bouchon C., and Louis M. (2004). L'ichtyofaune des herbiers de Phanérogames marines des Antilles françaises: intérêt de leur protection. *Revue Ecologie (Terre Vie)* **5**, 253-272.

3. Froese R. and Binohlan C. (2000). Empirical relationships to estimate asymptotic length, length at first maturity and length at maximum yield per recruit in fishes, with a simple method to evaluate length frequency data. *Journal of Fish Biology* **56**, 758-773.

4. Jackson E., Rowden A., Attrill M., Bossey S., and Jones M. (2001). The importance of seagrass beds as habitat for fishery species. *Oceanography and Marine Biology Annual Review* **39**, 269-303.

5. Louis M. and Guyard A. (1982). Contribution à l'étude des peuplements ichtyologiques dans les mangroves de Guadeloupe (Antilles françaises). *Bulletin Ecologie* **13**, 9-24.

6. Parrish J. (1989). Fish communities of interacting shallow-water habitats in a tropical oceanic region. *Marine Ecology Progress Series* **58**, 143-160.

7. Yañez-Arancibia A., Lara-Dominguez A. and Pauly D. (1994). Coastal lagoons as fish habitats. In: Kjerfve, B. (Ed.), *Coastal Lagoon Processes* **12**. Elsevier Science Publishers, Amsterdam, 363-376.

Marine Biology / Bacteriology

Colonization of Sunken Wood in the Caribbean Area: Influence of the Environment

M. Laurent and O. Gros

UMR-CNRS 7138, Systématique-Adaptation-Evolution, Equipe « Symbiose ». Université des Antilles et de la Guyane. UFR des Sciences Exactes et Naturelles, Département de Biologie. B.P. 592. 97159 Pointe-à-Pitre Cedex, Guadeloupe. France. olivier.gros@univ-ag.fr

Abstract

The work proposed here will focus on the question of the biodiversity, establishment, and function of organisms associated with marine wood falls, in the Caribbean area. This program relies on conducting both field studies on natural systems and experiments in various environments, particularly around Guadeloupe (16°N 61.5W) West Indies where some densities of wood falls could occur. Wood degradation and organisms establishment will be followed by regular field observations.

As an experimental strategy, we propose the deployment of wood parcels experimentally immerged between 600m and 2000m via anchors of Fish Aggregating Devices (FADs) and/or in shallow water environment (mangrove swamp and seagrass). Moreover, miniature in situ sensors will be deployed with the woods in order to monitor in situ physical and chemical parameters characterizing the wood interface during its decomposition in relation with the process of colonization by symbiotic organisms as mussels. Thus, we will be able to investigate the colonization process in relation to the environmental changes induced by wood decomposition and colonisation.

First results obtained using SEM and FISH observations are presented here showing that some of the organisms colonizing such woods possessed bacterial symbionts as observed in some protozoans and metazoans as nematodes.

Bacterial Symbiosis in Wood Fall Bivalves

M.C.Z. Laurent and O. Gros

UMR-CNRS 7138, Systématique-Adaptation-Evolution, Equipe « Symbiose ». Université des Antilles et de la Guyane. UFR des Sciences Exactes et Naturelles, Département de Biologie. B.P. 592. 97159 Pointe-à-Pitre Cedex, Guadeloupe. France - olivier.gros@univ-ag.fr

Abstract

During the Panglao cruise in the Bohol sea (Philippines) in May 2005, various bivalves associated with sunken wood were collected between 300 and 1800 meter depths.

Results from our study demonstrated the existence of bacterial symbionts in the lateral zone of the gill filaments. These bacteria are extracellular in the mytilids collected and intracellular in the lucinid species examined. Extracellular bacteria are located between microvilli at the apical surface of the cells all along the lateral zone of gill filaments while endocellular bacteria observed are envacuolated in large cells called bacteriocytes. Based on TEM observations, these gram negative bacteria are not methanotrophic due to the lack of concentric stacking of intracellular membranes in their cytoplasm. Based on FISH experiments, these bacteria are γ-Proteobacteria excepted in one sample where positive hybridizations were observed with β-Proteobacteria probes.

These results underline the diversity of organisms associated with sunken wood and the importance of chemosynthetic symbiosis in this kind of "ecosystems". Comparative studies on experimentaly sunken wood are in progress in the Caribbean area in various kinds of environments (mangrove swamp, seagrass and deep sea) in order to provide more data about biogeography and establishment and biodiversity of fauna associated with sunken wood.

Marine Biology / Bacteriology

Description Of The Extracellular Bacterial Interactions In Marine Nematodes From Thalassia testudinum Environment.

L. C. Maurin and O. Gros

UMR-CNRS 7138, Systématique-Adaptation-Evolution, Equipe « Symbiose ».
Université des Antilles et de la Guyane. UFR des Sciences Exactes et Naturelles, Département de Biologie.
B.P. 592. 97159 Pointe-à-Pitre Cedex, Guadeloupe. France. - olivier.gros@univ-ag.fr

Abstract

The marine free-living nematodes and particularly those belonging to the family of Stilbonematinae are usually found in the microoxic zone of the sulfidic sediments (Shiemer et al., 1990). In this study, we have investigated the nematodes living in the seagrass bed of T. testudinum known to posses sulfur-oxidizing organisms such as the lucinid clams.

The results presented here demonstrate the existence of extracellular bacteria located on the body surface of these nematodes by SEM and FISH analyses. At least four morphotypes of nematodes were identified harbouring bacteria on their cuticule. Based on SEM observations, each symbiotic nematode possesses a particular bacterial coat constituted by a typical bacterial morphotype characterized by its shape and size. Moreover, *in situ* hybridization (FISH) with oligonucleotide probes have shown that these extracellular symbionts are eubacteria. Experiments are in progress to identify the group of membership of these bacteria (α, β, γ or δ-Proteobacteria) by using other specific probes.

Such ectosymbionts may represent thioautotrophic bacteria as already described in various nematodes from other sulfidic environments. No phylogenetic analysis was done in this study to compare their DNA sequence to that of other marine invertebrate symbionts described to date.

Reference: Schiemer F., Novak R., and Ott J. 1990. Metabolic studies on thiobiotic free-living nematodes and their symbiotic microorganisms. Marine Biology 106: 129-137.

Observation of Marine Nematodes Along a Transect Beach-Seagrass Beds of *Thalassia testudinum*: a SEM Analysis

L.C. Maurin, C. Grateloup, M. Delannay and O. Gros

UMR-CNRS 7138, Systématique-Adaptation-Evolution, Equipe « Symbiose ». Université des Antilles et de la Guyane. UFR des Sciences Exactes et Naturelles, Département de Biologie. B.P. 592. 97159 Pointe-à-Pitre Cedex, Guadeloupe. France. olivier.gros@univ-ag.fr

Abstract

In the marine sediments, the most important taxon of the meiofauna is represented by free-living nematodes, which account for 60% to 90% of the total fauna (Coull, 1999). Some of them belonging to the family of Stilbonematinae present strong interactions with symbiotic bacteria (Polz et al., 1992).

The marine nematodes collected along a transect beach - marine seagrass bed in Guadeloupe were observed by Scanning Electron Microscope (SEM) in order to determine the presence of bacterial ectosymbionts on their cuticule.

The preliminary results obtained show a nematofaunic composition slightly different along the transect with 5 ectosymbiotic species of nematodes associated with T. testudinum sediment against 2 species collected in sand between the seagrass bed and the beach. Non-symbiotic nematodes were also observed : 4 species were frequently found in the sediment of the seagrass against 2 species outside *T. testudinum* environment. While non-symbiotic nematodes are characterized by a high abundance compared to the symbiotic ones, their specific diversity appeared lower.

These observations describe (i) the distribution of the ectosymbiotic and non-ectosymbiotic nematodes in shallow water *T. testudinum* beds and (ii) the diversity of the extracellular symbiotic interactions of the marine nematodes in sediment.

Further studies would be necessary to account for the whole of meiofauna in such ecosystem and evaluate all symbiotic organisms colonizing *T. testudinum* environment.

References:

Coull B.C. 1999. role of meiofauna in estuarine soft-bottom habitats. Australian Journal of Ecology 24: 327-343.

Polz M., Felbeck H., Novak R., Nebelsick M., Ott J. 1992. Chemoautotrophic, sulfur-oxidizing symbiotic bacteria on marine nematodes: morphological and biochemical characterization. Microbial Ecology 24: 313-329.

Table of contents

Health / Social Sciences

The Design and Application of a Biomedical Sensor for Blood Volume Pulsations 173
S. Cornwall, K. De Souza and R. Saunders
Modeling Economic Impact of Changes in Tourism for the French Overseas Region: the Guadeloupean Case 175
S. Mathouraparsad, A. Maurin and J.G. Montauban
Evaluation of Intensive Care in Trinidad – a Comparison with the Developed World 181
S. Hariharan, D. Chen
Fighting Against Sedentarity in the Caribbean Area: on the Interest of a Pluridisciplinar Approach 183
S. Antoine-Jonville, S. Sinnapah, S. Ruffié, S. Jacquelin, J.P. Donnet and O. Hue
Impact of Science on Gender Ideology in Society 184
K. Philip, N. Badrie and G. Sirju-Charran
Sickle Cell Trait Carriers: are they Comparable to Subjects with Normal Haemoglobin? From Cellular Biology to the Cardiovascular Approach 186
F. Sara, P. Connes, M.D. Hardy-Dessources, L. Marlin, M. Montout-Hedreville, J. Tripette, M. Etienne-Julan, C. Saint-Martin, J.C. Barthélémy and O. Hue
Comparing Physical Behaviors and Dietary Habits of Guadeloupeans Originating and Not Originating From India: Need for a Multidimensional Approach 188
S. Sinnapah, S. Antoine-Jonville, J.P. Donnet, S. Ruffié, and O. Hue
Factors Influencing Food Choices Among Secondary School Children in Trinidad, West Indies 190
N. Badrie, V. Leith, C. Serrette and T. Marie Rousseau
An Example of Applied Underwater Archaeological Studies in the West Indies 193
B. Vicens and J.S. Guibert
HLA Alleles Distribution Among a French Caribbean Population 195
M.O. Joannes, F. Agis and R. Chout
Neuroprotection: Activation of Novel Endogenous Pathways? 197
F.F. Youssef
Women in Sciences in the Caribbean: Some Data and Reflections 197
L. Alvarez-Diaz
Social Sciences, an Indispensable View on West Indian Health 198
J. Dumont, J. Pruneau, S. Ruffié, S. Laupa and G. Villoing
Social Dialogue in Conflictual Settings : The Case of Guadeloupe 198
F. Alvarez and H. Ernatus
Risk Factors of Acute Chest Syndrome in Guadeloupean Sickle Cell Anemia Children 199
V. Tarer, V. Chaar, M. Etienne-Julan, J.P. Diara, L. Doumdo, J. Elion and M. Romana
Sickle Red Cells Dynamic Behavior Under Venular Blood Flow 200
C. Allayous, A. Bruel, D. Schoëvaërt, R. Emilion and T. Marianne-Pepin
Sport and Sickle Cell Disease in 12-19 Years Old Adolescents in Guadeloupe: Best Enemies 200
J. Pruneau, F. Maillard and B. Philippon
The Effect of Tropical Environment on Sports Performances 201
S. Blonc, E. Senatus, C. Robin, M. Le Her and O. Hue
Modern Biotechnology and Biosafety Policy Issues for Guyana 201
J. C. Caesar
Eléments de Prospective et l'Environnement 202
M. Castellanos, J.G. Montauban, A. Rodrigue and L. Alvarez
Climate Change and Caribbean Economic Development: an Opportunity for Convergence of the Sciences 203
M. Attzs
A New Recombinant Geminivirus Infecting *Sida* in Jamaica 203
C.S. Stewart and M.E. Roye
Setting up of a Pet - Ct Center in Martinique: Interest and Feasibility 204
H. Azaloux, J. Baudin-Veronique, J.M. Caignon, C. Draganescu, M. Dieye and J. Smith-Ravin

Table of contents

Revitalizing Science and Technology Policy for Sustainable Development in Guyana: Leveraging Lessons from the Developing World 205
J. C. Caesar
Low brain cytochrome c oxydase activityIn two rabbit models of Alzheimer's Disease 205
T. Alleyne, J. Joseph, N. Mohan and A. Adogwa
The effect of *Apium graveolens* and *Momordica charantia* on plasma lipids and blood pressure in laboratory rats 206
E. Cummings and M. Varswyk
The Effects of *Apium graveolens* and *Trigonella foenumgraecum* on Plasmolipids in Laboratory Rats 206
E. Cummings and G. Coopsammy

Health / Social Sciences

Design and application of a biomedical sensor for blood volume pulsations

SIMEON CORNWALL, RAMSEY SAUNDERS AND KEITH DE SOUZA

Department of Physics, The University of the west Indies St Augustine, Trinidad - cornwall@myway.com

Abstract

The biomedical sensor developed makes use of Photoplethysmography (PPG) in the transmissive mode. The light source is a LED of wavelength 900nm and the detector a photodiode which are placed on opposite sides of the tissue. These devices are connected to a circuit of amplifiers and filters. The output is connected to a signal processing device which interfaces with a computer for analysis. The device has been applied to the measurement of vascular resistance of capillaries. The ratio of the rise time (Tg) of pulsations to fall time (Ta) of pulsations obtained were used in the determination of microvascular resistance. The subject was in a supine position and allowed to relax with the biomedical sensor attached to his/her finger and blood volume pulsations were taken for 50s to 100s. After taking about 2-3 sets of measurements for each subject, blood flow to the index finger region was then restricted by wrapping an elastic band tightly around the finger under test. This was left for four to five minutes after which the band was removed and the finger re-inserted into the sensor and further measurements taken.

Introduction

In this paper, circuitry for noninvasive monitoring of skin pulsations, using radiation of a near- infrared spectral range was developed. The method makes use of photoplethysmography. This technique was used to determine a quotient value for blood resistance. This was done by using the temporal parameters of a blood volume wave form. This waveform is derived due to the transmission of near – infrared light through the finger that has been modulated by periodic arterial blood volume changes.

The development of a non-invasive technique that detects the cardiovascular pulse wave, which propagates through the body, can contribute significantly to the evaluation of the quality of blood circulation. Since blood circulation is affected by a wide range of illnesses, such a technique can be of significant diagnostic value.

Firstly the design of the PPG sensor itself which was built using integrated circuits and other semiconductor parts. There are two types of PPG, one is reflection and the other which was the mode used in this study was transmission. In transmission mode the source and the detector are on opposite sides of the tissue under study. Photoplethysmography (PPG) is a noninvasive optical way of measuring variations in blood volume and perfusion in tissue. It is used in pulse oximetry. Several parameters of the cardiovascular system such as heart rate, arterial blood pressure and blood flow fluctuate spontaneously. In this study two aspects are being investigated, risetime, Tg and falltime, Ta

The study obtained the approval of the ethics Committee of The University of the West Indies.

Materials and Methods

The source was an infrared source with a peak spectrum at 900nm. This was chosen for its high penetrating ability. A portable device was designed for the processing and detection of skin transmitted optical signals from the finger of the body (See also Spigulis 2005) The signal is first amplified then filtered using a sallen-key configuration and the amplified again then it processed by a pico scope.

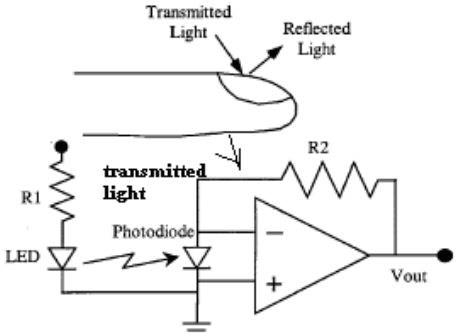

Fig.1 Photoplethysmograph fingernail sensor (Mascaro and Asada 2001)

Figure 1 shows the circuit diagram of the sensor used. The led used has a 900nm wavelength which is used for high penetration into the tissue. The Led illuminates the dermal blood vessels. The photodiode which in this case is positioned on the opposite side of the tissue detects the transmitted light through the finger. The amount of light that is transmitted depends on the volume of blood present in the vascular bed at that point in time. The greater the volume the less light is transmitted. The output voltage from the photodiode circuit will vary as blood volume varies with time. The opamp used is a standard 741 opamp. This in combination with resistors form an amplifier which amplifies the modulated signal

In the Medical Physics and Bioengineering lab within the physics department experimentation was carried out on 50 students. All students volunteered willing and also signed a consent form. Each student was made to lie in a supine position and was given some time to relax before readings were taken. Personal items such as rings, cell phones and bracelets were removed.

The sensor was attached to the index finger of the student was told to relax and to breathe normally. The sensor was designed in tramsmissive mode, which means that the light source and detector are on opposite sides of the finger. Two sets of readings were taken for a period between 50 to 100 seconds without obstruction to blood flow. The sensor was removed and a rubberband was tied tightly to the same finger and left for 4 to 5 minutes. The rubber band was then removed quickly and the finger was reintroduced into the sensor and two sets of 100 second readings were taken. The temperature of the room was recorded. The student then gave a medical background of himself/herself and family, such information was held in confidentiality. The ratio of times for the anacrota or risetime,Tg and catacrota or falltime,Ta was calculated using the Picoscope software which allows for temporal parameters to be calculated. The risetimes and falltimes were compared before and after the introduction of the rubberband. The modulated light signals from the index finger was fed from the sensor to amplifiers to amplify the signal and a sallen-key six pole lowpass filter was used to remove any high frequencies. The residual signal was amplified again and sent to the pico scope where signal processing was done. The picoscope interfaces with a computer allowing the signal to be seen in real-time.

Results

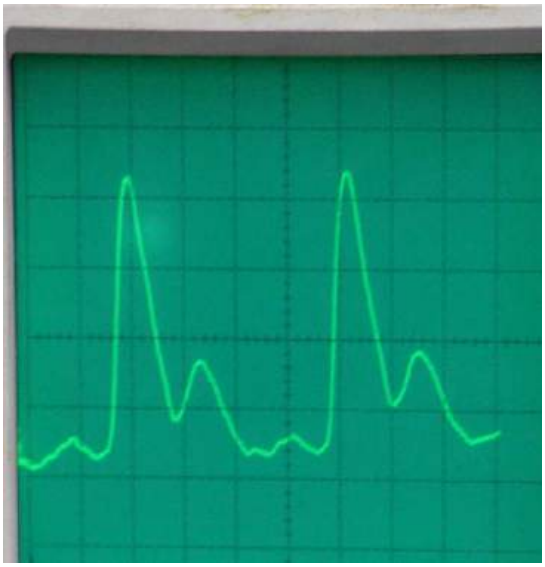

Fig.2 Output real-time display of device

Figure 2 shows what the real-time display is. Fifty three subjects were used. Of the fifty three who came to undergo the test, data from only 27 of them could be used because (1) the data was of poor quality so that calculations could not have been made, (2) some data was missing, (3) their bio-data showed they had an unhealthy habit which is known to affect the blood volume pulsations or (4) cardiovascular disease. What were left was about 27 useable data sets.

In Fig 3 ratio of Tg, the risetime on the time axis corresponds the
to A, and the temporal parameter Ta, falltime corresponds to (T-A). Figure 3 has the wave form as displayed in real time as the output from the device.

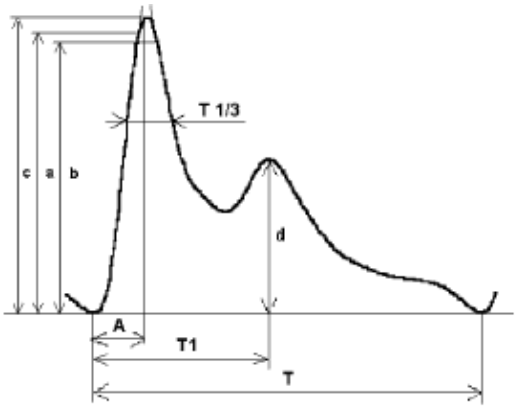

Fig. 3 Description of pulse wave. (See Korpas et al 2003)

Of the 27 data sets that were used 15 originated from data in which Tg/Ta was higher after the removal of the rubber-band compared to the values of unobstructed blood flow. In the remaining 12 data sets Tg/Ta was lower. When family history was considered only 13 from the first group and one from the second group could be used. Therefore, overall 13 cases Tg/Ta was higher and in one case it was lower.

Discussion

Although the sample size is small, there is clear evidence that for healthy subjects the ratio of Tg/Ta is higher after blood occlusion suggesting that this ratio is related to the micro vascular resistance in the blood vessels. Tg/Ta can therefore be used as a measure of the micro vascular resistance. In conclusion the device can be used in measurement of blood volume pulsations and in the measurement of micro vascular resistance. However, the results hold only in cases where there is no family or lifestyle factors that may influence the cardiovascular system. Alcohol use and cardiovascular diseases change the time parameters of the pulse waveform.

References:

Korpas D. Halek J, and Chlupova L.(2003). Surface artery volume pulse wave measurement verification method. Biomed. Papers 147(2),181 – 184

Spigulis J. (2005). Optical noninvasive monitoring of skin blood pulsations. Applied Optics 44(10), 1850-1857

Health / Social Sciences

Modeling Economic Impact of Changes in Tourism for the French Overseas Region: The Guadeloupean Case

Sébastien Mathouraparsad, Alain Maurin, Jean Gabriel Montauban
Laboratoire d'Economie Appliquée au Développement, Université des Antilles et de la Guyane, Campus de Fouillole, Guadeloupe, France
sebastien.mathouraparsad@univ-ag.fr, alain.maurin@univ-ag.fr, jean-gabriel.montauban@univ-ag.fr

Abstract

In using the Guadeloupean case as an example, this article seeks to contribute to the empirical studies currently being carried out elsewhere in the Caribbean region, with the aim of answering certain questions related to the modelling of changes within the tourism industry.
On the one hand it deals with enlarging the data base of similar empirical studies. Because the tourism sector is being made to occupy a strategic position, it is becoming increasingly necessary to identify the different related macroeconomic problems that may arise: forecasts of tourist arrivals, analysis of different scenarios for macroeconomic evolution, impact on specific sectors of demand variations within the sector, etc.
On other hand, it seeks to provide examples of the different types of economic analysis needed by decision makers, at both the local and national levels of government. It is evident that recent budgetary measures and investment incitements set up in Guadeloupe by local government bodies and by the French government show a certain amount of faith in the tourism sector, which is often viewed as a "magic cure" for generating economic activity and employment. In return for their commitment to providing financing, the authorities are now demanding a certain level of expertise capable of accurately determining the direct and indirect effects of tourism on economic activity and more specifically on the creation of wealth and employment.

Introduction

As far as both the international economy and more limited national or regional economies are concerned, the tourism sector has shown progressive development, especially since the liberalization of the airline industry in the 1990's. According to statistics provided by the WTO[1], the total number of tourist arrivals increased from 69.3 million in 1960 to 286.5 million in 1980, attaining 455.9 million in 1990 and 702.6 million in 2002. Thus, there were four times as many tourists travelling in 2002 than there were in 1960. Similarly, since the early 1990's, the evolutionary curve for this variable has been showing a steeper rise than during preceding periods.
Similarly, revenues from tourism have increased from 7 billion US dollars in 1960, to 103 billion in 1980 and 341 billion in 1994. International trade figures also show that tourism occupies a leading position among the various categories of goods and services being exchanged worldwide, well ahead of oil and automobiles.

In the developed countries which are the principal beneficiaries of revenues generated by international tourism, the sector plays an extremely important role, in terms of employment, consumption and investment. In most other countries therefore, the emergence of a tourism industry is considered to be a strategy for economic development. This is the case in certain Caribbean countries, such as Cuba and the Dominican Republic, where growth rates have been relatively high in recent years, due to economic policies which place a lot of emphasis on tourism.

Within the Caribbean region moreover, in the space of one decade since 1990, there has been a real shift in the distribution of the "tourist arrival cards" among certain countries. The big winners have in fact proven to be Cuba and the Dominican Republic, which both occupy the top spots. The number of visitors to the former grew by 1 400 000 between 1990 and 2001, resulting in Cuba's jumping from fifteenth place to the

[1] World Tourism Organization

number one position. During the same period, the Dominican Republic saw an additional 1 500 000 tourist arrivals, and moved from fourth to second place. Inversely, countries like the Bahamas, Barbados and Jamaica have shown relatively little progress or even slight regression in the Bahamian case.

These brief observations suffice to demonstrate the value of studies measuring the macro-economic impact of variations in tourist arrivals within a country and the need for forecasts in this domain. This value is multi-dimensional, as is highlighted by Witt and Witt (1995): "short term forecasts are required for scheduling and staffing, medium term forecasts for planning tour operator brochures and long term forecasts for investment in aircraft, hotels and infra-structure".

In using the Guadeloupean case as an example, this article seeks to contribute to the empirical studies currently being carried out elsewhere in the Caribbean region, with the aim of answering certain questions within the tourism industry.
On one hand it deals with enlarging the data base of empirical studies dedicated to modelling changes within the Caribbean's tourism industry. Because the tourism sector is being made to occupy a strategic position, it is becoming increasingly necessary to identify the different related macroeconomic problems that may arise: forecasts of tourist arrivals, analysis of different scenarios for macroeconomic evolution, impact on specific sectors of demand variations, etc.
On the other hand, it seeks to provide examples of the different types of economic analysis needed by decision makers, at both the local and national levels of government. It is evident that recent budgetary measures and investment incitements set up in Guadeloupe by local government bodies and by the French government show a certain amount of faith in the tourism sector, which is often viewed as a "magic cure" for generating economic activity and employment in Guadeloupe. In return for their commitment to providing financing, they are now demanding a certain level of expertise capable of accurately determining the direct and indirect effects of tourism on economic activity and more specifically on the creation of wealth and employment.

The text is developed in three parts. The first rapidly outlines the evolution of Guadeloupe's tourist industry, describes its positioning with regard to other Caribbean countries and discusses present-day stakes. The second reviews writings on the different approaches to modelling that are normally used to give an account of the dynamics of the principal variables responsible for tourism's evolution. The third section presents a SAM type model created for Guadeloupe and proposes its use in the elaboration of macroeconomic simulations of tourism's impact.

Materials & Methods

There is a relative abundance of literature proposing economic analyses of the tourism industry. Initially, these works took the form of structural econometric studies, during a period of considerable contribution in the field of Keynes-inspired macro-econometric modelling.
These studies were at first carried out in developed countries and they had a tendency to concentrate on the definition of behavioural patterns, in the aim of specifying the determining factors related to tourism demands.
The models produced within this context dealt for the most part with tourism-related earnings and expenditures, for which two types of variables were distinguished: those showing a price effect, aimed at taking account of visitor reactions to price and exchange rate modifications and, those showing a revenue effect, linked to a rise in tourist expenditure following an increase in their buying power (see Coulomb (1988)).
After this initial period, studies were progressively extended to include the rest of the world since the tourist trade was being increasingly placed at the heart of economic strategies in most countries. This holds true for activities directly or indirectly dependent on tourism as well as for activities related to employment or to the foreign trade balance.

In the Caribbean's very particular case, the first empirical implementations including forecasts of behavioural relations were proposed in the late 1980's (see Clarke et al. (1986), Belchere (1988), Rosensweig (1988) and Carey (1991)).

The almost systematic use of the OLS method was eventually phased out and in the ensuing years studies were carried out in a context which gradually approached that of modern econometrics. Consequently, publications from the late 1990's placed modern econometric techniques such as the use of non-stationary variables and Zellner's SUR (seemingly unrelated regression), at the heart of their methodological approaches.

Whether dealing with cases specific to individual countries or with comparative analyses of several economies, these studies paid particular attention to various issues, such as the price effects on tourism results, the problem of tourism maturity (Whitehall and Greenidge (1996)), the forecasting of tourist arrivals (Downes, Greenidge and Worrell (1997)), etc.

The methodological approach based on an input-output reasoning in national accounting and in computable general-equilibrium models has also retained the attention of many adepts of quantitative macroeconomics.

Adams and Parmenter (1992 and 1995), were the first to opt for an input-output type model. Since then, there has been widespread utilisation of general-equilibrium modelling, as can be noted in the many applications realized for the Australian economy, (Skene (1993), Madden and Thapa (2000), Woollett, Townsend and Watts (2001), Dwyer *et al*. (2003a, 2003b)), for the American economy (Blake *et al*., 2000), in Hawaii (Zhou *et al*., 1997), Spain (Blake, 2000), the United Kingdom (Blake, Sinclair and Sugiyarto, 2003) and in the Balearic Islands (Valle and Polo, 2004).

In the Caribbean, most of the work done in this domain was published in the late 1990's. These studies were consecrated to analysing the sectors most affected by tourist expenditure and by their contribution to economic growth. While pioneering authors such as Armstrong, Daniels and Francis (1974) managed to shed some early light on certain macroeconomic aspects of the tourism sector in the Caribbean, their focus was placed particularly on the Barbadian economy, based on a limited input-output table (13,13) and on figures from 1968. It was necessary to wait two decades for research work to attain a level corresponding to the importance of tourism within the region.

Thus, McDavid (2000) produced an application for the Jamaican economy in 2003, using an input-output table constructed with data from 1993, data which he also used to create a SAM and a CGE model, in order to respond to certain questions concerning the interdependent relationship between tourism and economic growth.

Finally, the temporal series approach, in as much as a methodological alternative, also held the interest of many researchers working on modelling the tourist trade.

Empirical investigations were undertaken with the aim of highlighting particular elements capable of being apprehended with a limited number of variables. This was achieved through the use of various methods of analyzing temporal series. For example, González and Moral (1995) proposed the use of a decomposition model including a revenue indicator, two price indices, an aleatory tendency and an aleatory seasonal component to explain Spain's external tourist demand. For a more general look at these studies, Witt and Witt's (1995) review can be consulted.

In the French West Indies, the first quantitative analyses concerning tourism only appeared in recent years.

First, in 2003, Fakhoury, Joeger and Naudet of the French National Institute of Statistics and Economic Studies (INSEE) and the French Development Agency (AFD) were able to make certain estimations concerning the economic fallout of international tourism on the different economic branches and aggregates in Guadeloupe. Their work was carried out as part of a project aimed at developing rapid economic accounts, and using the TABLO model, which is a Keynesian type quasi-accounting tool.

Then, in Martinique, while united for a convention, Carpin, Logossah, Marquès and Para from the INSEE, the Martinican tourism development agency (ARDTM) and the Martinican centre for research in economic/management modelling and computer applications (CEREGMIA) developed a satellite account for tourism in an attempt to meet a double objective: assess tourism's weight in the region's development and contribute to decision-making within the sector. From a technical standpoint, this

study is based on the calculation of the Leontief multiplier using the TEI developed by the INSEE and also on direct, indirect and induced effect multipliers.

Finally, in 2004, Mathouraparsad, Maurin and Montauban from the research centre for economic studies applied to development (LEAD) attached to the Université des Antilles et de la Guyane, also dealt with this question and created the first SAM model prototype, which they used to explore different scenarios related to macroeconomic evolution, including simulations for the tourism sector. The work presented here in fact represents a continuation of this production.

Results & Discussion

The simulations were realized based on a SAM elaborated from an input-output table created for Guadeloupe using the data available for 2000. This is the last year for which accounts were published. Dans un premier temps, nous avons estimé différents comptes synthétisant le secteur tourisme. This estimation was achieved by differentiating between the accounts of the original SAM and that in which tourist expenditures showed a 100% evolution. The different results obtained were then considered to be corresponding to those generated by the tourism account. Then, a simulation of tourism's impact on the economy was effected.

It is undeniable that tourism represents an important stake in Guadeloupe's economy. As a generator of employment, its financial repercussions on several branches of activity make it into a real axis for development. However, in recent years, this sector has been suffering a decrease in visitor numbers to the Guadeloupe archipelago. Touristes numbers have gone from 807 000 in 2000 to 773 400 in 2001. Terrorist attacks, airline company bankruptcy and hikes in ticket prices are just some of the possible reasons behind this 4% drop in tourist visitation. What are the economic consequences of this 4% drop in tourist expenditure?

Tourists spent 328 million euros during the course of 2000. The major areas of tourist expenditure were hotel accommodations and restaurant expenses, to which they consecrated 56% of their total budget. Following this were expenditures for vehicle rentals and consumer goods purchases.

Tourism represents 6% of the total GDP, 9% of total household consumption in Guadeloupe and its dependencies and 7 726 jobs. Tourists consume 11% of the local production of alcoholic drinks and 9% of services to individuals. Their presence accounts for almost one third of the turnover in the hotel and restaurant branch.

The SAM allows for the estimation of a branch account, of the different forms of intermediate consumption as well of certain aggregates.

The total weight of this sector of activity represents more than 7% of commercial production, or 674 million euros. It directly leads to 6% of imports and accounts for 8% of VAT and custom duty takings. Furthermore, it generates close to 6% of all salaries and 7% of total profits. It is responsible for 5% of total income tax earnings and 7% of corporate taxes. Finally, it generates net external earnings (tourist consumption – consecutive imports) of close to 533 million euros. It represents the primary form of export on the island and thus finances 47% of the trade deficit.

Tourism directly generates 469 million euros in production and 124 million in imports. The principal beneficiary branches are non-commercial services and construction.

It indirectly generated or induced production worth 205 million euros or 2.2% of total commercial production.

The analysis of tourism's repercussions on other branches has allowed for the identification of certain trickle-down effects, which are shown in the following table.

The branches which earn the most profit through tourism are the hotel and restaurant branch and that of other services to companies. Households rake in 215 million euros, which represents 5% of their total revenue.

We shall analyse tourism's multiplier effect which compares cumulated effects to direct effects. Direct production due to tourist expenditure estimated at 100 brings about a total global production of 144, because of indirect and induced effects.

We shall measure the economy's dependence on the tourism sector with the use of the touristicity coefficient, which indicates the different branches in which activities are heavily linked to tourism. The proportion of tourist-related production in relation to total commercial production stands at 8.35%. The consumer goods branch registers the highest percentage (38.44%), followed by the food processing industry (37.85%), intermediate goods (34.24%) and the hotel and restaurant branch (34.11%). The potential for development through tourism is very high in these branches.

Under the hypothesis of cyclical unemployment, the job-creation generated by tourism is assessed thanks to the ensuing productivity within the economy (AV/number of jobs). These jobs are of course attributed according to branch. An estimated 7 726 jobs are created, representing 6.5% of total job creation. These jobs are created mainly as a direct result of 69% of funding. The primary employer is the hotel/restaurant branch, with 36% of jobs.

A drop in tourist expenditure would entail, with all things remaining equal, a variation of the GDP by –0.25% and a 0.29% drop in production. As the following table shows, nearly all commercial activities would be affected by this decrease, except non-commercial services, which tends to show very little variation. The most concerned branches would be the hotel/restaurant branch, with an evolution of –1.45% and the sugar/rum branch whose decrease in activity would stand at about 1.28%. Approximately 309 jobs would be lost.

The earnings of the different economic agents are also affected by this decrease. Salaries and capital returns would also show a decrease of 0.23% and 0.27% respectively. This decrease would logically be followed by a drop in household consumption, estimated at 0.19% and a 0.25% drop in imports due to a slowdown of economic activity.

Since households would have less revenue at their disposition and would reduce their consumption, tax revenues would also be decreased. Income and corporate taxes would also be modified by –0.19% and –0.27% respectively. Total VAT earnings and customs duties would also drop by 0.33%.

The multiplier effect highlights the branches that are most closely related to the tourism sector. In other words, it is possible to pinpoint the sectors that are 'boosted' by tourism. Thus, the sugar/rum branch would have a 0.64% drop in activity. This is mostly due to the souvenirs carried away by tourists when they leave the island. Production in consumer goods industries would drop by 0.41% and activities in other service to companies branches by 0.62%. Finally, the most consequential variation would be registered in the hotel/restaurant branch, whose activity would be reduced by 1.44%. This minor crisis in tourism would provoke an income shortfall for firms and households to the tune of 0.19% and 0.27% respectively.

By breaking down the total of all revenues, it can be observed that the direct multiplier generates 55 production units out of a total of 83 for the sugar/rum branch, 6 units through indirect effects and 23 with the induced multiplier. Out of 145 production units in the consumer goods industries, direct effects are responsible for 55, indirect effects 18 and induced effects 72. The hotel/restaurant branch produces 560 units, with 200 by direct effects, 73 by indirect effects and 287 by induced effects. The revenue of economic agents is also affected, as already discussed. Households incomes are reduced by 4 482 euros which is a 0.19% drop in what they would have earned had this drastic reduction not taken place. Indirect (2 092) and induced (1 480) multipliers are the major driving forces behind the generation of this revenue.

The branches which respond most rapidly are the food-processing and trade industries. Direct production in food-processing industries due to a decrease in tourist expenditure estimated at 100, results in a general drop by 688 in production, because of indirect and induced effects.

References

Adams, P.D. et B.R. Parmenter, 1992, "The medium term significance of international tourism for the Australian economy". Canberra: Bureau of Tourism Research.

Adams, P.D. et B.R. Parmenter, 1995, "An applied general equilibrium analysis of the economic effects of tourism in a quite small, quite open economy", *Applied Economics*, 27, pp. 985-994.

Alleyne D. (2002), Forecasting tourist arrivals : the use of seasonal unit root pre-testing to improve forecasting accuracy, paper presented at the 23rd Annual Review Seminar, Central Bank of Barbados, july 9-12, Barbados.

Armstrong W.E., Daniel S. et Francis A.A. (1974), A structural analysis of the Barbados economy, 1968, with an application to the tourist industry, Social and economic study

Bacharach (1970) "Biproportionnal Matrices and Input-Output Change." Cambridge University Press, pp.42-58 et pp.75-86.

Blake, A., 2000, "A computable General Equilibrium Model of Tourism in Spain", mimeo.

Blake, A., R. Durbarry, T. Sinclair et G. Sugiyarto, 2000, "Modelling tourism and travel using tourism satellite accounts and tourism policy and forecasting models". Tourism and Travel Research Institute Discussion Paper 2001/4;

Blake, A., T. Sinclair et G. Sugiyarto, 2003, "Quantifying the impact of foot and mouth disease on tourism and the UK economy", *Tourism Economics*, in press.

Carpin G., Logossah K., Marquès B. Et Para G. (2004), Evaluations de l'impact économique du tourisme international à la Martinique: vers l'élaboration d'u compte satellite du tourisme, INSEE.

Coulomb F. (1988), L'économétrie des échanges touristiques de la France, Economie & Prévision, No 84, p. 41-59.

Daniel S., Francis A.A., Nelson D., Nembhard B., Ramjeesingh (1985), General equilibrium models for development policy, a World Bank research publication, Washington DC

Divay, J.-F. et Meunier, F. (1980) « Deux méthodes de confection du tableau entrées-sorties », *Annales de l'Insee*, n° 37, janvier-mars 1980, pp. 59-108.

Dwyer, L., P. Forsyth, R. Spurr et T. Ho, 2003b, "General equilibrium modelling in tourism, CRC for sustainable tourism, Australia", Monograph Series, in press.

Dwyer, L., P. Forsyth, R. Spurr et T. Ho, 2003a, "Contribution of tourism by origin market to a state economy: A multi-regional general equilibrium analysis", *Tourism Economics*, 9,(2), pp 117-132.

Fakhoury L., Joeger C et Naudet J.D. (2003), Baisse de la fréquentation touristique : une étude d'impact en Guadeloupe, Antiane n0 58, pp. 21-23

INSEE (1997), Les comptes économiques des Départements Français d'Amérique, Années 1993-1994-1995, Base 95, Les cahiers de l'INSEE.

Madden, J. , et P. Thapa, 2000, "The contribution of tourism to the New South Wales economy", Centre for Regional Economic Analysis, University of Tasmania.

McDavid H. (2003), An input-output analysis of the Jamaican hospitality and tourism sector, Social ans Economic Studies 52:1, pp. 161-184

Mathouraparsad S., Maurin A., Montauban J-G. (2004), La modélisation input-output : une approche pour mesurer l'impact des mesures économiques dans les DOM, papier présenté aux journées internationales du LEAD sous le thème "la macroéconomie appliquée au service de la politique économique", le 21 Mai 2004.

Maurin A., Montauban J-G. (2004), L'enjeu du développement économique insulaire, éditions SEDES.

Maurin A. and Watson P.K. (2000), "*Quantitative Modelling of the Caribbean Macroeconomy for Forecasting and Policy Analysis. Problems and Solutions*", Paper presented to the XXX Annual Monetary Studies Conference, Paramaribo.

Moore W. and Whitehall P. (2003), Modelling the tourism life cycle using regime switching models, Working Parpers 2003, Central Bank of Barbados.

Polo C., Valle E. (2004), An appraisal of tourism impact on the Balearic Islands economy

Samuel W.A. (1991), The contribution of tourism to the OECS economies, Carribean finance and management, 7 (1&2).

Simon O. (2003), Méthode de conception d'un tableau des échanges intermédiaires (TEI) pour le département de la Guadeloupe sur l'année 1999, INSEE

Skene, J., 1993, "The economic impact of the growth in visitor expenditure: A quantitative assessment", Bureau of Industry Economics Working Paper Nº 92.

Woollett, G., J. Townsend et and G. Watts, 2001, "Development of QGEM-T a computable general equilibrium model of tourism", Office of Economic and Statistical Research, Queensland Government Treasury.

Zhou, D., J.F. Yanagida, U. Chakravorty et P.Leung, 1997, "Estimating economic impacts from tourism", *Annals of Tourism Research*, vol. 24, nº1, pp. 76-89.

Health / Social Sciences

Evaluation of intensive care in Trinidad – a comparison with the developed world

S. HARIHARAN, D. CHEN

Anaesthesia and Intensive Care, Faculty of Medical Sciences, UWI, St. Augustine, Trinidad & Tobago
uwi.hariharan@gmail.com

Abstract

A therapeutic intervention scoring system (TISS-28) was applied to the intensive care units of Trinidad to evaluate the process of care, resource utilization, costs of intensive care therapy and prognosis of patients. Results showed that despite process of care and outcome of patients being comparable, the costs of intensive care were much cheaper to that of the developed world.

Introduction

Critical care has evolved as a specialty of its own in both the developed and developing countries. Intensive Care Units (ICU) becoming one of the vital areas of patient care in a hospital, they also consume a larger part of the budgetary allocations of a hospital. In recent years there has been an increase in the need for ICUs with more aggressive therapeutic procedures and/or for the increased use of adequate and invasive treatment for advanced diseases. Given the high-technology care offered in ICUs and the higher cost involved with this, proper utilization of the ICU resources should be of very high priority. This is especially true in developing countries such as ours where budgetary allocation has to be prudent to ensure minimal wastage of resources. We conducted a study to evaluate the ICU resources, their utilization and cost, and patient outcome by applying a model introduced in the Europe known as the Therapeutic Intervention Scoring System (TISS-28)

Materials and methods

TISS-28 was prospectively applied to patients consecutively admitted to the intensive care units (ICU) of three public teaching hospitals and two private hospitals in Trinidad on a daily basis for a period of eight weeks. Demographic data, diagnoses on admission, nurse-patient ratio, length of stay and hospital outcomes were recorded. Costs were calculated from data collected from various departments of the hospitals in relation to TISS score.

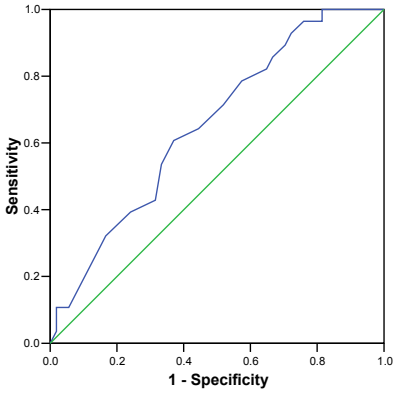

Figure 1: Receiver Operating Characteristic (ROC) curve for TISS-28

Results and Discussion

595 TISS-scored patient-days were analysed. The TISS scores in all the hospitals were comparable except Private Hospital II which had low therapeutic interventions (Table 1). The overall average TISS handled by a nurse was 26.2 per day which quantifies the nursing workload and comparable to the points reported from North America and Europe. In comparison to USA, the bed availability was very low. Also, the mean cost per patient and cost per TISS point were far less than that of USA, although the TISS score (process of care) and mortality (outcome of patients) were comparable. (Table 2). The discriminant function of TISS, which is the prognosticating ability, was fair, as shown by the area under the receiver operating characteristic (ROC) curve (0.65) (Figure 1).

INSTITUTION	Day-1 TISS* (Mean ± SD)	Last Day TISS* (Mean ± SD)	Average TISS per patient* (Mean ± SD)
Public Hospital I	28.1 ± 5.9	25.2 ± 8.1	27.1 ± 5.9
Public Hospital II	26.4 ± 10.4	25.6 ± 8.2	24.3 ± 6.2
Public Hospital III	30.2 ± 4.9	25.8 ± 5.0	28.1 ± 3.7
Private Hospital I	24.9 ± 5.5	21.0 ± 5.3	25.6 ± 1.9
Private Hospital II	20.5 ± 7.1	16.3 ± 3.8	18.2 ± 4.5

Table 1 TISS-28 scores in hospitals

Variable	T&T	U.S.A
Bed occupancy (%)	66.2	81
Bed availability per 100,000 population	2.0	30.5
Cost per patient (US $)	$ 5193	$ 40, 000
Cost per TISS Point (US $)	$ 26	$ 300
Mean Day-1 TISS	27.0	25.0
Standardized Mortality Ratio	0.9	0.96

Table 2 Comparison of process of care, costs

Conclusion

TISS-28 is a useful scoring system to evaluate the ICU resources, process of care, nursing workload, costs as well as to predict the prognosis of ICU patients. This assessment has allowed us to compare the performance of ICUs in Trinidad with those in the developed world. We could reasonably conclude that the resources, process of care, nursing workload in our ICUs are comparable to the developed world while costs are far less than the developed countries.

References :

1. Miranda DR, de Rijk A, Shaufeli W. Simplified therapeutic intervention scoring system: the TISS-28 items. Crit Care Med 1996; 24: 64-73
2. Apostolopoulou E, Nikoloudi P, Georgoudi E, Veldekis D. Utilisation of Intensive Care Unit: A multicentre study in Greece. ICUS Nurs Web J. 2005; 23: 1-6
3. Parviainen I, Herranen A, Holm A, Uusaro A, Ruokonen E. Results and costs of intensive care in a tertiary university hospital from 1996-2000. Acta Anaesthesiol Scand 2004; 48:55-60
4. Graf J, Graf C, Janssens U. Analysis of resource use and cost-generating factors in a German medical intensive care unit employing the Therapeutic Intervention Scoring System (TISS-28). Intensive Care Med 2002; 28:324-31
5. Zimmerman JE, Wagner DP, Knaus WA et al. The use of risk predictions to identify candidates for intermediate care units. Implications for intensive care unit utilization and cost. Chest 1995; 108: 490-9

Health / Social Sciences

Fighting Against Sedentarity In The Caribbean Area: On The Interest Of A Pluridisciplinar Approach

Antoine- Jonville S., Sinnapah S., Ruffié S., Jacquelin S., Donnet JP, Hue O.
Laboratoire ACTES, UFR STAPS, Université des Antilles et de la Guyane,
BP250, 97157 Pointe-à-Pitre cedex, Guadeloupe, France.
sophie.jonville@wanadoo.fr

Abstract

Obesity and related metabolic/cardiovascular diseases have become a major public health concern in the Caribbean area. The main risk factors associated with these conditions are identified, but there are no data available on the prevalence of insufficient aerobic fitness, nor on the physical activity behaviours of the population.

We assessed the cardiovascular risk on the Guadeloupean campus. A sample (n=137) of young Caribbean people was recruited among students, teachers and the administrative staff. Anthropometric data were collected about the whole group. Based on the body composition data obtained through bio-impedancemetry, the proportion of overweight women reached 24.6% and 1.7% in men. When related to the body mass index, these figures suggest that many women with normal weight have a percentage of fat in excess and a lack of muscle mass. The maximal oxygen uptake was measured through an incremental cycling exercise conducted up to exhaustion.

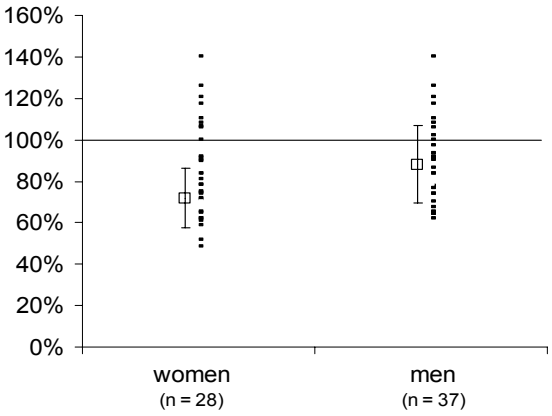

Distribution of the individual maximal oxygen uptake, expressed in percentage of the predicted value

This index of aerobic fitness reached 73.1%(±14.2%) of the predicted value in women, and 88.0% (±18.5%) in men.

Our observation on the population we have studied, educated and quite interested in their health since they have voluntarily participated, suggests that a large exercise program focusing on women is required.

As for public health, regular exercise - yet largely underexploited - can potentially prevent many cases of metabolic or cardiovascular diseases. Confronted with the strong prevalence of diabetes in Guadeloupeans of Indian origins, traditional medical care and prevention strategies meet their limits. A description of the physical activity levels is required to be able to study later the effects of regular exercise in the prevention of diabetes in such an ethnical subgroup. Results of our laboratory suggest that this population would be more sedentary than their counterparts. It is then important to be able to take into account the contribution of culture in the determination of physical behaviors. We presented a project in process apprehending the physical habits of young Guadeloupeans through different scientific approaches.

Acknowledgements

We are grateful to J Bangou (biochemistry department of the univesitary hospital), ML Persain and P Griffard (LMDE) for their efficient technical or financial support to that project.

Health / Social Sciences

Impact of Science on Gender Ideology in Society

PHILIP, K. [1], ALVAREDO V.[1], HEATH K[1], BADRIE, N. [2] AND SIRJU-CHARRAN, G. [1]

[1] Department of Life Sciences and [2] Department of Food Production, Faculty of Science and Agriculture, University of the West Indies, St. Augustine, Republic of Trinidad and Tobago
kezia.philip@gmail.com, nbadrie@yahoo.com, gcharran@fsa.uwi.tt

Abstract

Beliefs are ideological, when they are prevalent in a society not because they are true or reasonable, but because they serve to preserve or stabilise certain attributes. Historically, the *gender* ideology in society has viewed women as passive, emotional, subjective, less competent in mathematical and spatial abilities and therefore less capable of doing Science. In contrast, men have been seen as active, rational, objective and endowed with better mathematical and spatial skills, attributes purported to be better suited to being a scientist. Examples of research conducted in Biology and the Medical Sciences will be cited to demonstrate the impact of Science in maintaining this ideology and how in turn, this ideology influences the practice of modern/western science. An analysis of the current practices in certain disciplines taught at the St. Augustine campus of the University of the West Indies, which maintains this gender ideology will be explored and recommendations will be made to counteract any negative effects these may have on the participation of women in these disciplines.

Background

Historically, the ***gender*** ideology in society has portrayed women as passive, emotional, subjective, less competent in mathematical and spatial abilities and therefore less capable of doing Science. The perception of the way in which science is conducted is antithecal to femininity. Characteristics associated with masculinity are also associated with science viz reductionist; strategic; independent, void of interpersonal support while those associated with femininity are: holistic; seeking help; careers/nurturers; cooperative. This has been cited as a possible reason for the paucity of women in what is considered to be the 'Hard Sciences'.

Methodology

The research and materials presented are based on project reports done by students of the Gender and Science course at the University of the West Indies (U.W.I), St. Augustine and selected papers; Martin (1991), *'The Egg and the Sperm'* and Longino an Doell (1983), *'Body, Bias, Behaviour'*.

Findings

Computer Science

In Computer Science at the University of the West Indies, a discipline which was perceived to be male dominated, there was no significant difference between the numbers of female and male graduates. However, female participation was highest in the Computer Science and Management combination and decreases with increasing 'technical' combinations such as Computer Science and Electronics. This demonstrates the horizontal segregation within the discipline.

The majority of students in this discipline believed that males had a higher affinity for actual use and engagement with computers and computer technology and were also more adept at it. All of the female and some of the male students cited socialization, male domination and stereotyping as possible causes for this. 100% of the males students said they felt confident speaking up in class

because they wanted to make sure that they understood what was being taught and they felt that they would be credited for their ideas, whereas 80% of the female students were not confident speaking up for fear that their inadequacies will be revealed. They felt that either their answers were wrong, or that they would not be given credit for ideas.

Biology and Medical Sciences

The differences observed between males and females pursuing Computer Science at UWI reflect Martin's (1991) conclusion that the degree of metaphorical content in the descriptions of the egg and the sperm emphasizes and parallels cultural stereotypes of male and female behaviour. That is, the egg is seen as large and '**passive**' whereas the "sperms are small, 'streamlined,' and invariably '**active**'. The egg behaves 'femininely' while the behaviour of the sperm is described in very masculine terms, reinforcing this gender ideology in society.

This difference in male-female behaviour is also reinforced in the critique of research conducted in Biology by Longino and Doell (1983) when they stated: 'anthropologists' have argued that the social dominance of males is a function of hormonally determined behaviour. Such theorist credit aggression with the capacity to determine one's position in hierarchical social structures and then attribute aggressive behaviour to levels of testosterone circulating in the organism'.

The justification of the attribution of male-female behaviour to physiological (mainly hormonal) rather than environmental factors must be considered. Physiological explanations are clearly sexist in their description of assumed gender-dimorphic behaviour. For instance neuroendocrinologist describes 'tomboyism' as a preference for active outdoor play, preference for male over female play mates, greater interest in a career than housewifery, as well as less interest in small infants and less play rehearsal of motherhood roles. This reflects an initial acceptance of social prescriptions for sex-appropriate behaviour. Thus we can conclude that environmental factors (socialization) can influence a female students' preference for 'softer' disciplines and the lack of confidence in 'harder' ones.

References

Alvarado, V. and Heath, K. (2003), Why is There a Gender Imbalance in Computer Science*?* The University of the West Indies, St. Augustine, Trinidad and Tobago.

Martin, E. (1991). The Egg and the Sperm: How Science has constructed a romance based on sereotypical male-female roles. J. of Women in Culture and Society. 16 (3): 485-501.

Longino, H. E. and Doell, R. (1983). Body, Bias, Behaviour: A Comparative Analysis of Reasoning in Two Areas of Biological Science*.* Reprinted In*:* Feminism and Science, Eds. E. F. Keller and H. E. Longino, pp 73-90 Oxford University Press, Oxford UK (2003).

Health / Social Sciences

Sickle Cell Trait Carriers: are they like everyone? From cellular biology to the cardiovascular approach.

Fagnété Sara[1,2], Philippe Connes[1], Marie-Dominique Hardy-Dessources[2], Julien Tripette[1,2], Mona Montout-Hedreville[1,3], Laurent Marlin[1], Maryse Etienne-Julan[4], Christian Saint-Martin[4], Jean-Claude Barthélémy[5] and Olivier Hue[1].

[1]Laboratoire ACTES UPRES-EA 3596, Dpt de Physiologie, UFR STAPS, Université des Antilles et de la Guyane, Campus de Fouillole, Pointe-à-Pitre, Guadeloupe.
[2]INSERM, U763, Pointe-à-Pitre, Université des Antilles et de la Guyane, Pointe-à-Pitre, Guadeloupe.
[3]Service de Cardiologie, Centre Hospitalier Universitaire, Pointe-à-Pitre, Guadeloupe.
[4]Centre Caribéen de la Drépanocytose "Guy Mérault", Centre Hospitalier Universitaire, Pointe-à-Pitre, Guadeloupe.
[5]Laboratoire de Physiologie Clinique et de l'Exercice, groupe PPEH, Centre Hospitalier Universitaire, Saint-Etienne, France. pconnes@yahoo.fr

Abstract

Sickle cell trait (SCT) is the heterozygous form of sickle cell anemia (SCA). Although SCT is usually considered as a benign and asymptomatic condition, SCT carriers exhibit particular physical and physiological behaviour at rest and during exercise. Although epidemiological and experimental results demonstrated either a limitation or normal responses of SCT carriers in performing in endurance exercise (i.e. involving mainly aerobic metabolism), other works reported advantages of that population in performing exercise involving mainly anaerobic metabolism. Herein, we will address the issue of the lactic response paradox in SCT carriers during exercise. Finally, the medical complications and possible mechanisms of exercise related sudden death in SCT subjects will be discussed.

Introduction

SCT is the heterozygous form of SCA which is marked by the presence of both hemoglobin (Hb) S and A**.** Its prevalence is between 20 and 40% in the black population of Africa, 8-10% for Afro-Americans and 10% in the Caribbean Islands. The SCT, in contrast to SCA, is usually considered a benign disorder and the longevity and morbidity of SCT carriers seems to compare favorably with subjects with HbA[1]. However, exercise physiology and cardiovascular characteristics seem to differ between SCT and subjects with normal hemoglobin.

SCT carriers and aerobic metabolism

Several studies suggested that SCT is not a limiting factor to practice physical activities requiring aerobic metabolism. For example, it has been reported that 6.7% of SCT carriers were among the black football players in the National Football League[12]. Besides, SCT carriers usually exhibit identical maximal aerobic ability (as assessed by maximal oxygen consumption) than control subjects[2]. However, we recently demonstrated a one-third greater slow component amplitude in SCT carriers performing a prolonged and intense submaximal exercise compared with control subjects[3]. That suggests lower aerobic capacity and exercise intolerance in SCT carriers during prolonged and submaximal aerobic exercise.

SCT carriers and anaerobic metabolism

It has been hypothesized that the low affinity of HbS for O_2 within SCT carriers' red blood cells might cause repeated episodes of tissue hypoxia leading exercising muscles to develop anaerobic capacity to compensate for the hypothetical low oxidative capacity[9]. This hypothesis has been partly verified by Hue et al.[7] who observed that SCT carriers were able to reach higher performance during a jump-and-reach test than control subjects, suggesting greater alactic anaerobic ability in SCT carriers.

SCT carriers and lactic response paradox

Freund et al.[6] investigated the ability of SCT carriers to exchange and remove lactate from the circulation after a ramp exercise test (i.e. during recovery). Their results suggested that SCT carriers were likely to produce more lactate than controls or to have an impaired ability to clear circulating lactate[6]. However, they did not match SCT carriers and control subjects

according to physical activity. Thus, we compared the kinetics of lactate levels during and after the same kind of exercise tests between matched SCT carriers and controls[13] and we reported a surprising lower lactate levels in SCT carriers during the submaximal stage of exercise, at VO_{2max} and during the first minutes of recovery suggesting lower lactate production by exercising muscles and/or greater ability to clear circulating lactate. The greater activity recently found by our group for the red blood cell monocarboxylate transporter, namely MCT-1, in SCT carriers could contribute to a better regulation of lactate exchange between blood and other cellular compartments[14].

SCT carriers and exercise related sudden death

One of the most debated topics concerning the medical complications in SCT carriers is the exercise-related sudden death episodes[10]. Several authors have presented case reports of SCT carriers who have collapsed and died unexpectedly; nearly always under conditions of extreme exertion[8,10]. Among the potential patho-physiological mechanisms involved in these complications, those involved in painful crisis in SCA patients might play a role. We recently examined blood rheology changes in SCT carriers and control subjects in response to a short and supramaximal exercise test (1 min at 110% VO2max)[4]. Whole blood viscosity, plasma viscosity, hematocrit and red blood cell rigidity were assessed at rest, at the end of exercise and during recovery. All hemorheologic values, except red blood cell rigidity, were increased above resting values in both groups and these values remained higher until the 15th or 30th min of recovery as compared to resting values. Although, no significant difference was observed between the two groups for plasma viscosity and hematocrit, whole blood viscosity and red blood cell rigidity were higher in the SCT carriers at any time compared with the control group. This could very well constitute increased risks for microcirculatory complications[4]. In addition, results obtained by Monchanin et al.[11] suggest that vascular cell adhesion molecule (VCAM-1) might also be involved in the increased risk for microcirculatory disturbances during exercise in SCT carriers. Nevertheless, their results require caution because they did not take into account plasma volume variation occurring during exercise to correct their data. Besides, when hemoconcentration induced by exercise is used to correct raw values of VCAM-1 during exercise, no difference between SCT carriers and a control group is found (Tripette et al, unpublished data). At least, Connes et al.[5] recently measured coagulation markers (prothrombin time, activated partial thromboplastin time, plasma fibrinogen, antithrombin III activity, hematocrit and yield stress) in SCT carriers and control subjects at rest and at the end of a maximal exercise test. No difference was observed between the two groups at rest. At the end of exercise, only plasma fibrinogen was slightly higher in SCT carriers but was in the normal range. It could therefore be implied from these results that the increased risk for clinical complications in certain SCT carriers during exercise is not an increased blood coagulation activity. Further studies are required.

Conclusion

SCT carriers are not like every one. Their genetic conditions might constitute advantage or disadvantage during exercise, depending on the kind of exercise performed and on the conditions of exercise practice.

References

1-Ashcroft MT and Desai P. Mortality and morbidity in Jamaican adults with sickle-cell trait and with normal haemoglobin followed up for twelve years. *Lancet* 2: 784-786, 1976.

2-Bile A, Le Gallais D, Mercier B, Martinez P, Ahmaidi S, Prefaut C and Mercier J. Blood lactate concentrations during incremental exercise in subjects with sickle cell trait. *Med Sci Sports Exerc* 30: 649-654, 1998.

3-Connes P, Monchanin G, Perrey S, Wouassi D, Atchou G, Forsuh A, Debaud J, Djoda B, Owona FX, Francina A, Banga PE, Massarelli R, Thiriet P and Martin C. Oxygen uptake kinetics during heavy submaximal exercise: Effect of sickle cell trait with or without alpha-thalassemia. *Int J Sports Med* 27: 517-525, 2006.

4-Connes P, Sara F, Hardy-Dessources MD, Marlin L, Etienne F, Larifla L, Saint-Martin C and Hue O. Effects of short supramaximal exercise on hemorheology in sickle cell trait carriers. *Eur J Appl Physiol* 97: 143-150, 2006.

5-Connes P, Tripette J, Chalabi T, Beltan E, Etienne-Julan M, Chout R, Hue O and Hardy-

Dessources MD. Effects of strenuous exercise on blood coagulation activity in sickle cell trait carriers. *Clin Hemorheol Microcirc*, 2007 (in press).
6-Freund H, Lonsdorfer J, Oyono-Enguelle S, Lonsdorfer A, Dah C and Bogui P. Lactate exchange and removal abilities in sickle cell trait carriers during and after incremental exercise. *Int J Sports Med* 16: 428-434, 1995.
7-Hue O, Etienne-Julan M, Blonc S, Martin S, Hertogh C, Marlin L, Pallud C and Le Gallais D. Alactic anaerobic performance in subjects with sickle cell trait and hemoglobin AA. *Int J Sports Med* 23: 174-177, 2002.
8-Jones SR, Binder RA and Donowho EM, Jr. Sudden death in sickle-cell trait. *N Engl J Med* 282: 323-325, 1970.
9-Le Gallais D, Lonsdorfer J, Fabritius H, Bogui P, Sangare A and Cabannes R. Prevalence of the sickle cell trait among students in a physical education college in Cote-d'Ivoire. *Nouv Rev Fr Hematol* 31: 409-412, 1989.
10-Le Gallais D, Lonsdorfer J, Bogui P, Fattoum S, versus, Connes P, Hardy-Dessources MD and Hue O. Point-Counterpoint: Sickle cell trait should/should not be considered asymptomatic and as a benign condition during physical activity. *J Appl Physiol*, 2007 (in press).
11-Monchanin G, Serpero LD, Connes P, Tripette J, Wouassi D, Bezin L, Francina A, Ngongang J, de la Pena M, Massarelli R, Gozal D, Thiriet P and Martin C. Effects of progressive and maximal exercise on plasma levels of adhesion molecules in athletes with sickle cell trait with or without alpha-thalassemia. *J Appl Physiol* 102: 169-173, 2007.
12-Murphy JR. Sickle cell hemoglobin (Hb AS) in black football players. *Jama* 225: 981-982, 1973.
13-Sara F, Hardy-Dessources MD, Voltaire B, Etienne-Julan M and Hue O. Lactic response in sickle cell trait carriers in comparison with subjects with normal hemoglobin. *Clin J Sport Med* 13: 96-101, 2003.
14-Sara F, Connes P, Hue O, Montout-Hedreville M, Etienne-Julan M and Hardy-Dessources MD. Faster lactate transport across red blood cell membrane in sickle cell trait carriers. *J Appl Physiol* 100: 427-432, 2006.

Comparing Physical Behaviors And Dietary Habits Of Guadeloupeans Originating And Not Originating From India: Need For A Multidimensional Approach.

STEPHANE SINNAPAH, SOPHIE ANTOINE, JEAN PAUL DONNET and OLIVIER HUE
Laboratoire ACTES, UFR STAPS, Université des Antilles et de la Guyane, 97159 Pointe-à-Pitre. Guadeloupe, France - stephanesinnapah@hotmail.fr

Abstract

The physical activity and the dietary intakes of Asian Indians of Guadeloupe were measured by using three consecutive 24hr-recalls.. The results confirm the hypothesis of a tendency to sedentary behaviours but does not demonstrate dietary differences. Causes of the difference observed is hypothesized to be social and or cultural so that a study focused on the determinants of physical activity in asian indians is needed.

Introduction

South Asian Indians and their descents are overexposed to non insulin-dependent diabetes mellitus (NIDDM). The prevalence of the disease among Guadeloupeans originating from India is superior to 20% whereas it equals 2-5% in most of European countries. A genetic predisposition is very probable but environmental factors, including diet and physical behaviours may be involved..
We compared physical activity and dietary habits of Guadeloupeans originating and not originating from India.

Materials and methods

Forty-four Guadeloupeans originating from India (GOI) and 56 Guadeloupeans without this ethnic background participated (age range: 17-66 y). Reported energy expenditure (EE), energy intake (EI) and macronutrient intake were assessed by three consecutive 24-h recalls. EE was calculated by using the compendium of physical activities while the dietary logs were coded and entered into profile software for Windows (version 6.7.4; 4d Engine) based on the CIQUAL 1995 food composition table. Reported EI and reported macronutrient

	Asian Indians		Controls	
	Male (n=27)	Female (n=30)	Male (n=25)	Female (n=32)
Reported EE (kcal)°++	2615±420	2265±466	2920±608	2481±627
Physical Activity Level°+	1.47±0,14	1.63±0,23	1.64±0,33	1.74±0,34
Protein (% of EI)	15.19±1.65	15.09±1.58	15.72±1.63	14.79±2.20
Lipid (% of EI)	34.50±3.42	35.12±3.60	35.93±3.73	34.33±4.77
Carbohydrates (% of EI)	50.29±4,88	49.78±5.13	48.33±5.37	50.87±6.25
Reported EI (kcal)+ +	2520±470	2095±439	2468±343	1949±245

Table 1. *Dietary intakes and energy expenditureees by sex and ethnicity (n=114)*
+significant sex effect (p<0.05)

intake were expressed in kcal/day and percentage of reported EI, respectively. The effects of sex and ethnicity were studied using ANOVA tests with two group factors.

Results and Discussion

The main result of this study was that Asian Indians exhibited significantly less daily physical activity than the rest of the population. This was evidenced by lower physical activity level, reported energy expenditure and reported EE/reported EI. (Table1)

24-hr physical activity recall - Our study was based on self-reported energy expenditure, the validity of which has been demonstrated (Lof and Forsum, 2004) against the gold standard doubly labelled water technique (Schoeller and van Santen, 1982). The mean physical activity level of the sampling, 1.63±0.29, seems quite plausible regarding the standard of 1.55.

Energy expenditure - It was revealed that Asian Indians of Guadeloupe have a tendency to sedentary behaviours. This finding agrees with several studies that demonstrated that NIDDM-overexposed subgroups are often characterized by lower physical activity (Hahn et al, 1998; Hayes et al, 2002). Moreover, sedentary behaviour is a previously reported etiological source of NIDDM (Sigal et al, 2004).

Conclusion

Asian Indians of Guadeloupe are less physically active than their island counterparts. This could contribute to their reported over exposure to type two diabetes mellitus and coronary heart disease. This finding suggests that improving physical activity in this group might be an important prevention tool.

Acknowledgements

We thank the Centre Interprofessionnel de la Médecine du Travail for its support.

References

Lof M, Forsum E. Validation of energy intake by dietary recall against different methods to assess energy expenditure. J Hum Nutr Diet 2004: 17(5): 471-480.

Schoeller DA, van Santen E. Measurement of energy expenditure in humans by doubly labeled water method. J Appl Physiol 1982: 53(4): 955-959.

Hahn RA, Teutsch SM, Franks AL, Chang MH, Lloyd EE. The prevalence of risk factors among women in the United States by race and age, 1992-1994: opportunities for primary and secondary prevention. J Am Med Womens Assoc 1998: 53(2): 96-104, 107.

Sigal RJ, Kenny GP, Wasserman DH, Castaneda-Sceppa C. Physical activity/exercise and type 2 diabetes. Diabetes Care 2004: 27(10): 2518-2539.

Health / Social Sciences

Factors influencing food choices by secondary school children with specific reference to health and nutrition in Trinidad, West Indies

N. BADRIE [1], V. LEITH [2], C. SERRETTE [2] *, T. MARIE ROUSSEAU[2]

[1] *Department of Food Production and* [2] *Department of Agricultural Economics and Extension, University of the West Indies, St. Augustine, Republic of Trinidad and Tobago, West Indies*
nbadrie@yahoo.com

Abstract

Objective: To determine the factors which influence food choices of secondary school children in Trinidad, West Indies with specific reference to health.

Methodology: The structured-administered questionnaire was comprised of 13 questions, which were based on frequency of consumption of snack/lunch, influential factors for purchase of snack/lunch, reasons for choice of particular snack/lunch, perception to the amount of money allowance, preference of nutrition/taste versus taste and demographics. The subjects (91) were between the ages of 14 - 20 yr who attended 4 secondary schools. Data were analyzed by frequencies and percentages.

Results and Discussion: Most (67.6%) students would purchase snacks from the school cafeteria. The lack of time (31.4%) for preparation of snacks was a major reason for purchase. More students (72.4%) chose a particular snack/lunch for its taste than for its nutrition and health (27.6%). When students were asked for their reaction to the following excerpt: 'Imagine the following: (1) that your mother read in a magazine that it is very bad for your health to drink soft drinks and to eat fried foods such as chicken and chips; (2) she decides to stop buying soft drinks and to buy water instead. (3) stops preparing fried foods and instead prepares vegetables and asked you to stop buying chicken and chips', some students (36.9%) would react negatively. Some (40.4%) were 'satisfied' with their money allowance for purchase of snack/lunch, while 26.3% were 'somewhat satisfied', 16.2% 'very satisfied' and 17.2% 'never satisfied'. The majority (66.7%) of responses suggest that students over-ate 'sometimes', 24.5% 'never' and 8.8% 'always'. Students took meals with family members 'sometimes' (56.6%) and 16.2% 'always'.

Implications of the study: Taste of a snack/lunch was chosen over its health benefits and nutrition which suggest the need for school education on healthy food choices.

Introduction

According to the United Nations Food and Agriculture Organisation (UNFAO, 2002), 13% of Trinidad and Tobago population were under-nourished in 1997-1999. From among adolescents 13-19 years 4.6% were found to be overweight with a greater proportion of males than females (FAO, 2005). In the adult population 20 years and older, 16.8% are obese with the prevalence among women. Another 31.4% of this population are overweight, the prevalence being slightly higher in women than in men. Approximately 65 suffer from chronic energy deficiency. Most attention has been directed at the nutritional status of children and the need to provide meals in school to increase dietary intake in order to improve nutritional and educational outcomes (Walker *et al*., 1998; Gulliford *et al*., 2002). The objectives of the study were to determine the factors which influence food choices with emphasis on health nutrition by secondary school children in Trinidad, West Indies.

Methodology

Questionnaire

A questionnaire was administered by trained interviewers to 91 (40.7% male; 59.3% female) secondary school children who were between the ages of 14-20 yrs and attended 4 secondary schools. The % of students by age category were 17 yr old (25%), 15 yr (16%), 16 yr (15%), 18 yr old (11%), 14 yr (9%), 20 yr (3%) and 19 yr (2%). The survey comprised of 12 questions which asked questions on how often they brought lunch/snack to school; where did they purchase lunch/snack; why did they

purchase lunch/snack, influential factors affecting food choices and effect of choices of meals. Four questions requested demographic data. Twenty – five questionnaires were distributed to each of the four schools during the lunch breaks. Overall 93 questionnaires were returned and 91 questionnaires were analysed. Data were computed as frequencies and percentages using Minitab (version 14, release 2003, Minitab Inc, State College, Enterprise Drive, PA, USA).

Table 1 Purchase of snack/lunch

Questions	Response, % (n=91)
How often do you bring snack/lunch to school?	
never	32.7
varies	27.6
everyday	24.5
once per week	6.1
twice per week	1.0
thrice per week	3.1
four times per week	4.1
If you purchase snack/lunch, where do you purchase?	
school cafeteria	67.6
other	13.2
vendors outside school	10.3
food outlets outside of school	8.8
Why do you purchase snack/lunch?	
no time to prepare	31.4
taste	19.3
convenience	18.6
cheap	7.9
variety	9.3
not available at home	5.0
influence of friends	4.3
nutrition	2.9
religion	1.4
What are the reasons for your choice of a particular snack/lunch that you purchased?	
taste	24.0
cost	12.5
health/nutrition	11.5
quality	10.9
food safety	11.8
accustom	9.2
availability	7.9
convenience	7.6
religion	2.6
family influence	2.0

Purchase of snacks

Table 1 shows that when students were asked how often did they bring lunch/snack to school, the highest response was 'never'(32.7%), followed by 'variable'(27.6%) and 'every day' (24.5%). Most (67.6%) students purchased their snacks from the school cafeteria and indicated that time for pre-paration (31.4%) was one of the major reason for purchase. Taste was the most influential factor as a reason for purchase of snack/lunch.

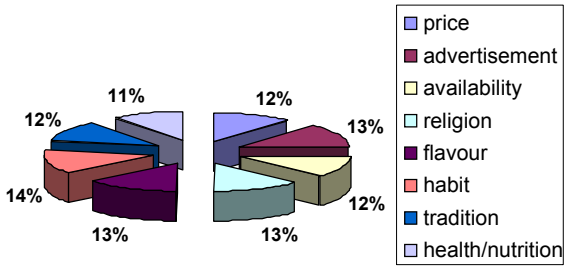

Fig 1. Factors which influence selection of a particular snack/lunch

Selection of particular snack/lunch

Fig 1 shows the % response, when students were asked to select which influential factor/s (n=357) affected their selection of a particular snack/lunch, flavour had the highest response rate (14.0%), followed by habit (13.7%), advertisement (13.2%) and religion (12.9%). In their choice of a particular snack/lunch, flavour had the highest influential response (54.9%) of which 44.0% was rated as 'important'. Health and nutrition was the least selected factor (41.8%) of which 26.4% rated it as 'important' 2.2% considered as 'not important'. Tradition was considered as 'not important'.

Health and nutrition

When students were given the following excerpt to read: 'Imagine the following: (1) that your mother read in a magazine that it is very bad for your health to drink soft drinks and to eat fried foods such as chicken and chips; (2) she decides to stop buying soft drinks and to buy water instead. (3) stopped preparing fried foods and instead prepares vegetables and asked you to stop buying chicken and chips', how would you react? Most students (61.5%) reacted positively, while others were 'negative' (36.9%) or were 'not sure' (15.4%). More students (72.4%) chose a particular snack/lunch more for its taste rather than for its

nutrition and health (27.6%). High fat food choices are common among adolescents (Dwyer, 1995, Bandini *et al*., 1999) particularly for snacks

Perception to money allowance & overeating

The following responses were given in respect to satisfaction of money allowance given for the purchase of snack/lunch, 40.4% were 'satisfied', 26.3% 'somewhat satisfied', 16.2% 'very satisfied' and 17.2% were 'never satisfied'. When the students were asked whether they overate, the majority (66.7%) felt that did so 'sometimes', 24.5% 'never' and 8.8% 'always'. Food insecurity could lead to overeating when food becomes available or to metabolic changes that permit efficient use of energy (Alaimo *et al*., 2001).

Family influence

When students were asked to respond to the following question: 'Last week, while you were at home with your family, how often did you have a meal together with your family?', the responses were 56.6% reported 'sometimes', 16.2% 'always; and 'infrequent; and 11.1% 'never'.

Intervention

Dietitians' efforts to educate adolescents about the benefits and healthfulness of foods would aid in intervention programs.

References

1) Alaimo, K., Olson, C.M, Frongillo, E.A. jr. (2001). Low family income and food insufficiency in relation to overweight in US children is there a paradox. Arch Pediatr Adolesc Med. 155: 1161-1167.

2) Bandini, L.G., Vu, D., Must, A., Cyr, H., Goldberg, A., Dietz, W.H. (1999). Comparison of high-calorie, low-nutrient-dense food consumption among obese and non-obese adolescents. Obesity Research. 7: 438-443.

3) Dwyrer, J. (1995). The school nutrition dietary assessment study. American Journal of Clinical Nutrition. 61 (supplement 1): 173S-177S (editorial).

4) FAO (2005) Nutrition country profiles. Trinidad and Tobago: Food and nutrition profiles. Economic and Social Development Department. FAO Country Profiles. http://www..fao.org/es/ESN/nutrition/tri-e-stm. Accessed 12th December, 2005.

5) Gulliford, M.c., Mahabir, D., Rocke, B.C.,Chinn, S., and Rona, R.J.(2002). Fresh school meals and children's social and nutritional status in Trinidad and Tobago. Public Health Nutrition. 5: 625-630.

6) UNFAO (2002). The state of food insecurity in the world. United Nations Food and Agriculture Organisation. United Nations Food and Agriculture Organization. The state of food security in the world. http://www.fao.org/docrep/003/y1500e/y1500e06.htm#P0_3 accessed 15 April 2002.

7) Walker, S.P., Powell, C.A., Hutchinson, S.e., Chang, s.m., Grantham-McGregor, S.M. (1998). School children's diets and participation in school feeding programmes in Jamaica. Public Health Nutrition. 1: 43-49.

Health / Social Sciences

An Example of Applied Underwater Archaeological Studies in the West Indies

Jean-Sébastien Guibert, Bernard Vicens
PREPASUB organization, Chemin de Tabanon, 97170 Petit Bourg, Guadeloupe FWI
prepasub.971@orange.fr

Abstract

On December 18th, 1809 under the pressure of an English fleet, two Napoleonic Period cargo ships, *corvettes de charge*, sank in Anse à la Barque on the west coast of Guadeloupe, south of the town of Bouillante. Both cargo ships navigating from France to Guadeloupe were transporting gold, money, weapons and soldiers to support Guadeloupe in its resistance against the English.

Historical context

At this period the West Indies are wasted by the consequences of the European Napoleonic wars. Guadeloupe is the last lesser island resisting the pressure of the English fleet composed by 25 ships blocking the island from any communication coming from France. On 1809, the French government decided to supply Guadeloupe by sending a squadron of two 'corvettes de charge' *la Seine* and *la Loire* escorted by two frigates. The squadron left France November 15 and reached the West Indies December 13, where it managed to force the blockade. Offshore Antigua the escorting frigates returned to France while both 'corvettes de charge' tried to go further on to Basse-Terre.

But the way to Basse-Terre was cut off by a part of the English fleet and the captain *Vincent de Comorre* decided to drop anchor at *Anse à la Barque* in order to unload both ships. On Dec. 18, still blocked in *Anse à la Barque* by more than 12 English ships the captain decided to scuttle his ships.

The discovery

In 2000, D. Cabarrus, found several canons that appeared after hurricane Lenny. He immediately alerted the Regional Council, who asked the 'Assosiation pour la Protection, Recherche et Etude du Patrimoine Subaquatique' (PREPASUB), a non profit organization studying and protecting underwater archaeological sites, to make an expertise.

PREPASUB's expertise

In 2001, PREPASUB set up a conservation project to protect the cargo ships and archaeological samples from damage caused by waves, light, taret mollusc or seaweed development that can deteriorate vestiges while waiting for authorization to excavate. The shipwrecks' site is located in an protected area very close from the shoreline.

Our first studies in historical sources strengthened our hypothesis that the ships were from the Napoleonic Period.

Several sources mentioned the shipwreck of the two Napoleonic ships, *corvettes de charge*, *La Seine* and *La Loire* [1,2]. Each ship measures 35 by 6 meters, has a bridge, an 800-barrel capacity, and three masts. This kind of ship is almost unknown, except by plans or by theoretical studies.

In 2003, The PREPASUB organized a first excavation's campaign whose goal was to confirm the historical sources and archaeological observations with DRASSM* agreement.

The completion of this campaign pointed out that the Napoleonic ships *La Seine* and *La Loire* were indeed the sunken ships in *Anse à la Barque*.

The discovery and study of archaeological samples proved the presence of such ships. Samples dating from the late 18th century and the very beginning of the 19th century have been expelled. Moreover, a great number of uniform ornaments were identified belonging to Napoleon's soldiers.

Ceramic, uniform ornaments, pipe and bullets

Our team worked on the back of *La Seine*, where we found the top keel and the bilge pump.

Currently, we are now in the process of a third campaign that took place in April 2006 under DRASSM's authorization. The objective was to localize both ships and to study ship-building more precisely.

The primary sources, mainly the captains' reports permitted us to identify both shipwrecks because they tell us that La Seine was northward of La Loire and that both starboards face the open sea [3].

Prospecting was made along the keels of both ships in order to find the mast foot and to confirm their orientation.

We found *La Seine*'s spanker mast foot close to its bilge pump.

The discoveries of those parts of the ship are very interesting in order to learn about the way one used to build ships, indeed spanker mast foot which is usually on the first bridge of such a ship was found on the top keel.

Moreover we found the entire pumping system of the Loire's main mast: a wooden pipe with its strain has been expelled to be studied.
Underwater excavation work consists in clearing selected areas limited by 3 meters squares with sediments aspirators. Archaeological samples found during this work are carefully expelled noticing the square from where it comes. Then archaeologists may draw a tri dimensional sketch-map of the part of the site they are working on.

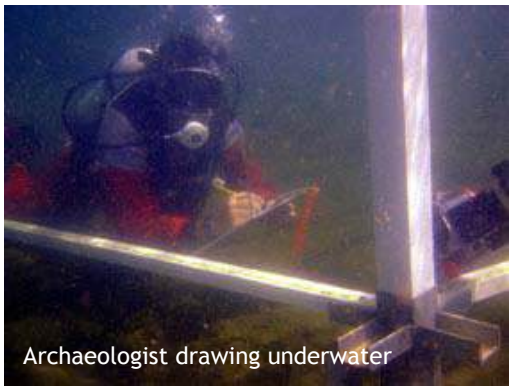

Archaeologist drawing underwater

By this method, we are now able to set up a first map of the site from the surveys done in 2003 and 2006 (See below).
To our surprise, while prospecting along the keels of *La Seine*, we found the remains of an entirely different ship. This one seems to be a coal carrier dating from the mid 19th century.
In addition, two ruins initially thought to be parts of the destroyed ships *La Seine* and *La Loire*, have turned out to be two brand new ships. One of them seems to be of local production because of its red-wood building.
The other sunk in the area of the shoreline is in very good state of conservation. This one may have been built by an English way.
Wooden samples of those ships have been extracted to be analyzed in order to determine the wood species.

Post excavation work
During both campaigns archaeological samples were expelled from the site in order to be studied in the PREPASUB's pre treatment laboratory.

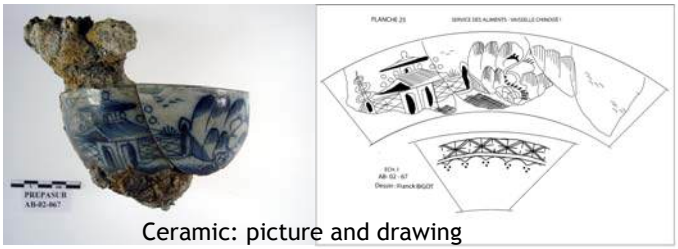

Ceramic: picture and drawing

Their study is a way to confirm or to invalidate a dating.
Dating an archaeological sample may be done by comparing it with a type, or by analyzing it in laboratory.
The archaeological samples have to be cleaned up, pictured and inventoried. During its pre-treatment (they are stocked in water to be unsalted) the archaeological samples are sketched, studied in order to be recorded in a data bank.
Some of them revealing a particular interest have been copied by molding.

As we are regularly trained by the DRASSM and regarding our experience we wish we worked with our Caribbean neighbors and their university concerning projects on Archaeological Researches.

References

[1] LACOUR Auguste, Histoire de la Guadeloupe, Basse-Terre, 1855.
[2] MOREAU, Jean Pierre, Guide des trésors archéologiques sous-marins des Petites Antilles, p. 136-137, Ed. Jean-Pierre Moreau, Clamart, 1988.
[3] Archives Nationales Marine BB4 307, Fo 44

* DRASSM : Département de Recherche en Archéologie Subaquatique et Sous-Marine

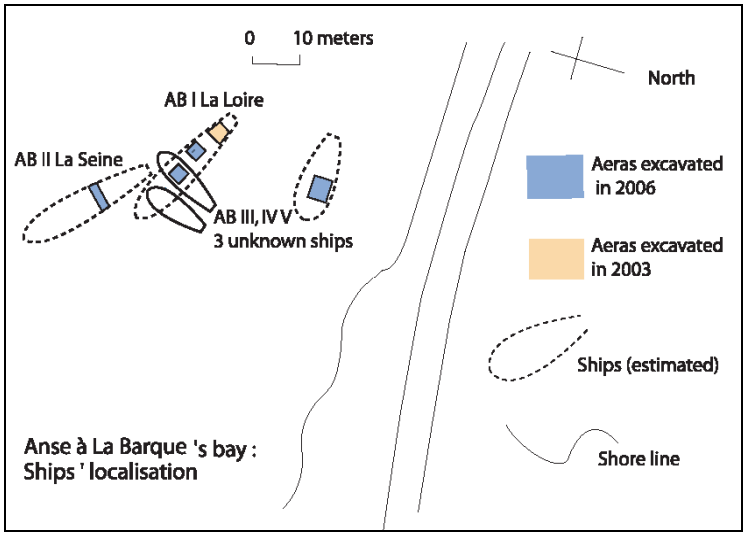

Photos : Prépasub
Plan : J S Guibert
Drawing : F Bigot

Health / Social Sciences

HLA Alleles Distribution Among A French Caribbean Population

M.O. Joannes [1,2,3], F. Agis [3], T. Marianne-Pépin [1], R. Chout [2,3].

[1] *Université des Antilles et de la Guyane, mojoanne@univ-ag.fr*
[2] *Equipe Epidémiologie Clinique et Médecine,*
[3] *Laboratoire d'Hématologie-Immunologie du CHU de Pointe-à-Pître Abymes, BP 465. 97159 Pointe-à-Pître Cédex. Guadeloupe, France.*

Introduction

The M.H.C. (*Major Histocompatibility Complex*) is a complex of genes encoding glycoproteins that play a key role in non-self recognition, in all mammalians.
Human M.H.C. molecules are called *Human Leucocytes Antigens* (H.L.A.)

HLA molecules present peptide antigens to T cells, initiating immune recognition of foreign antigens.

HLA genes are located on the short arm of chromosome 6. This complex occupies a large segment of DNA, extending about 3500 kb. These genes are divided into 3 classes:

- class I with notably HLA-A, B and C genes,
- class II with HLA-DR, DP and DQ notably,
- class III: genes encoding other proteins related to the immune response. For example, genes encoding C4, C2, and B factor, components of the complement system and others encoding critical cytokines such as TNF α and B (*Tumour Necrosis Factor*).

HLA system is one of the most polymorphic protein-encoding regions of the human genome. Furthermore, there are more than 450 and 520 known HLA-A and HLA-DRB alleles respectively.

Comparative analysis of HLA alleles revealed differences in the distribution of these alleles among different ethnic groups.

HLA alleles are well investigated. Their distribution has significant implications for analyzing human migration trends throughout history. Moreover, there are applications in forensic medicine, transplantation, association HLA-diseases.

This study aimed at estimate HLA allele frequencies among a population from Guadeloupe, a French West Indies island which inhabitants have various ethnic origins such as Africa, Europe, India…

Material and methods

One-hundred-and-fifty-five unrelated individuals from Guadeloupe were HLA class I and class II typed (80 men and 75 women aged from 18 to 72 years old).

Genomic DNA was extracted from whole blood collected on EDTA using a salting out method (**Miller S. et al., 1998**). HLA typing (class I: A and B and class II: DRB1) was performed by polymerase chain reaction-sequence specific primer (PCR-SSP) (One Lambda, Inc).
Data analysis: Statistical analysis was performed by computer package Arlequin 3.01 (**Excoffier et al. 2005**). This program estimated, by maximum likely-hood methods, HLA-A, B, and DR allele frequencies.

Results & Discussion

The results presented here are preliminary.
All individuals have been typed at a generic level.

Tables 1 to 3 show HLA-A, -B and –DRB1 allele frequencies in a population from Guadeloupe (for this population, only frequencies >4 are presented). Comparisons are made with similar data in Caucasian and African American populations.

Table 1. HLA-A allele frequencies in the studied population: comparison with known data

	Frequencies (%)		
Alleles	**Studied population**	**African American**	**Caucasian**
A*02	13.15	13.9	27.9
A*30	11.53	13.9	3.7
A*23	9.95	8.4	1.8
A*03	9.21	11.9	10.7
A*68	9.03	7.9	2.2
A*01	8.93	7.4	16.5
A*74	5.81	5	2.2
A*33	5.48	5.9	2.2
A*29	4.19	5.4	4
A*24	4.19	4.4	11

Table 2. HLA-B allele frequencies in the studied population: comparison with known data

	Frequencies (%)		
Alleles	**Studied population**	**African American**	**Caucasian**
B*53	14.52	13.8	0.4
B*07	11.29	8.5	16.3
B*44	6.77	9	14.7
B*58	5.48	5.3	0.4
B*35	5.16	6.4	11.2
B*45	5.16	2.1	-
B*08	4.84	6.4	11.2
B*42	4.84	-	-
B*57	4.52	3.2	3.5
B*18	4.19	4.2	2.3

Table 3. HLA-DR allele frequencies in the studied population: comparison with known data

	Frequencies (%)		
Alleles	**Studied population**	**African American**	**Cau-casian**
DRB1*15	14.74	12	9.3
DRB1*11	13.47	16.9	10.3
DRB1*13	11.88	17.6	12.1
DRB1*0301 & *0306	11.45	7	10.7
DRB1*04	7.38	7.7	15.9
DRB1*07	6.68	6.3	14.5
DRB1*01	5.75	9.8	9.6
DRB1*08	4.51	3.5	2.1

For A locus, 21 specificities were found. The most frequent alleles found were A*02 (13.15%), A*30 (11.53%) and A*23 (9.95%).
In this population, A*02 = [A*0201, A*0250]; A*30 = A*3001, A*23 = A*2301.

For B locus, 41 specificities were found. The most frequent alleles found were B*53 (14.52%), B*07 (11.29%), and B*44 (6.77%).
In this population, B*53 = B*5301; B*07 = [B*0701, B*0702, B*0704, B*0705]; B*44 = [B*4401, 4402, 4403, 4405].

For DR locus, 27 different HLA-DRB1 alleles were found. The most frequent alleles found were DRB1*1501 (14.71%), DR11 (i.e. DRB1*1101 and DRB1*1102) (13.47%), DRB1*1301 (11.88%), DR17 (i.e. DRB1*0301 and DRB1*0306) (11.47%).

Null alleles were found at each locus which requires further investigation, as HLA-sequencing, in order to identify these alleles.

Comparison of the allelic distribution in the studied population and distribution in other populations suggests that the Guadeloupean population is the result of an extraordinary interbreeding.

Some HLA alleles are involved in association with diseases. HLA-B27 positive individuals have 90 to 100 times greater chance of developing ankylosing spondilytis than do individuals HLA-B27 negative.
Other proved associations are narcolepsy and HLA-DRB1*1501; retinopathy birdshot and HLA-A29, type I diabetes mellitus and HLA DR3 and DR4 (this illness is a major health problem in Guadeloupe).
All these alleles are present in our studied population which is relevant to clinical diagnosis: HLA-B27 (1.29%); HLA-A29 (4.19%); HLA-DR3 (11.45%); HLA-DR4 (7.38%). However, the rationale for such associations is not always clearly defined.

Conclusion

This study has been conducted in order to estimate the distribution of HLA alleles in a general population from Guadeloupe for which such information were not available. HLA allele frequencies found in this population emphasize the various ethnic origin of this population (Africa, Europe, India…).
It also open new perspectives for other pathologies such as infectious complications in sickle cell disease particularly in children, spontaneous abortion and specific kidney graft rejection in population similar to the one studied. In these pathologies, HLA associations are highly suspected.

Acknowledgements:

The authors acknowledge the Conseil Régional de la Martinique and the Fonds Social Européen for their financial support.

References

EXCOFFIER L., LAVAL G and SCHNEIDER S. Arlequin ver 3.0: An integrated software package for population genetics data analysis. *Evolutionary Bioinformatics Online*, 2000.1: 47-50.

MILLER S.A., DYKES D.D. and POLESKY H.F. A simple salting out method for extracting DNA from human nucleated cells. *Nucleic Acids Research*, 1988. 16(3): 1215.

Allelic frequencies in worldwide populations are available on www.allelefrequencies.net

Health / Social Sciences

Neuroprotection: Activation of Novel Endogenous Pathways?

FARID F YOUSSEF

Physiology Unit, Faculty of Medical Sciences, University of the West Indies., St. Augustine Campus, Trinidad & Tobago - fmyoussef@ tstt.net.tt

Neurological disease continues to remain one of the major causes of morbidity and mortality worldwide, costing global society billions of dollars annually. While great strides have been made in elucidating the mechanisms behind many of these disease processes, progress on effective intervention strategies still remains limited. Many of the normal physiological pathways within the brain are designed to help prevent it from suffering injury. We have sought to examine these pathways with a view to understanding their mechanisms. In particular we have demonstrated that (i) a molecular form of learning and memory (long term potentiation) can reduce the effects of glutamate agonists and acute ischemia, (ii) activation of the endogenous cannabinoid pathway can modulate the effects of ischemia and (iii) activation of a sub-class of glutamate receptors (AMPA receptors) can induce receptor cross-talk and help attenuate epilepsy and migraine. These results suggest that activation of endogenous pathways may be critical to modulating the process of neurodegeneration and offer hope for the development of novel forms of intervention in the treatment of neurological disease.

Women in Sciences in the Caribbean: Some Data and Reflections

L. ALVAREZ-DIAZ

Ministery of Science, Technology and Environment of Cuba - lilliam@citma.cu

Abstract

The report contains country-level data on the presence of women in different scientific fields, having scientific degrees, occupying decision positions and comparisons with other countries in the Region, in particular in the Caribbean and other countries of Latin America. The figures show that the Cuba advances have been notorious.

The social analysis of the not-so-obvious problems is done from the perspective of women doing basic sciences, in particular women in Physics.

In Cuba, in spite of having for more than 40 years, a well established political will to open opportunities for everybody, opportunities to all the talent youth, including girls, still are present the stereotypes prejudices in our culture, and still we find professional bias, troubles in getting positions of leaderships in some sectors, lack of transparency in some decision-making levels, etc.

We discuss the importance of having women in leadership positions and how they can promote and serve as a pattern role model for the next generations. Also it is important to put in first place the support of the family, including parents and husbands as a factor of the success of many women in sciences, especially in the Third World.

The activity of the Third World Organization of Women in Sciences, TWOWS-TWAS, particularly in the Caribbean also is reported.

In addition, recommendations are made on ways of overcoming existing gender stereotypes among scientists, technologists, policy-makers and the community at large in Caribbean countries.

The necessity of mobilisation, to adopt recommendations on access to scientific careers, science policies, networking, and other important topics are crucial to shape the future of women in sciences in our countries.

Health / Social Sciences

Social Sciences, an Indispensable View on West Indian Health

J. DUMONT, J. PRUNEAU, S. RUFFIE, S. LAUPA AND G. VILLOING

Laboratoire ACTES – Université ANTILLES GUYANE, Campus de Fouillole 97159 Pointe-à-Pitre Guadeloupe, French West Indies. - jacques.dumont@univ-ag.fr

Abstract

The research laboratory ACTES, which subject is motricity in the Caribbean area, is regularly confronted with the issue of differences : either external ones, resulting from the tropical environment, or internal dealing with the population and its culture built by a singulary history. In our field, one question is coming out : How are the cultural and social norms determined, in particularly those hanging over the body, specifically the bruised body? This paper using several researches in the French West Indies, done or in process, wants to point out some of the certitudes on body normality that are supposed to shed light on body health. How are the differences thought ? How are they taken into account? Historically in the French West Indies, the statistical data are rare, either scattered or concentrated on few pathologies which gravity is sometimes diminished. The beginning of the military service in 1913 is a turning point insofar as health policies are set up in the French West Indies. However, even though the willingness is permanently reaffirmed, the measures are sporadic and the structures at their early stage. Moreover the validity of health indicators in effect are questioned. Could the morphological and physiological norms be used with black population, even though they are thought for white people? When we talk about pathologies their social visibility is brought out. For long, the bruised body has been hidden. The difference is a shame whether a simple step aside from the norm or a stigma. It's necessary to wait the eighties to have the society deal with handicap, pointing out the paradoxical right for difference and indifference. Physical activity can help to overcome the stigma, but can also reveal it sometimes as in the case of sickle cell disease. In today research the attention given to the genetic elements also questions the differences between populations leading somehow to a possible resurgence of the negatively connoted notion of race. Thus social sciences are indispensable for questioning health in the specific West Indian context.

Social Dialogue in Conflictual Settings : The Case of Guadeloupe

F. ALVAREZ (1) AND H. ERNATUS (2)

University of Antilles and Guyane, UFR SJE, Fouillole Campus, Guadeloupe
(1) Working group on " Management and Organizational Development ", LEAD, University of Antilles and Guyane ; associate researcher at CREFIGE, University of Paris-Dauphine. falvarez@univ-ag.fr
(2) Doctoral student at MATISSE (University of Paris 1) and LEAD (University of Antilles and Guyane). Helene.ernatus@wanadoo.fr

Abstract

In this world of globalisation, the small insular economies of French West Indies are meeting specific difficulties in terms of development, due to their size, but also to the conditions that govern commercial trade between French Caribbean territories and other Caribbean states. Besides, companies suffer from a lack of efficiency which is not caused only by material factors, but which is largely influenced by economic agent's behaviours, among which employers and trade unions.

Facing strong conflicting working relationships and a lack of structuring, recent studies have shown that a true and continuous social dialogue needs to be established in Guadeloupe. The heavy consequences of tensions and social conflicts on the local economy have been acknowledged by all social partners. Still, processes aimed at founding favourable conditions to create a sustainable social dialogue remain limited.

Why such conflicts? How can corporate social responsibility (CSR) initiatives, especially those related to implementing social dialogue, bring effective and relevant answers to the socio-economic problems of Guadeloupe?
The first part of the paper is dedicated to presenting the geographic, economic, social and cultural environment of Guadeloupe. The second part will analyse the causes of work conflicts. The last part of the paper focuses on the relevance of CSR initiatives- notably social dialogue- , for small companies for which institutional processes are difficult to implement. Moreover in such a context, social and cultural features have a strong impact on performance. Nevertheless, CSR initiatives seem to be a very strong lever to develop social dialogue or to change the way existing forms of dialogue are expressed.

Risk Factors of Acute Chest Syndrome in Guadeloupean Sickle Cell Anemia Children

V. TARER (1), V. CHAAR (1), M. ETIENNE-JULAN (1,2), J.P. DIARA (3),
L. DOUMDO (2), J. ELION (4) AND M. ROMANA (1)

(1) UMR 763 Inserm / Université des Antilles et de la Guyane - v.tarer@voila.fr
(2) *Centre Caribéen de la Drépanocytose "Guy Mérault", CHU de Pointe-à-Pitre, 97159, Guadeloupe,*
(3) *Service de Pédiatrie du CHU de Pointe à Pitre, CHU de Pointe-à-Pitre, 97159, Guadeloupe*
(4) *UMR 458 Inserm / Université Paris 7-Denis Diderot, Hôpital Robert Debré, 75019, Paris, France*

Abstract

Acute chest syndrome (ACS) is one of the most common causes of morbidity and mortality in sickle cell anemia (SCA) which is, as in other Caribbean islands, a major public health concern in Guadeloupe.
A prospective study was conducted on 239 SCA children followed up by the Guadeloupean sickle cell center between 1980 and 1999 (mean follow-up duration 7.8 ± 4.2 years), in order to provide information about incidence and risk factors of ACS in this population. Four hundred fifteen ACS episodes in 134 patients were analyzed. Potential predictors of first ACS were examined in a multivariate analysis and we performed a candidate gene study to identify associations between modulating genes and the occurrence of ACS. The overall incidence of this complication was 13.4/100 patients-years and ACS incidence was higner in male than in female (16.3/100 patients-years vs 10.8/100 patients-years, $p < 0.05$). A belated medical follow-up was associated with an increased risk for the first ACS [RR = 4.55 ; 95% CI (2.11 – 9.84)]. This result could be considerered as a new argument for the precocious medical follow-up of SCA patients. Three other risk factors of first ACS were identified: previous history of asthma [RR = 2.76 ; 95% CI (1.01 – 7.56)], steady state reticulocytes count [RR = 1.27 ; 95% CI (1.10 – 1.46)] and homozygous state for the T8002C variant of the endothelin -1 gene [OR = 4.30 ; 95% CI (1,21 – 15.20)]. As yet, asthma has never been formally identified as an independent risk factor for ACS. In the same way, if the involvement of ET-1 in the physiopathology of SCA is well-known, it is the first time that a polymorphism of its gene is described as a risk factor of a major complication of the disease. Ours results also suggested that *ecNOS* C-786, have a protective effect on the occurrence of first ACS [OR = 0,42 ; 95% CI (0,21 – 0,84)]. Furthers studies are warranted to confirm these results.

Health / Social Sciences

Sickle Red Cells Dynamic Behavior Under Venular Blood Flow

C. ALLAYOUS (1), A. BRUEL (2), D. SCHOËVAËRT (2), R. EMILION (3) AND T. MARIANNE-PEPIN (1)

(1) Université des Antilles et de la Guyane, Département de Biologie, Pointe-à-Pitre, Guadeloupe, France - Clara.Allayous@univ-ag.fr
(2) Unité INSERM U553, Hôpital Saint-Louis, Paris, France
(3) UMR 6822-MAPMO, Université d'Orléans, Orléans, France

Sickle Cell Disease (SCD) is a genetic vasculopathy caused by a mutation in the beta-globin gene (Glu6Val). Sickle hemoglobin molecules (HbS) have the property to polymerize when deoxygenated, forming sickle red blood cells. This polymerization initiates a cascade of events leading to vaso-occlusion, endothelial and inflammatory abnormalities and increased adhesive reactions. Vaso-occlusive crisis are initiated by the adhesion reaction between the activated blood vessel endothelium and sickle red cells (Walmet, 2003).
Hydroxyurea (HU) is a ribonucleotide reductase inhibitor that improves hematologic parameters and decreases adverse effects in patients with SCD. Currently, HU is the approved drug in the treatment of moderate and severe SCD. Recent studies showed that, under static conditions, HU affects the adhesion protein profile of the endothelial cells and decreases the adhesion of the sickle red cells onto the vessel endothelium (Brun, 2003; Conran, 2004).
The present study focuses on the adhesion between endothelial cells and sickle red cells, under venular flow conditions, using a human endothelial cell line, TrHBMEC. Our results show a difference in the dynamic behavior of the sickle red cells under various conditions such as 1°) TNFα and IFNγ; 2°) HU; and 3°) TNFα, IFNγ and HU.
These preliminary observations indicate that the dynamic behavior of the red blood cells, which is different between normal and SCD patients, might play a central role in the vaso-occlusive crisis.

Sport and Sickle Cell Disease in 12-19 Years Old Adolescents in Guadeloupe: Best Enemies

J. PRUNEAU, F. MAILLARD AND B. PHILIPPON

Laboratoire ACTES – Université ANTILLES GUYANE - Centre Caribéen de la Drépanocytose - Pruneau.j@wanadoo.fr

Abstract

In the Caribbean area, the Sickle cell disease is the most frequent genetic disease. In Guadeloupe, ten per cent of the population has the sickle cell trait (gene A and gene S), it means that 40000 people may transmit this disease to their child without being aware of it. From a strictly medical meaning, the disease can be managed via adapted care, since sickle cell disease is recognized as a priority of public health in France (1990). However, this disease affects not only the body of the patient but also its social identity. Then, the understanding of the disease calls upon an anthropological vision of human being, refusing to dissociate the man from its body and its sociocultural context.
Nevertheless, few anthropological studies have investigated the sickle cell disease (Benoit, 2004; Lainé, 2004). In addition, no study has focused on the relation between the anthropological aspects of this disease and physical activity. A possible explanation would be that physical practice is one of the principal factors of the sickle cell crisis onset. As a result, doctors caution against physical activity and it is often forbidden at school.
The aim of the present socio-anthropological study was therefore to investigate whether the adolescents suffering from this disease practiced a physical activity in spite of the doctor's contraindications. The main results showed that they practiced at school when physical activity was adapted and authorized by the administrative regulations. Moreover, adolescents practiced outside school even if it was proscribed, especially those who had the least serious form of the disease.
The results of the present socio-anthropological study question the problematic of physical activity and its interest in relation to this disease. Beyond the medical aspect, they suggest a new approach in terms of health for these adolescents to some extent: an adapted physical practice.

Health / Social Sciences

The Effect of Tropical Environment on Sports Performances

S. BLONC, E. SENATUS, C. ROBIN, M. LE HER AND O. HUE

Laboratoire ACTES, UFR STAPS UAG, Campus de Fouillole, BP 592, 97159 Pointe-à-Pitre Cedex, Guadeloupe FWI, France - stephen.blonc@univ-ag.fr

Abstract

It is well known that environmental factors can have impacts on physiological and psychological performances. Studies conducted in the FWI have showed three majors results.

Firstly/ In native to tropical climate, intensive and prolonged endurance exercise induces an overload regarding thermoregulatory and cardiac responses. In well-trained endurance athletes who trial acclimatization process, 14 days of exposure led to changes positives adaptations in physiological parameters such central temperature, sweat rate, body mass loss, heart rate and endurance performance, but were still insufficient to ensure complete acclimatization. Thus, the hot/wet climate induced impairment of physiological responses and constitute a limiting factor for aerobic performance.

Secondly/ When focused on anaerobic performances, it is well known that in temperate climate, short-term performances (cycle-sprint, jumps) varies throughout the day, and maximal anaerobic power is generally increased by the end of the afternoon, following the peak of the circadian temperature curve. Several studies conducted in the french Caribbean environment failed to show any daytime variation in maximal anaerobic performances which suggests that a hot and humid environment may have blunted the time-of-day effect by a passive warm-up effect. Thus, the warm exposure and the diurnal increase in body temperature influence muscle strength. However, the improvement in muscle contractility after these two passive warm-ups cannot be combined in order to improve force to a greater level. In conclusion, the tropical moderately warm and humid conditions does not affect anaerobic performance and permit in the opposite a stabilization of the performance whatever the time-of-day when compared to temperate climate.

Thirdly/ Cognitive studies in psychology showed a decrease of cognitive performance at hot room temperature for people living in temperate climate. This decrease in performance depends on the nature of the task (simple or complex cognitive tasks) and on the change of core temperature. The complex cognitive processes being the most vulnerable to hot and wet conditions (climate present in Guadeloupe), the aim of our studies was to determine the effects of heat stress on cognitive performance in native or not native people living in tropical climate.

Modern Biotechnology and Biosafety Policy Issues for Guyana

J. C. CAESAR

Department of Biology, Faculty of Natural Sciences, University of Guyana, Box 10-1110, Georgetown, Guyana - jccaesar@yahoo.com

Abstract

Agenda 21 and the *Convention on Biological Diversity* both recognise biotechnology can provide an important means by which biological diversity can be sustainably used. However, the techniques employed and/or the products derived therefrom may potentially pose risks to biological diversity. The basic product from modern biotechnology is transgenic, because the products are in the main derived from recombinant DNA technologies. In some arguments, the principles of genetics, reproductive biology and ecology have been used to indicate high probabilities of gene transfer reciprocity between transgenics and conventional or wild-type organisms. While the advent of the biotechnology age and

its attendant bioeconomy-driven development has been heralded as an important construct in the new-age development ethos, major international instruments, the *Convention on Biological Diversity* and the *Cartagena Protocol on Biosafety* recognize the need for ensuring the safety of biotechnology. Admittedly, the risks posed by biotechnology to biodiversity are best analysed on a case-by-case basis. However, the precautionary approach has been widely accepted as a plausible means for averting potentially unknown risks when there is lack of scientific certainty. Guyana, like many developing countries, is confronted with major policy issues regarding the potential and promise of biotechnology in alleviating hunger, disease and poverty as against the potential risks and how best to engage the twin issues of biotechnology development and biosafety. Guyana has been predominantly an agrarian economy with sugar and rice as the bedrock The European Union's preferential market restructuring necessitates innovative policy engineering. Issues of policy framework for leveraging safe bio-technologies as a developmental strategy, while sustainably using and safeguarding Guyana's relatively rich biodiversity wealth and assuring ecosystem health are highlighted and some suggestions advanced. As a small economy, a strategic regional collaborative approach may be more meaningful vis-à-vis the nations' biotechnology assimilation and exploitation capacity.

Eléments de Prospective et l'Environnement

M. CASTELLANOS (1), J.G. MONTAUBAN (2), R. ARISTIDE (2) AND L. ALVAREZ (4)

(1) PhD, DP-CITMA y Profesora Titular Adjunto del InSTEC - marlena@citma.cu
(2) PhD (4) Directora Ciencias CITMA - liliam@citma.cu

(Les îles de Cuba et de la Guadeloupe) •

Abstract

Les études sur la prospective, ses antécédents, ses définitions, ses conceptions basiques, les outils de sa mise en œuvre et ses très nombreuses applications, sont relativement aisées à recenser (*). Le travail ci-après présentera dans une première partie un bref récapitulatif relatif au champ de la prospective et en illustrera un aspect peut abordé, concernant la relation de la prospective à l'environnement.

Les thématiques abordées ici peuvent être approfondies en se référant aux ouvrages de la collection "Economie et environnement", dus à l'auteure de la pré-sente étude. Les deux premiers, "Nouvelles approches, réflexions et expériences actuelles", et "Introduction à la problématique de la valorisation économico - environnementale", traitent des bases conceptuelles et méthodologiques qui sont aujourd'hui celles de l'économie et de l'environnement.

Le troisième, "Applications relatives à la prospective et à la valorisation économico - environnementale", est un ouvrage collectif, regroupant 14 contributions sous la forme d'études pédagogiques et d'études de cas. Y ont participé 19 auteurs et 12 centres de recherches, dont l'U.A.G. et l'InsTEC.

(*) Godet (1994), Ortega (2003), Lugari (2003), Castellanos (2005), etc

Health / Social Sciences

Climate Change and Caribbean Economic Development: an Opportunity for Convergence of the Sciences

M. ATTZS

Department of Economics - University of the West Indies - St. Augustine, Trinidad and Tobago
mattzs@hotmail.com - mattzs@fss.uwi.tt

Abstract

Climate change has emerged as a significant challenge to sustainable development given its likely impacts on ecosystems. That Climate Change is a consequence of global warming due in large measure to anthropogenic factors is no longer an issue. The debate that remains is whether Caribbean socio-economic policy, at both the national and regional levels, should factor mitigation of GHGs and adaptation to climate change impacts into decision-making. That debate is guided, in part, by the paucity of solid national and regional scientific data to inform decision-making.

Decisions on whether to invest in GHG mitigation or adaptation strategies for Climate Change impacts ought to be based on specific triggers signalled by the national and regional scientific community. While there is consensus that the implementation of mitigation or adaptation policy should not necessarily be delayed until there is absolute certainty about the potentially negative impacts, there is concurrence that more research on "what is at risk" is needed at the regional and sub regional levels.

This paper focuses on the role of the "Sciences" in articulating climate change policy for sustainable national and regional economic development. The conclusion drawn in the paper is that effective policy to meet the challenges posed by climate change should begin with a convergence of the sciences.

A New Recombinant Geminivirus Infecting *Sida* in Jamaica

C.S. STEWART AND M.E. ROYE

The Biotechnology Centre, University of the West Indies, 2 St John's Close, Mona Kingston 7, Jamaica -

Abstract

Geminiviridae is the second largest group of plant viruses, with at least thirty-five new members being identified each year that are responsible for diseases that result in multi-billion dollar crop losses in the tropical and sub-tropical regions (Varma & Malathi, 2003). The genus Begomovirus contains the viruses which are most prevalent in the Western Hemisphere and most members of this genus are bipartite with the total genome represented by two separate DNA molecules designated DNA-A and DNA-B (Morales & Anderson, 2001). Weeds are known to act as reservoirs of geminiviral inoculum in the absence of crop hosts and some weed viruses also infect crops (Roye et al, 2003). Samples of the ubiquitous weed Sida which were exhibiting symptoms of golden mosaic typical of geminivirus infection were collected from agricultural areas in Jamaica. DNA was extracted and the degenerate geminivirus specific primers PAC1v1978/ PAV1c715 and PBC1v2039/ PBV1c800 used to amplify the DNA-A and DNA-B of the begomoviruses present respectively. Amplicons from a sample collected in Buckup, Manchester were cloned and sequenced. Multiple alignment with the DNA-A of Jamaican viruses as well as other viruses from this hemisphere revealed nucleotide similarity well below the 89 % threshold set by the International Committee on the Taxonomy of Viruses (ICTV) which makes this viral isolate a newly identified geminivirus. Nucleotide homology between this Buckup virus and other Jamaican Sida viruses ranged from 49 to 79 %. Pairwise comparison of the DNA-B of this virus with the Macroptilium golden mosaic virus Jamaica strain 2 (MGMV-[JM2])

revealed that the intergenic region (IR), hypervariable region and the nuclear shuttle protein (NSP) shared very high homology, with the IR of these viruses sharing a 96.8% identity. Additionally, the Buckup DNA-A IR shares an identity with MGMV-[JM2] of 93.3 % as well sharing the conserved Rep binding sites found in MGMV-[JM2] (Roye et al, 1999)

References

Morales, F.J.; Anderson, PK. 2001 "The emergence and dissemination of whitefly-transmitted geminiviruses in Latin America." Archives of Virology 146: 415-441.

Roye, M.E., Brown, S., Spence, J.D., Smith, K. and McLaughlin, W.A. 2003. "Ten Years of Molecular Biology Research on Whitefly Transmitted Geminivirus From Jamaica: A Review." Jamaican Journal of Science and Technology Vol. 14: 98 – 118.

Roye, M.E. McLaughlin, W.A., Spence, J.D. and Maxwell, D.P. 1999. The common weed Macroptilium lathyroides is not a source of crop-infecting geminiviruses from Jamaica. Journal of Tropical Agriculture. Trop Agric. (Trinidad) 76 (2):1-7. #308

Varma, A. and Malathi, V.G. 2003. "Emerging geminivirus problems: A serious threat to crop production." Ann. Appl. Biol. 142: 145-164.

Setting up of a Pet - Ct Center in Martinique: Interest and Feasibility

H. AZALOUX (1), J. BAUDIN-VERONIQUE (1), J.M. CAIGNON (1), C. DRAGANESCU (1), M. DIEYE (2) AND J. SMITH-RAVIN (2)

(1) Service de Médecine nucléaire, Oncologie, Biophysique, CHU de la Meynard, 97200, Fort de France, Martinique - azaloux@wanadoo.fr
(1) Registre des Cancers de la Martinique, AMREC, 97 200 Fort de France, Martinique
(1) Laboratoire de Biologie, Campus de Fouillole, 97 159 Pointe-à-Pitre, Guadeloupe

Abstract

Nowadays, Position Emission Tomography (TEP) is fully established in almost all the french regions including the island of "Réunion". Its setting up in Martinique will allow to medically covering the inter-region "Antilles-Guyane" (Guadeloupe, Guyane and Martinique). On the basis of medical territorial continuity, this will provide equal access to medical care in the French overseas territories in the Caribbean (DOM). An optimal use of this technique is already insured by the mean of a local cancer organisation which meets government requirements in the "plan cancer" set up in 2002. This structure, established several years ago, is multi-disciplinary and manages a cancer registry. For a long time, all its efforts were focused on medical care particularly radiotherapy (linear accelerators and curie therapy) of prostate cancers. Based on the registry data and the recognized standards related to different cancers, we have evaluated that the setting up of such apparatus is fully justified in order to respond to the needs of the french Caribbean islands not only on the medical care side but also in the field of research of novel biomarkers molecules (different from FDG-F18) and of abnormalities in cellular exchanges during oncogenesis. The presence of a cyclotron next to the TEP apparatus is essential, because of the short live (less than 2 hours) of the positrons used. Different collaborative research work will be possible with other institutions such as the "Université des Antilles et de la Guyane" in order to optimise such a highly sophisticated equipment.

Keywords: TEP-CT, Cyclotron, Tumor register, French West Indies

Health / Social Sciences

Revitalizing Science and Technology Policy for Sustainable Development in Guyana: Leveraging Lessons from the Developing World

J. C. CAESAR

Department of Biology, Faculty of Natural Sciences, University of Guyana, Box 10-1110, Georgetown, Guyana - jccaesar@yahoo.com

Abstract

The crucial roles of science and technology as important constructs in all facets of development can no longer be disputed. Most developing countries have recognized this imperative but the institutional frameworks needed to harness S&T as an engine for growth has not been adequately addressed. A case study on Guyana is presented.

Guyana, the only English-speaking country in South America has been touted as the gateway to the continent. However, this dream is yet to be realized. S&T has been recognized as an important cross-cutting instrument in Guyana's *National Development Strategy* and there is a draft *National Science and Technology Policy*. The Head of State, as Executive President, holds the Cabinet portfolio for S&T and there is a National Science Research Council. In principle, S&T has been given a high profile on the government agenda but actual outputs from a well structured framework is less than expected possibly due to other socio-economic demands and imperatives. This paper proposes to examine how some developing world experiences can be leveraged in re-establishing, strengthening and implementing the existing/emerging policy framework and developing the required capacity for reinforcing the national S&T agenda as a serious cross-cutting policy instrument for sustainable national development. The re-positioning of the University of Guyana as a strategic player in Guyana's S&T is advocated. The main thesis is that the transformation of articulated policy into active S&T enterprise as per other developing world paradigms is crucial to Guyana's regional and international competitiveness and national development in the epoch of globalisation.

Low Brain Cytochrome C Oxidase Activity in two Rabbit Models of Alzheimer's Disease

T. ALLEYNE, J. JOSEPH, N. MOHAN AND A. ADOGWA

Faculty of Medical Sciences - University of the West Indies, St. Augustine, Trinidad & Tobago trevnmar@tstt.net.tt

Abstract

Alzheimer's disease (AD), a debilitating neurodegenerative brain disorder, has in recent decades emerged as a major cause of death in the elderly, fueling the search for good animal models: One characteristic of this disease is low activity of brain cytochrome c oxidase (COX). In this study we evaluated two AD rabbit models, the Klatzo model and the Sparks model. Specifically, we isolated brain mitochondria and investigated the activity of brain COX for the two models; we also evaluated the spectral properties and protein composition of the brain mitochondria. Polarographic assay revealed that for the Klatzo model there was no significant change in Km but the Vmax of COX fell by between 25-68%: In some instances the well documented characteristic biphasic kinetics of the enzyme was replaced by a single phase. For the Sparks model 66% of the rabbits showed a decrease in COX activity. For this model the maximum decrease in Vmax was 43%. For the Sparks but not the Klatzo model, the brain mitochondria displayed decreased absorbance at 434nm further suggesting either a deficiency or decreased activity of COX. These results suggest that in so far as COX activity is concerned, both models are satisfactory AD models.

Health / Social Sciences

The effect of Apium graveolens and Momordica charantia on plasma lipids and blood pressure in laboratory rats

E. CUMMINGS , M. VARSWYK

Faculty of Health Sciences, University of Guyana, Turkeyen Campus, Guyana
rowepr1@yahoo.co.uk - ecummings@uog.edu.gy

Abstract

Apium graveolens (celery) and Momordica charantia (karela) are known to have both hypotensive and hypocholesterolemic effect but comparison of the 2 plants have not been examined. 40 laboratory rats were isolated and placed into 4 groups. 2 rats from each of the groups were sacrificed in order to obtain baseline data. Initial measurements included body weight, blood pressure, blood glucose and the plasma lipids (Total cholesterol, LDL, HDL and Triglycerides. 3 groups were then fed a high fat diet for 3 weeks. 4 rats from the each from the 4 groups were sacrificed and blood taken and the measurements were repeated. One of the groups was treated with water soluble extracts of celery another with karela (0.1 g/ml) for 3 weeks, the other 2 groups acted as normal control and high diet non treatment control. After 6 weeks the remaining rats were sacrificed and the above mentioned test were done. The results showed that the Karela supplemented rats recorded significant lower body weight ($P < 0.05$), lower blood pressure BP ($P < 0.05$) and increase HDL ($P < 0.05$).non significant lower Total cholesterol (TC), Triglycerides (TG) and Low density lipid Celery treated rats also recorded statistical significant decrease in body weight and blood pressure ($P < 0.05$). Non statistical significance decreases were observed for triglyceride, LDL, and increase in HDL. The study reveals for the first time that Celery is more effective in lowering BW while Karela is more effective in lowering BP

The Effects of Apium Graveolens and Trigonella Foenumgraecum on Plasmolipids in Laboratory Rats

E. CUMMINGS , G. COOPSAMMY

Faculty of Health Sciences, University of Guyana, Turkeyen Campus
rowepr1@yahoo.co.uk - ecummings@uog.edu.gy

Abstract

This study was carried out to determine the effects of the water soluble extracts of two plants, *Apium Graveolens* (celery) and *Trigonella foenum graecum* (fenugreek/methi) on Plasma Lipids in laboratory rats. The research was done in an attempt to find an affordable and effective and readily available treatment for persons suffering from hypercholesterolemia and related complications such as obesity and coronary artery disease.

Over a period of 7 weeks, 28 laboratory rats were isolated and placed into 3 groups. (A B&C). Group C was used as control while groups B and C were treated with an oral dose of methi and celery respectively after being fed with a high fat diet for a period of 3 weeks. Blood pressure body weight, blood glucose and plasma lipids (Total cholesterol, LDL, HDL and Triglycerides) were measured for obtain baseline data. These measurements were also done at the end of 3 weeks and at the end of 7 weeks.

The results showed that both *celery s* and *methi had* positive effects in lowering some of the plasma lipids. In the case of the rats that were fed celery there was a significant reduction in blood pressure, blood glucose and LDL. The reduction in total cholesterol, triglycerides and body weight these were not significant. In the case of the rats that were fed with *methi* there were statistically significant decreases in blood pressure, blood glucose, triglycerides, total cholesterol and LDL while the body weight decreased but not significantly. The results obtain in this study correlates with those obtain by other researchers.

The overall results suggest that both ThA. graveolens and T. graecum can exert favorable responses to the high levels for blood pressure, blood glucose a LDL, total cholesterol, triglycerides and body weight.